UNIVERSIDAD DE MURCIA

ESCUELA INTERNACIONAL DE DOCTORADO

Desert Truffle Cultivation: New Insights into Mycorrhizal Symbiosis, Water-Stress Adaptation Strategies and Plantation Management

Cultivo de la Trufa del Desierto: Nuevas Perspectivas sobre la Simbiosis Micorrícica, Estrategias de Adaptación al Estrés Hídrico y Manejo de Plantaciones

D. José Eduardo Marqués Gálvez

2019

UNIVERSIDAD DE MURCIA   **FACULTAD DE BIOLOGÍA**

DEPARTAMENTO DE BIOLOGÍA VEGETAL

DEPARTAMENTO DE BIOQUÍMICA Y BIOLOGÍA MOLECULAR-A

Desert truffle cultivation: new insights into mycorrhizal symbiosis, water-stress adaptation strategies and plantation management

Cultivo de la trufa del desierto: nuevas perspectivas sobre la simbiosis micorrícica, estrategias de adaptación al estrés hídrico y manejo de plantaciones

Memoria para optar al grado de Doctor en Biología Vegetal por la Universidad de Murcia presentada por:

JOSÉ EDUARDO MARQUÉS GÁLVEZ, MURCIA, 2019

Dª Asunción Morte Gómez, Catedrática de Universidad del Área de Botánica en el Departamento de Biología Vegetal, y Dª Manuela Pérez Gilabert, Catedrática de Universidad del Área de Bioquímica y Biología Molecular en el Departamento de Bioquímica y Biología Molecular-A,

AUTORIZAN:

La presentación de la Tesis Doctoral titulada "Desert truffle cultivation: new insights into mycorrhizal symbiosis, water-stress adaptation strategies and plantation management / Cultivo de la trufa del desierto: nuevas perspectivas sobre la simbiosis micorrícica, estrategias de adaptación al estrés hídrico y manejo de plantaciones", realizada por D. José Eduardo Marqués Gálvez, bajo nuestra inmediata dirección y supervisión, y que presenta para la obtención del grado de Doctor por la Universidad de Murcia.

En Murcia a 4 de Septiembre de 2019

Fdo: Dª Asunción Morte Gómez   Fdo: Dª Manuela Pérez Gilabert

Funding information

Scientific publications derived from this thesis

- **Marqués-Gálvez JE**, Morte A, Navarro-Ródenas A, García-Carmona F, Pérez-Gilabert M (2019) Purification and characterization of *Terfezia claveryi* TcCAT-1, a desert truffle catalase upregulated in mycorrhizal symbiosis. PloS One 14(7):e0219300. https://doi.org/10.1371/journal.pone.0219300.

- Andrino A, Navarro-Ródenas A, **Marqués-Gálvez JE**, Morte A. Desert truffle crop depends on agroclimatic parameters during two key periods. Manuscript accepted in Agronomy for Sustainable Development.

- **Marqués-Gálvez JE**, Kohler A, Miyauchi S, Navarro-Ródenas A, Arenas F, Paolocci F, Morin E, Auer L, Kuo A, Martin F, Morte A. Desert truffle genomes reveal survival adaptations to mycorrhizal lifestyle in dry land. Manuscript in preparation.

- **Marqués-Gálvez JE**, Morte A, Navarro-Ródenas A. Stomatal response to vapor pressure deficit in spring as a marker for desert truffle cultivation. Manuscript in preparation.

- **Marqués-Gálvez JE**, Navarro-Ródenas A, Arenas F, Guarnizo-Serrudo AL, Peguero-Pina J, Gil-Pelegrin E, Morte A. Elevated atmospheric CO_2 modifies desert truffle mycorrhizal plant flowering and response to water-stress. Manuscript in preparation.

Book chapters

- Morte A, Pérez-Gilabert M, Gutiérrez A, Arenas F, **Marqués-Gálvez JE**, Bordallo JJ, Rodríguez A, Berná LM, Lozano-Carrillo C, Navarro-Ródenas, A (2017) Basic and applied research for desert truffle cultivation. In: Varma A, Prasad R, Tuteja N (eds.) Mycorrhiza-Ecophysiology, Secondary Metabolites, Nanomaterials. Springer International Publishing pp. 23–24. https://doi.org/10.1007/978-3-319-57849-1_2.

Contribution to conferences and congresses

- Morte A, Arenas F, **Marqués-Gálvez JE**, Berná LM, Guarnizo-Serrudo AL, Gutiérrez A, Rodríguez A, Navarro-Ródenas A (2019) Turmiculture project: desert truffle crop against climate change and for rural development. 10th International Workshop on Edible Mycorrhiza Mushrooms (IWEMM10), Suwa City, Nagano Prefecture, Japan.

- Morte A, Andrino A, **Marqués-Gálvez JE**, Arenas F, Navarro-Ródenas A (2019) Desert truffle crop depends on agroclimatic parameters during two key periods. 10th International Workshop on Edible Mycorrhiza Mushrooms (IWEMM10), Suwa City, Nagano Prefecture, Japan.

- Navarro-Ródenas A, Andrino A, **Marqués-Gálvez JE**, Morte A (2017) Desert truffle cultivation: a bioclimatic model for suitable management and production. 9th International Conference on Mycorrhiza (ICOM9), Prague, Czech Republic.

- Morte A, Arenas F, **Marqués-Gálvez JE**, Gutiérrez A, Berna LM, Pérez-Gilabert M, Navarro-Ródenas A (2017) Advances in desert truffle cultivation in Spain. 9th International Workshop on Edible Mycorrhiza Mushrooms (IWEMM9), Texcoco, Mexico.

- **Marqués Gálvez JE**, Navarro-Ródenas A, Nicolás E, Morte A (2016) Combined effect of Vapour Pressure Deficit and irrigation on desert truffle mycorrhizal plants. 8th International Workshop on Edible Mycorrhiza Mushrooms (IWEMM8), Cahors, France.

Agradecimientos

Todo lo que en esta tesis está reflejado es fruto de éxitos y fracasos, de penas y glorias, de esfuerzo, dedicación, cansancio, sufrimiento y alegría, sobre todo alegría. Es curioso cómo, a veces, las emociones negativas se esfuerzan en llegar más hondo, en intentar perdurar más que las positivas. Precisamente por eso, me gustaría utilizar estas palabras para recordarme a mí mismo, y a quién lo necesite en el futuro, la importancia de la pasión por un trabajo duro, pero a la vez emocionante; el orgullo, por el trabajo bien hecho y la superación diaria; la confianza en uno mismo y en las personas que lo acompañan; la positividad ante los pequeños obstáculos que aparecen en el sendero; la felicidad, por los éxitos alcanzados y los grandes momentos vividos; y finalmente, el cariño por las personas que viajan con nosotros y por los recuerdos de un camino que ni se acaba ni empieza, sólo cambia.

Este documento ha sido posible gracias a personas, no sólo aquella que firma la autoría de la tesis, sino todas aquellas que, de una forma u otra, han aportado en su realización. Es por eso por lo que me gustaría mostrar mi agradecimiento.

En primer lugar, me gustaría agradecer a la Dra. Manuela Pérez Gilabert y a la Dra. Asunción Morte Gómez la confianza que han depositado en mí durante estos años y la oportunidad que me han brindado de dedicarme a aquello que me gusta. Gracias a ambas por sostener este maravilloso grupo de investigación y por esforzaros cada día en que todos los integrantes del grupo nos sintamos cómodos, motivados y contentos. Tomaré prestado aquel proverbio chino que de vez en cuando nos recuerda Asun: "Si caminas sólo irás más rápido, si caminas acompañado llegarás más lejos".

Gracias Manoli, este trabajo empieza contigo. Gracias por introducirme en el mundo de la investigación, por animarme para que fuera al departamento e ir poco a poco aprendiendo técnicas y cogiendo soltura en el laboratorio, por enseñarme a ser metódico y cuidadoso, por tus correcciones que tanto me han enseñado a lo largo de estos años, por los consejos que me has brindado y, sobre todo, por acompañarme en todo este largo camino, desde el TFG hasta ahora, que se dice pronto. Por último, gracias por hablarme de una empresa en la que podría hacer mis prácticas de fin de grado. Porque sin esa empresa y sin esas prácticas, no hubiera conocido a Asun.

A la Dra. Annegret Kohler y al Dr. Francis Martin gracias por permitirme realizar estancias cortas en el "Institute National de la Recherche Agronomique – Grand Est Nancy" (INRA-Grand Est Nancy) que me han permitido abrir nuevos horizontes y expandir mi deseo de conocimiento. A Shingo, gracias por enseñarme toda la bioinformática que he necesitado. A Veronica, Clemence, Felix y Milena por su acogida y simpatía, y por hacerme sentir como en casa.

A todo el personal de servicios de la Universidad de Murcia que ha colaborado para que esta tesis sea posible, del CAID, del SACE y, en especial al personal del SEAF, Almudena, José y María del Mar, gracias por estar siempre atentos y dispuestos. También a todos aquellos agricultores y recolectores de turmas como Paco de Lara o "El Zorro" que tanto colaboran y facilitan la investigación en campo.

A los profesores del Ala-C del departamento de Bioquímica y Biología molecular A, por haber aportado un granito de arena en mi formación permitiéndome realizar horas de docencia. A mis compañeros de bioquímica Sandra, Adrián, Paula, Samanta, Carolina, Susana, Rubén y Antonio, y todos aquellos, que aun de paso, me han marcado. Gracias por aceptarme como uno más aunque fuera un poco extranjero, por todas las comidas en el departamento y las comidas y cenas fuera de él.

Me gustaría acordarme también de todas esas personas que me acompañaron durante la carrera. A todos esos compañeros/as y amigos/as, aun habiendo perdido el contacto en mayor o menor medida, gracias por haberme ayudado a crecer. En especial, gracias a Ana Luisa. Por estar ahí cada vez que lo he necesitado, por darme la razón cuando la he tenido, y quitármela cuando no, gracias por ser una amiga de verdad. "A ver si nos vemos una vez al mes, por lo menos".

Gracias a todos mis tíos, tías, primos, primas, a aquellos que están cerca y veo más a menudo y a aquellos que están más lejos y veo en fechas señaladas. Me gustaría dedicaros unas líneas a cada uno de vosotros, pero de verdad, sois muchísimos, así que simplemente doy gracias precisamente por eso, porque seamos tantos y tan grandes, por los buenos ratos en comidas y cenas familiares. En especial a mis tíos Pepi y Juan, y a Victoria, Ramón y la pequeña Carolina, gracias por todo. A mi primo Juan Antonio, con el que he vivido buenos y malos momentos, gracias por estar ahí. A mis primas Inma y Virginia, sois como un rayo de luz que va iluminando todo a su paso. Gracias por todo, espero que la distancia y el tiempo no sea impedimento para que sigamos iluminándonos.

A mis amigos, es difícil describir con palabras y de manera resumida todo lo que me aportáis personalmente y todo lo que habéis sumado sin daros cuenta a ésta tesis. Gracias por habernos ayudados a crecer los unos a los otros desde que nacimos, desde el instituto o desde hace algo menos de tiempo, los lazos que creamos nos hacen ser lo que somos. Laura, David, Carmen, Santi, Jorge y Dani, gracias por estar ahí siempre, por vuestra alegría, comprensión, sinceridad y cariño.

A mis abuelos maternos Josefa y Eduardo, y paternos Josefa y Pepe, a los que aun estáis conmigo y a los que ya os fuisteis, gracias por todo vuestro tiempo y amor. Sin las grandes familias que un día creasteis, yo no estaría aquí. Gracias.

A mi hermana Alba, gracias por aportar siempre un punto de vista diferente, sin ti la vida habría sido más aburrida. A mi madre y mi padre, ni en diez vidas tendría el tiempo y las palabras suficientes para agradeceros todo lo que habéis hecho y aún hacéis por mí, día a día. Gracias por apoyarme desde el principio, por inculcarme valores tan importantes como el esfuerzo, la amabilidad, el cariño y la educación. Sin vuestro apoyo y sabiduría probablemente éste sería un trabajo inacabado. Este trabajo y cualquier éxito que coseche en la vida, son vuestros.

A Julia, otra vez las palabras se quedan cortas. Desde hace ya casi dos años lo único que he recibido de ti, es amor. Gracias por ser tan especial, por haberme apoyado desde el principio, por subirme el ánimo cuando lo tengo bajo y, sobre todo, por soportarme cuando me encuentro cargado de dudas y miedos. Sin tu optimismo y capacidad para ver siempre el lado bueno de las cosas hoy no estaría aquí. Gracias por la seguridad que me das y por hacerme sentir que nada malo puede pasar, y si pasa, no será tan malo contigo al lado.

"No es oro todo lo que reluce,
ni toda la gente errante anda perdida"

J.R.R. Tolkien – El Señor de los Anillos

Index of contents

Index of tables and figures

Chapter I: General introduction

Chapter III: Characterization and purification of *Terfezia claveryi* TcCAT-1, a desert truffle catalase upregulated in mycorrhizal symbiosis

Chapter IV: Desert truffle genomes reveal survival adaptations to mycorrhizal lifestyle in dry land

Chapter V: The crop of desert truffle depends on agroclimatic parameters at two key annual periods

Chapter VI: Stomatal response to vapor pressure deficit in spring as a marker for desert truffle cultivation

Chapter VII: Elevated atmospheric CO₂ modifies desert truffle mycorrhizal plant flowering and response to water-stress

Chapter VIII: General discussion

Appendix A: Supplementary protocol

Appendix B: Supplementary Tables

Appendix C: Supplementary Figures

Abbreviations

3-AT	3-Aminotriazol
AA	Auxiliary activity
ABA	Abscisic acid
ABTS	2,2'-Azino-bis (3-ethylbenzothiazoline-6-sulphonic acid)
AI	Aridity index
AM	Arbuscular mycorrhiza
AMBIC	Ammonium bicarbonate buffer
ANOVA	Analysis of the variance
APN	DNA lyase
AQP	Aquaporin
BCA	Bicinchoninic acid
BSA	Bovine serum albumin
BUSCO	Benchmark universal single copy orthologs
C&RT	Classification and regression tree
CAT	Catalase
CAZyme	Carbohydrate-active enzymes
CBM	Carbohidrate-binding module
CC	Control chamber
CD	Cyclodextrin
cDNA	Complementary deoxyribonucleic acid
CE	Carbohydrate esterase
CHAP	Cysteine, histidine-dependent amidohydrolases/peptidases
CO	Chitooligosaccharides
COX	Cyclooxygenase
Ct	Threshold cycle
DMATS	Prenyltransferase
DNA	Deoxyribonucleic acid
DOY	Day of the year

DOY$_{VPDt}$	Day of the year at which VPD threshold was stably reached
DSMP	Drought-stressed mycorrhizal plant
DSNMP	Drought-stressed non-mycorrhizal plant
DTT	Dithiothreitol
ECM	Ectomycorrhiza
EDO	European drought observatory
EEM	Ectendomycorrhiza
ERM	Ericoid mycorrhiza
ET0	Potential evapotranspiration
EXPN	Expansin
F'm	Maximum fluorescence during a light saturating pulse
FCWDE	Fungal cell wall degrading enzyme
FDR	False discovery rate
FLM	Free living mycelium
Fs	Steady state fluorescence
GH	Glycoside hydrolase
HC	High CO_2 chamber
HMG	High mobility group
HMM	Hidden Markov model
HPLC/MS	High-performance liquid chromathography / mass spectroscopy
IAA	Indole-3-acetic acid
IAM	Indole-3acetoamide
IPA	Indole-3-piruvic acid
IRGA	Infrared gas analyzer
iWUE	Intrinsic water use efficiency
JGI	Joint Genome Institute
LCO	Lipo-chitooligosaccharide
LMA	Leaf mass per area
LSC	Large subunit-size catalase
LTR	Long terminal repeat

MCWDE	Microbe cell wall degrading enzyme
MFS	Major facilitator superfamily
MHB	Mycorrhiza helper bacteria
MIP	Membrane intrinsic protein
MMN	Modified Melin-Norkrans
MMNo	Optimal Modified Melin Norkrans
mRNA	Messenger ribonucleic acid
MW	Molecular weight
MWCO	Molecular weight cut-off
NGS	Next generation sequencing
NIP	Nodulin 26-like intrinsic protein
NMDS	Non-multidimensional scaling
NMP	Non-mycorrhizal plant
NRPS	Non-ribosomal peptide synthase
ORM	Orquid mycorrhiza
PAR	Photosynthetic active radiation
PCoA	Principal coordinate analysis
PCR	Polymerase chain reaction
PCW	Plant cell wall
PCWDE	Plant cell wall degrading enzyme
perMANOVA	Permutational multivariate analysis of the variance
PGPR	Plant growth promoting rhizobacteria
PIP	Plasma membrane intrinsic protein
PKS	Polyketide synthase
PL	Polysaccharide lyase
PMF	Protein mass fingerprinting
PPFD	Photosynthetic photon flux density
PRINGO	Proteomic information navegation genome outlook
PSII	Photosystem II
rbcL	Large subunit-size Rubisco

rbcS	Small subunit-size Rubisco
RH	Relative humidity
RMSE	Root mean square error
RNA	Ribonucleic acid
ROS	Reactive oxygen species
rRNA	Ribosomal ribonucleic acid
RT-qPCR	Reverse transcription quantitative polymerase chain reaction
Rubisco	Ribulose-1,5-bisphosphate carboxylase/oxygenase
RuBP	Ribulose-1,5-bisphosphate
SAM	S-adenosylmethionine
SDS-PAGE	Sodium dodecyl sulfate–polyacrylamide gel electrophoresis
SIP	Small basic intrinsic protein
SMA	Simple moving average
SMS	Simple moving sum
SOD	Superoxide dismutase
SSC	Small subunit-size catalase
SSP	Small secreted protein
TE	Trasposable element
TFA	Trifluoroacetic acid
TINGO	Trasposon identification nominative genome overview
TIP	Tonoplast intrinsic protein
TPU	Triose phosphate use
TS	Terpene synthase
TX-114	Triton X-114
VOC	Volatile organic compound
VPD	Vapor pressure deficit
WWMP	Well-watered mycorrhizal plant
WWNMP	Well-watered non-mycorrhizal plant
XIP	X intrinsic protein

Resumen en castellano

El término **micorriza** (del griego *mykos*, hongo y *rhizon*, raíz) hace referencia a la asociación simbiótica entre las hifas de un hongo y las raíces de la mayoría de las plantas terrestres, entendiendo simbiosis como la asociación beneficiosa para ambas partes de organismos distintos. Las micorrizas juegan un papel vital para el crecimiento vegetal y los ciclos de nutrientes esenciales como el nitrógeno, fósforo y carbono en los ecosistemas. Entre los beneficios obtenidos por parte de la planta encontramos un aumento de la superficie activa de la raíz y, por tanto, una mejor entrada de nutrientes y agua a la planta, mejora de la resistencia a estreses bióticos y abióticos, o la formación de conexiones entre plantas que comparten el mismo hábitat permitiendo el transporte de nutrientes y la señalización. Los hongos, por su parte y salvo ciertas excepciones, son completamente dependientes de los fotoasimilados producidos por la planta para la obtención de carbono.

Se han descrito siete tipos de micorrizas: arbusculares, ectomicorrízas, ericoides, orquidiales, ectendomicorrizas, arbutoides y monotropoides. De entre éstos tipos, las **ectendomicorrízas (EEM)** son un grupo relativamente poco abundante pero que tiene un especial interés para el desarrollo de la presente tesis, puesto que la mayoría de las **trufas del desierto** en general, y *Terfezia claveryi* **Chatin** en particular, pertenecen a este grupo. Estructuralmente las EEM se distinguen porque forman estructuras típicas de las ectomicorrízas, como el manto (hifas apiladas que rodean a la raíz) o la red de Hartig (una red de hifas intercelulares) y, al mismo tiempo, hifas intracelulares en forma de *coils* o espirales. Además, en la raíz, estas estructuras pueden presentarse en solitario o al mismo tiempo, dependiendo, en muchos casos, del huésped y de las condiciones ambientales y/o experimentales. Por ejemplo, la micorriza de *T. claveryi* con *Helianthemum almeriense* Pau está influenciada por la condiciones de crecimiento: *in vitro* forma manto y red de Hartig, en maceta forma manto laxo o nulo, red de Hartig e hifas intracelulares y en condiciones de campo mayoritariamente hifas intracelulares con algo de red de Hartig. Además, se sabe que la abundancia de agua favorece la colonización intercelular, mientras que condiciones de estrés hídrico favorecen la colonización intracelular.

El conocimiento sobre las micorrizas en general sigue siendo escaso en comparación con lo que se sabe de hongos con otros estilos de vida, como los patógenos

o los saprófitos. Gracias a la reciente expansión de técnicas de secuenciación de genomas, transcriptomas y de análisis bioinformático, cada vez se conoce más acerca de la naturaleza de los hongos micorrícicos y sus características a nivel de genes y de la expresión de los mismos. La mayoría de genomas secuenciados pertenecen a los grupos mayoritarios de micorrizas arbusculares y ectomicorrízas, pero al inicio de esta tesis, sólo había sido secuenciado un genoma de ectendomicorríza, *Terfezia boudieri* Chatin. La **secuenciación de genomas micorrícicos** ha permitido inferir varias características comunes para todos o la mayoría de ellos y que se han denominado como la "**caja de herramientas micorrícica**": genomas grandes y con gran cantidad de elementos trasponibles, abundancia de las llamadas "proteínas pequeñas de secreción" (con menos de 300 aminoácidos) que son específicas a nivel de género o de especie, y que además están sobreexpresadas en simbiosis, y finalmente, la presencia de una reducida cantidad de proteínas implicadas en la remodelación de la pared celular vegetal y de metabolitos secundarios. Todas estas adaptaciones tienen como propósito evitar el sistema defensivo de la planta hospedante, algo que no siempre se consigue ya que una respuesta común de las plantas hospedantes a la micorrización es la producción de radicales libres. Este efecto provoca la inducción, por parte del sistema micorrício, de enzimas que se encargan de eliminar radicales libres, como la superoxido dismutasa o la **catalasa**.

Las trufas del desierto son hongos ascomicetos micorrícicos cuyo cuerpo fructífero, o ascocarpo, crece bajo el suelo, y cuyo hábitat se limita a zonas áridas o semiáridas, como la cuenca del Mediterráneo, norte de África, Oriente Medio, o los desiertos de Australia y América del Norte. Entre las trufas del desierto, los géneros más conocidos y apreciados son *Terfezia* y *Tirmania*. Especies pertenecientes a estos géneros forman ectendomicorrizas con plantas de la familia de las cistáceas, mayoritariamente con el género *Helianthemum*. El conocimiento que se tiene en la actualidad sobre las trufas del desierto es escaso en comparación con los numerosos estudios publicados sobre otras trufas comestibles como la trufa negra, la trufa de verano o la trufa blanca. Se desconoce exactamente su ciclo vital y su modo de reproducción, al igual que los mecanismos de reconocimiento y formación de la micorriza. Son apreciadas especialmente en los países de norte de África y en el Oriente Medio por sus cualidades gastronómicas y nutricionales, éstas últimas debidas en parte a su alto contenido en proteínas y fibra así como a su elevada actividad antioxidante. Esta tesis está centrada en el estudio de *T. claveryi*, especie que se encuentra mayoritariamente en el sudeste español,

más concretamente en la Región de Murcia, donde también se la conoce más popularmente como "turma" y que se puede encontrar localizando las grietas características que hace en el suelo, cerca de varias especies del género *Helianthemum*, como *H. almeriense*, *H. violaceum* o *H. hirtum*, entre otras, con las que establece simbiosis.

Actualmente sólo unas pocas especies de hongos micorrícicos comestibles son cultivables, como, la trufa negra (*Tuber melanosporum*), *Tuber borchii*, *Rhizopogon*, o el matsukate. Entre éstos, sólo dos trufas del desierto han sido cultivadas, *T. boudieri* en Túnez e Israel y *T. claveryi* en España. La primera plantación de *T. claveryi* se estableció en Zarzadilla de Totana, Murcia, España, en 1999 y desde entonces han ido surgiendo más plantaciones, sobre todo en el sudeste peninsular. Las plantaciones de *T. claveryi* comienzan a producir turmas entre la segunda y la tercera primavera tras la plantación; sus requerimientos son bastante escasos, limitándose a suelos pobres en materia orgánica, con pHs alcalinos. Las fructificaciones tienen lugar en primavera y pueden comenzar ya en diciembre y la temporada puede llegar a alargarse hasta junio, aunque la temporada suele ir desde febrero/marzo hasta abril/mayo. La producción media acumulada se encuentra en torno a 350 kg por hectárea a partir del séptimo u octavo año. Sin embargo, uno de los problemas más graves del manejo de estas plantaciones es la gran variación interanual de la producción, encontrándose años en los que las producciones estimadas alcanzan los 1000 kg por hectárea mientras que en otros la producción es nula o testimonial, dependiendo de las lluvias acaecidas. De las diversas plantas que actúan como huésped de *T. claveryi*, *H. almeriense* fue la primera usada para sintetizar la micorriza *in vitro* y la más utilizada para su cultivo. Se trata de un arbusto que presenta una fenología típica de plantas caducifolias y semicaducifolias de verano: el desarrollo vegetativo comienza tras las primeras lluvias de otoño y continúa hasta la primavera, cuando se produce la floración y la fructificación de las turmas; el máximo de fotosíntesis se da en invierno y la colonización micorrícica es mayoritariamente intracelular durante todo el año, aunque en verano apenas es perceptible.

Entre las **zonas áridas y semiáridas** habitadas por las trufas del desierto destaca la **cuenca Mediterránea**. Los territorios con climas mediterráneos suponen entre el 1 y el 4 % de la superficie terrestre, y la **sequía**, provocada principalmente por la **escasez de precipitaciones** y un **alto déficit de presión de vapor**, es el principal factor limitante para el desarrollo vegetal y la producción de los cultivos mediterráneos. La

transición entre la primavera y el invierno es la etapa del año en donde se produce un característico incremento de sequía en los climas mediterráneos. La sequía suele afectar a diversos parámetros vegetales tales como la fotosíntesis, la conductancia estomática, la conductancia del mesófilo, la morfología foliar (representada por el peso específico foliar), el potencial hídrico de tallo o de hoja, y la expresión de muchos genes, entre los que destacan las acuaporinas o la Rubisco. Además, las plantas también responden al estrés hídrico mediante la producción de especies reactivas al oxígeno como el anión superóxido, hidróxido o el peróxido de hidrógeno. En este contexto, las catalasas vuelven a jugar un papel importante debido a su implicación en la dismutación del peróxido de hidrógeno en agua y oxígeno. Las micorrizas en general son conocidas por mejorar la respuesta al estrés hídrico de las plantas que colonizan, bien mejorando la conductancia hidráulica de las raíces, mejorando los parámetros de intercambio gaseoso o minimizando los daños oxidativos producidos como consecuencia del propio estrés hídrico. *T. claveryi*, en particular, mejora la respuesta de *H. almeriense* frente al estrés hídrico mediante mejoras fisiológicas y nutricionales, al mismo tiempo que modifica la expresión de acuaporinas de la planta y también la suya propia (TcAQP1).

El estrés hídrico afecta, no sólo a los parámetros fisiológicos y moleculares de las plantas, sino también a la productividad de los cultivos. Diversas encuestas a recolectores y algunos estudios apuntan a que tanto las lluvias otoñales, como el tipo de suelo y las temperaturas primaverales son factores que afectan a la productividad de este cultivo. Además, está por ver cómo el cambio climático y su consiguiente aumento en la concentración de CO_2 atmosférico, aumento de temperaturas y mayor riesgo de desertificación, afectarán al cultivo de *T. claveryi*.

Con todo lo expuesto anteriormente, el **objetivo principal** de esta tesis doctoral consiste en aumentar el conocimiento básico y aplicado de la simbiosis micorrícica entre la trufa del desierto *Terfezia claveryi* y *Helianthemum almeriense* y de los métodos para su explotación agrícola. Para ello se proponen los siguientes **objetivos específicos**:

1. Evaluar el papel de las catalasas fúngicas en la simbiosis *T. claveryi* x *H. almeriense*, centrándonos en la formación de la micorriza y en la respuesta al estrés hídrico.

2. Describir las características genómicas de las trufas del desierto, centrándonos en su modo reproductivo, el desarrollo de las distintas estructuras micorrícicas que estos hongos forman con las raíces de sus plantas simbiontes y la adaptación a los climas áridos.

3. Determinar qué parámetros agroclimáticos pueden estar positiva o negativamente relacionados con la producción de la trufa del desierto *T. claveryi,* y conocer los periodos de tiempo críticos durante los cuales esos parámetros son más importantes.

4. Caracterizar las respuestas de la planta turmera *H. almeriense* a los cambios ambientales que se producen en primavera para buscar marcadores morfo-fisio-moleculares que puedan ayudar a rastrear los cambios fenológicos de la planta, y relacionar estos marcadores con la producción de trufa del desierto.

5. Evaluar los efectos del aumento de CO_2 atmosférico sobre las respuestas fisiológicas de la simbiosis micorrícica de *H. almeriense* x *T. claveryi*, y su interacción con los incrementos de temperatura y sequía que se producen durante la primavera mediterránea, periodo de fructificación de la turma.

Para poder responder a los objetivos propuestos, se llevaron a cabo distintos ensayos, cuya metodología, resultados, discusión y conclusiones están resumidos en los siguientes apartados.

1. Caracterización y purificación de TcCAT-1, una catalasa de Terfezia claveryi que se encuentra sobre-expresada durante la simbiosis micorrícica.

Las catalasas son enzimas importantes para el normal funcionamiento de los organismos. Son las principales responsables de la dismutación del peróxido de hidrógeno en agua y oxígeno y, en hongos, pueden tener tanto funciones constitutivas como de respuesta a estreses bióticos y abióticos e incluso de señalización, debido a que el peróxido de hidrógeno, a bajas concentraciones, puede actuar cómo molécula de señalización. Es por esto por lo que se purificó a homogeneidad y se caracterizó una catalasa, denominada TcCAT-1, a partir de ascocarpos de *T. claveryi*.

De forma muy breve, para la extracción de esta enzima en primer lugar se trituraron trozos de ascocarpo de *T. claveryi* congelados con nitrógeno líquido; el polvo resultante se resuspendió en tampón fosfato 0,1 M pH 7 y este extracto crudo fue sometido a partición de fases con el detergente no iónico Triton X-114. El sobrenadante obtenido tras la partición de fases se separó mediante ultrafiltración con membranas Amicon Ultra de 100.000 kDa de tamaño de poro; la muestra retenida tras la ultrafiltración se purificó mediante dos etapas cromatográficas: con una columna de interacción hidrofóbica (HiTrap® Phenyl HP 1 mL); las fracciones con actividad catalasa eluídas de esta columna se cargaron en una columna de exclusión molecular (Superdex® 200 10/300 GL). Tras estas etapas se consiguió una purificación de 33,7 veces y una recuperación de actividad del 19,3%. La proteína purificada se sometió a electroforesis en gel de poliacrilamida para determinar su peso molecular; posteriormente, mediante la técnica de "huella peptídica", se confirmó que era una catalasa y se identificó su secuencia de aminoácidos; esta secuencia permitió analizarla filogenética y bioinformáticamente. La caracterización de la proteína junto con su análisis filogenético y el modelado por homología de su estructura tridimensional indicaron que TcCAT-1 era un homotetrámero perteneciente al grupo de catalasas de alto tamaño de subunidad, más concretamente al clado 2. La actividad de TcCAT-1 se determinó espectrofotométricamente siguiendo la caída de absorbancia a 240 nm; esta caída se corresponde con el consumo del sustrato de la reacción, el H_2O_2. Tras determinar los valores óptimos de pH y temperatura, se estudió el efecto de la concentración de sustrato, un ensayo necesario para determinar la constante de Michaelis o K_m; también analizamos el efecto de distintos inhibidores. Se determinó que, al igual que se ha descrito para otras catalasas, esta proteína posee un amplio rango de actividad a distintos pHs y temperaturas.

Por último, mediante PCR cuantitativa, se analizó la expresión diferencial del gen que codifica la proteína TcCAT-1 en micelio libre, ascocarpo y micorrizas, tanto bien regadas como sometidas a estrés hídrico. Se observó un aumento en la expresión del gen *TcCAT-1* en tejido micorrícico en comparación con el micelio libre y el ascocarpo. En condiciones de estrés hídrico, la colonización micorrícica de *T. claveryi* aumentó y *TcCAT-1* no se encontró sobreexpresado, aunque los niveles de peróxido bajaron significativamente en las raíces micorrizadas de *H. almeriense* x *T. claveryi* sometidas a estrés hídrico. Por tanto, esta bajada no puede ser atribuida a un aumento de los niveles de expresión de *TcCAT-1* y probablemente sea el resultado bien de un aumento en la

actividad de ésta u otras enzimas o de la presencia de compuestos antioxidantes de naturaleza no enzimática.

Todos estos resultados sugieren que TcCAT-1 posee las características típicas de una catalasa de subunidad grande, y que el aumento de su expresión en raíces micorrizadas puede jugar un papel en el proceso de micorrización de ésta especie. Además, se han comprobado los efectos beneficiosos de la micorriza a nivel de modulación del estrés oxidativo, aunque no se ha podido correlacionar la bajada de niveles de peróxido de hidrógeno con un aumento en el nivel de transcritos de *TcCAT-1*.

2. El genoma de las trufas del desierto revela adaptaciones relacionadas con la supervivencia de las micorrizas en regiones áridas.

Las trufas del desierto crecen en regiones áridas y semiáridas y, ya que está previsto que la superficie de estas regiones aumente en los próximos años debido a los efectos del cambio climático, el cultivo de estas especies es de gran interés. Para profundizar en el estudio de estos hongos, en colaboración con el Joint Genome Institute de California (USA) y dentro del proyecto "1000 Fungal Genomes", se secuenciaron y analizaron los genomas de dos de las especies de trufas del desierto más apreciadas: *Terfezia clavery* Chatin y *Tirmania nivea* Trappe; además, se estudió el transcriptoma de *T. claveryi* con el objetivo de analizar las singularidades de éstas especies con respecto a otras especies micorrícicas comestibles que no están adaptadas a regiones secas como la trufa negra (*Tuber melanosporum)* o la trufa blanca (*Tuber magnatum)*. La secuenciación de estos genomas ha permitido revelar singularidades de las ectendomicorrízas que hasta ahora no habían sido descritas.

T. claveryi T7 y *T. nívea* G3 se cultivaron en matraces con medio líquido MMNo y su micelio se cosechó para realizar extracciones de ADN y ARN. Una vez extraído el ADN y el ARN, fueron secuenciados y ensamblados por el Joint Genome Institute. Una vez secuenciados, estos genomas fueron analizados empleando distintas herramientas bioinformáticas. Para el ensayo transcriptómico se extrajo RNA de la simbiosis micorrícia de *H. almeriense* x *T. claveryi* en distintas condiciones: micelio de vida libre (sólo RNA de *T. claveryi*), planta sin micorrizar (sólo RNA de *H. almeriense*), micorriza bien regada y micorriza sometida a estrés hídrico (RNA de raíces, mezcla de *T.

claveryi y *H. almeriense*). Tras realizar la transcripción reversa de este RNA mediante la enzima retrotranscriptasa se secuenció el cDNA resultante y se llevó a cabo el análisis bioinformático del transcriptoma. Además, gracias al RNA extraído de raíces micorrícicas se pudo ensamblar *de novo* un transcriptoma parcial de *H. almeriense* y estudiar la expresión de estos genes en las distintas condiciones previamente descritas.

La secuenciación del genoma de *T. claveryi* y *T. nivea* ha permitido revelar distintas características de estos hongos. Al igual que otros hongos micorrícicos, estas trufas del desierto poseen genomas grandes, relacionados con una gran cantidad de elementos trasponibles, así como un reducido conjunto de enzimas degradadoras de la pared celular vegetal y una gran cantidad de pequeñas proteínas secretadas que, en el caso de *T. claveryi,* están mayoritariamente sobreexpresadas en el tejido micorrícico. En comparación con otros hongos micorrícicos, se han observado ganancias en el número de genes relacionados con el procesamiento del RNA ribosómico y pérdidas en genes relacionados con el transporte transmembrana. Ambos eventos podrían estar relacionados con mecanismos de adaptación a climas áridos. Además, por primera vez, hemos descrito el modo de reproducción de las trufas del desierto, ya que se han identificado genes relacionados con la reproducción sexual (genes *MAT*), no sólo en *T. claveryi* y *T. nívea*, sino también en *Terfezia boudieri* y *Kalahariituber pfeilii*. Tres de las cuatros trufas del desierto analizadas (*T. claveryi*, *T. boudieri* y *T. nívea*) son heterotálicas, lo que quiere decir que sólo poseen uno de los dos haplotipos de genes *MAT* (*MAT 1-1-1* y *MAT 1-2-1*) y por lo tanto, son autoestériles y necesitan de cruzamiento para su correcta reproducción sexual. En el caso de *K. pfeilii* se encontraron ambos haplotipos en el mismo genoma, lo que indica que esta especie es homotálica y que, por tanto, es capaz de autocruzarse.

En cuanto a los genes implicados en la degradación de la pared celular vegetal, resulta curioso que las especies de trufa del desierto poseen un menor número de enzimas degradadoras de pectina que, por ejemplo, otras especies del género *Tuber*. Además, estas enzimas y, en general, todas las enzimas que degradan la pared celular vegetal se encuentran reguladas a la baja durante estrés hídrico, al mismo tiempo que el tipo de micorriza formada entre *T. claveryi* y *H. almeriense* cambia, en rasgos generales, de intercelular a intracelular. Estas características genómicas y transcriptomicas parecen estar asociadas al estilo de vida ectendomicorrícico, que a su vez, parece una adaptación a la vida en regiones áridas y semiáridas

En conclusión, se han descrito una serie de características genómicas y transcriptómicas relacionadas con el modo de reproducción de las trufas del desierto, así como con el estilo de vida ectendomicorrício y con sus adaptaciones a climas secos. Estos datos servirán para abordar nuevas estrategias de cultivo de trufas del desierto y para aumentar nuestro conocimiento sobre las adaptaciones a climas áridos y las respuestas al estrés hídrico.

3. El cultivo de las trufas del desierto depende de parámetros agroclimáticos durante dos periodos anuales clave.

Tal y como se ha mencionado anteriormente, la gran variabilidad interanual en la cosecha de trufas del desierto es uno de los principales problemas de este cultivo. Según diversas encuestas realizadas a recolectores de trufas del desierto, las precipitaciones o el tipo de suelo son los factores que más afectan a las fructificaciones. Para dilucidar esta cuestión, realizamos un estudio estadístico en una parcela experimental de cultivo de la especie *T. claveryi* usando como planta simbionte *H. almeriense*. Los datos ambientales de esta parcela experimental, situada en Zarzadilla de Totana (Murcia), se obtuvieron tanto de una de las estaciónes meteorológicas del Instituto Murciano de Investigación y Desarrollo Agrario (IMIDA), como de la estación meteorológica instalada en la propia plantación. Estos datos ambientales se compararon con los datos de producción de trufas del desierto obtenidos durante 15 años. Para llevar a cabo estos análisis se realizaron correlaciones de Pearson y árboles de clasificación y regresión.

La producción media de trufas del desierto de esta plantación fue de 355 kg por hectárea, aunque con una desviación estándar de ± 318 kg por hectáreaa. Prácticamente todos los parámetros estudiados (índice de aridez, evapotranspiración (ET0), temperatura media, humedad relativa media, precipitaciones, déficit de presión de vapor (DPV), potencial hídrico de suelo y potencial hídrico de suelo anómalo) mostraron correlaciones con la producción de trufa del desierto durante algún periodo del año. La mayoría de las correlaciónes, sin embargo, se acumulan principalmente en otoño y en menor medida en primavera. De entre los parámetros ambientales estudiados, el potencial hídrico de suelo y el índice de aridez parecen ser los más determinantes. También construimos árboles de clasificación y regresión de 4 parámetros: ET0, precipitaciones, índice de aridez y el potencial hídrico de suelo, lo que nos permite estimar la producción de trufas de desierto

mediante valores umbrales para el otoño y la primavera de cada uno de los parámetros. A raíz de estos resultados, proponemos 4 estrategias de manejo de plantaciones de trufa del desierto basadas en el índice de aridez, en el potencial hídrico de suelo, en una combinación de ambos o en el potencial hídrico del suelo anómalo.

En conclusión, se han identificado dos períodos anuales clave para la producción de las trufas del desierto, otoño y primavera, y se han estudiado los parámetros ambientales que más la determinan: índice de aridez y potencial hídrico de suelo. Esto ha permitido diseñar diversas propuestas de manejo del riego que servirán para mejorar, no sólo la producción total de trufas del desierto, sino también para estabilizar la gran variabilidad interanual existente en este cultivo.

4. La respuesta estomática al déficit de presión de vapor como un marcador para el cultivo de la trufa del desierto.

En la misma línea que la sección anterior, en este capítulo se aborda la mejora de la producción de la trufa del desierto. Tal y como se ha mencionado, el déficit de presión de vapor (DPV) y el potencial hídrico de suelo son dos de los parámetros que más determinan el rendimiento de un cultivo de trufa del desierto. Además, bajo nuestra propia experiencia y la de múltiples recolectores, algunos eventos fenológicos de la planta como la floración o la senescencia foliar están relacionados con el inicio y el fin de la temporada de fructificación y, por tanto, pueden afectar a la producción total. El objetivo de este capítulo fue la caracterización en campo de diversas variables morfo-fisio-moleculares de la planta *H. almeriense* micorrizada con *T. claveryi* para intentar correlacionarlas con la producción de ascocarpos.

Durante la primavera de 2016 (desde abril hasta junio) se monitorizó una plantación experimental de *H. almeriense* x *T. claveryi* localizada en el Campus de Espinardo (Murcia). Durante ese periodo y con una frecuencia de dos o tres veces por semana, se estimaron parámetros de intercambio gaseoso (asimilación neta de CO_2, conductancia estomática, transpiración, concentración de carbono intercelular, eficiencia intrínseca del uso de agua) empleando una cámara de intercambio gaseoso Li-6400xt (Li-COR Inc., Lincoln, NE, EEUU). También se midió el potencial hídrico de tallo con una cámara de Scholander y se recolectaron hojas para medir su área, el peso seco y el peso

específico foliar (peso seco/área) y para realizar la extracción de ARN. Una vez extraído el ARN, fue retrotranscrito a cDNA con una retrotranscriptasa. Se usaron cebadores específicos para cinco acuaporinas de *H. almeriense* (*HaPIP1.1*, *HaPIP1.2*, *HaPIP2.1*, *HaPIP2.2* y *HaTIP1.1*) y para la subunidad grande de Rubisco (*HarbcL*) y se realizó una PCR cuantitativa a tiempo real para cuantificar la expresión de estos genes a lo largo de la primavera de 2016. Además, se recogieron datos climáticos de la plantación con una estación automática y se correlacionaron con todos los parámetros morfo-fisio-moleculares de la planta.

Prácticamente todos los parámetros estudiados correlacionaron con algún parámetro ambiental, lo que puso de manifiesto la gran influencia del ambiente en el comportamiento de las plantas. De entre estas relaciones, las más estadísticamente significativas fueron las establecidas entre la conductancia estomática y el DPV, por un lado, y entre los potenciales hídricos de tallo y suelo, por otro. Utilizando la relación entre el DPV y la conductancia estomática se estableció un umbral de DPV que explicaba en mayor medida los cambios significativos y bruscos entre la primavera temprana (hasta el 8 de mayo) y la primavera tardía (desde el 9 de mayo). En cuanto a la expresión de Rubisco, parece estar fuertemente correlacionada con la conductancia estomática, mientras que las acuaporinas mostraron una regulación fina sólo durante la primavera tardía, es decir, la planta sólo regula la expresión de estas acuaporinas cuando las condiciones de estrés hídrico son más severas, para maximizar la adquisición de agua a la vez que se minimiza la pérdida de la misma.

Una vez caracterizadas estas variables durante la primavera de 2016, se seleccionó aquella que mejor explicaba el cambio brusco que se produjo en la fenología de las plantas micorrizadas de *H. almeriense*, la conductancia estomática, y, gracias a su relación con el DPV, se seleccionó un valor umbral de DPV medio (0,93 kPa) en el que las plantas experimentan este brusco cambio. Comparando el día del año en el que se alcanzó este umbral con las fructificaciones de ascocarpos de *T. claveryi* en otra plantación situada en Zarzadilla de Totana (Murcia) durante los últimos 18 años, se comprobó que la producción está correlacionada con este parámetro y que, por lo tanto, los años en los que se alcanza tarde este valor umbral de DPV son años más productivos.

Por último, durante las primaveras de 2017 y 2018, se realizó un ensayo preliminar en una tercera parcela experimental de *H. almeriense* x *T. claveryi,* situada en Corvera (Murcia), en la cual se instalaron unos sombrajes sobre ciertos grupos de plantas

con el propósito de retrasar la subida de DPV y así mejorar tanto las variables fotosintéticas de las plantas como, en última instancia, la producción de trufas del desierto. Además, estos sombrajes se combinaron con irrigación. No se observaron cambios ni en las variables fotosintéticas ni en la producción de ascocarpos para el tratamiento combinado de sombraje e irrigación, debido probablemente a que los efectos positivos del riego y de la leve bajada de DPV se vieron contrarrestados por la disminución de luz debida al sombraje.

En conclusión, gracias a la profunda caracterización de varios parámetros fisiológicos de la planta micorrizada *H. almeriense* durante la primavera, hemos sido capaces de encontrar un marcador del estado fenológico de la planta que se correlaciona con la producción de trufas del desierto. Esto puede ser utilizado como herramienta de selección de las mejores áreas para este cultivo, como diagnóstico de plantaciones o incluso, se puede intentar modificar la DPV, como se ha realizado en el ensayo preliminar descrito en este capítulo, para mejorar la producción de trufas del desierto.

5. Alto CO_2 atmosférico modifica la floración y la respuesta al estrés hídrico de las plantas de trufas del desierto.

Se estima que para finales del siglo XXI las concentraciones atmosféricas de CO_2 estén entre los 700 y 800 ppm, a la vez que las temperaturas aumentarán entre 2 y 4 ºC de media y las precipitaciones serán más escasas y con patrones más irregulares, dando lugar a una expansión de las zonas desérticas o semi-desérticas. Aunque el cultivo de la trufa del desierto está bien adaptado a las condiciones de sequía y, en general, a los climas áridos y semiáridos, se desconoce cómo afectará el aumento de CO_2 a la fisiología de su planta huésped así como a la relación planta-hongo.

Para dilucidar esto, se realizó un ensayo en el que se pusieron 72 plantas de *H. almeriense* micorrizadas con *T. claveryi* repartidas en 2 cámaras de cultivo. En ambas cámaras se fueron cambiando de igual manera las condiciones de temperatura, humedad y fotoperiodo para imitar 4 escenarios propios de la transición entre invierno y verano del clima mediterráneo (invierno, primavera temprana, primavera tardía y verano). La única diferencia entre las dos cámaras es que, durante todo el ensayo, en una de ellas se enriqueció la atmósfera de CO_2 en torno a los 800 ppm y en otra se mantuvo en torno a

400 ppm. Para cada escenario, en ambas cámaras se midieron parámetros de intercambio gaseoso empleando una cámara de intercambio gaseoso Li-6400xt (Li-COR Inc., Lincoln, NE, EEUU) y potencial hídrico de tallo con la cámara de Scholander. También se midió biomasa de la parte aérea, el contenido en clorofila de las hojas, el área de la hoja, los pesos seco y específico foliar. Además, se estudió la intensidad de micorrización en raíces y el contenido en almidón y azúcares libres de las mismas. Para estudiar en más profundidad las variables de intercambio gaseoso, se realizaron curvas de respuesta al CO_2, gracias a las cuales se pudieron estimar parámetros como la conductancia del mesófilo, la velocidad de carboxilación máxima de la Rubisco o la tasa máxima de flujo de la cadena de transporte de electrones.

En conjunto, las plantas se comportaron de manera diferente según las estaciones y la concentración de CO_2 atmosférico y parámetros como la fotosíntesis, la conductancia estomática o el potencial hídrico de tallo fueron disminuyendo para ambos tratamientos de CO_2 a lo largo de las estaciones simuladas. Sin embargo, tanto la fotosíntesis como la eficiencia en el uso del agua fueron mayores en las plantas con alta concentración de CO_2, lo que les permitió soportar mejor el estrés hídrico como indica una mayor biomasa vegetal durante el verano. Además, la floración se vio alterada, ya que entre la primavera tardía y el verano aparecieron un número significativamente mayor de botones florales y flores en el tratamiento de alto CO_2. Por último, la micorrización fue aumentando con el paso de las estaciones, en ambos tratamientos por igual, y ni la concentración de almidón ni la de azúcares libres en raíz se vio alterada en ningún momento y/o tratamiento.

De estos resultados se puede concluir que el aumento de la concentración de CO_2 afecta, en general, positivamente a los parámetros fisiológicos de *H. almeriense* en respuesta al estrés hídrico progresivo que se da entre invierno y verano en el clima mediterráneo, sin perjudicar la relación simbiótica con *T. claveryi*. Los cambios en floración y, en general, la exacerbación de las diferencias entre primavera temprana y primavera tardía han de ser estudiados más profundamente, puesto que estos cambios están relacionados con las fructificaciones de la trufa del desierto *T. claveryi*.

CHAPTER I

General Introduction

1.1. Mycorrhizal fungi

Mycorrhizas (from Greek *mykos*, fungi, and *rhizon*, root) were first described by the German botanist Frank (1885) and can be defined as the **symbiotic association** between the hyphae of some **fungi** and the **roots** of some higher plants, understanding symbiosis as the mutually **beneficial associations** between different organisms (de Bary, 1887). Mycorrhizas are abundant, between 85% and 92% of angiosperms are estimated to form some type of mycorrhizal symbiosis, while most of non-mycorrhizal plant species are nutritional specialist such as carnivores or parasites, or habitat specialists as hydrophytes and epiphytes. They are also present in almost all ecosystems, such as desert, arable lands or tropical forest (Brundrett 2009; Brundrett and Tedersoo 2018).

Mycorrhizas play a central role in plant growth, diversity and in C, N and P cycles in ecosystems (van der Heijden et al., 2015). Mycorrhizal symbiosis is known to be advantageous for both organisms involved. On the plant side:

1. It has been confirmed that mycorrhizas, not roots, are the main responsible for nutrient uptake by land plants. This is mainly because mycorrhizal fungi confer a larger physiologically active area for the roots, and possess more efficient systems to mobilize and acquire nitrates and phosphates from the soil than plant roots (Marchsner and Bell, 1994; Smith and Read, 2008).

2. Mycorrhizas increase plant tolerance to several biotic (pathogens, nematodes) and abiotic stresses (water deficit, heavy metals, among others) (Pozo and Azcón-Aguilar, 2007; Nadeem et al., 2014).

3. Mycorrhizal fungi also connect plants below ground *via* an hyphal network, informally named "wood wide web", allowing the movement of resources and signalization among coexisting plants in a shared habitat (Helgason et al., 1998).

On the fungus side, with a few exceptions, mycorrhizal fungi are completely dependent on the plant for organic carbon (Smith and Read, 2008).

For all the benefits provided to the plant, these organisms have been widely studied and worldwide used for improvement of agricultural production (Nadeem et al., 2014). However, the agricultural use of these fungi is not only limited to the improvement of plant crops: during their life cycle, some mycorrhizal fungi, especially ectomycorrhizal

fungi, form edible fruiting bodies which are highly appreciated for human consumption, such as mushrooms and truffles (Murat et al., 2008). In the last years, some of these edible fungi, such as saffron milk caps, matsutake, boletus, black truffles or desert truffles have been successfully domesticated in order to have controlled production (Hall et al., 2003) and, thus, mycorrhizal fungi have become a new target for agro-economic exploitation. For more information about this issue, see **Section 1.4**.

1.1.1. Types of mychorrizal associations

There are seven types of mycorrhizas described: **arbuscular mycorrhiza** (**AM**), **ectomycorrhiza** (**ECM**), ericoid mycorrhiza (ERM), orchid mycorrhiza (ORM), **ectendomycorrhiza** (**EEM**), arbutroid mycorrhiza and monotropoid mycorrhiza. The two major mycorrhizal types in terms of abundance and quantity of research performed are AM and ECM (Smith and Read, 2008).

AM is the most abundant type of mycorrhizal symbiosis, as recent estimations suggest that 71% of all land plants form AM symbiosis, with 315 described fungal species belonging to *Glomeromycota* division (Brundrett and Tedersoo, 2018), AM association emerged over 407 million of years ago (Mya) and is considered ancestral in land plant evolution (Spatafora et al., 2016; Strullu-Derrien et al., 2018). AM can be recognized by two characteristic structures formed in the roots by the mycorrhizal fungi: **arbuscules** and **vesicles** (**Figure 1.1A; 1.1B; 1.1C**). Arbuscules are dichotomously branched, terminal hyphae that develop within cortical root cells but remain apoplastic, since plant plasma membrane invaginates around the arbuscules forming the **periarbuscular membrane** which is considered the exchange structure of nutrients between fungus and plant. Vesicles contain lipids and are assumed to have storage function. Outside the root, there is **extraradical mycelium** that can be very extensive but does not form any complex structure comparable to the mantle formed by ECM (Harrison, 1997). AM fungi are obligate symbionts, so they cannot be cultivated *in vitro* without the presence of the host plant (Read and Smith, 2008), and play a key role in agriculture, as they enhance plant growth and production of most arable crops under different conditions, including various soil stresses (Miransari, 2010; Nadeem et al., 2014).
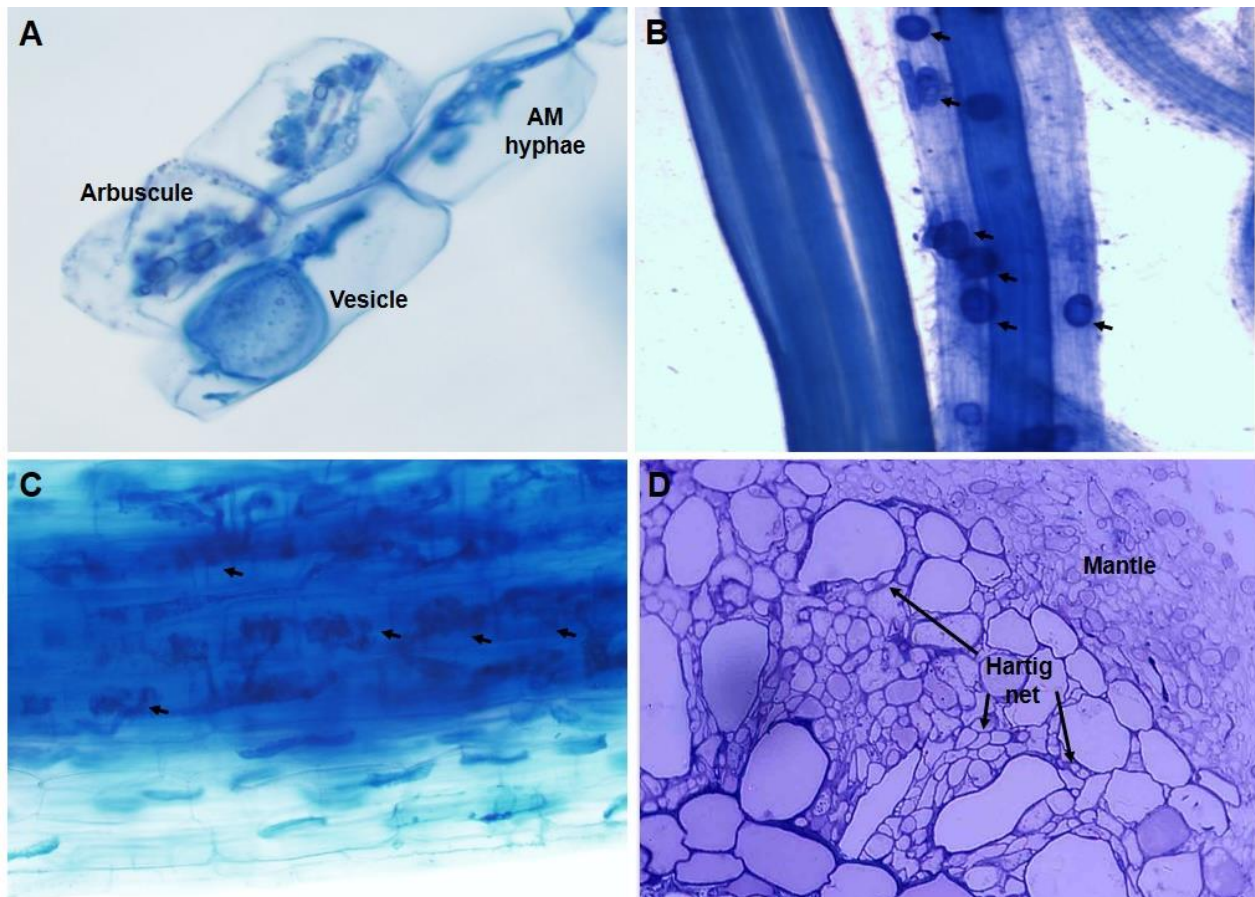
Figure 1.1. Typical morphological structures of AM and ECM under optical microscope.
(A) Cortical root cells with hyphae, an arbuscule and a vesicle **(B)** Longitudinal root section with vesicles (arrows). **(C)** Longitudinal root section with arbuscules (arrows). **(D)** Semi-thin cross section of an *in vitro* ECM structure between *Terfezia claveryi* and *Helianthemum almeriense*, where mantle and Hartig net can be visualized, picture extracted from (Gutiérrez et al., 2003).

ECM are formed between approximately 6,000 different tree species and more than 20,000 different fungal species belonging to *Basidiomycota* and *Ascomycota* divisions. The oldest ECM fossils were found in *Pinus* roots, 48.7 Mya and presented a convergent evolution: 78 to 82 independent times (Tedersoo and Smith, 2017) from white-, brown-rot fungi and soil saprophytes to the actual ECM (Kohler et al., 2015). The vast majority of ECM share three typical structures: an intercellular hyphal network called **Hartig net**, where the nutrient exchange takes place, a sheathing **mantle** around the roots, with an intense nutrient transport activity and **extraradical mycelium** that explores and acquires nutrients from the surrounding rhizosphere (**Figure 1.1D**). Although ECM fungi are symbionts, depending on the host to obtain C, most of them can be grown alone *in vitro* using simple sugars as source of C (Read and Smith, 2008).

1.1.1.1. Ectendomycorrhizal fungi

EEM deserve a special mention in this chapter, as the main species that have been studied in this thesis belong to this group. EEM are of restricted occurrence, and therefore, have received limited attention from the scientific community. EEM were first called "ectendotrophic mycorrhizas" by Melin (1922) although these days "ectendomycorrhiza" is more used. Structurally, EEM are characterized by the **co-occurrence** of both **intercellular Hartig net** and **intracellular hyphae** penetrating the cortex cells, normally forming **coils** (Morte et al., 1994) (**Figure 1.2**). In addition, there is usually a thin and disordered **mantle** surrounding the root, or even lack of it (Yu et al., 2001; Roth-Bejerano et al., 2014).

Several fungal species are known to form this type of mycorrhiza, for instance *Wilcoxina mikolae*, *Wilcoxina rehmii*, *Sphaerosporella brunnea* or *Tricharina mikolae*, mainly with *Pinus* and *Larix* species as host plants (Yu et al., 2001). Fungal species that belong to the **desert truffle** group (more information in **Section 1.3**) are also able to form EEM associations with their hosts (Roth-Bejerano et al., 2014).
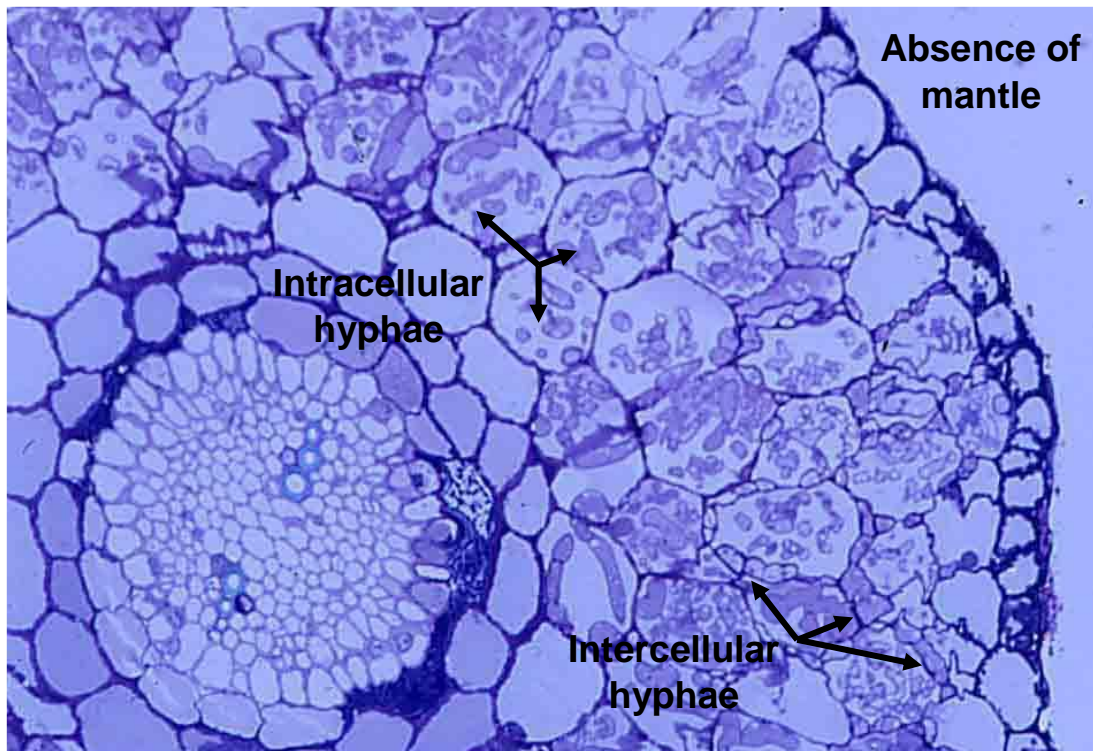
Figure 1.2. Transversal semi-thin cut of *H. almeriense x T. claveryi* EEM typical structure viewed under optical microscope (Navarro-Ródenas et al., 2011).

One feature shared by EEM fungi is their ability to form intra-, inter- or both types of mycorrhiza at the same time, depending on the host, the environment, and/or experimental conditions (Yu et al., 2001), although some of the experimental conditions seem inconsistent for different species. Some examples of this phenomenon:

1. *W. mikolae* forms EEM symbiosis with *Pinus banksiana* (Scales and Peterson, 1991a) or *Pinus resinosa* (Piché et al., 1986) in semi-aseptic pot cultures, while it forms ECM with *Picea mariana* or *Betula alleghaniensis* in growth pouches (Scales and Peterson, 1991b).

2. Increases in phosphorous or nitrogen fertilization can increase the amount of intracellular colonization by EEM fungi in *Pinus sylvestris* (Pachelewski et al., 1991-1992).

3. *H. almeriense* x *T. claveryi* mycorrhiza is influenced by the growth conditions: ECM *in vitro* (high P availability), EEM with majority of intercellular hyphae and without mantle formation in greenhouse (medium P availability) and EEM with majority of intracellular colonization in field conditions (low P availability) (Gutiérrez et al., 2003; Navarro-Ródenas et al., 2012a).

4. Auxin, phosphate and its interaction are capable of determining the type of mycorrhiza formed between transformed *Cistus* roots and *Terfezia boudieri* (Zaretsky et al., 2006a). This study concluded that the type of mycorrhiza formed depends on the genetic background of both the fungal isolate and the plant clone, the concentration of phosphate in the growth medium, the plant sensitivity to auxins and the level of auxin secretion by the fungal isolate.

5. Water conditions influence the type of mycorrhiza formed between *T. claveryi* and *H. almeriense*. Navarro-Ródenas et al. (2013) proposed that more than one type of mycorrhiza may be observed along the root system of a single plant at the same time, calling this phenomenon *ectendomycorrhizal continuum*, and showed that the overall percentage of colonization increases and the relative abundance of intercellular and intracellular colonization varies, favoring intracellular colonization, under water-stress conditions.

1.1.2. Genomic and transcriptomic tools for the study of mycorrhizal fungi

The **genome** of an organism is defined as its complete set of **DNA**, including all of its genes, while the **transcriptome** is defined as the sum of all RNA molecules in a cell, tissue or organ, although often the term transcriptome makes reference only to the **messenger RNA** (**mRNA**). The genome of an organism encodes the set of instructions that define its **lifestyle**, while its transcriptome show how these genes are regulated in a specific moment, condition and/or tissue. Because of the multiple types of plant-fungal associations (pathogens, symbionts or endophytes), in recent decades, the study of plant and fungal genomes is gaining great relevance as a useful tool to unravel the reasons for their different lifestyles (Kuo et al., 2014). Unlike plant genomics, which is very advanced, fungal genomics is still developing; in the last years, large scale international projects such as **1000 Fungal Genomes**, whose main goal is to document the diversity of fungal genomics at the family level, have promoted its progress (Grigoriev et al., 2014).

One of the reasons for the rapid advancement is the development of new, faster and cheaper sequencing techniques. The first major technology for genome sequencing was the Sanger sequencing (Sanger et al., 1977) but lately, it has been replaced by high-throughput techniques, also called **Next Generation Sequencing** (**NGS**). NGS produce shorter and with higher error rate reads, but yields thousands of times more output at a much cheaper cost per base pair. Among the most common sequencing platforms we can find Sanger, Illumina (Illumina Inc, California, USA) SOLiD (Thermo Fisher Scientific Inc, Massachusetts, USA) 454 (Roche Holding AG, Switzerland) or PacBio (Pacific Biosciences Inc, California, USA), each of them with its own features (Kuo et al., 2014).

Using some of the techniques mentioned and within the frame of the 1000 Fungal Genomes initiative, only a few mycorrhizal species have been sequenced to date, and especially focused on AM and ECM (for a detailed list consult Joint Genome Institute, JGI website, https://genome.jgi.doe.gov/mycocosm/home). Mycorrhizal genomes and transctiptomes, along with functional and *in silico* studies, have revealed new insights into the mycorrhiza lifestyle (see **Section 1.2**). It is important to highlight that there are only three EEM desert truffles among the list of sequenced fungi: *Tirmania nivea*, *T. claveryi* and *Terfezia boudieri*, and only *T. boudieri* genome has been published and analyzed (Murat et al., 2018), but together with other *Pezizomycete* truffle genomes such

as *Tuber aestivum*, *Tuber magnatum* or *Tuber borchii*, and, thus, there was not a deep analysis on their specific biological features.

1.2. Fungal "symbiosis toolkit" for mycorrhiza lifestyle

Most mycorrhizal fungal genomes sequenced to date have general features that are common to the mycorrhizal lifestyle, and that have been defined as the fungal "**symbiosis toolkit**" (Kohler et al., 2015). The main characteristics of the mycorrhizal lifestyle are an **expansion in the genome size**, usually accompanied by the expansion in the content of **transposable elements** (**TEs**), the **expansion in orphan small secreted proteins** (**SSPs**), upregulated during mycorrhization, and reduced sets of **carbohydrate-active enzymes** (**CAZymes**), including **plant cell wall degrading enzymes** (**PCWDEs**), and **secondary metabolism** related genes in the genome. **Figure 1.3** summarizes some of these essential features in different lifestyles.
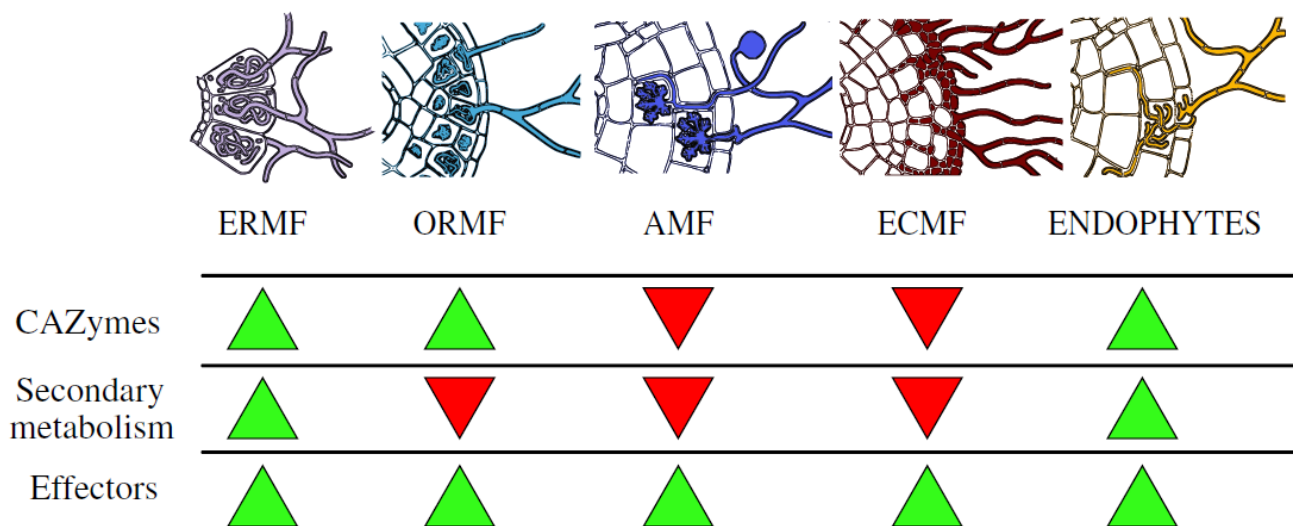
Figure 1.3. Schematic representation of important genomic features of mycorrhizal fungi and root endophytes. Green and red arrows indicate either high or low abundance, respectively, for carbohydrate-active enzymes (CAZymes), secondary metabolism enzymes and effector encoding genes. ERMF = ericoid mycorrhizal fungi, ORMF = orchid mycorrhizal fungi; AMF = arbuscular mycorrhizal fungi; ECMF = ectomycorrhizal fungi. Figure adapted from Perotto et al. (2018).

1.2.1. Genome size and transposable elements

Genomes of mycorrhizal fungi sequenced so far present sizes between 38 and 192 Mb for ECM and up to 1 Gb for AM, with a predicted gene content ranging from 10,000 to 23,000 genes for ECM and 21,000 to 31,000 for AM. In general terms, these **large genomes** are accompanied by a **large proportion of repeated sequences**, mainly **TEs**. For instance, *Cenoccocum geophilum*, the only mycorrhizal species (ECM) within the *Dothideomycetes* fungal class, has a genome 4 times larger than other non-mycorrhizal *Dothideomycetes* such as *Glonium stellatum* or *Lepidopterella palustris;* 81% of this genome consists on repeated elements but the number of genes is similar to that reported for the other two species (Peter et al., 2016). The same trend is found for other mycorrhizal fungi, regardless of their lineage and mycorrhizal type, such as *Laccaria bicolor* (*Basidiomycota*), *Rhizophagus irregularis* (*Glomeromycota*) or several *Tuber* species (*Ascomycota*) (Martin et al., 2008; 2010; Tisserant et al., 2013; Murat et al., 2018). Furthermore, in *Tuberaceae*, a great correlation between genome size and the proportion of repeated elements was found, which suggests that the expansion of the genome is mainly due to the proliferation of TEs (Murat et al., 2018).

The increased content in TEs is also found in most of plant pathogenic fungi, especially in those that are considered (hemi) biotrophic. It is known that TEs contribute to the plasticity and adaptability of fungi to their environment and, therefore this feature may play a role in the co-evolution of these fungi with their hosts (Raffaele and Kamoun, 2012). It is important to note that, although this feature is quite common, there are exceptions, such as the ECM fungi *Hebeloma cylindrosporum* and *Amanita muscaria*, with low contents in TEs, so this feature might not be a prerequisite of the biotrophic lifestyle (Peter et al., 2016).

1.2.2. Signaling and recognition: effectors and small secreted proteins (SSPs)

The study of **plant-fungal interactions** in mycorrhizal fungi has historically been very important, since it may answer key questions about the specificity of these interactions or about how mycorrhizal fungi avoid the plant´s immune system, among others. Thanks to the genomic advances, new insights about these issues have been

elucidated. Both AM and ECM interactions have been studied in depth and recently reviewed by Bonfante and Genre (2015) and Pellegrin et al. (2019). Among the molecules that are known to play a role in plant-fungal interaction, we can mention strigolactones, cutin and flavonoids, produced by the plant, and fungal lipo-chitooligosaccharides (LCOs), chitin oligosaccharides (COs), auxins, several volatile compounds and **SSPs**, among others, that are produced by the fungus. SSPs are of special importance because an expansion has been found in orphan SSPs for all mycorrhizal genomes sequenced so far, including different lineages and mycorrhizal types (Martin et al., 2008; 2010; Tisserant et al., 2013; Murat et al., 2018).

It has been hypothesized that these species-specific SSPs are involved in the plant-fungal interaction. In fact, there is already evidence of the key roles played by some of these SSPs, such as SP7 from *R. irregularis* (Kloppholz et al., 2011) or MiSSP7 from *L. bicolor* (Plett et al., 2011; 2014). In both cases, it has been shown that these effectors interact indirectly and mitigate, at least partially, the plant´s defense system through the transcription factors *ERF19* for *R. irregularis* SP7 (Kloppholz et al., 2011), or *JAZ6* for *L. bicolor* MiSSP7 (Plett et al., 2014). With the sequencing and analysis of an increasing number of mycorrhizal fungal genomes, the search for more species-specific effectors for different types of mycorrhizal symbiosis is considered an actual hotspot in the field of plant-microbe interactions.

1.2.3. Cell wall remodeling, secondary metabolites and plant defense system in mycorrhizal symbiosis

Another general feature of mycorrhizal lifestyle is the **constrained amount of PCWDEs** and **microbe cell-wall-degrading enzymes** (**MCWDEs**). AM and ECM fungi sequenced to date share a limited repertoire of genes coding for PCWDEs and MCWDEs. However, this trend is not found in ERM and ORM, which are more similar to pathogens and saprophytes in their PCWDE genomic repertoire (Kohler et al., 2015; Martino et al., 2018; Morin et al., 2019). It has been proved that ECM lifestyle has evolved polyphiletically from diverse decayer and decomposer saprophytic fungi. This evolution is marked by significant constraints of the ancestral saprophyte apparatus. In the case of ERM and ORM, they also evolved from these ancestors but have retained an extensive

decaying apparatus that is probably exploited by the plant for the supply of carbohydrate (Kohler et al., 2015).

As stated above, ECM fungi have retained some limited PCWDE and MCWDE activities and, to a lesser extent, also participate in organic matter decay (Averill et al., 2014). Moreover, those PCWDE are also involved in the remodeling of the plant cell wall during the establishment of the ECM symbiosis. Veneault-Fourrey et al. (2014) studied the expression of several PCWDEs and fungal cell wall degrading enzymes (FCWDEs) during the mycorrhization of *L. bicolor* with *Populus trichocarpa* and found that several PCWDE acting on hemicellulose were related to the first stages of the mycorrhiza, while PCWDE acting on cellulose and pectin were related to later stages. In addition, several PCWDE targeting **pectin** were related to degradation of **middle lamella** and specific formation of **Hartig net**. They also found a fungal expansin-like gene that may act both in the remodeling of plant and fungal cells (Veneault-Fourrey et al., 2014).

Fungal secondary metabolites can be divided into four chemical classes: poliketides, terpenoids, shikimic acid derived compounds and non- ribosomal peptides. In fungal genomes, several genes related to the biosynthesis of secondary metabolites can be found: polyketide synthase (PKS), prenyl transferase (DMATS), non-ribosomal peptide synthase (NRPS) and terpene synthase (TS). Many secondary metabolites are involved in pathogenic interactions, but biotrophic lifestyles such as mycorrhiza, possess fewer genes involved in their biosynthesis probably as an adaptive mechanism to avoid the host defense systems (Pusztahelyi et al., 2015), although they are not always successful. In fact, an **oxidative burst** (accumulation of **reactive oxygen species** or **ROS**) on the plant side has been reported during the AM colonization of roots of *Medicago trunculata* and *Phaseolus vulgaris*, as well as in the ECM symbiosis of *Castanea sativa* (Salzer et al., 1999; Lambais et al., 2003; Baptista et al., 2007). The oxidative burst is usually accompanied by the subsequent induction of ROS-scavenging activities in the mycorrhizal root, such as superoxide dismutase (SOD), **catalase** (**CAT**) and peroxidase, in order to alleviate this process and achieve the colonization.

1.3.   Desert truffles

Truffles can be widely defined as **ascomycetes** with **hypogeous** (growing under soil surface) or semi-hypogeous, **macroscopic sporocarps**. Therefore, "**desert truffle**" is not a phylogenetic nor a taxonomic term, but refers to edible hypogeous fungi (truffles) growing in **arid** and **semiarid areas**. All truffles known so far, desert truffles included, form mycorrhizal associations. The following genera are typically considered to belong to the desert truffle group: *Carbomyces*, *Elderia*, *Eremiomyces*, *Kalaharituber*, *Mattirolomyces*, *Mycoclelandia*, *Picoa*, *Stouffera*, *Terfezia*, *Tirmania*, and *Ulurua* (Moreno et al., 2014). All of these genera belong to *Pezizaceae* family, *Pezizomycetes* class, except for *Carbomyces*, which belongs to *Carbomycetaceae* family, and *Picoa*, to *Pyronemataceae* family. In addition, there are other species that do not belong to this genera but that can be considered as desert truffles such as *Tuber gennadii*. Among desert truffles, the best known and appreciated genera are **Terfezia** and **Tirmania**. Species belonging to these genera form **ectendomycorrhizal symbiosis** mainly with members of **Cistaceae** plant family, including different species of the *Helianthemum* genus (Morte et al., 1994; Kagan-Zur and Roth-Bejerano 2008; Roth-Bejerano et al., 2014; Moreno et al., 2014; Kovács and Trappe 2014).

As stated above, the only approaches to the study of desert truffles at genomic level have been the cDNA–AFLP analysis of the mycorrhiza formed between *T. boudieri* and *Cistus incanus* (Zaretsky et al., 2006b) and the recently published genome of *T. boudieri* (Murat et al., 2018), but there is still a lack of knowledge in this area. This section will be focused on **Terfezia claveryi** **Chatin** and **Tirmania nivea** **Trappe**.

1.3.1.   Life cycle and sexual reproduction

Mycorrhizal fungi are difficult to study. Unlike edible saprophytic fungi, whose life cycles are well known and can be grown *in vitro*, mycorrhizal fungi depend on their host to complete their life cycle which is much less known. On general basis, all edible ECM or EEM fungi, desert truffle included, possess three differentiated phases on their **life cycle**: (i) a **vegetative stage**, which corresponds to the hyphal growth in the underground soil ecosystem after spore germination; (ii) a **symbiotic stage** when the

mycorrhizal association is established; and (iii) a **reproductive stage** leading to the organization of **fruiting bodies** (Murat et al., 2008).

Both **sexual reproduction** and life cycle are still unclear for desert truffles. So far, no *MAT* **genes**, and therefore, no signs of sexual reproduction have been found in any desert truffle, neither self-fertilization (homothallism), nor outcrossing (heterothallism). *MAT* genes encode transcription factors that are the master loci controlling sexual reproduction and development in fungi. All known heterothallic ascomycetes have a single locus with two alternative *MAT* genes, while two different locus containing these two alternative genes each are found in homothallic species. In the case of heterothallism, the genes of opposite mating types are located on the same chromosomal locus but are dissimilar in sequence: one encodes a protein with an α-box domain (*MAT 1-1-1*), whereas the other encodes a high mobility group (HMG) protein (*MAT 1-2-1*) (Debuchy et al., 2010). Evidence of heterothallism has been found in other truffles belonging to *Tuberaceae* family, such as *Tuber melanosporum*, *Tuber aestivum* or *Tuber magnatum* (Martin et al., 2010; Rubini et al. 2011; Murat et al., 2018), and this finding has supposed a great impact on black truffle cultivation (Rubini et al., 2011; Zampieri et al., 2012; Linde and Selmes, 2012; Murat et al., 2013; Rubini et al 2014; Le Tacon et al. 2014).

Although the current dogma for *Ascomycetes* states that the mycorrhizal mycelium together with the sterile veins of the gleba are homokariotic, while the short living ascogenous hyphae are heterokariotic, Roth-Bejerano et al. (2004) found heterokariotic nuclei also in sterile hyphae of *T. boudieri*. These findings suggest the possibility of a long-term heterokariotic hyphae, but the lack of further studies makes this issue still controversial. Therefore, more studies are necessary to elucidate both life cycle and sexual reproduction of desert truffles.

1.3.2. Desert truffle ecology

Drylands are the areas that are exposed to greater potential annual evapotranspiration (ET0) than annual precipitation, calculated as the ratio between both factors and called **aridity index** (AI) (UNESCO, 1979). The ET0 is the sum of the humidity loss on a soil surface because of direct evaporation and plant transpiration. The

arid climates can be subdivided into hyper-arid (AI < 0.03), arid (0.03 < AI < 0.2), and semiarid (0.2 < AI < 0.5). A fourth aridity type called dry subhumid (0.5 < AI < 0.65) can be recognized as an intermediate category between dry and humid climate types. Furthermore, in some of these climates, aridity can be more pronounced in some seasons or even be present only temporally (Moreno et al., 2014).

Desert truffles have been historically found in all the climates that fill the definition of dry land. As stated before, desert truffles are mycorrhizal fungi, and therefore, they need a host to develop their full life-cycle. Species from *Terfezia* and *Tirmania* genera usually form mycorrhizal associations with plants endemic of the regions that they are inhabiting (for instance the *Cistaceae* family in the Mediterranean basin). For more information about drylands in general, and Mediterranean environmental factors in particular, go to **Section 1.5**.

1.3.3. Commercial, nutritional and medicinal value

The first records of gathering and use of desert truffles go back to the Bronze Age Amorites, and nowadays the Bedouins collect and consume desert truffles in the same places. They conform the culture with the longest recorded history on the use of desert truffles. Hence, it is in the **Middle East** where desert truffles have the best developed market, and where they can reach the highest prices that range between **20 to 200 USD per kg** (Shavit, 2014).

The most popular desert truffles in these regions are species of *Terfezia* and *Tirmania*, popular mainly in the Middle East, Mediterranean basin and Northern Africa. Historically, desert truffles have been used as important components of the **diet**, as a survival food in the desert for nomad tribes, as **medicines** against eye and skin diseases or even as **cosmetics** and **aphrodisiacs** (Shavit, 2014). Although the nutritional value of desert truffles presents some small variations between different species, they contain around 20-27 % of protein, 3-7.5 % of fat, 55-60 % of carbohydrates 7-13% of fiber, between 2-5 mg/100 mg of ascorbic acid and a high content on mineral nutrients (Martínez-Tomé et al., 2014). In addition, they present important **antioxidant activities**, similar or even higher than some common food antioxidants such as α-tocopherol or propyl gallate (Martínez-Tomé et al., 2014).

As mentioned before, desert truffles have historically been used for medicinal purposes, but it was not until the beginning of the XXI century when these activities were evaluated with more precise techniques. Studies carried out by Mandeel and Al-Laith (2007), Janakat et al. (2004; 2005) or Aldebasi et al. (2012) proved that some species of desert truffles such as *T. claveryi*, *Terfezia arenaria, T. boudieri* or *Tirmania pinoyi* possess antibacterial (against *Escherichia coli*, *Chlamydia trachomatis*, *Staphylococcus aureus*, *Pseudomonas aeruginosa…*) and antifungal (against *Candida albicans…*) activities, and have potential to be used as therapeutic agents against a range of human pathogens (Shavit and Shavit, 2014).

1.3.4. *Terfezia claveryi* Chatin

The genus **Terfezia** (Tul. & Tul.) Tul. & Tul. was raised by Tulasne and Tulasne (1851) and it belongs to *Pezizaceae* family, *Pezizales* order, *Pezizomycetes* class, *Ascomycota* division. The hypogeous fruiting bodies of the species comprising this genus are very appreciated mainly around the **Mediterranean countries**, from the south of Europe to the north of Africa and the **Middle East**. In **Spain** they receive different common names, depending on the region where they are usually collected: "turma", "patata de monte", "tumba crilla", "patata tumba" or "patata de turmera" in the southeast of Spain, especially in Region de Murcia. In Extremadura, western Andalucía, Madrid or Castilla-León they call them "criadillas de tierra" or "criadillas vaqueras", and in the Canary Islands they are called "papas crías" or "criadas". *Terfezia* name comes from the Arab "Terfas", common name that Arabs use to call these truffles, using also other names such as "Faq'a", "Kumba", "Kamah", "Kamé" or "Kholasis" (Honrubia et al., 2003).

Terfezia claveryi Chatin (**Figure 1.4**) was first described by Chatin (1892) and named after M. Clavery, Minister of Foreign Affairs from Siria that sent the sample from Damasco's market to Europe, for its analysis. *T. claveryi* forms a globose ascocarp from 2 to 10 cm diameter and between 50-200 g weight. Its peridium is thin, smooth and brownish. The inner part of the ascocarp is formed by hyphae that are differentiated in hypotecium (the first and sterile layer of hyphae) and glebe (internal combination of ascogenous and sterile hyphae). The gleba has a pinkish color and, in contact with air, it changes to yellowish-brownish (Chatin, 1892). The ascocarps lack the strong aroma of other truffles such as black truffle (*Tuber melanosporum*) or summer truffle (*Tuber*

aestivum) caused by the volatile organic compounds (VOCs). Inside the gleba, fertile hyphae forms globose asci of 70-80 µm diameter containing round, with hyaline, and reticulated ornamented spores of 17-24 µm diameter and a large lipid vacuole inside them. In later stages of maturation, these spores can be found outside the ascus and with verrucosal ornamentation (Gutiérrez, 2001).
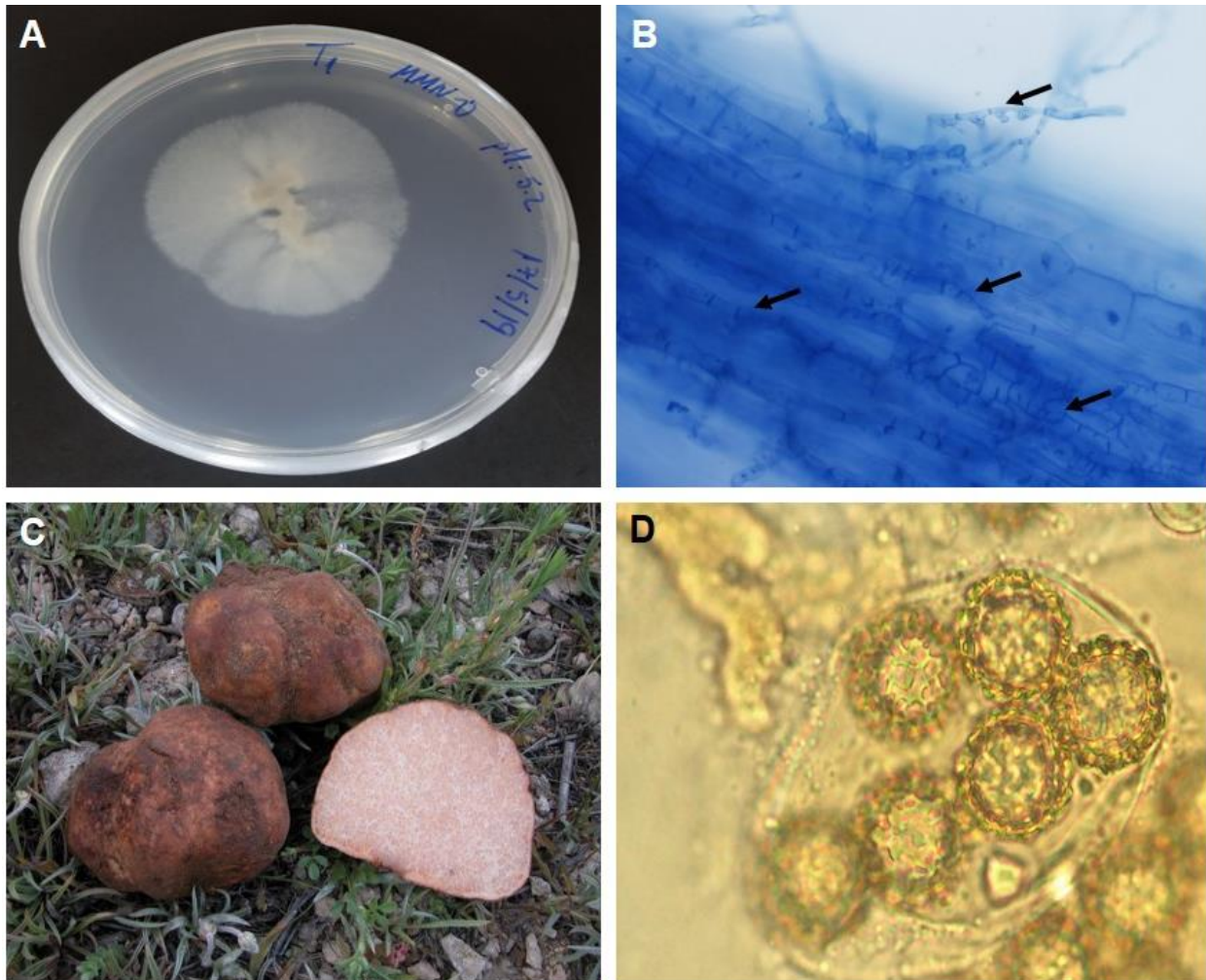
Figure 1.4. Mycelium of *T. claveryi* cultured *in vitro* (A), mycorrhiza with *H. almeriense* in pot conditions (arrows indicate hyphae) (B), ascocarps (C) and spores (D). Photographs C and D ceded by Antonio Rodríguez.

Desert truffles of *T. claveryi* can be found in several countries from the Mediterranean basin, but in **Spain** its collection is especially important due to cultural and historical reasons and the possibility of cultivation (see **Section 1.4** for more details). In the southeast of Spain, *T. claveryi* can be found in **calcareous soils** associated to several plants of the ***Helianthemum*** genus: *H. almeriense* Pau, *H. violaceum* (Cav.) Pers,

H. ledifolium (L.) Mill. or *H. hirtum* (L.) Mill. The diversity of host plants allows this species to colonize different types of habitats, from coastal habitats at sea level, associated with halophytic bushes, to areas at 1200 meters from sea level in annual *Helianthemum* meadows. The accompanying vegetation of these *Helianthemum* species colonized with *T. claveryi* can vary depending on the ecosystem, but some of the typical species that can be found are *Andryala ragusina*, *Artemisia lucentica*, *Brachypodium retusum*, *Dittrichia viscosa*, *Dorycnium pentaphyllum*, *Fumana ericoides*, *Fumana hispidula*, *Plantago albicans*, *Rosmarinus officinalis*, *Sideritis murgetana*, *Stipa tenacissima*, *Teucrium capitatum*, *Teucrium murcicum*, *Thymelaea hirsuta*, *Thymus membranaceus* and *Thymus vulgaris*, among others (Navarro-Ródenas, 2011). *T. claveryi* can be found in different types of soil (from heavy clay-rich to sandy soils), but with the condition of **neutral to basic soil pHs** (7 - 8.7) and **low organic matter input** (Honrubia et al., 2007). The **fructifications** are in **spring**, usually from late February to early May, but the first fructifications can occur as soon as in December and the last as late as in June.

1.3.4.1. *Enzymes in Terfezia claveryi ascocarps*

Apart from its morphological and ecological features, several enzymes have been characterized from *T. claveryi* ascocarps. Because of the importance of phosphorous on the cycle of *T. claveryi*, an **alkaline and acid phosphatases** have been characterized, localized, and their role under water-stress have been studied (Navarro-Ródenas et al., 2009; Navarro-Ródenas et al., 2012a). An **esterase** and two oxidorreductases (a fully latent **tyrosinase** and a **lipoxygenase**) from *T. claveryi* ascocarps have also been purified and characterized using different biochemical methods (Pérez-Gilabert et al. 2001a; 2001b; 2005a; 2005b). Although the physiological role of these enzymes is not clear, their activity may affect some basic features of the ascocarps such as flavor, color or texture, and therefore, to the overall quality of the ascocarps (Pérez-Gilabert et al., 2014).

1.3.5. *Tirmania nivea* Trappe

The genus ***Tirmania*** was erected by Chatin (1892) in order to differentiate several species from the genus *Terfezia*. It takes its name in honor of M. Tirman, the governor-general of Algeria, who sent the type collection to Chatin, while ***Tirmania***

nivea (**Figure 1.5**) takes its name from the latin word *niveus* (snowy white), because of the white color of the gleba and the young peridium (Alsheikh and Trappe, 1983). The genus *Terfezia* and *Tirmania* are quite close but they differ mainly in the morphology of the spores that are globose and ornamented in *Terfezia* and ellipsoid and smooth in *Tirmania*, and in the reaction of their asci to Meltzer's reagent, since asci and spores from *Tirmania* spp. become blue, while those from *Terfezia* spp. do not (Trappe, 1979).

T. nivea is more popular in the **Arab countries** than in Europe, and can be collected from the eastern Morocco to the deserts of Iraq and the Arabian Peninsula, while in the south of Spain there have only been rare collections of this species (Moreno et al., 2000). It forms a hypogeus to partially emergent subglobose to turbinate ascocarp from 6 to 15 cm diameter. Its peridium is 0.5-1.5 mm thick, glabrous, unpolished and often cracked to expose the gleba, with a yellowish white or pinkish brown color. The gleba is solid and fleshy with white or near to white sterile veins. Their asci are ellipsoid to piriform, with a diameter between 40 to 90 µm, containing 8 spores in mature state. The spores are from 10 to 18 µm diameter and are ellipsoid and smooth (Alsheikh and Trappe, 1983).
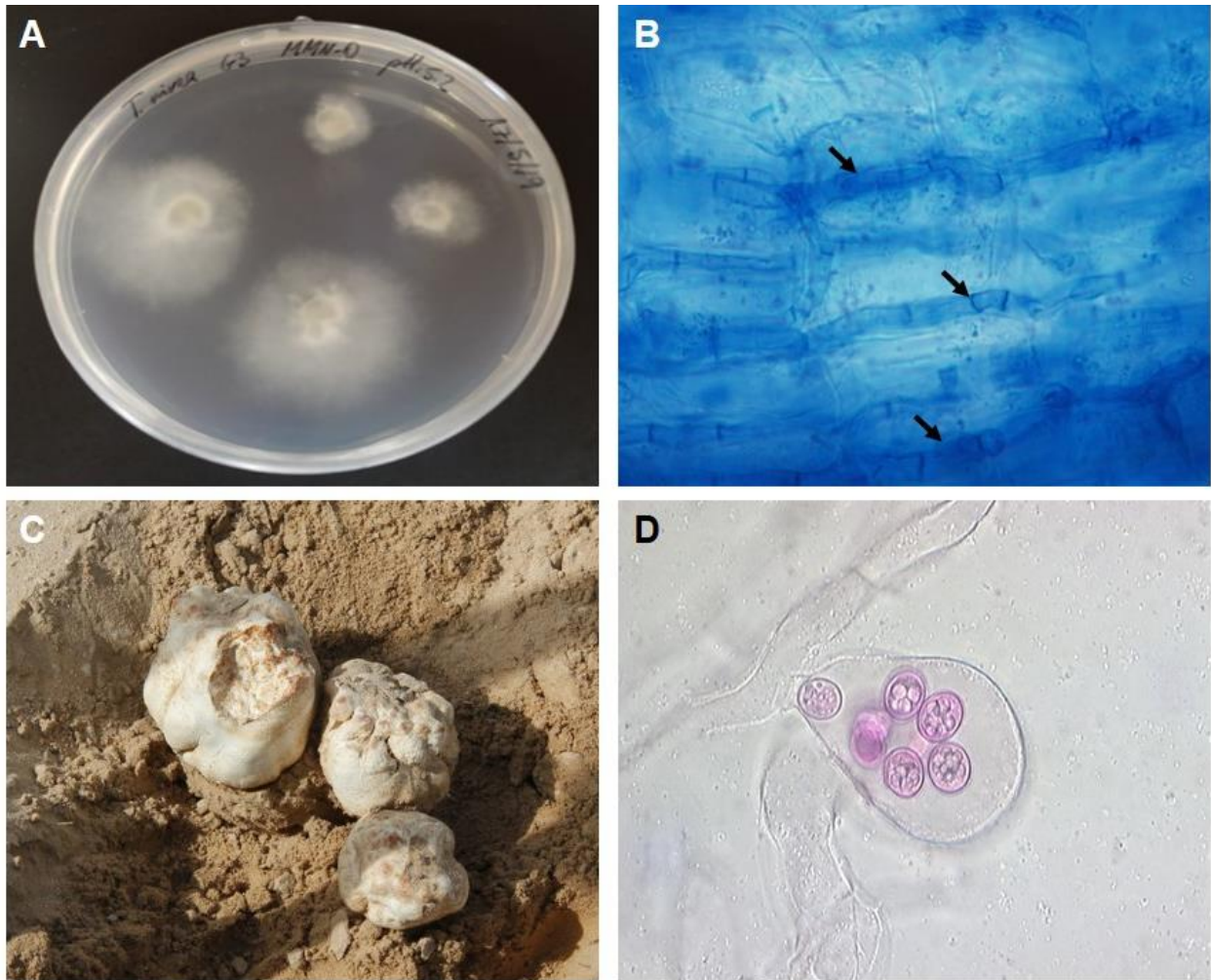
Figure 1.5. Mycelium of *Tirmania nivea* **cultured** *in vitro* **(A), mycorrhiza with** *H. lippi* **in pot conditions (arrows indicate hyphae) (B), ascocarp (C) and spores (D).** Photographs C and D ceded by Asunción Morte.

1.4.   Desert truffle cultivation

Edible mycorrhizal mushrooms and truffles include some of the most **expensive foods** in the world and have a global market worth billions of dollars. Despite this, only a few species, such as, saffron milk caps, matsutake, boletus, black truffles or desert truffles, have been domesticated with varying degrees of success, and not in large volumes. Cultivation of edible mycorrhizal fungi finds several obstacles, such as the need to be associated with a host plant, contamination with other mycorrhizal species before and after the establishment of plantations, and a general lack of understanding of the biology of each of these species (Hall et al., 2003).

From the **desert truffles** group only two of them have been reported to be successfully cultivated: ***Terfezia claveryi*** in **Spain** (Honrubia et al., 2001; Morte et al., 2008) and *Terfezia boudieri* in Tunisia and Israel (Slama et al., 2010; Kagan-Zur et al., 2014). More recently, mycorrhizal plants with *Picoa lefebvrei* and *Tirmania nivea* have been planted in 2014, and with *Terfezia arenaria* in 2015, in Spain, but fruiting ascocarps have not yet been obtained (Morte et al., 2017). In the present section, only *T. claveryi* cultivation will be discussed.

Figure 1.6. Different *H. almeriense* x *T. claveryi* plantations. **(A)** Detail from an *H. almeriense* x *T. claveryi* plant in the field. **(B)** and **(C)** Details of an *H. almeriense* x *T. claveryi* plant during spring, with desert truffle fructification (arrows). **(D)** Desert truffle plantation in spring located in Corvera (Murcia). **(E)** Desert truffle plantation located in Caravaca de la Cruz (Murcia).

The first plantation of the desert truffle *T. claveryi* was established in 1999 in southeastern Spain (Murcia) (Honrubia et al., 2001). Since then, more plantations have emerged, also in the southeast area of the Iberian Peninsula, and the current state of

knowledge about this crop comes mainly from the information gathered from all these plantations.

T. claveryi **fructification** usually occurs during the **second or third spring** after plantation, depending on site suitability, season and framework of the plantation, as well as on the management practices, which consist mostly on irrigation and weed elimination (Morte et al., 2008; 2012). The soil requirements for the cultivation of *T. claveryi* are the same as those required for natural production: **basic soils** with **low content in organic matter**. In most plantations, carpophores fructified yearly and production increased over time with average productions of 35-40 g m^{-2} per year, which extrapolated can bring productions between **350 and 400 kg per hectare** (Morte et al., 2012, 2017). However, **the annual yield is erratic** and there is still a lot of research to do in order to increase the management knowledge and to minimize large interannual fluctuations. Together with some biotic factors, such as the accompanying microbiome on the plantation site, or possible contaminations with other mycorrhizal species, the most likely reasons for the large fluctuations in the yields of the desert truffle are **environmental factors**.

T. claveryi cultivation is also known in Spain as "turmicultura" (turmiculture), due to the vernacular name "turma" given to *T. claveryi* ascocarps in the south of the Iberian Peninsula (Honrubia et al., 2014). This crop has been growing during the past years and now it is starting to become a potential alternative crop for arid lands. The rising interest on turmiculture has resulted in the foundation of research and development companies, such as Thader Biotechnology SL, a spin-off company from "Universidad de Murcia" created with the purpose of enhancing the applied research on desert truffle cultivation and to produce and sell high quality desert truffle mycorrhizal plants. It also resulted in the creation of a national association called "Asociación Española de Turmicultura", which groups different desert truffle farmers or "turmicultores" and experienced gatherers in order to promote and announce the benefits of this crop.

1.4.1. *Helianthemum almeriense* Pau as a host for *T. claveryi* cultivation

From the several host known by being colonized by *T. claveryi*, **H. almeriense** was the first to have mycorrhiza synthetized and the first used for its cultivation (Morte et al., 1994; 2008). *H. almeriense* is a **drought-deciduous Mediterranean woody perennial shrub** belonging to *Cistaceae* family. It usually appears in open dry, stony, limestone, mica or marl places with gypsum or sandy soils, at altitudes between 0 to 500 m. Its habitat is the southeast arid regions of Iberian Peninsula, although it can also be found in Morocco (Morte and Honrubia, 1997). Phenology is defined as the study of periodic events in the life cycles of living beings, as influenced by the environment. The annual phenology of *H. almeriense* is typical of other deciduous or semi-deciduous shrubs of the Mediterranean summer (Nilsen and Muller, 1981; Haase et al., 2000; Gulías et al., 2009) and consists on a **vegetative period** that lasts from autumn (bud breaking) to spring, **blooming events** that start at the end of winter and finish in spring and **leaf senescence** at the end of spring/beginning of summer. Maximum photosynthesis is found in winter, and mycorrhizal colonization in the field is mainly intracellular at above 40% of mycorrhization average, except for summer, where few signs of mycorrhiza are found (Gutiérrez et al., 2003; Morte et al., 2010; Navarro-Ródenas et al., 2015) (**Figure 1.7**).
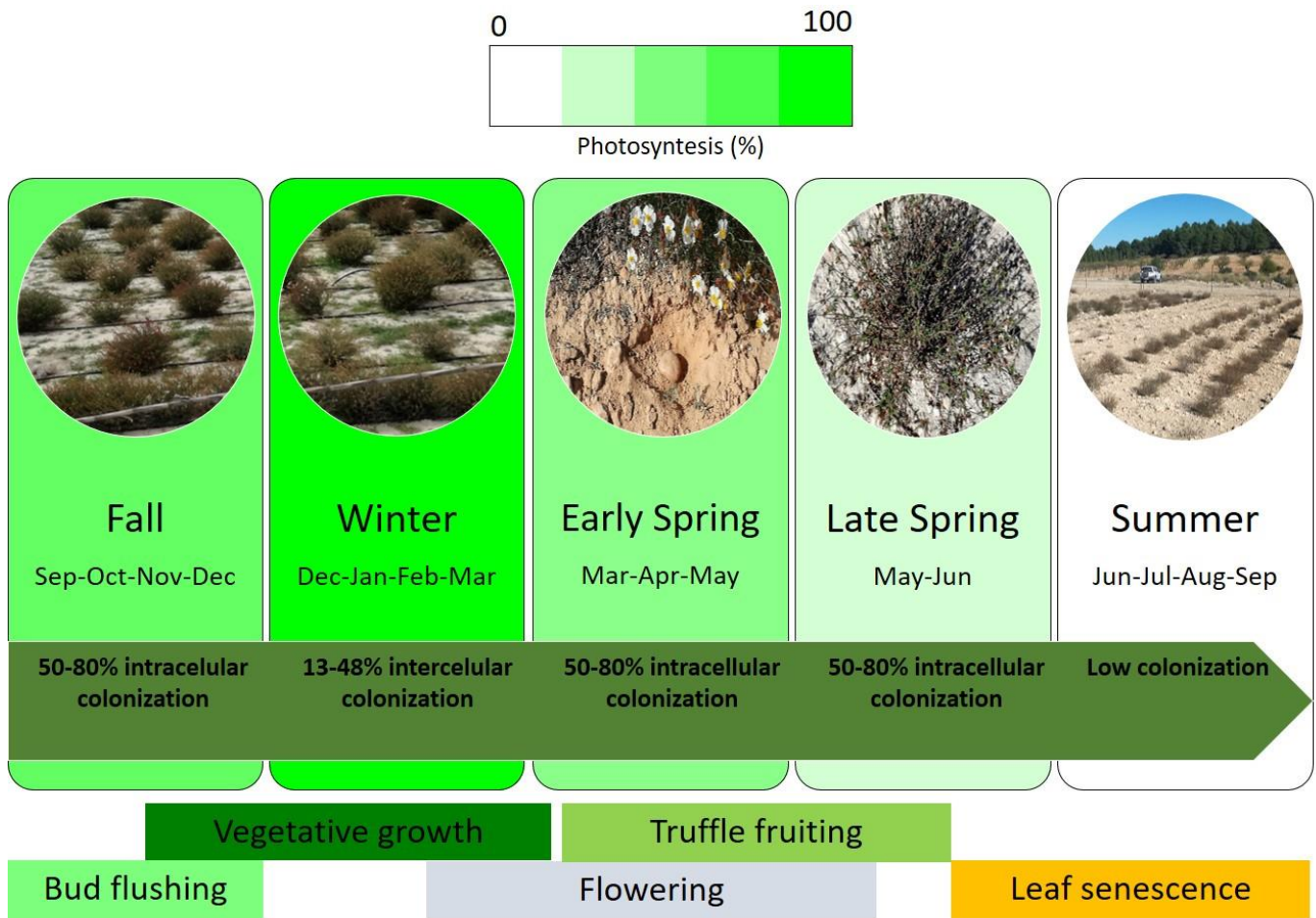
Figure 1.7. Schematic representations of a typical phenological year of *H. almeriense* x *T. claveryi* mycorrhizal plants.

Due to the increasing demand of desert truffle crops in the semiarid areas of the southeast of Spain, the research on the **production** of high quality **mycorrhizal plants** (*H. almeriense* x *T. claveryi*) has been enhanced during the last years. The production of *H. almeriense* mycorrhizal plants can be achieved both *in vivo* or *in vitro* or mixing strategies (*i.e.* plant production *in vitro* plus mycorrhizal inoculum production *in vivo*, or viceversa) (Morte et al., 2008). A summary of the different options for plant production is shown in **Figure 1.8**. The main issues faced when producing mycorrhizal plants are poor survival rates of the seeds, high dependency on the spore inoculum and low percentages of mycorrhization (Morte et al., 2017). High mortality of *H. almeriense* seeds during the first stages of germination can be solved using **plants micropropagated *in vitro*** (Morte et al., 1994) or adding native **plant growth promoting rhizobacterias** (PGPR), which are bacteria inhabiting the rhizosphere of the roots and able to improve

plant development specially under biotic and abiotic stresses (Glick, 1995). In the case of *H. almeriense*, some PGPR of the genus *Pseudomonas* have shown an improvement in seed survival, a reduction in production time and a higher plant quality during the early stages of plant development (Navarro-Ródenas et al., 2016).

The dependency on spore inoculum can be solved using mycelium grown *in vitro* as inoculum. In this sense, both the use of ciclodextrins (CDs) and the use of polyethylenglycol (PEG) to subject the mycelium to a moderate water-stress were able to stimulate mycelial growth *in vitro* (López-Nicolás et al., 2013; Navarro-Ródenas et al., 2012a). In addition, the production *in vitro* of *T. claveryi* mycelium was improved using a Modified Melin-Norkrans (MMN) culture medium, recently optimized by Arenas et al. (2018). Even with these advances, the growth of *T. claveryi in vitro* is far from being stable and substantial enough to be considered the main source of fungal inoculum. At last, fungal colonization has also been improved with the use of native mycorrhizal helper bacteria (MHB) (Navarro-Ródenas et al., 2016).
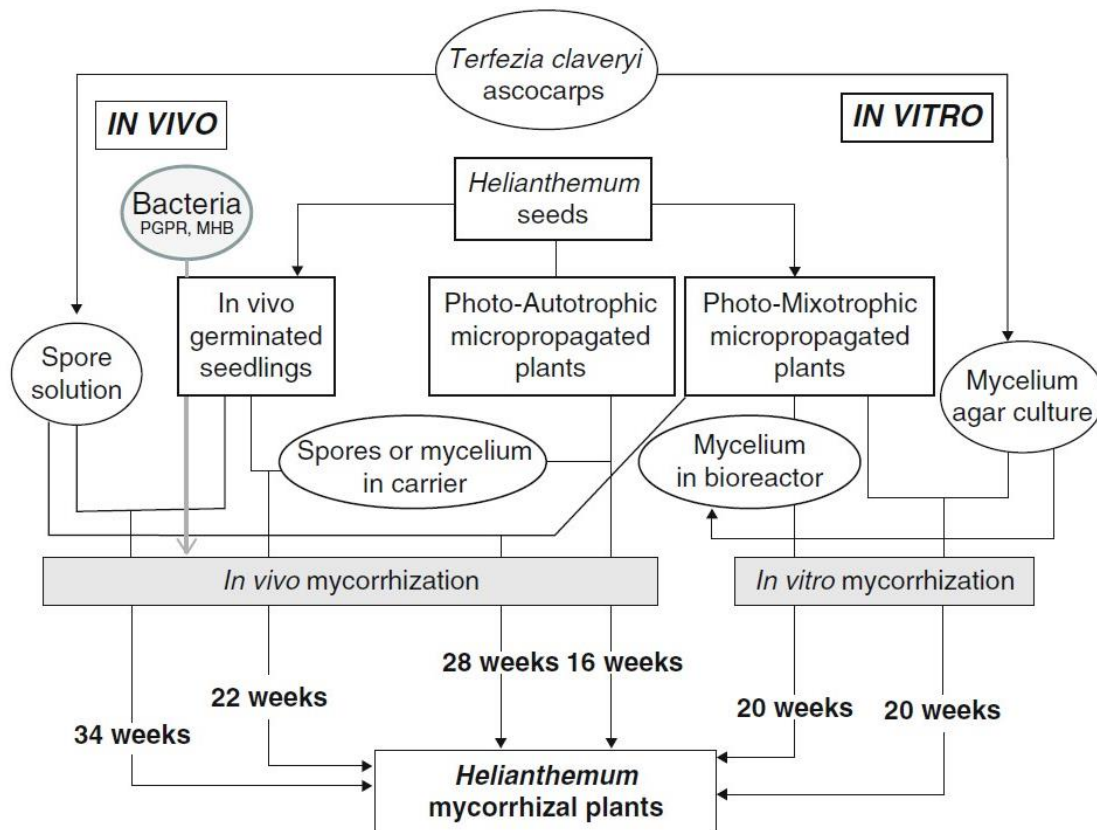
Figure 1.8. *In vivo* and *in vitro* methods for production of desert truffle mycorrhizal plants and the period of time required for each of them. PGPR = plant growth-promoting rhizobacteria, MHB = mycorrhiza helper bacteria. Figure extracted from Morte et al. (2017).

1.5. Water-stress: drought and vapor pressure deficit

As stated before, **drylands** are the areas of the globe where the ET0 exceeds the precipitations, resulting in **AI < 0.65**. Here, we will focus on one type of dry land, the **Mediterranean climate**, which is localized between 32º and 40º latitude north south and supposes between 1 and 4% of the total area of the Earth, being the Mediterranean basin the major exponent of this climate (Aschman, 1973; di Castri, 1981; Mooney, 1982). The climate on the Mediterranean basin is characterized by **low total precipitations** (200 to 500 mm per year), **cold winters**, and **hot and dry summers** (Köppen, 1923), restricting the favorable period for plant development to autumm and spring and, therefore, originating the idea that the biomass productivity of the Mediterranean plants is low. However, in terms of maximum photosynthesis, Flexas et al. (2014) showed that Mediterranean plants are no less productive than their non-Mediterranean counterparts.

Drought can be defined as a transient environmental situation of extreme soil water content scarcity, mostly due to low precipitations, while the **vapor pressure deficit** (VPD) can be defined as the difference between the amount of moisture in the air and how much moisture the air can hold when saturated. These two parameters are the main limiting factors for the photosynthesis, survival and growth of plants inhabiting Mediterranean ecosystems (Bacelar et al., 2009). The sum of those two factors (lack of precipitations and high VPD) during the transition from Mediterranean winters to summers is translated into a **water-stress** state for the plants, which affects several physiological parameters. Water-stress affects virtually all the physiological processes of plants, such as cell expansion, cell wall, chlorophyll, nitrate reductase and, in general, the reduction of protein synthesis, the accumulation of abscisic acid (ABA), antioxidants or organic solutes such as sugars, and leaf senescence (Jones, 2004). Here, we will focus only on some of those responses, such as **gas-exchange responses**, **leaf morphology**, **hydraulic status** and the regulation of **aquaporins**, **Rubisco** and **antioxidant** enzymes, and their interactions.

1.5.1. Gas-exchange parameters

The **gas-exchange** parameters of the plant refer to the exchange of O_2, CO_2 and water vapor between the leaves and the environment, and affect the biological processes of the plant, such as respiration or **photosynthesis**. The gas-exchange parameters can be estimated through the use of infrared gas analyzers (IRGAs) systems used as portable photosynthesis systems. By combining gas-exchange measurements with chlorophyll fluorescence measurements, they can estimate the photosynthetic parameters of plants, such as **net carbon assimilation** (A_N), transpiration (E), substomatic or intercellular CO_2 concentration (C_i), **stomatal conductance** to H_2O (g_s), **mesophyll conductance** to CO_2 (g_m), chloroplastic CO_2 concentration (C_c) photosystem II efficiency (ΦPSII), electron transport flux (J_{flu}) or maximum carboxylation rate of Rubisco (V_{cmax}), among others. Some of these parameters are calculated by the portable photosynthesis system using the differentials between CO_2 and water vapor before and after passing through the leaf and using the model from Farquar et al. (1980), while others, such as gm, C_c or V_{cmax}, can be calculated using other mathematical models, such as the one proposed by Harley et al. (1992) or Either and Livingston (2004), and require data from response curves to CO_2 concentration (called A_N-C_i curves). Most of the physiological responses of plants to water-stress result in A_N reduction, together with gs and gm decrease, and the increase in the **intrinsic water use efficiency** (**iWUE**), which is the ratio between A_N and gs. Some other parameters, such as V_{cmax}, remain generally unchanged, but may experience a decrease under long-term water-stresses (Flexas et al., 2006a).

1.5.2. Leaf morphology

C3 angiosperms present leaves composed of three different tissues: epidermis, mesophyll and vascular tissue. Most of the chloroplasts are contained in the mesophyll, which is protected by the epidermis and is intermingled with the vascular transport system. The **leaf mass per area** (**LMA**) is the simplest indicator of leaf structure and is composed of the ratio between leaf dry mass and leaf area. It is a powerful parameter that gives information about plant strategies: in general terms, the better adapted a plant is to water-stress, the higher LMA presents. Although LMA is a structural parameter and does not vary rapidly, it is known to respond to long-term stresses. LMA usually increases as

a response to long-term water-stress, mainly by reducing the leaf area (Poorter et al., 2009). LMA is also known to be related to the gas-exchange parameters of the plant such as gm: although it determines the maximum value of gm, it does not correlate with the real value of this parameter (Flexas et al., 2008).

1.5.3. Water potential

Water potential (**Ψ**) is defined as the free energy per volume of water (Boyer, 1995); it is assumed that pure water has a Ψ of 0 in standard conditions of temperature and pressure. This parameter determines the direction and strength of the water exchanges between different parts of the plant or between the plant and the soil. Another typical response to water-stress is a decrease of the water potential (Ψ) of different plant organs such as leaves or shoots.

1.5.4. Aquaporins

Aquaporins (**AQPs**) are integral membrane proteins that are present in the plasma and intracellular membranes of several organisms (animals, plant, fungi, eubacteria and archaebacteria) and serve as channels that facilitate and regulate the passive movement of water and other small solutes and gases across the membrane (Zardoya 2005). They belong to the ancient protein family of the **major intrinsic proteins** (**MIP**, Pfam code PF00230 v 32.0). The first and main interest in the study of plant AQPs lies in their capacity to transport **water**. However, the discovery that plants can also transport **small solutes** and **gases** has related AQPs to several key functions such as transpiration, tissue expansion and desiccation, CO_2 transport, nutrient uptake (Maurel et al. 2008; Maurel et al., 2016) and O_2 transport (Zwiazek et al. 2018).

Depending on the similarities in the aminoacid sequences and in the typical subcellular location, the plant´s AQPs or MIPs can be subdivided into five subfamilies: plasma membrane intrinsic proteins (PIP), tonoplast intrinsic proteins (TIP), nodulin26-like intrinsic proteins (NIP), small basic intrinsic proteins (SIP) and X intrinsic proteins (XIP). Moreover, PIPs can be subdivided into two subgroups, PIP1 and PIP2 (Maurel et al., 2008).

AQPs are 23-35 kDa proteins whose structure is quite conserved and consists of six hydrophobic transmembrane α-helices that delimit a narrow pore. The transmembrane helices are connected by five loops (Verkman et al., 2000) (**Figure 1.9**). One of the citoplasmatic loops and one of the extracellular loops are connected by the motif NPA (Asn-Pro-Ala) which is characteristic of these proteins. Moreover, homo- and heterotetramers are usually formed, each of them forming and independent pore (Zardoya, 2005). Normally, the heteromerization of AQPs PIP2 and PIP1 is necessary for their proper functioning, since some PIP1 can be retained intracellularly and are not capable of transporting water, requiring coexpression with PIP2 and then heteromerization to be located in the plasma membrane and be functional (Yaneff et al. 2014; Bienert et al., 2018).
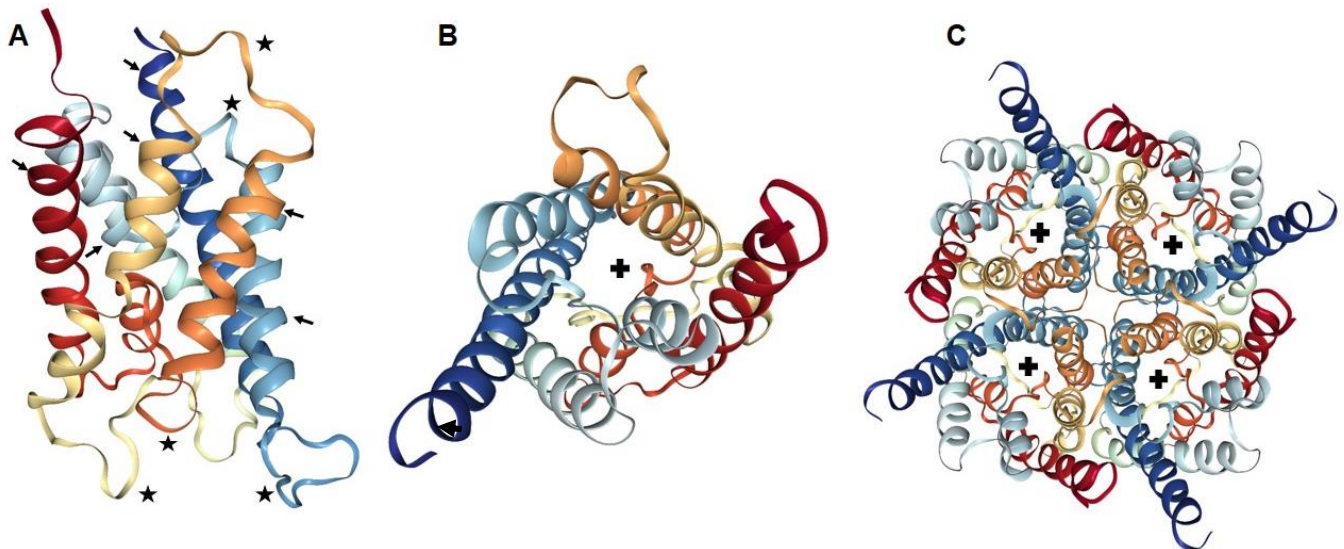
Figure 1.9. Typical aquaporin structure. Human aquaporin, PDB entry: 4CSK. (**A**) Longitudinal view of an AQP monomer with the helices (arrows) and the loops (stars). (**B**) Transversal view of an AQP monomer with the pore (cross). (**C**) Transversal view of an AQP tetramer with 4 pores (cross).

The plant´s AQPs play an important role in water-stress tolerance. In **roots**, water transport is a combination of three different pathways: **apoplastic** (water flows around the cells), **symplastic** (cell to cell *via* plasmodesma) and **transcellular** (cell to cell though cell membranes). It is in the transcellular pathway where the AQPs are important regulators of the water transport in roots (Steudle, 2000). In **leaves**, AQPs are also important, not only for water transport, but also for CO_2 transport, as AQPs can determine the **path of CO_2 through the mesophyll** and affect gas-exchange parameters

of the plant such as g_m or A_N (Kaldenhoff et al., 2008; Maurel et al., 2016). AQP regulation can be achieved *via* transcriptional regulation or post-transcriptionally by gating, whereby the rate of flux through the channel is controlled, or by trafficking, whereby aquaporins are shuttled from the intracellular storage sites to the plasma membrane (Törnroth-Horsefield et al., 2010). Transcriptional regulation of AQPs in response to drought stress is always difficult to interpret, since plants can have multiple AQPs isoforms (*i.e.* 35 for *Arabidopsis*) and each of them responds differently to drought stress. AQP upregulation in water-stress conditions can be a way of increasing hydraulic conductance but downregulation might be also a way of minimizing water loss (Alexandersson et al., 2005).

1.5.5. Rubisco

Ribulose-1,5-bisphosphate carboxylase/oxygenase (**Rubisco**) (EC 4.1.1.39) is an enzyme found in the chloroplasts of autotrophic organisms that, in the case of plants, represents between 30 and 50% of the total protein in the leaf (Parry et al., 2013). During **photosynthesis**, Rubisco catalyzes the **fixation of CO_2** to ribulose-1,5-bisphosphate (RuBP) being the key enzyme in Calvin-Benson-Bassham cycle and, thus, in the photosynthesis. At the same time, it is also able to function as an oxygenase by **incorporating** an O_2 molecule to RuBP in the **photorespiration** process (Bracher et al., 2017). Because of these two functions, Rubisco is a central protein for life on Earth. It is also one of the largest enzymes, has a molecular mass of approximately 560 kDa and is composed of 16 polypeptides, eight of them are encoded by *rbcS* genes and form the **small subunit** (15 kDa each), while the other eight form the **large subunit** (55 kDa each) and are encoded by *rbcL* genes (Spreitzer and Salvucci, 2002).

Water-stress is known to induce decreases in Rubisco activity in several plant species (Boyer, 1976; Lawlor 1995; Flexas et al., 2006b; Abdallah et al., 2018). The mechanism of Rubisco activity decrease in these conditions and may vary from fast responses (biochemical regulation, like adjustments in the activation state) to long term water-stress, which can involve changes in gene expression (directly regulation of *rbcS* and *rbcL* genes or indirectly, *via* regulation of Rubisco inhibitors) (Flexas et al., 2006; Parry et al., 2008).

1.5.6. Antioxidants

One of the main responses of plants to water-stress is the increase in the production of free radicals or **reactive oxygen species** (**ROS**), such as superoxide anion (O_2^-), **hydrogen peroxide** (**H_2O_2**) or hydroxyl radicals ($^*OH$). Thus, the plant antioxidant systems, both enzymatic (catalases, superoxide dismutases, peroxidases…) and non-enzymatic (gluthation, ascorbate, α-tocopherol…), must be involved in mechanisms of tolerance to water-stress.

With regard to **catalases**, they are the main enzymes responsible for the **dismutation of H_2O_2** into water and dioxygen. Catalase activity has been observed in three groups of enzymes: "**typical**" **monofunctional heme-catalases** (the largest and most extensively studied), **bifunctional catalases-peroxidases** and **non-heme catalases**. In addition, low levels of catalase activity are found in many heme-containing proteins that are not normally considered catalases (Switala and Loewen, 2002). Monofunctional heme-catalases have been classified following two criteria: subunit size and phylogeny. Based on the subunit size they are divided in two groups: the **large subunit size** catalases, "LSCs" (>75 kDa), present only in bacteria and fungi and the **small subunit size** catalases "SSCs" (<60 kDa). LSCs are classified in **L1** and **L2** subgroups. In fungi, L1-type catalases are not inducible and usually accumulate in spores, while those from the L2-type are usually induced by different stressors and are extracellular enzymes (Chelikani et al., 2004; Hansberg et al., 2012). Both LSCs and SSCs have proved to be active as tetramers and dimers, but not as monomers (Díaz et al., 2005). On the other hand, typical catalases are divided in three main evolutionary clades: **Clade 2**, comprising LSCs and **Clade 1** and 3 comprising SSCs. Clade 1 includes SSCs from bacteria, green algae and plants. Clade 2 groups the LSCs from bacteria and fungi while **Clade 3** contains SSCs from most phyla, including fungi, but not Viridiplantae (Hasnberg et al., 2012).

1.5.7. Mycorrhizal symbiosis and water-stress tolerance

As indicated in **Section 1.1**, mycorrhizal fungi provide the root system with a larger physiologically active area, which translates into a **better capacity to extract water from the soil**. One of the reasons, is that the diameter of the hyphae, between 2 and 5 μm, allows them to access certain sites in the soil structure that the root cannot. In

addition, hyphae also have the ability to extract water from soils with a lower water potential than the roots (Theodorou y Bowen, 1970)

The capacity of the mycorrhiza to improve the state of the plant against water-stress is not always accompanied by an improvement in the water hydraulics of the roots. When comparing the results obtained in different studies with mycorrhizal and non-mycorrhizal plants subjected to water-stress, most of the times mycorrhization improves the hydraulics of the plant root, although in other cases, no or even negative effects have been found (Augé, 2001; Letho and Zwiazek, 2011). Moreover, sometimes mycorrhizas are able to impact on the expression of plant´s AQP and also collaborate in the improvement of roots water hydraulics by regulating the expression of their own fungal AQPs (Lehto and Zwiazek, 2011).

There are several reports on the benefits of mycorrhiza to the tolerance to water-stress in terms of gas exchange and hydraulic parameters. The most common responses are **improvement in transpiration**, **stomatal conductance** and leaf and shoot **water potential**. However, the influence of mycorrhiza on tissue hydration and foliar gas exchange are often subtle, transient and probably also depend on the specific circumstances and symbionts involved (Augé, 2001).

Another mechanism by which mycorrhizal associations may improve the plant responses to water-stress may lie in their ability to **detoxify** the **ROS** accumulated during water-stress. In soybean inoculated with AM, a decrease in oxidative damage to root lipids during water-deficit conditions has been reported, while under drought stress, roots of AM *Digitaria eriantha* plants showed lower levels of H_2O_2 and higher catalase activity than their non-mycorrhizal counterparts (Porcel et al., 2004; Ruiz-Lozano et al., 2008; Pedranzani et al., 2016).

1.5.7.1. *T. claveryi beneficial effects to H. almeriense responses to water-stress*

So far we have discussed the general benefits that mycorrhizae provide to their hosts, but in this section we will focus on the beneficial effects of **T. claveryi** for its most common plant host, **H. almeriense**.

H. almeriense plants inoculated with *T. claveryi* performed better under water-stress than those without mycorrhizal colonization. These improvements consisted of **greater water potential**, **transpiration**, **stomatal conductance** and **net assimilation**, together with the modification of the **nutrient status** of the plants, concluding that mycorrhization with *T. claveryi* partially mitigates the detrimental effects of water-stress through specific physiological (transpiration, water use efficiency) and nutritional (P, N and K) alterations (Morte et al., 2000). Moreover, in field conditions, the inoculation with *T. claveryi* **improved the survival rates** of the *H. almeriense* host and confirmed that the *H. almeriense* mycorrhizal plants maintain good physiological parameters with drought conditions (Morte et al., 2010).

As already mentioned in **Section 1.1.1.1**, the nature of the mycorrhizal colonization of *T. claveryi* with *H. almeriense* depends on the water status of the system, as the colonization is more intense and **favors the intracellular colonization** in situations of water-stress (Morte et al., 2010; Navarro-Ródenas et al., 2013). Moreover, Navarro-Ródenas et al. (2013) characterized **five *H. almeriense* AQPs** (*HaPIP1.1*, *HaPIP1.2*, *HaPIP2.1*, *HaPIP2.2* and *HaTIP1.1*) and also reported a **fine-tune regulation** of these AQPs in *H. almeriense* x *T. claveryi* plants only under water-stress conditions. In addition, a fungal AQP from *T. claveryi* (**TcAQP1**) was characterized and proved to be quite efficient in the transport of water and CO_2. It was proposed that TcAQP1 played a role in the tolerance to water-stress, since it was upregulated in *T. claveryi* mycelium grown under drought stress (Navarro-Ródenas et al. 2012b) and it was also fine-tune regulated during drought stress in mycorrhizal plants (Navarro-Ródenas et al., 2013).

More recently, it has been described an alternative ribosomal RNA (rRNA) post-transcriptional maturation, called "**hidden gap**" that may be related to the capacity of this fungus to resist water-stress (Navarro-Ródenas et al., 2018).

All these findings show that *T. claveryi* has different mechanisms related to its adaptation to drylands and that its symbiosis with *H. almeriense* plants is beneficial for the host, making this system an alternative crop for arid and semiarid regions.

1.5.8. Water-stress as a determining factor in the production of desert truffles

It seems that water-stress is not only affecting the physiological and molecular parameters of plants. In fact, the **yields** of some Mediterranean crops, such as the olive tree, are also strongly **influenced by water-stress** (usually a combination of drought and high VPD) and other environmental parameters such as the ET0 or the AI (both previously defined in **Section 1.3.2**) (Ben-Gal et al., 2009). Regarding **desert truffle fructification**, there is limited knowledge about the factors that affect it. Based on personal communications from interviews with desert truffle gatherers and farmers (known as "turmicultores"), in general, truffles show up more frequently during March-April, and according to desert truffle gatherers, factors such as **rain** (97.8%), **soil type** (62.2%) and **host plant** influence the yield of the desert truffle. Around 80 % of the gatherers think that **winter showers** are an important factor that allows the truffle to reach a good size, and **spring precipitations** or **spring temperatures** were important for 9.1% and 25% of the interweaved pickers, respectively (Mehmet, 2017).

Another factor that also varies highly among years and that may be related to total production are the **start and end dates of the recollection season**. Most gatherers and "turmicultores" indicate that during this period **mild temperatures** together with some **soil moisture** are needed for fructifications and that they occur together with some **phenological changes** of the plant: *i.e.* the start of the fructification coincides with the **blooming**, while the end is related to **flower disappearance** and **leaf senescence** (**Figure 1.7**).

Apart from the valuable general knowledge that comes from years of experience of gatherers and "turmicultores", there have been certain scientific approaches to understand how the environment affects desert truffle fructifications. Bradai et al. (2015) found that the natural fructifications of desert truffle were closely related to the accumulated **precipitations from October–December**, probably determining the development of truffles after the dry period (summer). Morte et al. (2012) observed a statistical correlation, according to Pearson's test, between the amount of **precipitations during autumn** (September, October, and November) of a year and the *T. claveryi* desert truffle harvest in spring of the following year. Honrubia et al. (2014) recommended that irrigation should be provided at the end of summer/beginning of autumn and, if the dry

conditions continue, an extra irrigation of 50–80 L m^{-2} at the beginning of the fructification season could greatly improve crop in base of their own experience.

1.5.9. Desert truffle cultivation in the frame of climatic change

Predictions of global **climatic change** point to a greater risk of **desertification**, since the increase in temperature, together with shorter, less frequent and less widespread precipitation events, can induce the expansion of drylands. Drylands are currently home to more than 38% of the global population and therefore represent the most sensitive areas of the world (Schlesinger et al., 1990; Krinner et al., 2013; Huang et al., 2016). Moreover, global climate change is also closely related to the **spring phenology** of plants (Badeck et al., 2004; Cleland et al., 2007), especially for arid and semiarid plants, such as Mediterranean shrubs (Bernal et al., 2010; León-Sánchez et al., 2016), since the climate change is already causing spring to occur earlier (Corell, 2005). The increase in potential dry areas makes the cultivation of desert truffles an even more interesting alternative for agricultural exploitation, not only in the present, but also in the future. Therefore, basic and applied research of desert truffles should be expanded to establish them as a successful crop in these potential dry regions and to provide new insights in their water-relationships and their spring phenology (Morte et al., 2017).

Global warming and increasing drought are a consequence of the **increase in atmospheric concentrations of CO$_2$**. Although drought can negatively affect several biological processes of plants, described in **Section 1.5**, such as the decrease in A$_N$, high atmospheric CO$_2$ concentrations usually increase A$_N$ without effect or a slight decrease in their gs (Ainsworth and Rogers, 2007). The main consequence of this is an **increase in the photosynthetic intrinsic water use efficiency** (iWUE) of the plants. The more carbon is able to assimilate a plant with less water loss, the more efficient it is considered. Therefore, this increased use of the water by the plants with a rising concentration of atmospheric CO$_2$ could reduce predictions of future drought stress due to climatic change (Swann et al., 2016). How the increased atmospheric CO$_2$ concentrations will affect *H. almeriense x T. claveryi* mycorrhizal system and desert truffle cultivation remains unknown, but a meta-analysis from Alberton et al. (2005) with several responses of mycorrhizal fungi and mycorrhizal plants to elevated CO$_2$ concentrations reveals that, in general terms, positive responses could be expected.

References

Abdallah MB, Dalila T, Antonella P, Elena DZ, Mauro S, Andrea S, et al. (2018) Unraveling physiological, biochemical and molecular mechanisms involved in olive (*Olea europaea* L. Cv. Chétoui) tolerance to drought and salt stresses. J. Plant. Physiol. 220(November 2017):83–95. https://doi.org/10.1016/j.jplph.2017.10.009.

Ainsworth EA, Rogers A (2007) The response of photosynthesis and stomatal conductance to rising [CO_2]: mechanisms and environmental interactions. Plant Cell Environ. 30(3):258–70. https://doi.org/10.1111/j.1365-3040.2007.01641.x.

Alberton O, Kuyper TW, Gorissen A (2005) Taking mycontrism seriously: mycorrhizal fungal and plant responses to elevated CO_2. New Phytol. 167:859-868. https://doi.org/10.1111/j.1469-8137.2005.01458.x.

Aldebasi YH, Nouh WG, Abdel-Atti NM (2012) Comparative pathological studies on the healing effect of natural (*Terfezia claveryi*) and synthetic (vigamox) antimicrobial on corneal ulcers in rabbits. J. Pharm. Biomed. 2(6):66–77.

Alexandersson E, Fraysse L, Sjövall-Larsen S, Gustavsson S, Fellert M, Karlsson M, Johanson U, Kjellbom P (2005) Whole gene family expression and drought stress regulation of aquaporins. Plant Mol. Biol. 59(3):469–84. https://doi.org/10.1007/s11103-005-0352-1.

Alsheikh AM, Trappe JM (1983) Desert truffles: The genus *Tirmania*. Trans. Br. Mycol. Soc. 81(1):83–90. http://dx.doi.org/10.1016/S0007-1536(83)80207-1.

Arenas F, Navarro-Ródenas A, Chávez D, Gutiérrez A, Pérez-Gilabert M, Morte A (2018) Mycelium of *Terfezia claveryi* as inoculum source to produce desert truffle mycorrhizal plants. Mycorrhiza 28(7): 691-701. https://doi.org/10.1007/s00572-018-0867-3.

Aschmann H (1973) Distribution and peculiarity of Mediterranean ecosystems. In: Di Castri F, Mooney HA, eds. Mediterranean Type Ecosistems: Origin and Structure. Springer Verlag, New York. pp. 405.

Augé RM (2001) Water relations, drought and vesicular-arbuscular mycorrhizal symbiosis. Mycorrhiza 11:3–42. https://doi.org/10.1007/s005720100097.

Averill C, Turner BL, Finzi AC (2014) Mycorrhiza-mediated competition between plants and decomposers drives soil carbon storage. Nature 505(7484):543–45. https://doi.org/10.1038/nature12901.

Bacelar, EA, Moutinho-Pereira JM, Gonçalves BC, Lopes JI, Correia CM (2009). Physiological responses of different olive genotypes to drought conditions. Acta Physiol. Plant. 31(3):611-621. https://doi.org/10.1007/s11738-009-0272-9.

Badeck FW, Bondeau A, Böttcher K, Doktor D, Lucht W, Schaber J, Sitch S (2004) Responses of spring phenology to climate change. New Phytol. 162(2):295–309. https://doi.org/10.1111/j.1469-8137.2004.01059.x.

Baptista P, Martins A, Pais MS, Tavares RM, Lino-Neto T (2007) Involvement of reactive oxygen species during early stages of ectomycorrhiza establishment between *Castanea sativa* and *Pisolithus tinctorius*. Mycorrhiza 17(3):185–193. https://doi.org/10.1007/s00572-006-0091-4.

Ben-Gal A, Agam N, Alchanatis V, Cohen Y, Yermiyahu U, Zipori I, Presnov, E, Sprintsin M, Dag, A (2009) Evaluating water stress in irrigated olives: Correlation of soil water status, tree water status, and thermal imagery. Irrig. Sci. 27:367–376. https://doi.org/10.1007/s00271-009-0150-7.

Bernal M, Estiarte M, Peñuelas J (2010) Drought advances spring growth phenology of the Mediterranean shrub *Erica multiflora*. Plant Biol. 13(2):252–57. https://doi.org/10.1111/j.1438-8677.2010.00358.x.

Bienert MD, Diehn TA, Richet N, Chaumont F, Bienert GP (2018) Heterotetramerization of plant PIP1 and PIP2 aquaporins is an evolutionary ancient feature to guide PIP1 plasma membrane localization and function. Front. Plant Sci. 9:382. https://doi.org/10.3389/fpls.2018.00382.

Bonfante P, Genre A (2015) Arbuscular mycorrhizal dialogues: do you speak 'plantish' or 'fungish'?. Trends Plant Sci. 20(3):150–54. https://doi.org/10.1016/j.tplants.2014.12.002.

Boyer JS (1976) Photosynthesis at low water potentials. Phil. Trans. R. Soc. Lond. B. 273(927):501–512.

Boyer J (1995) Measuring the water status of plants and soils. Academic Press Inc., San Diego.

Bracher A, Whitney SM, Hartl FU, Hayer-Hartl M (2017) Biogenesis and metabolic maintenance of Rubisco. Annu. Rev. Plant Biol. 68:29–60.

Bradai L, Bissati S, Chenchouni H, Amrani K (2015) Effects of climate on the productivity of desert truffles beneath hyper-arid conditions. Int. J. Biometeorol. 59(7):907-915. https://doi.org/10.1007/s00484-014-0891-8.

Brundrett MC (2009) Mycorrhizal associations and other means of nutrition of vascular plants: understanding the global diversity of host plants by resolving conflicting information and developing reliable means of diagnosis. Plant Soil 320(1–2):37–77. https://doi.org/10.1007/s11104-008-9877-9.

Brundrett MC, Tedersoo L (2018) Evolutionary history of mycorrhizal symbioses and global host plant diversity. New Phytol. 220(4):1108–15. https://doi.org/10.1111/nph.14976.

Chatin MA (1892). Contribution a l'histoire naturelle de la truffe. Bulletin de la Societe Botanique de France 38:54-64.

Chelikani P, Fita I, Loewen PC (2004) Diversity of structures and properties among catalases. Cell Mol. Life Sci. 61:192–208. https://doi.org/10.1007/s00018-003-3206-5.

Cleland E, Chuine I, Menzel A, Mooney H, Schwartz M (2007) Shifting plant phenology in response to global change. Trends Ecol. Evol. 22(7):357–65. https://doi.org/10.1016/j.tree.2007.04.003.

Corell R (2005) Arctic climate impact assessment. Bulletin of the American Meteorological Society. 86(6):860.

De Bary A (1887) Comparative morphology and biology of the fungi, mycetozoa and bacteria. Claredon press. Vol 2.

Di Castri F, Goodall DW, Specht RL (1981) Ecosystems of the world 11: Mediterranean-Type Shrublands of the World. Elsevier Scientific Publishing Company.

Debuchy R, Berteaux-Lecellier V, Silar P (2010) Mating systems and sexual morphogenesis in ascomycetes. In: Borkovich KA, Ebbloc DJ, eds. Cellular and Molecular Biology of Filamentous Fungi. American Society of Microbiology Press, Washington DC pp. 501-535. https://doi.org/10.1128/9781555816636.ch33.

Díaz A, Muñoz-Clares RA, Rangel P, Valdás VJ, Hansberg W (2005) Functional and structural analysis of catalase oxidized by singlet oxygen. Biochimie. 87(2):205–214. https://doi.org/10.1016/j.biochi.2004.10.014.

Ethier G, Livingston N (2004) On the need to incorporate sensitivity to CO_2 transfer conductance into the Farquhar–von Caemmerer–Berry leaf. Plant Cell Environ. 27:137–153. https://doi.org/10.1111/j.1365-3040.2004.01140.x.

Farquhar GD, von Caemmerer S, Berry JA (1980) A biochemical model of photosynthetic CO_2 assimilation in leaves of C3 species. Planta 149:78–90. https://doi.org/10.1007/BF00386231.

Flexas J, Bota J, Galme J, Medrano H, Ribas-Carbó M (2006a) Keeping a positive carbon balance under adverse conditions: responses of photosynthesis and respiration to water stress. Physiol. Plant. 127:343–352. https://doi.org/10.1111/j.1399-3054.2006.00621.x.

Flexas J, Bota J, Henkle M, Medrano H (2006b) Decreased Rubisco activity during water stress is not induced by decreased relative water content but related to conditions of low stomatal conductance and chloroplast CO_2 concentration. New Phytol. 172:73–82. https://doi.org/10.1111/j.1469-8137.2006.01794.x.

Flexas J, Ribas-Carbó M, Diaz-Espejo A, Galmés J, Medrano H (2008) Mesophyll conductance to CO_2: current knowledge and future prospects. Plant Cell Environ. 31:602–621. https://doi.org/10.1111/j.1365-3040.2007.01757.x.

Flexas J, Diaz-Espejo A, Gago J, Gallé A, Galmés J, Gulías J, Medrano H (2014) Photosynthetic limitations in Mediterranean plants: A review. Environ. Bot. 103:12-23. https://doi.org/10.1016/j.envexpbot.2013.09.002.

Frank AB (1885) On the nutritional dependence of certain trees on root symbiosis with belowground fungi. Translated by Trappe JM (2005) An English translation of AB Frank's classic paper of 1885. Mycorrhiza 15:267-75.

Glick BR (1995) The enhancement of plant growth by free-living bacteria. Canadian J. Microbiol. 41:109–117. https://doi.org/10.1139/m95-015.

Grigoriev IV, Nikitin R, Haridas S, Kuo A, Ohm R, Otillar R, et al. (2014) MycoCosm portal: Gearing up for 1000 fungal genomes. Nucleic Acids Res. 42(D1):699–704. https://doi.org/10.1093/nar/gkt1183.

Gulías J, Cifre J, Jonasson S, Medrano H, Flexas J (2009) Seasonal and interannual variations of gas exchange in thirteen woody species along a climatic gradient in the Mediterranean island of Mallorca. Flora-Morphology, Distribution, Functional Ecology of Plants 204(3):169–81. https://doi.org/10.1016/j.flora.2008.01.011.

Gutiérrez A (2001) Caracterización, micorrización y cultivo en campo de las trufas del desierto. Dissertation. Dpto de Biología Vegetal. University of Murcia, Murcia pp. 264.

Gutiérrez A, Morte A, Honrubia M (2003) Morphological characterization of the mycorrhiza formed by *Helianthemum almeriense* Pau with *Terfezia claveryi* Chatin and Picoa lefebvrei (Pat.) Maire. Mycorrhiza 13(6):299–307. https://doi.org/10.1007/s00572-003-0236-7.

Haase P, Pugnaire FI, Clark SC, Incoll LD (2000) Photosynthetic rate and canopy development in the drought-deciduous shrub *Anthyllis cytisoides*. J. Arid Environ. 46(1):79–91. https://doi.org/10.1006/jare.2000.0657.

Hall IR, Yun W, Amicucci A (2003) Cultivation of edible ectomycorrhizal mushrooms. Trends Biotechnol. 21 (10): 433-438. https://doi.org/10.1016/S0167-7799(03)00204-X.

Hansberg W, Salas-Lizana R, Domínguez L (2012) Fungal catalases: function, phylogenetic origin and structure. Arch Biochem. Biophys. 525(2):170–80. http://dx.doi.org/10.1016/j.abb.2012.05.014.

Harley PC, Loreto F, Marco G Di, Sharkey TD (1992) Theoretical considerations when estimating the mesophyll conductance to CO_2 flux by analysis of the response of photosynthesis to CO_2. Plant Physiol. 98:1429–1436. https://doi.org/10.1104/pp.98.4.1429.

Harrison MJ (1997) The arbuscular mycorrhizal symbiosis: an underground association. Trends Plant. Sci. 2(2):54-60. https://doi.org/10.1016/S1360-1385(97)82563-0.

Helgason T, Daniell TJ, Husband R, Fitter AH, Young JPW(1998) Ploughing up the wood-wide web?. Nature394(6692):431. https://doi.org/10.1038/28764.

Honrubia M, Gutiérrez A, Morte A (2001) Desert truffle plantation from southeast Spain. In: Edible Mycorrhizal Mushrooms and Their Cultivation: Proceedings of the Second International Conference on Edible Mycorrhizal Mushrooms. Christchurch, New Zealand pp 3–5.

Honrubia M, Morte A, Gutiérrez A, González F, Dieste C (2003) Las turmas o trufas de desierto. In: Esteve Selma MA, Lloréns Pascual del Riquelme M, Martínez Gallur C (eds.) Los Recursos Naturales de la Región de Murcia. Un Análisis Interdisciplinar. Servicio de Publicaciones de la Universidad de Murcia, Murcia pp. 277–279.

Honrubia M, Morte A, Gutiérrez A (2007) Las Terfezias. Un cultivo para el desarrollo rural en regiones áridas y semi-áridas. In: Reyna S, ed. Truficultura, Fundamentos y Técnicas. Ediciones Mundi-Prensa, Madrid, pp 365-397.

Honrubia M, Andrino A, Morte A (2014) Preparation and maintenance of both man-planted and wild plots. In: Kagan-Zur V, Roth-Bejerano N, Sitrit Y, Morte A, eds. Desert Truffles: Phylogeny, Physiology, Distribution and Domestication. Berlin, Heidelberg: Springer Berlin Heidelberg pp. 367-387. https://doi.org/10.1007/978-3-642-40096-4_22.

Huang J, Haipeng Y, Guan X, Wang G, Guo R (2016) Accelerated dryland expansion under climate change. Nat Clim. Change 6(2):166–71. https://doi.org/10.1038/nclimate2837.

Janakat S, Al-Fakhiri S, Sallal AK (2004) A promising peptide antibiotic from *Terfezia claveryi* aqueous extract against *Staphylococcus aureus in vitro*. Phytother. Res. 18(10):810-813. https://doi.org/10.1002/ptr.1563.

Janakat SM, Al-Fakhiri SM, Sallal AK (2005) Evaluation of antibacterial activity of aqueous and methanolic extracts of the truffle *Terfezia claveryi* against *Pseudomonas aeruginosa*. Saudi medical journal 26(6):952-955.

Jones HG (1998) Stomatal control of photosynthesis and transpiration. J. Exp. Bot. 49(Special):387–98. https://doi.org/10.1093/jxb/49.Special_Issue.387.

Kagan-Zur V, Roth-Bejerano N (2008) Desert Truffles. Fungi 1 (Special Issue: Truffles) 1:32–37.

Kagan-Zur V, Roth-Bejerano N, Sitrit Y, Morte A (2014) Desert Truffles. Phylogeny, Physiology, Distribution and Domestication. Soil Biology, volume 38, Springer-Verlag, Berlin, Heidelberg. ISBN 978-3-642-40095-7.

Kaldenhoff R, Ribas-Carbó M, Sans JF, Lovisolo C, Heckwolf M, Uehlein N (2008) Aquaporins and plant water balance. Plant Cell Environ. 31:658–666. https://doi.org/10.1111/j.1365-3040.2008.01792.x.

Kloppholz S, Kuhn H, Requena N (2011) A secreted fungal effector of *Glomus intraradices* promotes symbiotic biotrophy. Curr. Biol. 21(14):1204–9. https://doi.org/10.1016/j.cub.2011.06.044.

Kohler A, Kuo A, Nagy LG, Morin E, Barry KW, Buscot F, et al. (2015) Convergent losses of decay mechanisms and rapid turnover of symbiosis genes in mycorrhizal mutualists. Nat. Gen. 47(4): 410–415. https://doi.org/10.1038/ng.3223.

Köppen W (1923) *Die klimate der Erde*. Bornträger, Berlin pp. 369.

Kovács G, Trappe J (2014) Nomenclatural history and genealogies of desert truffle. In: Kagan-Zur V, Roth-Bejerano N, Sitrit Y, Morte A, eds. Desert Truffles. Phylogeny, Physiology, Distribution and Domestication. Soil Biology, volume 38, Springer-Verlag, Berlin, Heidelberg pp. 57–67. https://doi.org/10.1007/978-3-642-40096-4_2.

Krinner G, Shongwe M, Bony S, Booth B, Brovkin V, et al. (2013) Long-term climate change: projections, commitments and irreversibility. In Climate Change 2013. The Physical Science Basis: Working Group I Contribution to the Fifth Assessment Report of the Intergovernmental Panel on Climate Change. https://doi.org/10.1017/CBO9781107415324.024.

Kuo A, Bushnell B, Grigoriev, IV (2014) Fungal genomics: Sequencing and annotation. In: Grimm B, ed. Advances in Botanical Research (1st ed., Vol. 70). Elsevier Ltd pp. 1-52. https://doi.org/10.1016/B978-0-12-397940-7.00001-X.

Lambais MR, Ríos-Ruiz WF, Andrade RM (2003) Antioxidant responses in bean (*Phaseolus vulgaris*) roots colonized by arbuscular mycorrhizal fungi. New Phytol. 160(2):421–428. http://doi.wiley.com/10.1046/j.1469-8137.2003.00881.x.

Lawlor DW (1995) The effects of water deficit on photosynthesis. In: Smirnoff N, ed. Environment and plant metabolism. Flexibility and acclimation. Oxford, UK: BIOS Scientific Publishers pp. 129–160.

Le Tacon F, Marçais B, Courvoisier M, Murat C, Montpied P, Becker M (2014) Climatic variations explain annual fluctuations in French Périgord black truffle wholesale markets but do not explain the decrease in black truffle production over the last 48 years. Mycorrhiza 24 (1):115–125. https://doi.org/10.1007/s00572-014-0568-5.

Lehto T, Zwiazek J (2011) Ectomycorrhizas and water relations of trees: a review. Mycorrhiza 21(2):71–90. https://doi.org/10.1007/s00572-010-0348-9.

León-Sánchez L, Nicolás E, Nortes PA, Maestre FT, Querejeta JI (2016) Photosynthesis and growth reduction with warming are driven by nonstomatal limitations in a Mediterranean semiarid shrub. Ecol. Evol. 6 (9): 2725-2738. https://doi.org/10.1002/ece3.2074.

López-Nicolás JM, Pérez-Gilabert M, García-Carmona F, Lozano-Carrillo MC, Morte A (2013) Mycelium growth stimulation of the desert truffle *Terfezia claveryi* Chatin by β-cyclodextrin. Biotechnol Prog. 29(6):1558-1564. https://doi.org/10.1002/btpr.1791.

Linde CC, Selmes H (2012) Genetic diversity and mating type distribution of *Tuber melanosporum* and their significance to truffle cultivation in artificially planted truffieres in Australia. Appl. Environ. Microbiol. 78(18):6534-6539. . https://doi.org/10.1128/AEM.01558-12.

Mandeel QA, Ameer A, Al-Laith A (2007) Ethnomycological aspects of the desert truffle among native Bahraini and non-Bahraini peoples of the kingdom of bahrain. J. Ethnopharmacol. 110(1):118–29. https://doi.org/10.1016/j.jep.2006.09.014.

Marschner H, Dell B (1994) Nutrient uptake in mycorrhizal symbiosis. Plant and Soil. 159(1):89-102. https://doi.org/10.1007/BF00000098.

Martin F, Aerts A, Ahrén D, Brun A, Danchin EGJ, Duchaussoy F, et al. (2008) The genome of *Laccaria bicolor* provides insights into mycorrhizal symbiosis. Nature 452(7183): 88–92. https://doi.org/10.1038/nature06556.

Martin F, Kohler A, Murat C, Balestrini R, Coutinho PM, Jaillon O, et al. (2010) Périgord black truffle genome uncovers evolutionary origins and mechanisms of symbiosis. Nature 464(7291): 1033–1038. https://doi.org/10.1038/nature08867.

Martínez-Tomé M, Maggi L, Jiménez-Monreal AM, Murcia MA, Marí JAT (2014) Nutritional and antioxidant properties of *Terfezia* and *Picoa*. In: Kagan-Zur V, Roth-Bejerano N, Sitrit Y, Morte A, eds. Desert Truffles. Phylogeny, Physiology, Distribution and Domestication. Soil Biology, volume 38, Springer-Verlag, Berlin, Heidelberg pp. 261–275. https://doi.org/10.1007/978-3-642-40096-4_17.

Martino E, Morin E, Grelet GA, Kuo A, Kohler A, Daghino S, et al. (2018) Comparative genomics and transcriptomics depict ericoid mycorrhizal fungi as versatile saprotrophs and plant mutualists. New Phytol. 217(3): 1213-1229. https://doi.org/10.1111/nph.14974.

Maurel C, Verdoucq L, Luu D, Santoni V (2008) Plant aquaporins: membrane channels with multiple integrated functions. Ann. Rev. Plant Biol. 59(1):595–624. https://doi.org/10.1146/annurev.arplant.59.032607.092734.

Maurel C, Verdoucq L, Rodrigues O (2016) Aquaporins and plant transpiration. Plant Cell Environ. 39(11):2580–87. https://doi.org/10.1111/pce.12814.

Mehmet A (2017) Ethnomycological aspects of traditional usage and indigenous knowledge about the arid-semi arid truffles consumed by the residents of the Eastern Anatolia Region of Turkey. Gazi Univ J. Sci. 30(4): 57-70.

Melin E (1922) On the mycorrhizas of *Pinus sylvestris* L. and *Picea abies* Karst. A preliminary note. J. Ecol. 9:254–257.

Miransari M (2010) Contribution of arbuscular mycorrhizal symbiosis to plant growth under different types of soil stress. Plant Biol. 12(4):563–69. https://doi.org/10.1111/j.1438-8677.2009.00308.x.

Mooney HA (1982) Mediterranean-type ecosystems: research progress and opportunities. S. Afr. J. Sci. 78:5–7.

Moreno G, Diez J, Manjón JL (2000) *Picoa lefebvrei* and *Tirmania nivea*, two rare hypogeous fungi from Spain. Mycol Res. 104(3):378-381. https://doi.org/10.1017/S0953756299001227.

Moreno G, Alvarado P, Manjón JL (2014) Hypogeous desert fungi. In: Kagan-Zur V, Roth-Bejerano N, Sitrit Y, Morte A, eds. Desert Truffles. Phylogeny, Physiology, Distribution and Domestication. Soil Biology, volume 38, Springer-Verlag, Berlin, Heidelberg pp. 57–67. https://doi.org/10.1007/978-3-642-40096-4_1.

Morin E, Miyauchi S, San Clemente H, Chen ECH, Pelin A, de la Providencia, I, et al. (2019) Comparative genomics of *Rhizophagus irregularis*, *R. cerebriforme*, *R.diaphanus* and *Gigaspora rosea* highlights specific genetic features in Glomeromycotina. New Phytol. 222(3): 1584–1598. https://doi.org/10.1111/nph.15687.

Morte A, Cano A, Honrubia M, Torres P (1994) *In vitro* mycorrhization of micropropagated *Helianthemun almeriense* plantlets with *Terfezia claveryi* (desert truffle). Agric. Sci. Finl. 3: 309–314. https://doi.org/10.23986/afsci.72700.

Morte A, Lovisolo C, Schubert A (2000) Effect of drought stress on growth and water relations of the mycorrhizal association *Helianthemum almeriense-Terfezia claveryi*. Mycorrhiza 10(3):115–119. https://doi.org/10.1007/s005720000066.

Morte A, Honrubia M, Gutiérrez A (2008) Biotechnology and cultivation of desert truffles. In: Varma A, ed. Mycorrhiza. Springer Berlin Heidelberg pp. 467–483. https://doi.org/10.1007/978-3-540-78826-3_23.

Morte A, Navarro-Ródenas A, Nicolás E (2010) Physiological parameters of desert truffle mycorrhizal *Helianthemun almeriense* plants cultivated in orchards under water deficit conditions. Symbiosis 52(2–3):133–139. https://doi.org/10.1007/s13199-010-0080-4.

Morte A, Andrino A, Honrubia M, Navarro-Ródenas A (2012) *Terfezia* cultivation in arid and semiarid soils. In: Zambonelli A, Bonito GM, eds. Edible Ectomycorrhizal Mushrooms: Current Knowledge and Future Prospects. Springer-Verlag, Berlin Heidelberg pp. 241–263. https://doi.org/10.1007/978-3-642-33823-6_14.

Morte A, Pérez-Gilabert M, Gutiérrez A, Arenas F, Marqués-Gálvez JE, Bordallo JJ, Rodríguez A, Berná LM, Lozano-Carrillo C, Navarro-Ródenas, A (2017) Basic and applied research for desert truffle cultivation. In: Varma A, Prasad R, Tuteja N, eds. Mycorrhiza-Ecophysiology, Secondary Metabolites, Nanomaterials. Springer International Publishing pp. 23–24. https://doi.org/10.1007/978-3-319-57849-1_2.

Murat C, Mello A, Abbà S, Vizzini A, Bonfante P (2008) Edible mycorrhizal fungi: identification, life cycle and morphogenesis. In: Varma A, ed. Mycorrhiza. Springer Berlin Heidelberg pp. 707–732. https://doi.org/10.1007/978-3-540-78826-3_33.

Murat C, Rubini A, Riccioni C, De la Varga, H, Akroume E, Belfiori B, et al. (2013) Fine-scale spatial genetic structure of the black truffle (*Tuber melanosporum*) investigated with neutral microsatellites and functional mating type genes. New Phytol. 199(1): 176-187. https://doi.org/10.1111/nph.12264.

Murat C, Payen T, Noel B, Kuo A, Morin E, Chen J, et al. (2018) Pezizomycetes genomes reveal the molecular basis of ectomycorrhizal truffle lifestyle. Nat. Ecol. Evol, 2(12): 1956–1965. https://doi.org/10.1038/s41559-018-0710-4.

Nadeem SM, Ahmad M, Zahir AZ, Javaid A, Ashraf M (2014) The role of mycorrhizae and plant growth promoting rhizobacteria (PGPR) in improving crop productivity under stressful environments. Biotechnol. Adv. 32(2):429–48. https://doi.org/10.1016/j.biotechadv.2013.12.005.

Navarro-Ródenas A, Morte A, Pérez-Gilabert M (2009) Partial purification, characterization and histochemical localization of alkaline phosphatase from ascocarps of the edible desert truffle *Terfezia claveryi* Chatin. Plant Biol. 11(5):678-685. https://doi.org/10.1111/j.1438-8677.2008.00172.x

Navarro-Ródenas A (2011) Caracterización de la actividad fosfatasa y estudio de la respuesta a la sequía en la simbiosis micorrícica de *Helianthemum almeriense* Pau y *Terfezia claveryi* Chatin. Dissertation. Dpto de Biología Vegetal. University of Murcia, Murcia. pp. 295.

Navarro-Ródenas A, Pérez-Gilabert M, Torrente P, Morte A (2012a) The role of phosphorus in the ectendomycorrhiza *continuum* of desert truffle mycorrhizal plants. Mycorrhiza 22(7): 565-575. https://doi.org/10.1007/s00572-012-0434-2.

Navarro-Ródenas A, Ruíz-Lozano JM, Kaldenhoff R, Morte A (2012b) The aquaporin TcAQP1 of the desert truffle *Terfezia claveryi* is a membrane pore for water and CO_2 transport. Mol. Plant Microbe Interact. 25(2):259–66. https://doi.org/10.1094/mpmi-07-11-0190.

Navarro-Ródenas A, Bárzana G, Nicolás E, Carra A, Schubert A, Morte A (2013) Expression analysis of aquaporins from desert truffle mycorrhizal symbiosis reveals a fine-tuned regulation under drought. Mol. Plant Microbe Interact. 26(9):1068–78. https://doi.org/10.1094/MPMI-07-12-0178-R.

Navarro-Ródenas A, Nicolás E, Morte A (2015) Effect of irrigation on desert truffle mycorrhizal plants in field. XXI Reunión de la Sociedad Española de Fisiología Vegetal, Toledo, Spain.

Navarro-Ródenas A, Berná LM, Lozano-Carrillo C, Andrino A, Morte A (2016) Beneficial native bacteria improve survival and mycorrhization of desert truffle mycorrhizal plants in nursery conditions. Mycorrhiza 26(7):769–79. https://doi.org/10.1007/s00572-016-0711-6.

Navarro-Ródenas A, Carra A, Morte A (2018) Identification of an alternative rRNA post-transcriptional maturation of 26S rRNA in the Kingdom Fungi. Front. Microbiol. 9(MAY):1–8. https://doi.org/10.3389/fmicb.2018.00994.

Nilsen ET, Muller WH (1981) Phenology of the drought-deciduous shrub *Lotus scoparius*: climatic controls and adaptive significance. Ecol. Monogr. 51(3):323–41. https://doi.org/10.2307/2937277.

Pachelewski R, Kermen J, Chrusiak E, Trzcinka M (1991–1992) Studies on pine ectendomycorrhizae in nurseries. Acta Mycol. 27:49–61.

Parry MAJ, Keys AJ, Madgwick PJ, Carmo-Silva AE, Andralojc PJ (2008) Rubisco regulation: a role for inhibitors. J. Exp. Bot. 59(7):1569–80. https://doi.org/10.1093/jxb/ern084.

Parry MAJ, Andralojc PJ, Scales JC, Salvucci ME, Carmo-Silva AE, Alonso H, Whitney SM (2013) Rubisco activity and regulation as targets for crop improvement. J. Exp. Bot. 64:717–730. https://doi.org/10.1093/jxb/ers336.

Pedranzani H, Rodríguez-Rivera M, Gutiérrez M, Porcel R, Hause B, Ruiz-Lozano JM (2016) Arbuscular mycorrhizal symbiosis regulates physiology and performance of *Digitaria eriantha* plants subjected to abiotic stresses. Mycorrhiza 26(2):141-52. https://doi.org/10.1007/s00572-015-0653-4.

Pellegrin C, Martin F, Veneault-Fourrey C (2019) Molecular signalling during the ectomycorrhizal symbiosis. In: Hoffmeister D, Gressler M, eds. Biology of the Fungal Cell. The Mycota (A Comprehensive Treatise on Fungi as Experimental Systems for Basic and Applied Research), vol 8. Springer, Cham. https://doi.org/10.1007/978-3-030-05448-9_6.

Pérez-Gilabert M, Morte A, Honrubia M, García-Carmona F (2001a) Monophenolase activity of latent *Terfezia claveryi* tyrosinase: characterization and histochemical localization. Physiol. Plant. 113:203–09. https://doi.org/10.1034/j.1399-3054.2001.1130207.x.

Pérez-Gilabert M, Morte A, Honrubia M, García-Carmona F (2001b) Partial purification, characterization, and histochemical localization of fully latent desert truffle (*Terfezia claveryi* Chatin) polyphenol oxidase. J. Agric. Food Chem. 49:1922–1927. https://doi.org/10.1021/jf001009n.

Pérez-Gilabert M, Sánchez-Felipe I, García-Carmona F (2005a) Purification and partial characterization of lipoxygenase from desert truffle (*Terfezia claveryi* Chatin) ascocarps. J. Agric. Food. Chem. 53:3666–3671. https://doi.org/10.1021/jf048087l.

Pérez-Gilabert M, Morte A, Ávila-Gónzalez R, García-Carmona F (2005b) Characterization and histochemical localization of nonspecific esterase from ascocarps of desert truffle (*Terfezia claveryi* Chatin). 53:5754–5759. https://doi.org/10.1021/jf050334d.

Pérez-Gilabert M, García-Carmona F, Morte A (2014) Enzymes in *Terfezia claveryi* ascocarps. In: Kagan-Zur V, Roth-Bejerano N, Sitrit Y, Morte A, eds. Desert Truffles. Springer Berlin Heidelberg pp. 243–261. https://doi.org/10.1007/978-3-642-40096-4_16.

Perotto S, Daghino S, Martino E (2018) Ericoid mycorrhizal fungi and their genomes: another side to the mycorrhizal symbiosis? New Phytol. 220(4):1141–47. https://doi.org/10.1111/nph.15218.

Peter M, Kohler A, Ohm RA, Kuo A, Krützmann E, Morin E, et al. (2016) Ectomycorrhizal ecology is imprinted in the genome of the dominant symbiotic fungus *Cenococcum geophilum*. Nat. Comm. 7(7):12662. https://doi.org/10.1038/ncomms12662.

Piché Y, Ackerley CA, Peterson RL (1986) Structural characteristics of ectendomycorrhizas synthesized between roots of *Pinus resinosa* and the E-strain fungus *Wilcoxina mikolae* var. mikolae. New Phytol. 104:447–452.

Plett JM, Kemppainen M, Kale SD, Kohler A, Legué V, Brun A, et al. (2011) A secreted effector protein of *Laccaria bicolor* is required for symbiosis development. Curr. Biol. 21(14):1197-1203. https://doi.org/10.1016/j.cub.2011.05.033.

Plett JM, Daguerre Y, Wittulsky S, Vayssieres A, Deveau A, Melton SJ, et al. (2014) Effector MiSSP7 of the mutualistic fungus *Laccaria bicolor* stabilizes the *Populus* JAZ6 protein and represses jasmonic acid (JA) responsive genes. Proc. Natl. Acad. Sci. USA 111(22): 8299–8304. https://doi.org/10.1073/pnas.1322671111.

Poorter H, Niinemets U, Poorter L, Wright I, Villar R (2009) Causes and consequences of variation in leaf mass per area (LMA): a meta-analysis. New Phytol. 182(3):565–88. http://dx.doi.org/10.1111/j.1469-8137.2009.02830.x.

Porcel R, Ruiz-Lozano JM (2004) Arbuscular mycorrhizal influence on leaf water potential, solute accumulation, and oxidative stress in soybean plants subjected to drought stress. J. Exp. Bot. 55(403):1743–1750. https://doi.org/10.1093/jxb/erh188.

Pozo MJ., Azcón-Aguilar C (2007) Unraveling mycorrhiza-induced resistance. Curr. Opin Plant Biol. 10(4):393–98. https://doi.org/10.1016/j.pbi.2007.05.004.

Pusztahelyi T, Holb IJ, Pocsi I (2015) Secondary metabolites in fungus-plant interactions. Front Plant Sci. 6(August):1–23. https://doi.org/10.3389/fpls.2015.00573.

Raffaele S, Kamoun S (2012) Genome evolution in filamentous plant pathogens: why bigger can be better. Nat. Rev. Microbiol. 10: 417–430. https://doi.org/10.1038/nrmicro2790.

Roth-Bejerano N, Li YF, Kagan-Zur V (2004) Homokaryotic and heterokaryotic hyphae in *Terfezia*. Antonie van Leeuwenhoek 85(2):165–68. https://doi.org/10.1023/B:ANTO.0000020283.99376.55.

Roth-Bejerano N, Navarro-Ródenas A, Gutiérrez A (2014) Hypogeous desert fungi. In: Kagan-Zur V, Roth-Bejerano N, Sitrit Y, Morte A, eds. Desert Truffles. Phylogeny, Physiology, Distribution and Domestication. Soil Biology, volume 38, Springer-Verlag, Berlin, Heidelberg pp. 57–67. https://doi.org/10.1007/978-3-642-40096-4_5.

Rubini A, Belfiori B, Riccioni C, Tisserant E, Arcioni S, Martin F, Paolocci F (2011) Isolation and characterization of MAT genes in the symbiotic ascomycete *Tuber melanosporum*. New Phytol. 189(3): 710–722. https://doi.org/10.1111/j.1469-8137.2010.03492.x.

Rubini A, Riccioni C, Belfiori B, Paolocci F (2014) Impact of the competition between mating types on the cultivation of *Tuber melanosporum*: Romeo and Juliet and the matter of space and time. Mycorrhiza 24(1):19-27. https://doi.org/10.1007/s00572-013-0551-6.

Ruiz-Lozano JM, Porcel R, Aroca R (2008) Evaluation of the possible participation of drought-induced genes in the enhanced tolerance of arbuscular mycorrhizal plants to water deficit. In: Varma A, ed. Mycorrhiza. Berlin, Heidelberg: Springer pp. 185–205. https://doi.org/10.1007/978-3-540-78826-3_10.

Salzer P, Corbière H, Boller T (1999) Hydrogen peroxide acculation in *Medicago truncatula* roots colonized by the arbuscular mycorrhiza-forming fungus *Glomus intraradices*. Planta 208(3):319–25. https://doi.org/10.1007/s004250050565.

Sanger F, Nicklen S, Coulson AR (1977) DNA sequencing with chain-terminating inhibitors. Proc. Nat. Acad. Sci. USA 74(12):5463-5467. https://doi.org/10.1073/pnas.74.12.5463.

Scales PF, Peterson RL (1991a) Structure and development of *Pinus banksiana–Wilcoxina ectendomycorrhizae*. Can. J. Bot. 69:2135–2148.

Scales PF, Peterson RL (1991b) Structure of ectomycorrhizae formed by *Wilcoxina mikolae* var. mikolae with *Picea mariana* and *Betula alleghaniensis*. Can. J. Bot. 69:2149–2157.

Schlesinger WH, Reynolds JF, Cunningham GL, Laura F, Jarrell WM, Virginia RA, et al. (1990) Biological feedbacks in global desertification conceptual models for desertification. Science 247(4946): 1043–1048. https://doi.org/10.1126/science.247.4946.1043.

Shavit E (2014) The history of desert truffle use. In: Kagan-Zur V, Roth-Bejerano N, Sitrit Y, Morte A, eds. Desert Truffles. Phylogeny, Physiology, Distribution and Domestication. Soil Biology, volume 38, Springer-Verlag, Berlin, Heidelberg pp. 217–243. https://doi.org/10.1007/978-3-642-40096-4_15.

Shavit E, Shavit E (2014) The medicinal value of desert truffles. In: Kagan-Zur V, Roth-Bejerano N, Sitrit Y, Morte A, eds. Desert Truffles. Phylogeny, Physiology, Distribution and Domestication. Soil Biology, volume 38, Springer-Verlag, Berlin, Heidelberg pp. 323–343. https://doi.org/10.1007/978-3-642-40096-4_20.

Slama A, Fortas Z, Boudabous A, Neffati, M (2010) Cultivation of an edible desert truffle (*Terfezia boudieri* Chatin). Afr. J. Microbiol. Res. 4(22): 2350–2356.

Smith, SE, Read D (2008) Mycorrhizal Symbiosis (Third Edition), 1-9. London: Academic Press.

Spreitzer RJ. Salvucci ME (2002) Rubisco: Structure, regulatory interactions, and possibilities for a better enzyme. Ann. Rev. Plant. Biol. 53(1):449–75. https://doi.org/10.1146/annurev.arplant.53.100301.135233.

Steudle E (2000) Water uptake by plant roots: an integration of views. Plant and soil 226(1):45-56. https://doi.org/10.1023/A:1026439226716.

Strullu-Derrien C, Selosse MA, Kenrick P, Martin F (2018) The origin and evolution of mycorrhizal symbioses: from palaeomycology to phylogenomics. New Phytol. 220(4): 1012–30. https://doi.org/10.1111/nph.15076.

Swann, ALS, Hoffman FM, Koven CD, Randerson JT (2016) Plant responses to increasing CO_2 reduce estimates of climate impacts on drought severity. Proc. Natl. Acad .Sci. USA 113(36):10019–24. https://doi.org/10.1073/pnas.1604581113.

Switala J, Loewen PC (2002) Diversity of properties among catalases. Arch. Biochem. Biophisics 401:145–54. https://doi.org/10.1016/S0003-9861(02)00049-8.

Tedersoo L, Smith ME (2017) Biogeography of Mycorrhizal Symbiosis Ecological Studies, vol. 230. Springer. https://doi.org/10.1007/978-3-319-56363-3.

Theodorou C, Bowen GD (1970) Mycorrhizal responses of radiata pine in experiments with different fungi. Australian Forestry 34:183-191.

Tisserant E, Malbreil M, Kuo A, Kohler A, Symeonidi A, Balestrini R, et al. (2013) Genome of an arbuscular mycorrhizal fungus provides insight into the oldest plant symbiosis. Proceed. Natl. Acad. Sci. USA 110(50):20117-20122. https://doi.org/10.1073/pnas.1313452110.

Trappe M (1979) The orders, families, and genera of hypogeous Ascomycotina (truffles and their relatives). Mycotaxon 9:297-340.

Tulasne LR, Tulasne C (1851). Fungi Hypogaei: Histoire et Monographie des Champignons Hypogés. Klincksieck, Paris.

Törnroth-Horsefield S, Hedfalk K, Fischer G, Lindkvist-Petersson K, Neutze R (2010) Structural insights into eukaryotic aquaporin regulation. FEBS Letters 584(12):2580–88. https://doi.org/10.1016/j.febslet.2010.04.037.

United Nations Educational, Scientific and Cultural Organization (UNESCO) (1979) Map of theworld distribution of arid regions: map at scale 1:25,000,000 with explanatory note. MAB Technical Notes 7, UNESCO, Paris.

Van der Heijden MG, Martin F, Selosse MA, Sanders IR (2015) Mycorrhizal ecology and evolution: the past, the present, and the future. New Phytol. 205(4):1406-1423. https://doi.org/10.1111/nph.13288.

Veneault-Fourrey C, Commun C, Kohler A, Morin E, Balestrini R, Plett J, et al. (2014) Genomic and transcriptomic analysis of *Laccaria bicolor* CAZome reveals insights into polysaccharides remodelling during symbiosis establishment. Fungal Genet. Biol. 72: 168–181. https://doi.org/10.1016/j.fgb.2014.08.007.

Verkman AS, Mitra AK (2000) Structure and function of aquaporin water channels. Am. J. Physiology-Renal Physiol. 278(1):F13-F28.

Yaneff A, Sigaut L, Marquez M, Alleva K, Pietrasanta LI, Amodeo G (2014) Heteromerization of PIP aquaporins affects their intrinsic permeability. Proc. Natl. Acad. Sci. USA 111(1):231–36. https://doi.org/10.1073/pnas.1316537111.

Yu TE, Egger KN, Peterson LR (2001) Ectendomycorrhizal associations - Characteristics and functions. Mycorrhiza 11(4):167–177. https://doi.org/10.1007/s005720100110.

Zampieri E, Rizzello R, Bonfante P, Mello A (2012) The detection of mating type genes of *Tuber melanosporum* in productive and non productive soils. Appl. Soil Ecol. 57:9-15. https://doi.org/10.1016/j.apsoil.2012.02.013.

Zardoya, R (2005) Phylogeny and evolution of the major intrinsic protein family. Biol. Cell 97(6):397–414. https://doi.org/10.1042/BC20040134.

Zaretsky M, Kagan-Zur V, Mills D, Roth-Bejerano N (2006a) Analysis of mycorrhizal associations formed by *Cistus incanus* transformed root clones with *Terfezia boudieri* isolates. Plant Cell. Rep. 25(1): 62–70. https://doi.org/10.1007/s00299-005-0035-z.

Zaretsky M, Sitrit Y, Mills D, Roth-Bejerano N, Kagan-Zur V (2006b) Differential expression of fungal genes at preinfection and mycorrhiza establishment between *Terfezia boudieri* isolates and *Cistus incanus* hairy root clones. New Phytol. 171(4): 837–846. https://doi.org/10.1111/j.1469-8137.2006.01791.x.

Zwiazek J, Xu H, Tan X, Navarro-Ródenas A, Morte A (2017) Significance of oxygen transport through aquaporins. Sci. Rep. 7:1–11. https://doi.org/10.1038/srep40411.

C H A P T E R   II

Objectives

The aim of this thesis is to deepen the knowledge of the mycorrhizal symbiosis *Terfezia claveryi* x *Helianthemum almeriense*, its water relations and cultivation.

In order to address this overall purpose, the following specific objectives are proposed:

1. To assess the role of fungal catalases in the *T. claveryi* x *H. almeriense* symbiosis, especially during mycorrhiza formation and in drought conditions.

2. To describe the genomic features of desert truffles that are relevant to their cultivation, focusing on their reproductive mode, the development of the different symbiotic structures that these fungi form in the roots of their hosts, and their adaptations to semiarid environments.

3. To determine which agroclimatic parameters can be positively or negatively correlated with the productivity of desert truffles and to know the critical periods thorughout the year in which these agroclimatic parameters most importantly determine truffle crops.

4. To characterize the responses of the desert truffle plant *H. almeriense* to the environment in spring, to search for morpho-physio-molecular markers that could help us to track easily the changes in phenology and to evaluate the relationships between the markers of the plant phenology and productivity of desert truffle.

5. To evaluate the effects of the increase in atmospheric CO_2 concentration and its interaction with the increasing drought of the Mediterranean springs to the physiological responses of the *H. almeriense* x *T. claveryi* mycorrhizal symbiosis.

Characterization and purification of *Terfezia claveryi* TcCAT-1, a desert truffle catalase upregulated in mycorrhizal symbiosis

3.1. Introduction

Desert truffles are a group of edible hypogeous ascomycetes that form mycorrhizal symbiosis with plants of the Cistaceae family. Some species of *Terfezia, Tirmania* and *Picoa* belong to this group of truffles, which are distributed in arid and semiarid areas, mainly around the Mediterranean countries, from the South of Europe to the North of Africa. **Terfezia claveryi** Chatin is one of the best known desert truffle species because of its great ecological and commercial value (Morte et al., 2008). The type of association formed between this species and *Helianthemum* genus plants is an **ectendomycorrhiza**, characterized by the presence of both intercellular Hartig net and intracellular hyphae penetrating the cortex cells (Roth-Bejerano et al., 2014). Furthermore, biotechnological advances have allowed cultivation and subsequent commercialization of this species using **Helianthemum almeriense** Pau as host plant (Morte et al., 2012; 2017).

Drought is one of the main limiting factors for photosynthesis, growth and survival of Mediterranean plants (Bacelar et al., 2009). One of the consequences of hydric deficit in plants is oxidative stress, which implies an excessive accumulation of reactive oxygen species (ROS) such as superoxide anion and **hydrogen peroxide** (**H_2O_2**). Therefore, antioxidant systems, both enzymatic and non-enzymatic, must be involved in water-stress tolerance mechanisms. It is well known that mycorrhizal fungi modify water relations in the host (Nelsen et al., 1987). The majority of studies about this topic have been carried out in arbuscular mycorrhiza (AM) symbiosis and they suggest several mechanisms by which this symbiosis can alleviate drought stress in host plants (Ruiz-Lozano et al., 2008). One of these mechanisms is the protection against the oxidative damage generated by drought. In soybean inoculated with AM, there is a decrease in the oxidative damage to lipids in roots during water-deficit conditions (Porcel et al., 2004). Under drought stress, roots of AM *Digitaria eriantha* plants showed lower levels of H_2O_2 and higher catalase activity than their non-mycorrhizal counterparts (Pedranzani et al., 2016). Thus, fungal enzymes involved in the control of the levels of H_2O_2 may be involved in the enhanced resistance to drought stress of mycorrhizal plants. Mycorrhizal plants of *H. almeriense* with *T. claveryi* are well adapted to semiarid conditions and the negative effects of drought are reduced in these plants by specific physiological (transpiration, water use efficiency, aquaporin expression), nutritional (P, N and K

content) and morphological alterations due to the mycorrhizal colonization (Morte et al., 2000; 2010; Navarro-Ródenas et al., 2013).

It is well known that H_2O_2 at high concentrations is toxic to cells, but there are evidences involving this molecule in signaling, apoptosis or cell differentiation (Díaz et al., 2001). The intracellular colonization of the AM *Funneliformis mosseae* is known to be limited by the oxidative burst produced in *Medicago trunculata* host roots (Salzer et al., 1999). Baptista et al. (2007) stated that during the early stages of ectomycorrhizal establishment of *Pisolithus tinctorious* x *Castanea sativa*, H_2O_2 accumulates following a pattern similar to the one showed by pathogenic fungi (Wojtaszek, 1997) and it is a candidate signaling molecule for symbiosis (Navarro-Ródenas et al., 2015).

Catalases are the main enzymes responsible for the dismutation of H_2O_2 into water and dioxygen. Catalase activity has been observed in three groups of enzymes: "typical" monofunctional heme-catalases (the largest and most extensively studied), bifunctional catalases-peroxidases and non-heme catalases. In addition, low levels of catalase activity are found in many heme containing proteins not normally considered to be catalases (Switala and Loewen, 2002). Monofunctional heme-catalases have been classified following two criteria: subunit size and phylogeny. Based on subunit size they are divided in two groups: the **large subunit size catalases**, "**LSCs**" (>75 kDa), present only in bacteria and fungi and the **small subunit size catalases** "**SSCs**" (<60 kDa) (Hansberg et al., 2012; Chelikani et al., 2004). LSCs are classified in **L1** and **L2** subgroups. In fungi, L1-type catalases are not inducible and usually accumulate in spores, while those from the L2-type are usually induced by different stressors and are extracellular enzymes (Hansberg et al., 2012). Both LSCs and SSCs have proved to be active as tetramers and dimers, but not as monomers (Díaz et al., 2005). On the other hand, typical catalases are divided in three main evolutionary clades: **Clade 2**, comprising LSCs and **Clade 1** and **3** comprising SSCs. Clade 1 includes SSCs from bacteria, green algae and plants. Clade 2 groups the LSCs from bacteria and fungi while **Clade 3** contains SSCs from most phyla, including fungi, but not Viridiplantae (Hansberg et al., 2012).

There is little knowledge about the physiological role of catalases in fungi, even less in mycorrhizal fungi, but catalases may be involved both in mycorrhiza formation and in defense against drought stress. Thus, in order to test the relevance of fungal catalases in these processes, here we report on the purification and biochemical characterization of a catalase from *T. claveryi*, named TcCAT-1, as well as its expression

profile across different stages of *T. claveryi* life cycle and in *Helianthemum* plants mycorrhized with *T. claveryi* under different water treatments.

3.2.   Materials and methods

3.2.1.   Biochemical and sequence analysis

3.2.1.1.   *Enzyme extraction and purification*

Pieces of *T. claveryi* ascocarps collected in Zarzadilla de Totana (Lorca, Murcia, Spain) under *H. almeriense* shrubs, were homogenized using liquid nitrogen with a mortar and pestle and then suspended in 0.1 M sodium phosphate at pH 7.0 in a ratio of 1:4 (w/v). The homogenate was then centrifuged at 7,000 g for 20 min at 4 °C in a Sigma 2-16K centrifuge with a 12141-H rotor (Sigma, Osterode am Harz, Germany). The resultant supernatant was subjected to temperature phase partitioning with a 10% (w/v) final concentration of Triton X-114 (TX-114) prepared in the same buffer. The mixture was placed in a thermostatic bath at 37 °C for 30 min or until phase partitioning was achieved. This solution was centrifuged at 7,000 g for 20 min at 30 °C. After centrifugation, the supernatant was either used immediately or stored at -80 °C (where it was stable for more than one month). The buffer of the phase-partitioning supernatant was changed to buffer A (1.5 M ammonium sulphate in 10 mM Tris-HCl pH 6.9) by ultrafiltration using Amicon ®Ultra-4, 100,000 MWCO, (Merck Millipore Ltd., Ireland). Aliquots of 1 mL of this extract were loaded onto a HiTrap® Phenyl HP 1 mL column (GE Healthcare Life Sciences, Barcelona, Spain) connected to an Äkta purifier (GE Healthcare Life Sciences, Barcelona, Spain) and equilibrated with buffer A at a flow rate of 0.75 mL.min^{-1}. After the injection, the column was washed with buffer A and catalase activity was eluted from the column using a linear gradient 0-100% of buffer B (10 mM Tris-HCl pH 6.9). Aliquots containing catalase activity were then mixed and concentrated by filtration using Amicon ®Ultra-4, 10,000 MWCO centrifugal tubes. Aliquots of 100 µL were loaded onto a Superdex® 200 10/300 GL column (GE Healthcare Life Sciences, Barcelona, Spain) and eluted using buffer C (NaCl 150 mM in 50 mM sodium phosphate buffer pH 7.0) at a flow rate of 0.5 mL.min-1. The separation was followed at 280 nm and column fractions were assayed routinely for catalase activity in the standard reaction medium described below.

3.2.1.2. *Molecular mass determination*

Molecular mass of the native purified enzyme was estimated using Superdex® 200 10/300 GL gel filtration column, at the above mentioned conditions. Dextran blue, apoferritin (443 kDa), β- amylase (200 kDa), alcohol dehydrogenase (150 kDa), albumin (66 kDa), carbonic anhydrase (29kDa) and cobalt chloride were used as standards (**Figure 3.1**).

The graph shows a calibration plot with K_{av} on the y-axis (ranging 0 to 0.8) and Log_{10} molecular mass (Dalton) on the x-axis (ranging 4 to 5.4). The equation is:

$$y = -0.3912x + 2.3533$$
$$r^2 = 0.9875$$
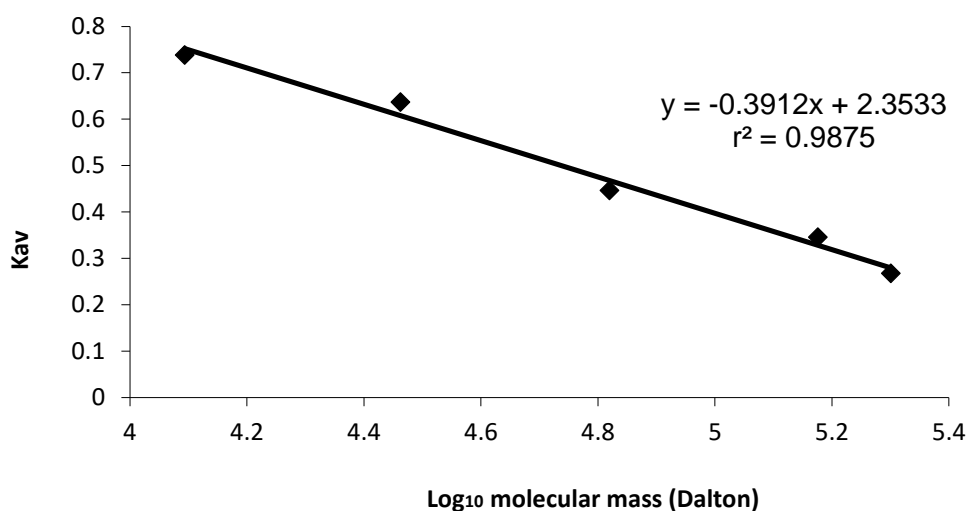
Figure 3.1. Standard calibration curve for molecular mass analysis by gel filtration. $K_{av} = (V_e-V_o) / (V_t-V_o)$, where K_{av} is the phase distribution coefficient, V_e is the elution volume, V_o is the void volume calculated with blue dextran and V_t is the total volume of the column.

The molecular mass determination of a TcCAT-1 monomer was performed by SDS-PAGE (sodium dodecyl sulfate gel electrophoresis) using a 10% gel. Samples from each purification stage and a commercial protein ladder (PageRuler™ Unstained High Range Protein Ladder, ThermoFisher), which consisted of protein standards of known molecular mass, were loaded on the same gel. After running and processing the gel (see **Appendix A: Supplementary protocols** for details) it was scanned. The images were analyzed using ImageJ software (https://imagej.net) and the molecular mass was calculated using a standard calibration curve (**Figure 3.2**). The band corresponding to the purified protein was further analyzed by mass spectrometry.
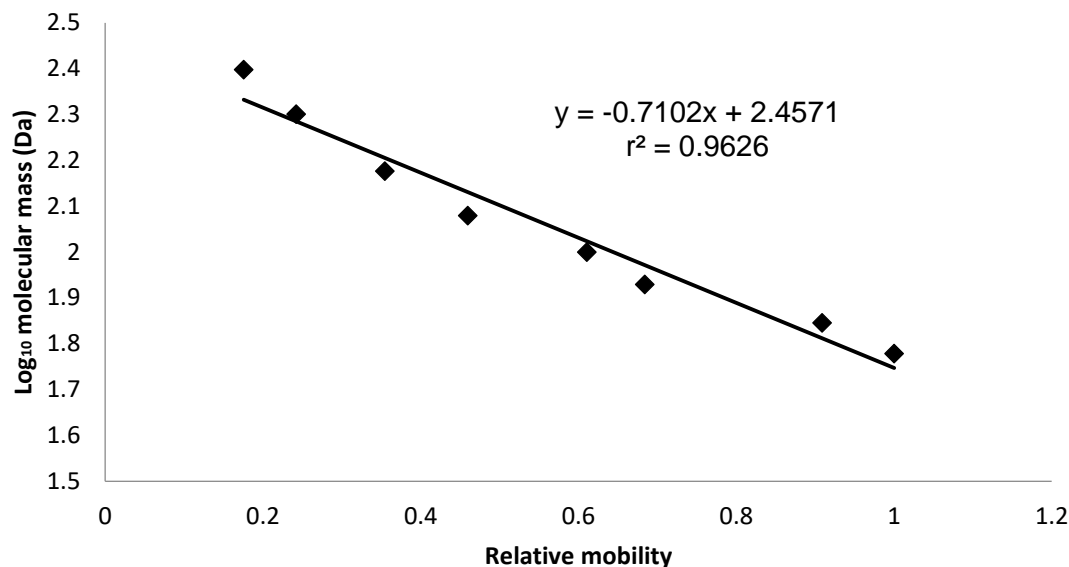
Figure 3.2. Standard calibration curve for monomer molecular, mass determination by SDS-PAGE. Each point represents the relative mobility of a protein standard (PageRuler™ Unstained High Range Protein Ladder, ThermoFisher).

3.2.1.3. Identification of the purified protein by mass spectrometry

The band corresponding to the purified protein was excised from the gel and distained with 50% acetonitrile–25 mM ammonium bicarbonate buffer (AMBIC) for 30 min at 37 °C. Then, it was dried with a vacuum evaporator, reduced with 20 mM dithiothreitol (DTT) (20 min at 56 °C) and alkylated with iodoacetamide 100 mM for 30 min at room temperature in the dark. The supernatant was removed and the bands were washed at 37 °C, with 25 mM AMBIC pH 8.5 and then with the same buffer in 50% acetonitrile, 15 min each time. After drying, the band was incubated with 0.5 µg of Trypsin Gold Proteomics Grade (Promega Corporation, Madison, MI, U.S.A) and 0.01 % ProteaseMax surfactant for 10 min at 4 °C and then at 37 °C for 3h. The supernatant was collected and residual peptides were washed out of the band with 50% acetonitrile in 0.5% trifluoroacetic acid (TFA) and 100% acetonitrile. Both extracts were combined, dried in a vacuum evaporator and resuspended in water/acetonitrile/formic acid (94.9:5:0.1). Analysis of the tryptic digests of the sample was carried out in an HPLC/MS system consisting of an HPLC connected to an Ion Trap XCT Plus Mass Spectrometer (Agilent Technologies, Santa Clara, CA, USA) using an electrospray interface, operating in the positive mode. Sample was injected onto a Waters XBridge BEH C18 HPLC column (Waters Corporation, USA), thermostatted at 40 °C, at a flow rate of 10 µl min^{-1}.

After washing with water/acetonitrile/formic acid (94.9:5:0.1) the digested peptides were eluted using a linear gradient 0-80% of water/acetonitrile/formic acid (10:89.9:0.1), for 150 min. Data processing was performed with Data Analysis program for LC/MSD Trap Version 3.3 (Bruker Daltonik, GmbH, Germany) and Spectrum Mill MS Proteomics Workbench (Revision A.03.02.060B, Agilent Technologies, Santa Clara, CA, USA) and peptides were matched against *Terfezia claveryi* database from the Joint Genome Institue (https://genome.jgi.doe.gov/programs/fungi/index.jsf).

3.2.1.4. *Sequence analysis*

Sequences of several fungal catalases were collected from the following public databases: MycoCosm, GenBank, Protein Data Bank and UniprotKB. A total of 29 selected fungal sequences (**Table 3.1**) were aligned using Clustal Omega (Sievers et al., 2011); the multiple sequence alignment obtained was cut, saving only the conserved core region (from residue 66 to 557, numbering for TcCAT-1). An unrooted phylogenetic tree was generated with MEGA 6.0 (Tamura et al., 2013) using the Maximum-Likelihood method.

TcCAT-1 homology modeling was carried out with Swiss-Model (Biasini et al., 2014) using as template the coordinates of a catalase from *Scytalidium thermophilum* (PDB: 4AUE). Model and template were superimposed using the command MatchMaker from UCSF Chimera package (Pettersen et al., 2004). The sequences of the modeled TcCAT-1, together with those of 4AUE and catalases from *Penicillium vitale* (2XF2) and *N. crassa* (3EJS) and the two other catalases from *T. claveryi* genome, ID 1091969 and ID 1248402, were aligned using Clustal Omega (Sievers et al., 2011). The alignment, was displayed using ESPript (Robert et al., 2014).

Table 3.1. Catalase fungal sequences used for the phylogenetic tree construction

Species	Name	Database	Accesion Number
Alternaria alternata	Alt_alt_L2	NCBI/GenBank	OWY51759.1
Aspergillus fumigatus	Asp_fum_L2	NCBI/RefSeq	XP_748550
Aspergillus nidulans	Asp_nid_L2	NCBI/RefSeq	XP_682608.1
Aspergillus nidulans	Asp_nid_S	NCBI/GenBank	AAG45152.2
Aspergillus oryzae	Asp_ory_L1	NCBI/GenBank	BAC56946.1
Aspergillus oryzae	Asp_ory_S	NCBI/GenBank	BAE63583.1
Bipolaris_maydis	Bip_may_L2	NCBI/RefSeq	XP_014078299.1
Botrytis cinerea	Bot_cin_L2	NCBI/GenBank	AAK77951.1
Candida albicans	Can_alb_S	NCBI/RefSeq	XP_718818.1
Coccidioides immitis	Coc_imm_L1	UniportKB	J3K0Y0
Coccidioides immitis	Coc_imm_S	NCBI/GenBank	EAS33312.3
Histoplasma capsulatum	His_cap_L1	NCBI/Genbank	AAF01462.1
Leptosphaeria maculans	Lep_mac_L1	NCBI/RefSeq	XP_003841429.1
Mycosphaerella graminicola	Myc_gra_L1	Mycocosm/JGI	98331
Neurospora crassa	Neu_cra_L1	UniportKB	Q9C168
Neurospora crassa	Neu_cra_L2	PDB	3EJ6
Neurospora crassa	Neu_cra_S	NCBI/GenBank	EAA32637.1
Penicillium citrinum	Pen_cit_L2	NCBI/GenBank	ABB89950.1
Penicillium vitale	Pen_vit_ L2	PDB	2XF2
Scytalidum thermophilum	Scy_the_L2	PDB	4AUE
Terfezia boudieri	Ter_bou_783759	Mycocosm/JGI	783759
Terfezia boudieri	Ter_bou_817666	Mycocosm/JGI	817666
Terfezia boudieri	Ter_bou_841489	Mycocosm/JGI	841489
Terfezia claveryi	Ter_cla_1091969	Mycocosm/JGI	1091969
Terfezia claveryi	Tc_CAT_1	Mycocosm/JGI	1216276
Terfezia claveryi	Ter_cla_1248402	Mycocosm/JGI	1248402
Trichoderma virens	Tri_vir_L1	Mycocosm/JGI	38844
Tuber melanosporum	Tub_mel_6264	Mycocosm/JGI	6264
Tuber melanosporum	Tub_mel_2118	Mycocosm/JGI	2118

3.2.1.5. Biochemical characterization

Unless otherwise stated, the standard reaction medium to measure TcCAT-1 activity consisted of 1 U of enzyme, 10 mM H_2O_2 and 0.1 M sodium phosphate buffer pH 7.0, in a final volume of 1 mL. One unit of enzyme activity (U) is defined as the amount of enzyme that decomposes one µmol of H_2O_2 per minute at room temperature in the standard reaction medium. The reaction was started by adding the enzyme, and the decrease in absorbance at 240 nm was followed in a Jasco V-650 spectrophotometer. A

blank without enzyme was prepared for each measurement. The H_2O_2 concentration was calculated using $\varepsilon_{240} = 39.4$ $M^{-1}cm^{-1}$ (Nelson et al., 1974).

To determine the effect of pH, TcCAT-1 activity was followed at 25 °C in the standard reaction medium using the following buffers 0.1 M: acetate (pH 4-5), phosphate (pH 5-12), Tris-HCl (pH 7-10) and carbonate (pH 10-11).

The optimum temperature was determined using the standard reaction medium described above. The measurements were recorded on a Shimadzu UV-2401PC spectrophotometer equipped with a Peltier thermoelectric temperature controlling unit (TCC-240A). Once the medium was taken to the desired temperature the reaction was started by adding the enzyme.

To study the thermostability of TcCAT-1, the enzyme was incubated at different temperatures, in phosphate buffer 0.1 M pH 7.0 for 1 h and the residual activity was measured at 25 °C, in the standard reaction medium. The range of temperatures used in both assays was between 20 °C and 70 °C.

The effect of H_2O_2 concentration on TcCAT-1 activity was determined measuring the initial rate of the H_2O_2 consumption spectrophotometrically in the standard reaction medium changing the H_2O_2 concentration from 0.15 mM to 70 mM. The apparent K_m and V_{max} were calculated by nonlinear regression fitting of the experimental points to the Michaelis-Menten equation.

Monofunctional heme-catalases are sensitive to a number of compounds, such as hydroxylamine, 2-mercaptoethanol and 3-aminotriazole (3-AT) (Switala et al., 2002). The inhibition of TcCAT-1 was measured using different concentrations of hydroxylamine (up to 0.5 µM), mercaptoehanol (up to 5 mM) or 3-aminotriazol (3-AT) (up to 20 mM) in the standard reaction medium. Inactivation by 3-AT was studied by incubating the enzyme with 3-AT in 0.1 M phosphate buffer pH 7.0 for one hour. At 10 min intervals, aliquots were withdrawn from this incubation media (1 U of enzyme per mL of 10 mM 3-AT) and the reaction was started by adding H_2O_2 (10 mM final concentration).

In order to evaluate if the purified TcCAT-1 presented also peroxidase activity, a reaction medium consisting of 1 U enzyme, 2,2'-azino-bis (3-ethylbenzothiazoline-6-sulphonic acid) (ABTS) 2 mM, H_2O_2 1 mM and 0.1 acetate buffer pH 4.0, final volume

1 mL was prepared and changes in absorbance were measured at 405 nm in a Jasco V-650 spectrophotometer. Different amounts of enzyme were tested and a blank without enzyme was prepared for each measurement.

Effect of pH, temperature, substrate and inhibitor concentration and peroxidase activity assays were performed in triplicate and the mean and standard deviation were plotted.

3.2.2. TcCAT-1 expression and drought stress assay

3.2.2.1. Biological material

Mature ascocarps of *T. claveryi* were collected in Zarzadilla de Totana (Lorca, Murcia, Spain) under *H. almeriense* shrubs and rinsed carefully with water to remove any soil debris. Gleba and peridium were carefully separated flash frozen in liquid nitrogen and stored at -80 °C until use. Mature ascocarps collected in the above location were used to isolate *T. claveryi* mycelium, strain T7, which was grown in vitro in Erlenmeyer flasks containing Modified Melin-Norkrans optimal (MMNo) medium (Arenas et al., 2018) . The cultures were shaken at 100 rpm and maintained in the dark at 23 °C for three months. Then, and then mycelium was collected, flash frozen in liquid nitrogen and stored at -80 °C until used (for detailed medium composition see **Appendix A: Supplementary protocols**).

H. almeriense seeds were collected in the same location and germinated according to Navarro-Ródenas et al. (2013), with some modifications. Briefly, they were scarified and surface sterilized with 10 % H_2O_2 (20 min) and germinated in 75 cc pots with a substrate consisting of peat moss:perlite mix, 1:1 (v:v). After two months of growth, they were transferred to 230 cc pots. Approximately 10^5 *T. claveryi* spores were mixed with the new substrate and added to the pots during the transference of the plants. These spores were obtained from mature ascocarps as explained in Morte et al., (2008). Mycorrhizal status was checked by microscopy methods three months after spore inoculation and then half of the plants were subjected to drought stress before taking measurements. Non-mycorrhizal plants, both well-watered (WWNMP) and drought-stressed (DSNMP) controls were also grown. A total of six plants per treatment: well-watered mycorrhizal plants (WWMP), drought-stressed mycorrhizal plants (DSMP),

WWNMP and DSNMP were obtained. Shoot water potential (Ψ) was measured periodically to check the water status of the plant. To this aim, 5 cm-long plant apices were covered in dark during one hour, cut and immediately placed in a pressure chamber (Soil Moisture Equipment Co; Santa Barbara, CA, U.S.A.) according to Scholander et al., (1965). Furthermore, relative soil moist content was calculated periodically by the gravimetric method (Brakensiek et al., 1979). It was over 75 % in well watered treatments while it reached 40 % in drought treatments. The moisture content was maintained at these values for all the treatments until WWMP and WWNMP showed a $\Psi > -1$ MPa and DSMP and DSNMP $\Psi < -2$ MPa, values considered as moderate drought stress for this species according to previous works (Morte et al., 2010; Navarro-Ródenas et al., 2013). When reached, secondary and tertiary roots containing apical tips, were rinsed to remove soil, harvested and immediately stained and observed under an Olympus BH2 microscope, as explained later or flash frozen in liquid nitrogen and stored at -80 °C for RNA extraction.

3.2.2.2. *RNA isolation and quantitative real-time PCR*

In order to study TcCAT-1 in different phases of *T. claveryi* life cycle and during drought stress, RNA isolation and quantitative real-time PCR was performed in several biological samples and conditions, explained before. 100 mg of WWMP and DSMP roots, mycelium and ascocarp were homogenized in liquid nitrogen with the help of mortar and pestle. RNA was extracted from secondary and tertiary roots (including apical tips) of WWMP and DSMP according to Chang et al. (1993) (detailed protocol in **Appendix A: Supplementary protocols**), and from mycelium cultures and ascocarps using RNAeasy Plant Mini Kit (Qiagen, Hilden, Germany Qiagen), following manufacturer instructions. cDNA was synthetised by Reverse-Transcrption Polymerase Chain Reaction (RT-PCR) from 0.5 µg of total RNA from each sample using QuantiTect Reverse Transcription Kit (Qiagen, Hilden, Germany), following manufacturer´s instructions.

Expression of TcCAT-1 was studied by real-time PCR using a QuantStudioTM 5 Flex (Applied Biosystems, Foster City, California, USA). TcCAT-1 forward (and TcCAT-1 reverse primers were designed in the 3'untraslated region using http://www.idtdna.com (**Table 3.2**). Each 15 µl reaction contained 1.5 µl of 1:10 cDNA

template, 0.11 µl of primer mix 5 µM each and 7.5 µl of SyBR Green Master Mix (Applied biosystems, Foster City, California, USA). The PCR program consisted of 10-min incubation at 95 °C, followed by 40 cycles of 15s at 95 °C and 1 min at 60 °C, where the fluorescence signal was measured.

The efficiency of the primer set was evaluated by performing real-time PCR on several dilutions of cDNA. Real-time PCR threshold cycle (Ct) was determined in triplicate. 2-ΔΔCt method was used to evaluate the expression of each gene [33] normalizing gene expression to the geometric mean of elongation factor (EF1-alfaII) (JF491354, NCBI) and actin (ID1089750, Mycocosm) levels (**Table 3.2**). These genes have been confirmed as a proper reference genes in different conditions using transcriptomics analyses (unpublished results) and geNorm, included in qbase+ software, version 3.0 (Biogazelle, Zwijnaarde, Belgium (www.qbaseplus.com). All primers were tested on all different samples to test specificity and cross amplification (**Table 3.2**). Real-time PCR experiments were carried out in six separate biological samples and non-template controls were performed in all PCR reactions.

Table 3.2. Primers used in the study, *geNorm* M score and cross amplification test. NMP = Non-mycorrhizal plants; FLM = Free living mycelium; A = Ascocarp. For Ct mean calculation three biological replicates and three technical replicates were used.

Primer	Gene	Sequence (forward and reverse respectively)	Efficiency (%)	Stability (geNorm)	Sample	Ct mean
TcCAT-1	Catalase	5'GGAGAGGGTTGGTGTAATTCTT'3 5'GCTGCCCTTGATAACCCTATT'3	80.9	nd	NMP	Undetermined
					FLM	25.365 ± 0.177
					A	24.742 ± 0.707
					WWMP	28.150 ± 0.584
					DSMP	28.590 ± 0.671
TcActin	Actin	5'CACTGGAGCATGGGATTGT'3 5'GTACTGGATGCTCCTCAGAAAG'3	99.5	0.342	NMP	Undetermined
					FLM	26.367 ± 0.182
					A	26.537 ± 0.308
					WWMP	33.525 ± 0.880
					DSMP	33.404 ± 0.820
TcEF	Elongation Factor	5'TCCGTTAAGGAAATTCGTCG'3 5'GTCCAGGGTGGTTCATCAAG'3	97.71	0.312	NMP	Undetermined
					FLM	21.042 ± 0.720
					A	20.655 ± 0.182
					WWMP	30.686 ± 0.915
					DSMP	30.674 ± 0.884

3.2.2.3. H_2O_2 root content determination

150 mg of frozen roots from WWMP, WWNMP, DSMP and DSNMP treatments were homogenized in liquid nitrogen using mortar and pestle. They were resuspended in 1 mL of phosphate 0.1 M buffer containing 0.1% trichloroacetic acid (TCA). They were centrifuged at 12000 g for 10 min and pellet was discarded. Supernatant was diluted and H_2O_2 content was measured using a fluorimetric H_2O_2 assay kit (Sigma, Madrid, Spain). The protein content was measured according to the bicinchoninic acid method (Smith et al., 1985) using BSA as standard (for detailed protocol see **Appendix A: supplementary protocols**). H_2O_2 content was normalized using total protein of the extract. Six biological replicates of each treatment were measured.

3.2.2.4. Fungal colonization

Fungal colonization of each plant (n=6) for each treatment: WWMP, DSMP, WWNMP and DSNMP was measured under an Olympus BH2 microscope, after staining their roots with trypan blue as described in Gutiérrez et al. (2003). To calculate the mycorrhization status, 100 secondary and tertiary root sections per sample were observed under the microscope and were classified as mycorrhizal or nonmycorrhizal depending on the presence/absence of *T. claveryi* mycorrizal structures (for detailed protocol see **Appendix A: supplementary protocols**).

3.2.2.5. Statistical analyses

TcCAT-1 expression, H_2O_2 content and fungal colonization were subjected to analysis of the variance (ANOVA) and to Tukey test using R studio (version 1.1.456). Before the analysis, data were subjected to normality (Shaphiro-Wilk) and homoscedasticity (Levene) tests. Data plotting was carried out using Sigmaplot v 10.0 (Systat Software, UK).

3.3.   Results

3.3.1.   Biochemical and sequence analysis

3.3.1.1. Enzyme extraction and purification

In the supernatant obtained after phase partitioning of the crude extract with TX-114, a two-fold purification of the enzyme was obtained (**Table 3.3**). Submitting this aqueous phase to ultrafiltration removed 63 % of the proteins. Loading the enzyme onto HiTrap® Phenyl HP 1 mL column resulted in a 23.2 fold purification and a recovery of 71.2 % of total activity, while TcCAT-1 was finally purified to apparent homogeneity using gel filtration chromatography. By this final step, 33.7-fold purification was obtained and the residual activity was 19.3 %. The purified catalase was stable at -20°C for at least one month.

Table 3.3. **Purification of *T. claveryi* CAT (2 g of gleba).**

	Volume (mL)	Total activity (U)	Total protein (mg)	Specific activity (U mg^{-1})	Recovery (%)	Purification (fold)
Crude extract	8.0	303.8	34.7	8.8	100	1
10%TX-114 supernatant	4.5	296.8	16.7	17.8	97.7	2.0
100K MWCO filtration	1.0	267.4	6.2	43.1	88.0	4.9
HiTrap Phenyl HP	4.5	216.3	1.1	202.7	71.2	23.2
Superdex 200 10/300 GL	2.0	58.8	0.2	295.4	19.3	33.7

3.3.1.2. Molecular mass determination

The molecular mass of the purified catalase was estimated to be 357.8 kDa by gel filtration (**Figure 3.3A**). When the enzyme was analyzed by SDS-PAGE, a value of 90.4 kDa for the monomer was obtained (**Figure 3.3B**).
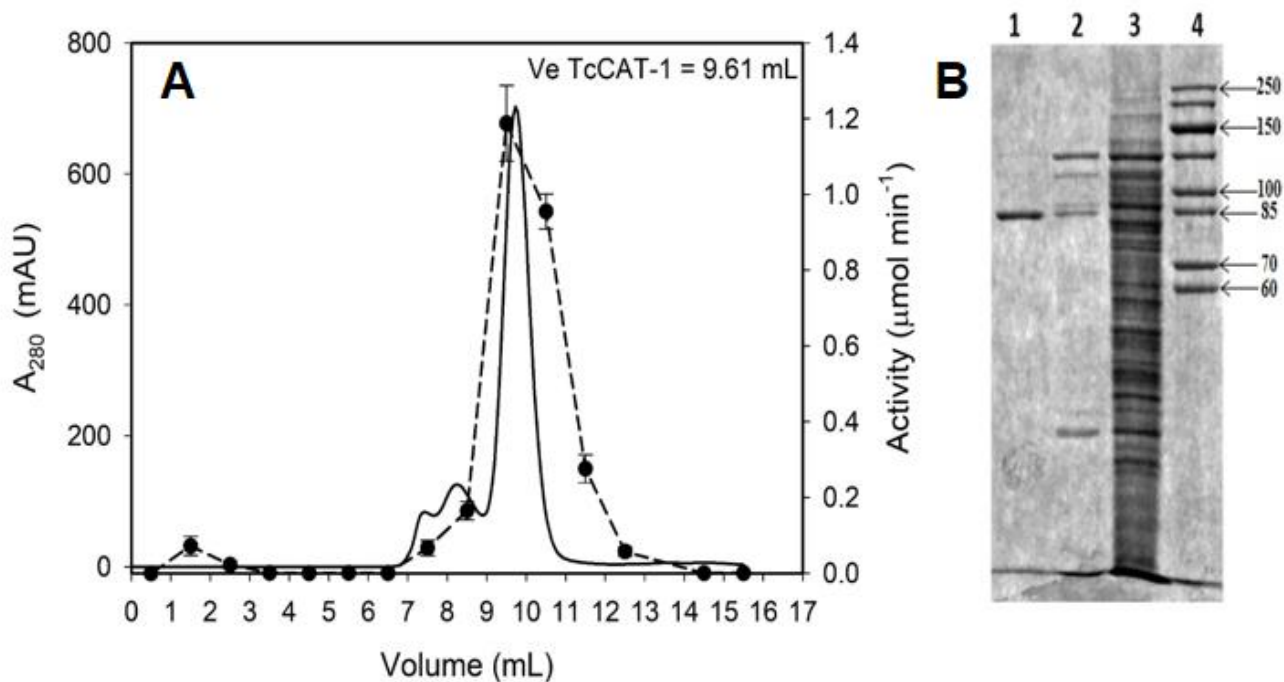
Figure 3.3. Molecular mass determination of TcCAT-1. (A) Gel filtration chromatogram. Absorbance at 280 nm is represented with solid line and TcCAT-1 activity measured in the standard reaction medium is represented with dashed line. **(B)** SDS-PAGE (10%). Lane 1: CAT eluted in Superdex® 200 10/30 GL. Lane 2: CAT eluted in HiTrap Phenyl HP. Lane 3: crude extract. Lane 4: SDS unstained molecular mass marker, mass indicated in kilodaltons.

3.3.1.3 pH and temperature

TcCAT-1 remained maximally active over a broad range of pH (from 5-11) using phosphate buffer and no optimal pH was observed. No activity was detected at pH 12.0 (**Figure 3.4A**). The enzyme showed very little activity at acid pHs. This decrease in activity is also caused by acetate buffer, since the activity at pH 5.0 was considerably higher when acetate was replaced by phosphate. The effect of temperature on the initial rate of TcCAT-1 (**Figure 3.4B**) indicates that, in a range from 20°C to 65°C, TcCAT-1 remains maximally active and presents a relative activity between 80-100 %, losing only 32 % of activity at 70 °C. After incubating the enzyme for one hour at each temperature, the thermostability test showed a 50% loss of enzyme activity (T_{50}) around 50 °C and that the enzyme retains 28% of activity at 70 °C (**Figure 3.4B**).
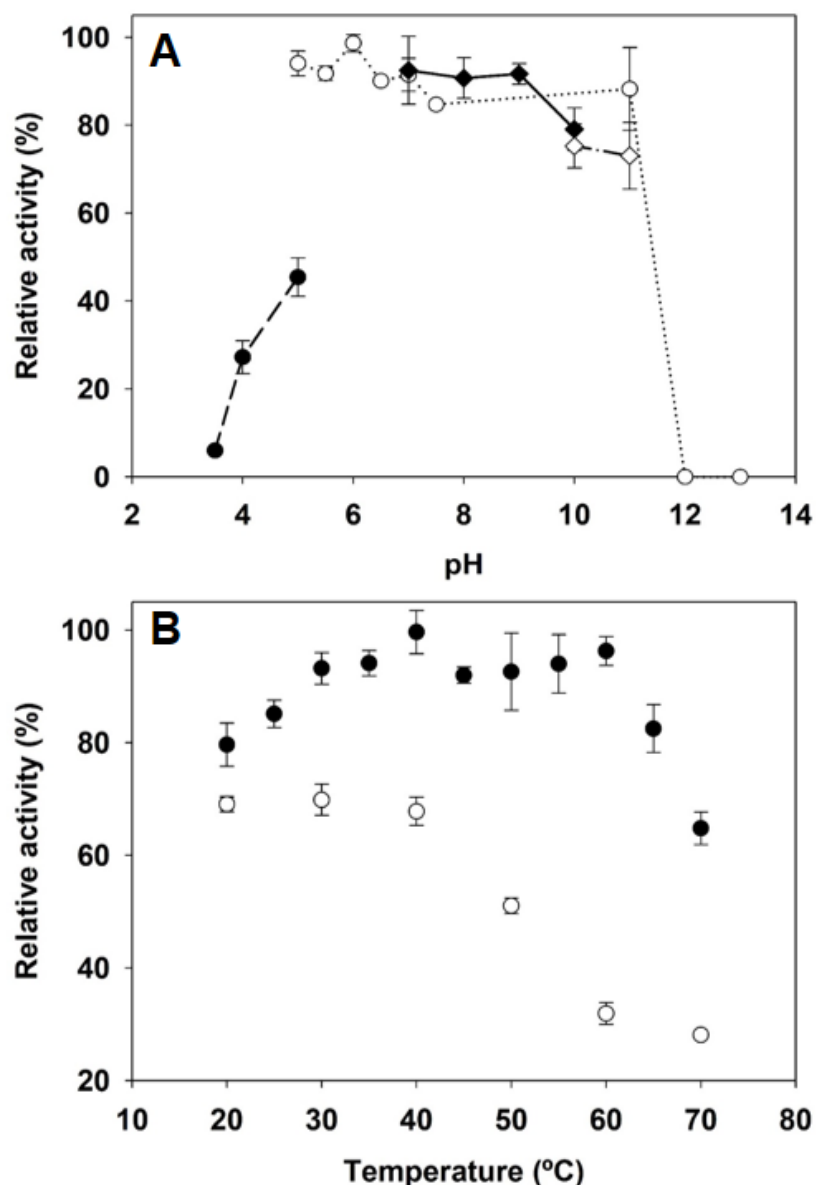
Figure 3.4. Effect of pH (A) and temperature (B) on CAT activity. (A) Acetate (●), phosphate (○), Tris-HCl (♦) and carbonate (◊) buffers are represented. **(B)** Determination of activity in a reaction medium at different temperatures (●) and thermostability of the enzyme: activity measured after 60 min of CAT incubation at each temperature (○). Values are the mean of 3 replicates. Bars indicate standard error.

3.3.1.4. Substrate concentration

The effect of H_2O_2 concentration on the initial rate of TcCAT-1 was analyzed spectrophotometrically increasing the substrate concentration up to 70 mM The experimental results were adjusted to the Michaelis-Menten equation and a good correlation was observed (**Figure 3.5**). The values obtained for the apparent K_m and V_{max} were 35.5 mM and 5.5 µmol min^{-1}, respectively.
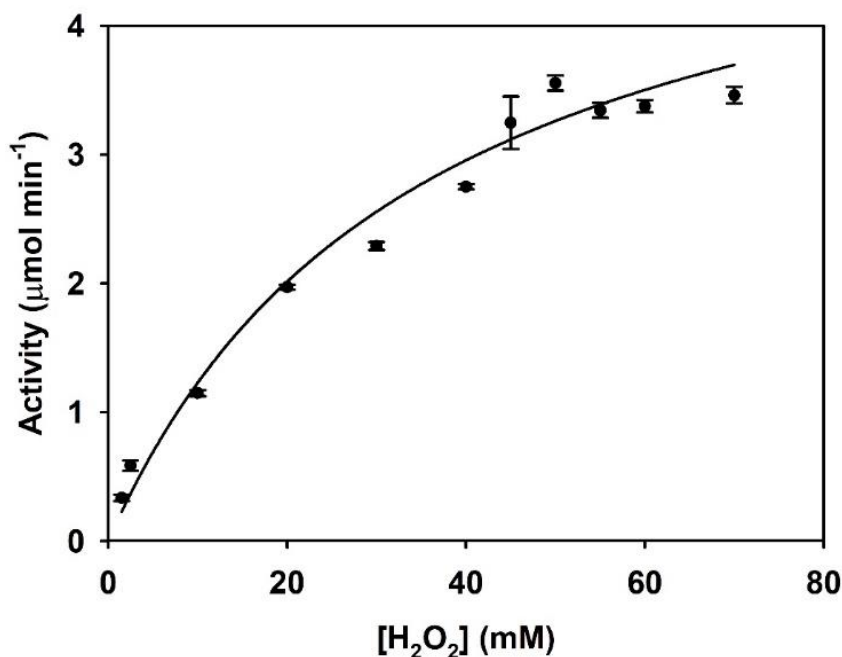
Figure 3.5. Effect of substrate concentration on TcCAT-1 activity. Each point represent experimental data from 3 replicates, bars indicate standard error and solid line is the fit to Michaelis-Menten equation.

3.3.1.5. Inhibitors

The concentration of inhibitor required for 50% inhibition (IC_{50}) calculated for hydroxylamine was 0.1 µM and 0.125 mM for 2-mercaptoethanol (**Table 3.4**). The inhibition produced in TcCAT-1 activity by the presence of 3-AT (up to 20 mM) in the reaction medium was only of 10%. However, a time-dependent decrease in the activity of TcCAT-1 was observed when the enzyme was incubated in the presence of 10 mM 3-AT (**Table 3.4**). In these conditions, 50 % of activity was lost in 10 min. Peroxidase-like activity was not detected using ABTS and H_2O_2 as substrates.

Table 3.4. Effect of inhibitor on TcCAT-1 activity from *T. claveryi*. See Material and methods for details.

Inhibitor	IC_{50}
Hydroxilamine	$0.10 \pm 0.01\,\mu M$
2-Mercaptoethanol	0.13 ± 0.02 mM
3-Aminotriazol (3-AT)	10 mM, after 10 min incubation

3.3.1.6. *Sequence identification*

The genome of *T. claveryi* has been recently published by Joint Genome Institute (JGI, California, USA) (https://genome.jgi.doe.gov/programs/fungi/index.jsf). Three different sequences coding for catalases were found in this genome (proteins ID 1216276, 1091969 and 1248402). The Protein Mass Fingerprinting (PMF) presented a 41% sequence coverage and 25 matched peptides with protein ID 1216276 automatically annotated as a "mono-functional catalase" in that database and did not match with any of the other two annotated catalases from *T. claveryi* genome (ID 1091969 and ID 1248402).

The percentage of sequence identity of TcCAT-1 with the other two *T. claveryi* catalases, determined by multiple sequence alignment, was 44.7% for ID 1248402 (76.7% of coverage) and 24.9% for ID 1091969 (52.3% coverage).

Figure 3.6. Multiple sequence alignment of TcCAT-1 with other fungal catalases. *Scytalidium thermophilum* (4AUE), *Neurospora crassa* Cat-3 (3EJ6) and *Penicillium vitale* (2XF2). The alignment was carried out with Clustal Omega (Sievers et al., 2011) and the output was generated with ESPript 3.9 (Robert, 2014). The secondary structure corresponding to the modeled TcCAT-1 is displayed above, where springs represent α helix or 3₁₀ helix (η) and arrows β strands. White characters on a black backround indicate residues strictly conserved. (●) represents the conserved key residues, while (▲) represents the glycosilation sites, predicted in TcCAT-1 and observed in 3EJ6.

The multiple sequence alignment of TcCAT-1 (ID 1216276) and fungal catalases from other species (**Figure 3.6**) shows a high percentage of identity (62%) with *Scytalidum thermophilum* (4AUE) and 58% with *Penicillium vitale* (2XF2) and *Neurospora crassa* (3EJ6). This high percentage of sequence identity with other catalases of known structure allowed to build a homology model of TcCAT-1, the topology diagram of which is shown on top of **Figure 3.6**. **Figure 3.7** shows main-chain superposition of TcCAT-1 model and its template (4AUE). The overall structure of the modeled monomer is similar to those described for other catalases (Díaz et al., 2009).
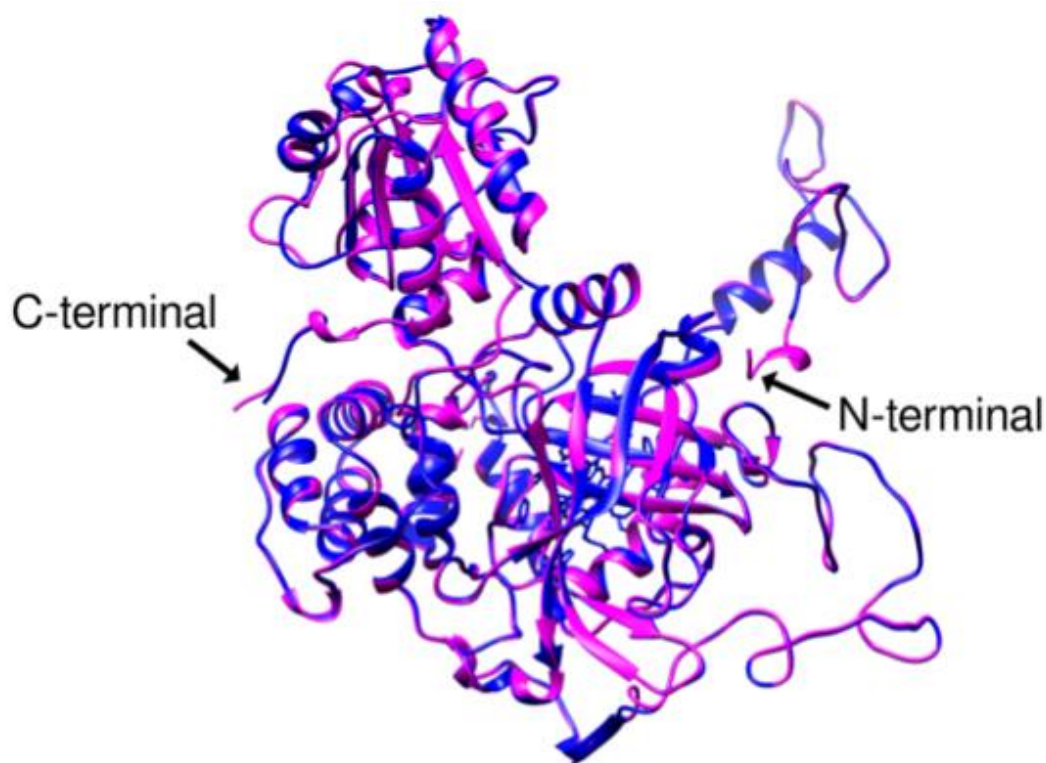
Figure 3.7. Main-chain superposition of TcCat-1 model (magenta) and 4AUE (blue).

3.3.1.7. *Phylogenetic analysis*

In order to gain more information on TcCAT-1, a phylogenetic tree was built using sequences of catalases from truffles (*T. claveryi*, *Terfezia boudieri* and *Tuber melanosporum*) and other Ascomyota (**Figure 3.8**). TcCAT-1 has been identified as a catalase belonging to L2 group.
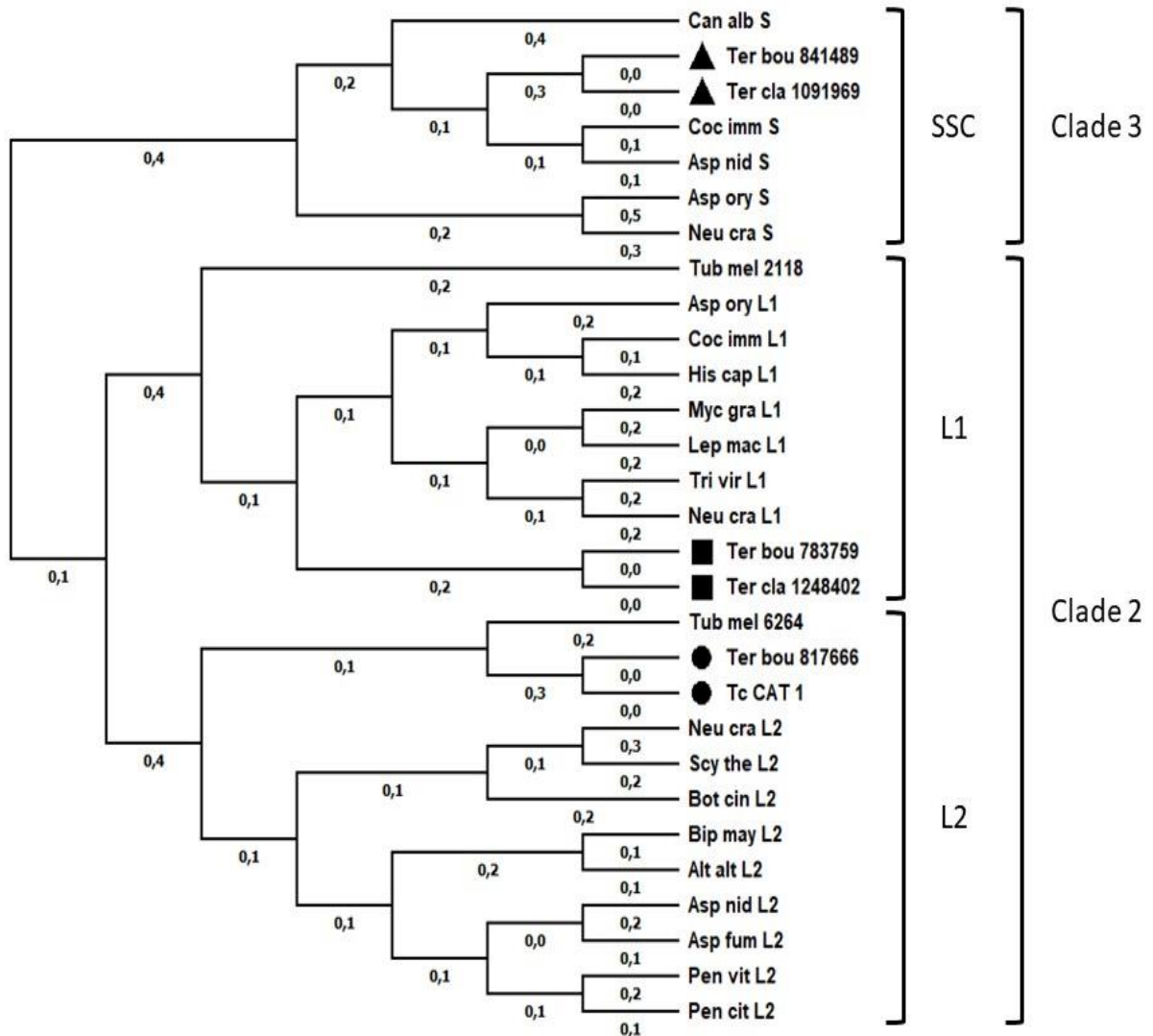
Figure 3.8. Maximum-Likelihood unrooted tree of fungal catalases. *T. claveryi* and *T. boudieri* novel catalases were identified as L1 (■), L2 (●) or SSC (▲).The percentage of replicate trees in which the associated taxa clustered together in the bootstrap test (1000 replicates) and the branch length are shown next to and below the branches, respectively. For information about the sequences see **Table 3.1**.

3.3.2. TcCAT-1 expression and drought stress assay

3.3.2.1. TcCAT-1 mRNA levels during T. claveryi life cycle

Analysis of RT-qPCR revealed the lowest expression levels in free living mycelium (FLM) and no significant fold-change in the ascocarp. mRNA levels of *TcCAT-1* were upregulated in WWMP showing a 3.79 Log2 fold-change (**Figure 3.9**). No amplification was obtained when using *TcCAT-1* primers in non-mycorrhizal plants (**Table 3.2**).
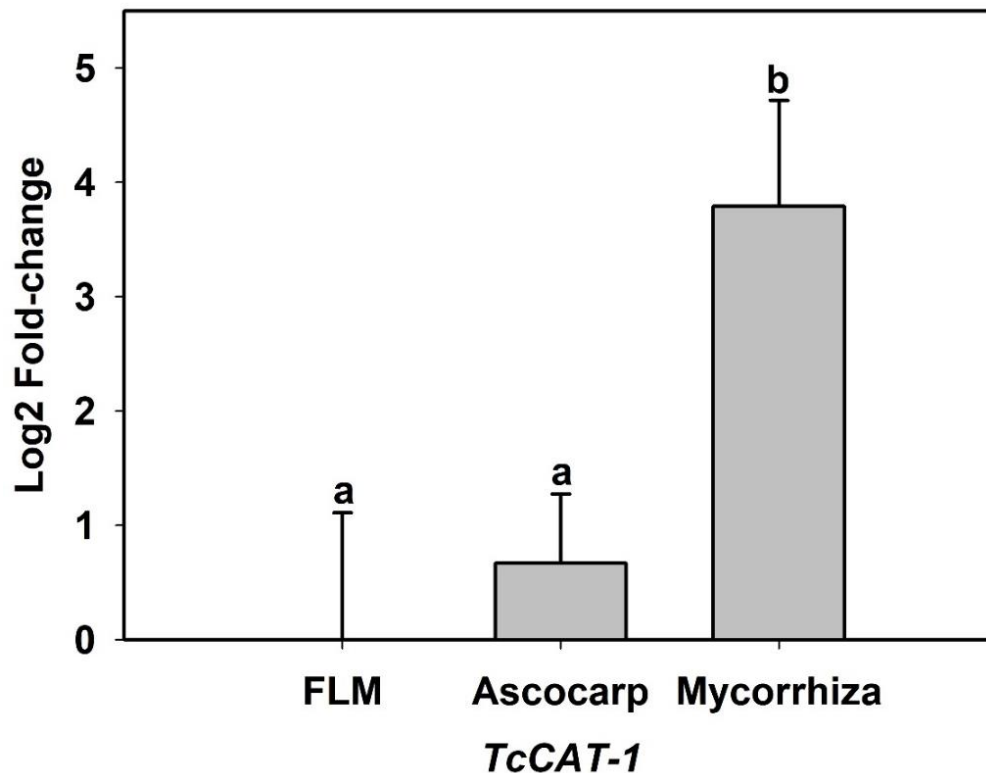
Figure 3.9. Log2 fold-change of *TcCAT-1* during different stages of *T. claveryi* biological cycle. FLM = free living mycelium; Mycorrhiza = well-watered mycorrhizal plants. Fold-change data was calculated by normalizing to actin (ID1089750, Mycocosm) and elongation factor (JF491354, NCBI) levels. Bars show the means ± standard error ($n = 6$). Different letters indicate different significance groups when $p < 0.05$, as determined by analysis of variance (ANOVA) and a Tukey test.

3.3.2.2. *TcCAT-1 mRNA levels and H$_2$O$_2$ content during drought stress*

When comparing *TcCAT-1* expression between WWMP and DSMP, no significant change was observed (**Table 3.5**). At the same time, H$_2$O$_2$ content in roots was significantly lower only in DSMP compared to well-watered treatments (**Figure 3.10**).

Table 3.5. TcCAT-1 expression pattern in WWMP and DSMP. WWMP = well-watered mycorrhizal plant; DSMP = drought-stressed mycorrhizal plant.

Sample	Relative expression
WWMP	1 ± 0.27 a
DSMP	1.07 ± 0.43 a
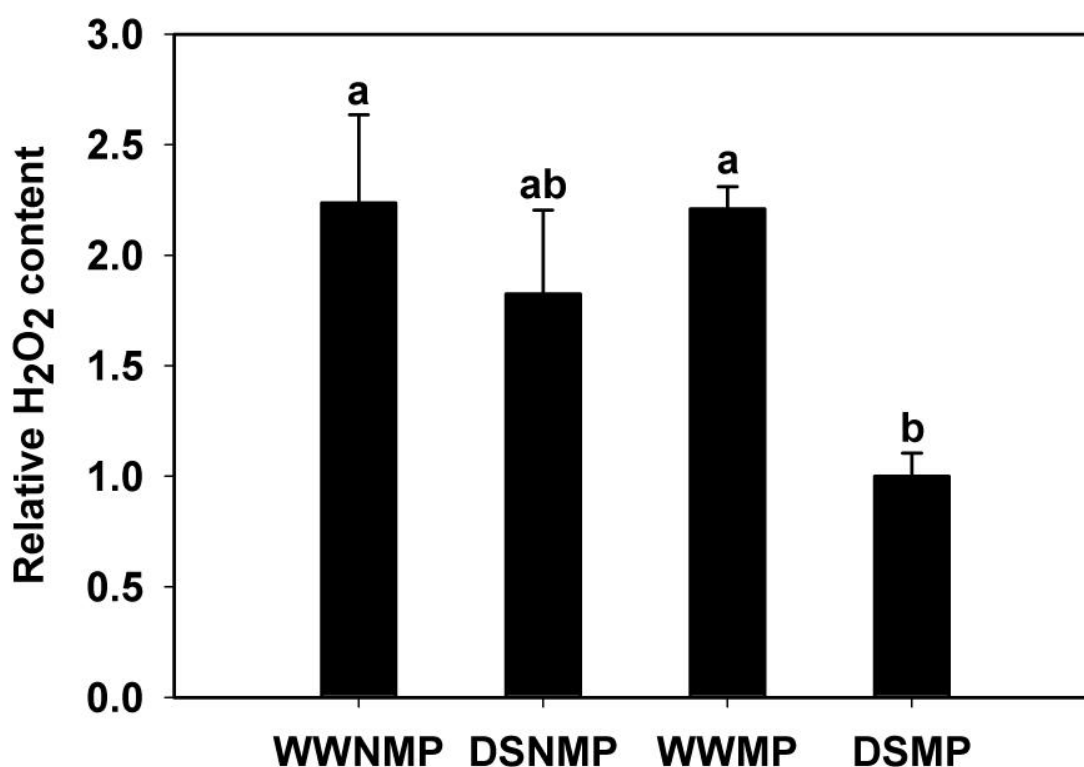
Figure 3.10. Relative H$_2$O$_2$ content in roots of plants with different mycorrhiza and water treatments. Bars show the means ± standard error (n = 6). Different letters indicate different significance groups between treatments when $p < 0.05$, as determined by by analysis of variance (ANOVA) and a Tukey test. WWMP = well-watered mycorrhizal plants; DSMP = drought-stressed mycorrhizal plants; non mycorrhizal treatments, WWNMP = well-watered non-mycorrhizal plant; DSNMP= drought-stressed non-mycorrhizal plant.

3.3.2.3. *Fungal colonization during drought stress*

Fungal colonization in each treatment was measured, finding a higher mycorrhization percentage in DSMP (48.8 %) than in WWMP (27.8 %), while no colonization was observed in non-mycorrhizal controls (**Table 3.6**). Along the root system, ecto- (**Figure 3.11A**), ectendo- and endo- (**Figure 3.11B**) mycorrhizal structures were observed.

Table 3.6. Fungal colonization of *H. almeriense* x *T. claveryi* mycorrhizal plants. WWMP = well-watered mycorrhizal plants; DSMP = drought-stressed mycorrhizal plants; WWNMP = well-watered non-mycorrhizal plants; DSNMP = drought-stressed non-mycorrhizal plants. Different letters indicate different significance groups when $p < 0.05$, as determined by Student's t-test.

Sample	Mycorrhization percentage (%) ± Standard Error
WWMP	27.8 ± 5.8 a
DSMP	48.8 ± 6.4 b
WWNMP	Mycorrhiza undetected
DSNMP	Mycorrhiza undetected
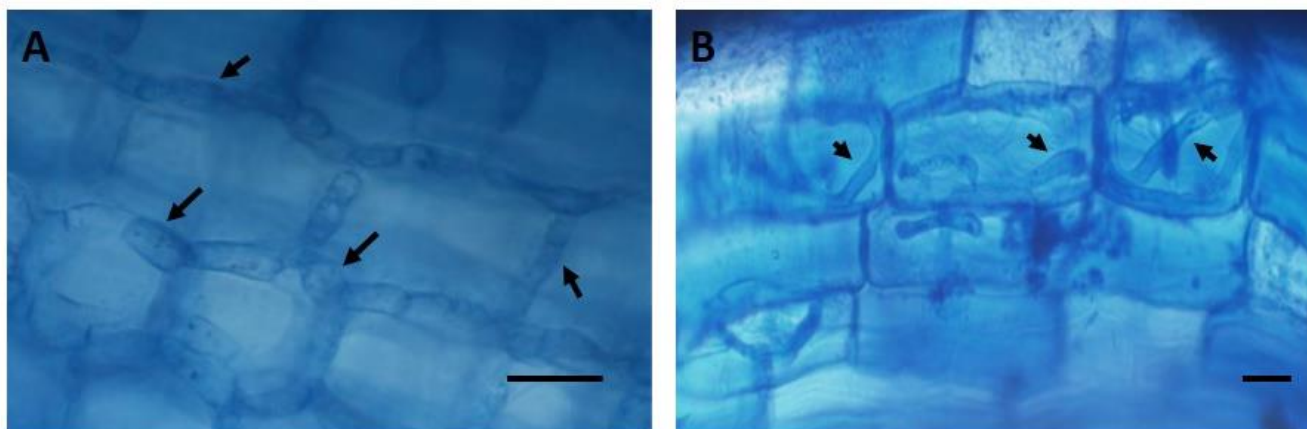
Figure 3.11. Fungal colonization of *T. claveryi* in *H. almeriense* roots. Arrows indicate inter- or intracellular hyphae and scale bar represents 20 μm. **(A)** Intercellular colonization. **(B)** Intracellular colonization.

3.4. Discussion

We have purified TcCAT-1 from ascocarps of *T. claveryi* and performed a biochemical and sequence analysis. The presence of phenolic compounds and other metabolites, which can bind to proteins and modify their properties, difficult enzyme purification in fungal extracts. In addition, *T. claveryi* ascocarps are rich in lipids which impair spectrophotometric measurements in crude extracts. To remove all these compounds, phase partitioning with TX-114 was used since this method gave good results with other enzymes from this fungus (Pérez-Gilabert et al., 2001a; 2001b; 2005a; 2005b). The whole process of purification (**Table 3.3**) was considered good according to the yield and purification levels and when compared to other catalase purifications (Fu et al., 2014; Kimoto et al., 2012).

Molecular masses obtained by gel chromatography and by SDS-PAGE (**Figure 3.3**) suggest that TcCAT-1 is a homotetramer and belongs to the LSCs group of monofunctional heme-catalases. Gel filtration separates molecules according to size, which is dependent on both molecular mass and shape. Thus, the shape of the protein could affect the molecular mass measured by gel filtration and may explain, in part, the discrepancies found between the molecular masses of the monomer and tetramer determined experimentally. On the other hand, the experimental MW of this tetramer is very similar to the 354 kDa determined for CAT-1 from *Neurospora crassa* (Díaz et al., 2001). The MW of this sequence was estimated as 82,017 Da with the ProtParam tool from Expasy (Gasteiger et al., 2005). The differences between the estimated and the experimental MW (90.4 kDa) are very similar to the described above for the glycoprotein CAT-1 from *N. crassa* (Díaz et al., 2001)*,* thus suggesting that TcCAT-1 is also a glycoprotein. In fact, when TcCAT-1 sequence was analyzed with ScanProsite tool (De Castro et al., 2006) three predicted sites of N-glycosilation were detected. The alignment (**Figure 3.6**) confirms the conservation in the sequence of TcCAT-1 of the N-glycosilation sites reported for *N. crassa* Cat-3 (Díaz et al., 2009). Conserved residues marked in Fig 4 are characteristic of the catalase family. For example, catalytic histidine H62, stabilized by an arginine (R100) and a valine (V104) and a tyrosine (Y350), which serves as the heme proximal side ligand, are within conserved regions.

TcCAT-1 belonged to L2 group (**Figure 3.8**) when a phylogenetic analysis was performed. With exceptions, such as the plant pathogen *Ustilago maydis* that only has a

catalase-peroxidase but no catalase genes (Kamper et al., 2006), most *Ascomycota* have several monofunctional heme catalases, usually one to four SSCs and two LSCs, one L1 and one L2. In addition to TcCAT-1, other two catalases, ID 1248402 and ID 1091969, with low sequence identity to TcCAT-1 (no higher than 24.9%) have been found in *T. claveryi* fungal genome, the former belonging to L1 and the latter to the SSC phylogenetic groups (**Figure 3.8**).

The pH, optimum temperature profile and thermostability shown by TcCAT-1 (**Figure 3.4**) are typical of monofunctional catalases (Díaz et al., 2001; Switala et al., 1999; Seah et al., 1973). The apparent K_m (**Figure 3.5**) is similar to the estimated for CAT-1 of *N. crassa* at concentrations of H_2O_2 below 100 mM (Díaz et al., 2001) and to those described for CAT from the bacteria *P. aeruginosa* (Switala and Loewen, 2002). The sensitivity of TcCAT-1 to hydroxylamine (**Table 3.4**) is similar to the reported for CAT from *Aspergillus niger, E. coli or N. crassa* (IC_{50} of 0.4, 0.12 and 0.19 respectively) (Díaz et al., 2001; Hansberg et al., 2012), while its sensitivity to 3-AT (**Table 3.4**) is similar to the reported for CAT-1 from *N. crassa*.

Catalase activity in fungi has been related to stress conditions (high and low water content, high and low temperature, presence of competing species, etc) and also to development of their life cycle (Hansvberg et al., 2012), in the case of edible mycorrhizal fungi it consists on a free-living mycelium phase, a symbiotic mycorrhizal phase and a fruiting body phase (Wang et al., 2017), but the role of the vast majority of these fungal enzymes remains to be elucidated.

The saprophytic edible fungi *Pleorotus ostreatus* and the entomopathogen *Beauveria bassiana,* present both several catalases with different expression levels, in different life cycle stages, suggesting distinct functions during their life cycle (Chantasingh et al., 2013; Wang et al., 2017). However, until now the expression and function of fungal catalases during mycorrhiza life-cycle has not been studied. The upregulation of *TcCAT-1* in mature mycorrhiza reported in this paper (**Figure 3.9**) suggests that this enzyme may be playing a role in mycorrhizal symbiosis of *T. claveryi* and *H. almeriense*. In any case, mRNA data should be treated with caution, since it has been shown that, at steady-state, mRNA levels mainly explain protein concentrations, while during dynamic phases such as cellular differentiation or stress response, post-

transcriptional regulation may deviate this ideal correlation between transcript and protein levels (Liu et al., 2016).

In AM associations, the accumulation of ROS and the induction of plant ROS-scavenging enzymes, such as superoxide dismutase, catalase and peroxidase during the mycorrhization process have been reported (Salzer et al., 1999; Lambais et al., 2003). Baptista et al. (2007) reported an increase in H_2O_2 production, with a pattern similar to the observed for pathogenic infections, during early stages of ECM establishment between *Castanea sativa* and *Pisolithus tinctorius*. However, in order to establish a successful association, the fungal symbiont must be able to elude the host´s defense response and this response could explain the higher expression level of *TcCAT-1* in *H. almeriense* x *T. claveryi* mycorrhizal roots. Phylogenetic analysis reinforces this idea since it shows that TcCAT-1 clusters with L2 catalases, which are usually extracellular enzymes induced by different stressors (Hansberg et al., 2012).

Catalases are the main responsible for the dismutation of the H_2O_2, one of the ROS that can be produced during drought stress (Porcel et al., 2005). One of the advantages of mycorrhization is to favor the adaptation of the host plant to water deficit through various processes, being protection against oxidative damage one of them. In this sense, different studies have reported decreases in H_2O_2 content, usually correlated with an induction in catalase activity, in mycorrhizal roots undergoing drought stress (Pedranzani et al., 2016; Wu et al., 2006). At the same time, it is already known that *T. claveryi* mitigates the negative effects of drought by physiological and nutritional alterations in *H. almeriense* (Morte et al., 2000; Navarro-Ródenas et al., 2013). However, to what extent drought induces oxidative stress in *H. almeriense* has not been investigated yet. The results here presented are the first approach of how oxidative stress is managed by the *H. almeriense x T. claveryi* mycorrhiza under water-deficit conditions. A significant decrease in the H_2O_2 root content is observed only in mycorrhizal plants submitted to drought stress (**Figure 3.10**). The increase in mycorrhization levels (**Table 3.6**) could play a role in the H_2O_2 decrease. This decrease is not observed in non-mycorrhizal plants (**Figure 3.10**), suggesting that the beneficial effects of mycorrhiza during water deficit at cellular level may involve a relief of oxidative stress. However, there is no increase in TcCAT-1 expression levels (**Table 3.5**). This result suggests that TcCAT-1 is not responsible for the decrease in the H_2O_2 levels observed in DSMP and other ROS scavenger enzymes or even antioxidant compounds may be involved. Future

and more exhaustive research will be needed to fully comprehend the role that plant and fungal enzymes and/or non-enzymatic compounds may have in the oxidative response of the mycorrhiza against the drought.

In conclusion, TcCAT-1 purified and characterized in this study shows an interesting expression pattern during the life cycle of *T. claveryi*. It seems to play a significant role in the mycorrhizal symbiosis of *T. claveryi* and *H. almeriense* since it is upregulated in mature mycorrhiza compared to free living mycelium and fruit body stage. Mycorrhization has a beneficial effect in terms of oxidative stress relief, but the transcriptional profile of this enzyme does not seem to be the responsible of the H_2O_2 decrease observed in the mycorrhizal plants during water deficit. Future investigation would be, thus, needed to assess the role of TcCAT-1 and other fungal ROS scavengers in mediating mycorrhiza formation and plant resistance to drought stress.

References

Arenas F, Navarro-Ródenas A, Chávez D, Gutiérrez A, Pérez-Gilabert M, Morte A (2018) Mycelium of *Terfezia claveryi* as inoculum source to produce desert truffle mycorrhizal plants. Mycorrhiza 28(7):691-701. https://doi.org/10.1007/s00572-018-0867-3.

Bacelar EA, Moutinho-Pereira JM, Gonçalves BC, Lopes JI, Correia CM (2009) Physiological responses of different olive genotypes to drought conditions. Acta Physiol. Plant. 31(3):611–21. https://doi.org/10.1007/s11738-009-0272-9.

Baptista P, Martins A, Pais MS, Tavares RM, Lino-Neto T (2007) Involvement of reactive oxygen species during early stages of ectomycorrhiza establishment between *Castanea sativa* and *Pisolithus tinctorius*. Mycorrhiza 17(3):185–193. https://doi.org/10.1007/s00572-006-0091-4.

Biasini M, Bienert S, Waterhouse A, Arnold K, Studer G, Schmidt T, Kiefer F, Gallo Cassarino T, Bertoni M, Bordoli L, Schwede T (2014) SWISS-MODEL : modelling protein tertiary and quaternary structure using evolutionary information. Nucleic Acid Res. 42(April):252–258. https://doi.org/10.1093/nar/gku340.

Brakensiek DL, Osborn HB, Rawls WJ (1979) Field Manual for Research in Agricultural Hydrology. Agriculture Handbook, Science and Education Administration, US Department of Agriculture.

Chang S, Puryear J, Cairney J (1993) A simple and efficient method for isolating RNA from pine trees. Plant Mol. Biol. Report. 11(2):113–116. https://doi.org/10.1007/BF02670468.

Chantasingh D, Kitikhun S, Keyhani NO, Boonyapakron K, Thoetkiattikul H, Pootanakit K, Eurwilaichitra L (2013) Identification of catalase as an early upregulated gene in *Beauveria bassiana* and its role in entomopathogenic fungal virulence. Biol. Control. 67(2):85–93. http://dx.doi.org/10.1016/j.biocontrol.2013.08.004.

Chelikani P, Fita I, Loewen PC (2004) Diversity of structures and properties among catalases. Cell Mol. Life Sci. 61:192–208. https://doi.org/10.1007/s00018-003-3206-5.

De Castro E, Sigrist CJA, Gattiker A, Bulliard V, Langendijk-Genevaux PS, Gasteiger E, Bairoch A, Hulo N (2006) ScanProsite: detection of PROSITE signature matches and ProRule-associated functional and structural residues in proteins. Nucleic Acids Res. 34:362–365. https://doi.org/10.1093/nar/gkl124.

Díaz A, Muñoz-Clares RA, Rangel P, Valdás VJ, Hansberg W (2005) Functional and structural analysis of catalase oxidized by singlet oxygen. Biochimie. 87(2):205–214. https://doi.org/10.1016/j.biochi.2004.10.014.

Díaz A, Rangel P, Montes de Oca Y, Lledías F, Hansberg W (2001) Molecular and kinetic study of catalase-1, a durable large catalase of *Neurospora crassa*. Free Radic. Biol. Med. 31(11):1323–33. https://doi.org/10.1016/S0891-5849(01)00637-2.

Díaz A, Valdés VJ, Rudiño-Piñera E, Horjales E, Hansberg W (2009) Structure-function relationships in fungal large-subunit catalases. J. Mol. Biol. 386(1):218–232. https://doi.org/10.1016/j.jmb.2008.12.019.

Fu X, Wang W, Hao J, Zhu X, Sun M (2014) Purification and characterization of a catalase from marine bacterium *Acinetobacter* sp. YS0810. Biomed. Res. Int. 2014:409626. http://doi.org/10.1155/2014/409626.

Gasteiger E, Hoogland C, Gattiker A, Duvaud S, Wilkins MR, Appel RD, Bairoch A (2005) Protein identification and analysis tools on the ExPASy Server. In: Walker JM, ed. The Proteomics Protocols Handbook. Human Press Inc, Totowa, NJ pp. 571–608. https://doi.org/10.1385/1-59259-890-0:571.

Gutiérrez A, Morte A, Honrubia M (2003) Morphological characterization of the mycorrhiza formed by *Helianthemum almeriense* Pau with *Terfezia claveryi* Chatin and *Picoa lefebvrei* (Pat.) Maire. Mycorrhiza 13(6):299–307. https://doi.org/10.1007/s00572-003-0236-7.

Hansberg W, Salas-Lizana R, Domínguez L (2012) Fungal catalases: function, phylogenetic origin and structure. Arch. Biochem. Biophys. 525(2):170–80. http://dx.doi.org/10.1016/j.abb.2012.05.014.

Kamper J, Kahmann R, Bolker M, Ma L, Brefort T, Saville BJ, et al. (2006) Insights from the genome of the biotrophic fungal plant pathogen *Ustilago maydis*. Nature 444:97–101. https://doi.org/10.1038/nature05248.

Kimoto H, Yoshimune K, Matsuyma H, Yumoto I (2012) Characterization of catalase from psychrotolerant *Psychrobacter piscatorii* T-3 exhibiting high catalase activity. Int. J. Mol. Sci. 2012;13(2):1733–1746. https://doi.org/10.3390/ijms13021733.

Laemmli UK (1970) Cleavage of structural proteins during the assembly of the head of bacteriophage T4. Nature 227:680–685. https://doi.org/10.1038/227680a0.

Lambais MR, Ríos-Ruiz WF, Andrade RM (2003) Antioxidant responses in bean (*Phaseolus vulgaris*) roots colonized by arbuscular mycorrhizal fungi. New Phytol. 160(2):421–428. http://doi.wiley.com/10.1046/j.1469-8137.2003.00881.x.

Liu Y, Beyer A, Aebersold R (2016) On the dependency of cellular protein levels on mRNA abundance. Cell 165(3):535-550. https://doi.org/10.1016/j.cell.2016.03.014.

Livak KJ, Schmittgen TD (2001) Analysis of relative gene expression data using real-time quantitative PCR and the 2-$\Delta\Delta$CT method. Methods 25(4):402–408. https://doi.org/10.1006/meth.2001.1262.

Morte A, Lovisolo C, Schubert A (2000) Effect of drought stress on growth and water relations of the mycorrhizal association *Helianthemum almeriense-Terfezia claveryi*. Mycorrhiza 10(3):115–119. https://doi.org/10.1007/s005720000066.

Morte A, Honrubia M, Gutiérrez A (2008) Biotechnology and cultivation of desert truffles. In: Varma A, ed. Mycorrhiza. Springer Berlin Heidelberg pp. 467–483. https://doi.org/10.1007/978-3-540-78826-3_23.

Morte A, Navarro-Ródenas A, Nicolás E (2010) Physiological parameters of desert truffle mycorrhizal *Helianthemun almeriense* plants cultivated in orchards under water deficit conditions. Symbiosis 52(2–3):133–139. https://doi.org/10.1007/s13199-010-0080-4.

Morte A, Andrino A, Honrubia M, Navarro-Ródenas A (2012) *Terfezia* cultivation in arid and semiarid soils. In: Zambonelli A, Bonito GM, eds. Edible Ectomycorrhizal Mushrooms: Current Knowledge and Future Prospects. Springer-Verlag, Berlin Heidelberg pp. 241–263. https://doi.org/10.1007/978-3-642-33823-6_14.

Morte A, Pérez-Gilabert M, Gutiérrez A, Arenas F, Marqués-Gálvez JE, Bordallo JJ, Rodríguez A, Berná LM, Lozano-Carrillo C, Navarro-Ródenas, A (2017) Basic and applied research for desert truffle cultivation. In: Varma A, Prasad R, Tuteja N, eds. Mycorrhiza-Ecophysiology, Secondary Metabolites, Nanomaterials. Springer International Publishing pp. 23–24. https://doi.org/10.1007/978-3-319-57849-1_2.

Murat C, Mello A, Abbà S, Vizzini A, Bonfante P (2008) Edible mycorrhizal fungi: identification, life cycle and morphogenesis. In: Varma A, ed. Mycorrhiza. Springer Berlin Heidelberg pp. 707–732. https://doi.org/10.1007/978-3-540-78826-3_33.

Navarro-Ródenas A, Bárzana G, Nicolás E, Carra A, Schubert A, Morte A (2013) Expression analysis of aquaporins from desert truffle mycorrhizal symbiosis reveals a fine-tuned regulation under drought. Mol. Plant Microbe Interact. 26(9):1068–78. https://doi.org/10.1094/MPMI-07-12-0178-R.

Navarro-Ródenas A, Xu H, Kemppainen M, Pardo AG, Zwiazek JJ (2015) *Laccaria bicolor* aquaporin LbAQP1 is required for Hartig net development in trembling aspen (*Populus tremuloides*). Plant Cell Environ. 38(11):2475–86. https://doi.org/10.1111/pce.12552.

Nelsen CE (1987) The water relations of vesicular-arbuscular mycorrhiza systems. In: Safir GR, ed. Ecophysiology of VA Mycorrhizal Plants. CRC Press, Boca Raton, Florida pp 71-92.

Nelson DP, Kiesow LA (1972) Enthalphy of decomposition of hydrogen peroxide by catalase at 25°C (with molar extinction coefficients of H_2O_2 solutions in the UV). Anal Biochem. 49:474–478. https://doi.org/10.1016/0003-2697(72)90451-4.

Pedranzani H, Rodríguez-Rivera M, Gutiérrez M, Porcel R, Hause B, Ruiz-Lozano JM (2016) Arbuscular mycorrhizal symbiosis regulates physiology and performance of *Digitaria eriantha* plants subjected to abiotic stresses by modulating antioxidant and jasmonate levels. Mycorrhiza 26(2):141–152. https://doi.org/10.1007/s00572-015-0653-4.

Pérez-Gilabert M, Morte A, Honrubia M, García-Carmona F (2001a) Monophenolase activity of latent *Terfezia claveryi* tyrosinase: characterization and histochemical localization. Physiol Plant. 113:203–09. https://doi.org/10.1034/j.1399-3054.2001.1130207.x.

Pérez-Gilabert M, Morte A, Honrubia M, García-Carmona F (2001b) Partial purification, characterization, and histochemical localization of fully latent desert truffle (*Terfezia claveryi* Chatin) polyphenol oxidase. J. Agric. Food Chem. 49:1922–1927. https://doi.org/10.1021/jf001009n.

Pérez-Gilabert M, Sánchez-Felipe I, García-Carmona F (2005a) Purification and partial characterization of lipoxygenase from desert truffle (*Terfezia claveryi* Chatin) ascocarps. J. Agric. Food. Chem. 53:3666–3671. https://doi.org/10.1021/jf048087l.

Pérez-Gilabert M, Morte A, Ávila-Gónzalez R, García-Carmona F (2005b) Characterization and histochemical localization of nonspecific esterase from ascocarps of desert truffle (*Terfezia claveryi* Chatin). J. Agric. Food. Chem. 53:5754–5759. https://doi.org/10.1021/jf050334d.

Pettersen EF, Goddard TD, Huang CC, Couch GS, Greenblatt DM, Meng EC, Ferrin TE (2004) UCSF Chimera - A visualization system for exploratory research and analysis. J. Comput. Chem. 25(13):1605–12. https://doi.org/10.1002/jcc.20084.

Porcel R, Ruiz-Lozano JM (2004) Arbuscular mycorrhizal influence on leaf water potential, solute accumulation, and oxidative stress in soybean plants subjected to drought stress. J. Exp. Bot. 55(403):1743–1750. https://doi.org/10.1093/jxb/erh188.

Robert X, Gouet P (2014) Deciphering key features in protein structures with the new ENDscript server. Nucleic Acids Res. 42(W1):320–324. https://doi.org/10.1093/nar/gku316.

Roth-Bejerano N, Navarro-Ródenas A, Gutiérrez A (2014) Types of mycorrhizal association. In: Kagan-Zur V, Roth-Bejerano N, Sitrit Y, Morte A, eds. Desert Truffles. Phylogeny, Physiology, Distribution and Domestication. Soil Biology, volume 38, Springer-Verlag, Berlin, Heidelberg pp. 69–80. https://doi.org/10.1007/978-3-642-40096-4_5.

Ruiz-Lozano JM, Porcel R, Aroca R (2008) Evaluation of the possible participation of drought-induced genes in the enhanced tolerance of arbuscular mycorrhizal plants to water deficit. In: Varma A, ed. Mycorrhiza. Springer, Berlin, Heidelberg: Springer pp. 185–205. https://doi.org/10.1007/978-3-540-78826-3_10.

Salzer P, Corbière H, Boller T (1999) Hydrogen peroxide accululation in *Medicago truncatula* roots colonized by the arbuscular mycorrhiza-forming fungus *Glomus intraradices*. Planta 208(3):319–25. https://doi.org/10.1007/s004250050565.

Scholander PF, Bradstreet ED, Hemmingsen EA, Hammel HT (1965) Sap pressure in vascular plants. Science 148(3668):339–346. https://doi.org/10.1126/science.148.3668.339

Seah TCM, Kaplan JG (1973) Purification and properties of the catalase of bakers' yeast. J. Biol. Chem. 248(8):2889–2893.

Sievers F, Wilm A, Dineen D, Gibson TJ, Karplus K, Li W, et al. (2011) Fast, scalable generation of high-quality protein multiple sequence alignments using Clustal Omega. Mol. Syst. Biol. 7(539):1–6. https://doi.org/10.1038/msb.2011.75.

Smith PK, Krohn RI, Hermanson GT, Mallia AK, Gartner FH, Provenzano MD, Fujimoto EK, Goeke NM, Olson BJ, Klenk DC (1985) Measurement of protein using bicinchoninic acid. Anal. Biochem. 150:76–85. https://doi.org/10.1016/0003-2697(85)90442-7.

Switala J, Loewen PC (2002) Diversity of properties among catalases. Arch. Biochem. Biophisics 401:145–54. https://doi.org/10.1016/S0003-9861(02)00049-8.

Switala J, Neil JOO, Loewen PC (1999) Catalase HPII from *Escherichia coli* exhibits enhanced resistance to denaturation. Biochemistry 38:3895–3901. https://doi.org/10.1021/bi982863z.

Tamura K, Stecher G, Peterson D, Filipski A, Kumar S (2013) MEGA6: molecular evolutionary genetics analysis version 6.0. Mol. Biol. Evol. 30(12):2725–2729. https://doi.org/10.1093/molbev/mst197.

Wang L, Wu X, Gao W, Zhao M, Zhang J, Huang C (2017) Differential expression patterns of *Pleurotus ostreatus* catalase genes during developmental. Genes 8(335):1–12. https://doi.org/10.3390/genes8110335.

Wojtaszek P (1997) Oxidative burst : an early plant response to pathogen infection. Biochem. J. 692:681–692. https://doi.org/10.1042/bj3220681.

Wu QS, Xia RX, Zou YN (2006) Reactive oxygen metabolism in mycorrhizal and non-mycorrhizal citrus (*Poncirus trifoliata*) seedlings subjected to water stress. J. Plant Physiol. 163(11):1101–1110. https://doi.org/10.1016/j.jplph.2005.09.001

Desert truffle genomes reveal survival adaptations to mycorrhizal lifestyle in dry land

4.1.   Introduction

The term **desert truffle** refers to edible hypogeous fungi growing in **arid** and **semiarid areas** (Kovács and Trappe, 2014). These areas are characterized by an aridity index (AI), lower than 0.5 (UNESCO, 1979) and by poorly fertile soils with sandy texture and low inputs of organic matter (Bonifacio and Morte, 2014). Since most climate models point to temperature increases and precipitation decreases during the next decades, the area of arid and semiarid ecosystems is expected to increase (Schlesinger et al., 1990; Lavee et al., 1998). Thus, desert truffles are becoming an alternative crop increasingly interesting in places such as the Mediterranean region and the Middle East, where the risk of desertification is getting higher, and their basic and applied research needs to be expanded in order to establish them as a successful crop in these regions (Morte et al., 2017).

To the desert truffle group belong species of the genus *Carbomyces*, *Elderia*, *Eremiomyces*, *Kalaharituber*, *Mattirolomyces*, *Mycoclelandia*, *Picoa*, *Stouffera*, *Terfezia*, *Tirmania*, and *Ulurua;* in addition, some species of the *Tuber* genus, such as *Tuber gennadii*, are also known as desert truffles (Moreno et al., 2014). Among these species, those of *Terfezia* and *Tirmania* genera are the best known and commercially, as well as nutritionally appreciated (Kagan-Zur & Roth-Bejerano, 2008). ***Terfezia claveryi*** (Honrubia et al., 2001, Morte et al., 2008) and ***Terfezia boudieri*** (Slama et al., 2010, Kagan-Zur et al., 2014) are the only ones that have been successfully cultivated in Spain (*T. claveryi*), Tunisia and Israel (*T. boudieri*). ***Tirmania nivea*** is a desert truffle highly appreciated in the Arab countries. Stimulation of natural fructifications of *T. nivea* has been achieved in Abu Dhabi (UAE) through irrigation, spore inoculation and fencing certain natural zones (Gouws et al., 2014). ***Kalaharituber pfeilii***, also known as "n'abba" or "sand potato", has been less studied that the rest of desert truffle mentioned and, although a relevant part of the diet of habitants of South Africa, Botswana, Angola or Namibia, its cultivation has not been reported so far (Trappe et al., 2008).

Most desert truffles establish symbiosis with their hosts, normally annual and perennial shrubs belonging to the *Cistaceae* family (Roth-Bejerano et al., 2014). Thanks to this mutual relationship, desert truffle species improve the performance of their host plants in arid and semiarid conditions. As an example, by altering physiological and

nutritional parameters (Morte et al., 2000; 2010), such as the expression of plant and fungal aquaporins (Navarro-Ródenas et al., 2013) and the hydrogen peroxide (H_2O_2) content in roots (Marqués-Gálvez et al., 2019), *T. claveryi* mycorrhizae helps its host plant *Helianthemum almeriense* to cope with drought periods. The type of mycorrhizae formed by these fungi, known as **ectendomycorrhizae** (**EEM**), is quite rare and peculiar. EEMs are characterized by the co-occurrence of both intercellular Hartig net and intracellular hyphae penetrating the cortex cells, normally forming coils. In addition, there is usually a thin and disordered fungal mantle surrounding the root (Morte et al., 1994; Yu et al., 2001; Roth-Bejerano et al., 2014). Yet, the occurrence of either intercellular or intracellular mycorrhizal structures depend on several factors: *in vitro* conditions, high auxin, phosphate and/or water content favor the intercellular type, while field conditions, low auxin, phosphate and/or water availability favor the intracellular type (Gutiérrez et al., 2003; Zaretsky et al., 2006a; Navarro-Ródenas et al., 2012; 2013).

Since the first mycorrhizal genome, that of *Laccaria bicolor,* was published (Martin et al., 2008), many fungal genomic and transcriptomic data became available thanks to recent advances in sequencing techniques such as **Next Generation Sequencing** (NGS) (Kuo, et al., 2014) and to large-scale international projects such as the **1000 Fungal Genomes Project** by **Joint Genome Institute** (JGI, California, USA) (Grigoriev et al., 2014). These advances allowed the study of specific evolutionary features of the mycorrhizal lifestyle, known as the fungal "**symbiosis toolkit**" (Kohler et al., 2015), to discover and functionally characterize signaling molecules important for mycorrhizal associations, such as MiSSP7 in *L. bicolor* x *Populus* species (Plett et al., 2014) and to shed light on their reproductive mode (Martin et al., 2010; Murat et al., 2018). Other important genomic features of mycorrhizae, revealed thanks to genome sequencing, are the **carbohydrate-active enzymes** (**CAZymes**), especially those that are secreted and target the plant and/or microbial cell walls, since they usually reflect the lifestyle of fungi (Kohler et al., 2015). Moreover, the study of **transposable elements** (**TEs**-transposable elements, transposons or jumping genes) is also becoming important. They are DNA (DNA transposons) or RNA (retrotrasposons, with or without long terminal repeats (LTRs)) sequences that can change their position within a genome, creating in some cases mutations and altering the genome size. Transposons are one of the factors driving speciation and evolution and may be related to the plasticity and

adaptability of fungi to their environment (Raffaele and Kamoun, 2012; Casacuberta and González, 2013).

Desert truffles have been historically less studied than other truffles such as the well-known Perigord black truffle (*Tuber melanosporum*) or the white truffle (*Tuber magnatum*), and the knowledge on these and other species have benefited from the sequencing of their genomes (Martin et al., 2010; Murat et al., 2018). Although cDNA–AFLP analysis has been carried to identify genes related to *T. boudieri* x *Cistus incanus* symbiosis (Zaretsky et al., 2006b) and the genome of *T. boudieri* has been recently published (Murat et al., 2018), many key aspects of their biology remain to be elucidated. Among them, the **reproductive mode** and the genetic determinants underlying the development of the different symbiotic structures that these fungi form on their hosts, as well as their adaptations to different environments, are of basic and applied relevance.

To this end, in the present study, we compared the genomes of two desert truffles, *T. claveryi* strain T7 and *Tirmania nivea* strain G3, with those of 9 *Pezizomycetes*, and assessed the transcriptomes of *T. claveryi* free living mycelia and *T. claveryi* x *H. almeriense* mycorrhizae under both control and dry conditions. Our findings represent a step forward in our understanding of sexual and vegetative propagation modes of the desert truffles and highlight the singularities in their mycorrhizal interaction with the host plant that are reflected in their genomes, with respect to the other Pezizomycetes.

4.2. Materials and methods

4.2.1. Fungal strains for genome sequencing

Terfezia claveryi strain T7 was isolated from an ascocarp collected in an *H. almeriense x T. claveryi* experimental field located in Zarzadilla de Totana (Murcia, Spain) in April 2007. *Tirmania nivea* strain G3 was isolated from an ascocarp collected close to *Helianthemum lippi* plants in an arid natural site, located in Abu Dhabi (United Arab Emirates), in February 2014. Both strains have been maintained *in vitro* by subculturing every 3-6 months, using Modified Melin-Norkrans (MMN) and/or optimal Modified Melin-Norkrans (MMNo) (Arenas et al., 2018) liquid (75 rpm) and solid media,

at 23ºC in the dark, (for detailed medium composition see **Appendix A: Supplementary protocols**).

4.2.1   Genome sequencing, assembly and annotation

Genomic DNA and total RNA from axenic liquid cultures of *T. claveryi* and *T. nivea* mycelia were isolated by the CTAB method (Chang et al., 1993). Prior to sequencing, DNA and RNA were treated with RNAse (Thermofisher, US) and DNAse I (Thermofisher, US), respectively. In addition, the bacteria contamination was checked with the 16S amplification and the quality and integrity of DNA and RNA was controlled by gel electrophoresis, fluorometric quantification (Qubit), ratios 260/280 - 260/230 and RNA electrophoresis Bioanalyzer system (2100 Bioanalyzer, Agilent Technologies). All samples met the requirements specified by the JGI for genome sequencing (for detailed DNA and RNA protocols, see **Appendix A: Supplementary protocols**).

Genomes of *T. claveryi* and *T. nivea* were sequenced by the US Department of Energy (DOE), Joint Genome Institute (JGI), using PacBio sequencing, assembled with Falcon, and annotated with the JGI Annotation Pipeline, as detailed in Kohler et al. (2015). The transcriptome was sequenced with Illumina and assembled with Trinity (Grabherr et al., 2011).

4.2.2.   Comparative genomics

For phylogenetic tree construction and genome comparison, 13 fungal genomes belonging to Pezizomycetes class were selected (**Table S1** in **Appendix B: supplementary Tables**). Except for *T. claveryi* and *T. nivea*, the rest of genomes used have been already published (Martin et al., 2010; Murat et al., 2018; Traeger et al., 2013).

4.2.2.1. Tree construction

Orthologous genes (genes that arise from a common DNA ancestral sequence and diverged after speciation event, *i.e.* genes with a similar sequence and function that appear in two or more different species) among the selected fungi were identified using

FastOrtho with the parameters set to 50% identity, 50% coverage, inflation 3.0 (Wattam et al., 2014). The protein sequences used in this process were genome-wide protein assemblies from JGI fungal portal MycoCosm (https://genome.jgi.doe.gov/mycocosm/home). Clusters with single copy genes were identified and aligned with MAFFT 7.221 (Katoh & Standley, 2013), ambiguous regions (regions containing gaps and poorly aligned) were eliminated, and single-gene alignments were concatenated with Gblocks 0.91b (Cruickshank, 2000). A phylogenetic tree was constructed with RAxML 7.7.2 (Stamatakis, 2006) using the standard algorithm, the PROTGAMMAWAG model of sequence evolution and 1,000 bootstrap replicates.

4.2.2.2. Comparative genome feature analysis

Statistics of JGI genome assemblies (*i.e.* N50, number of genes and scaffolds, genome size) were obtained from JGI Mycocosm (https://genome.jgi.doe.gov/programs/fungi/index.jsf). Genome completeness with single copy orthologues was calculated using BUSCO v3.0.2 (Benchmarking Universal Single-Copy Orthologs) with default parameters (Sima et al., 2015). The coverage of TEs in genomes was calculated using a custom pipeline Transposon Identification Nominative Genome Overview (TINGO; Morin et al., 2019). The information above was combined and visualized.

Theoretical secretomes were predicted as described previously (Pellegrin et al., 2015). The count and ratio of total (present in the genomes) and theoretically secreted CAZymes, lipases, proteases and small secreted proteins (< 300 amino acid), plant cell wall degrading enzymes (PCWDEs) and microbe cell wall degrading enzymes (MCWDEs) were calculated, visualized and compared. Global trends of ecological groups were evaluated using Non-metric Multi Dimensional Scaling (NMDS) with the count of total and theoretically secreted CAZymes. The dissimilarities among the ecological groups were calculated and the relationship was converted into distances in the two dimensional space with the function metaMDS in R vegan package (Oksanen et al., 2016). Output files generated above were combined and visualised with custom R scripts, Proteomic Information Navigated Genomic Outlook (PRINGO; available on request) incorporating R packages ggplot2, ggtree, and egg (Auguie 2017; Yu et al., 2017; Wickam 2009).

4.2.2.3. *Pfam domain enrichment*

The Pfam database (El-Gebali et al., 2019) is a large collection of protein families, each represented by multiple sequence alignments and hidden Markov models (HMMs). Domains are functional regions of a protein; a protein can be composed of one or more domains and the same domain can appear in different proteins. The identification of the domains present in a protein can give clues about the function of that protein. First, the top 100 more frequent Pfam domains (https://pfam.xfam.org/, v 32.0) from the 13 fungi analyzed were selected. The frequency values of those domains were transformed into z-scores, which are a measure of relative enrichment and depletion. The hierarchical clustering was done with a Euclidian distance metric and average linkage clustering method. The data were visualized and clustered using MULTIEXPERIMENT VIEWER (http://mev.tm4.org). Then, with the objective of highlighting the families that were overrepresented or underrepresented in the four desert truffles (*T. claveryi*, *T. boudieri, T. nivea* and *K. pfeilii*) compared to the other 9 *Pezizomycetes*, the Mann-Whitney-Wilcoxon test was performed to each Pfam family.

4.2.3. MAT and related genes identification

MAT 1-1-1 genes were automatically annotated by JGI in the genomes of *T. nivea* and *K. pfeilii*. To search for all putative *MAT* genes in *T. claveryi*, *T. boudieri, T. nivea* and *Kalarituber pfeilii* genomes, a local BLASTP was performed on JGI website using the *MAT1-1-1* and *MAT 1-2-1* genes of filamentous ascomycetes as queries and the default parameters. The genomic regions surrounding the *MAT* locus in these species were then scanned to search for conserved genes. Full CDS of *MAT 1-1-1* and HMG domain of *MAT 1-2-1* genes were aligned using MAFFT 7.221 (Katoh & Standley, 2013) and Maximum-Likelihood analysis was done in IQ-TREE (Nguyen et al., 2014) using ultrafast bootstrap with 1000 replicates and the best-fit model (VT+I), chosen according to Bayesian Information Criterion (BIC), determined with ModelFinder (Kalyaanamoorthy et al., 2017). Phylogenetic trees were visualized using Mega X (Kumar et al., 2018). Genes related to pheromone biosynthesis and signaling were also searched in *T. claveryi* and *T. nivea* by BLASTP using orthologous genes already identified in other *Pezizomycetes* as queries (Murat et al., 2018).

4.2.4. Biological material and experimental conditions for transcriptome analysis

In vitro T. claveryi mycelium strain T7 was grown in Erlenmeyer flasks containing liquid MMNo medium (Arenas et al., 2018). The cultures were shaken at 75 rpm and maintained in the dark at 23 °C for three months and then mycelium was collected, flash frozen in liquid nitrogen and stored at -80 °C until later use.

For host plant production, *H. almeriense* seeds were collected in Zarzadilla de Totana (Murcia, Spain) and germinated as explained in Morte et al. (2008). After two months of growth, 36 plants were transferred to 300 cc individual pots where they were inoculated with approximately 10^5 *T. claveryi* spore solution. These spores were obtained from mature ascocarps from the same location stated above. Twelve plants were not inoculated with *T. claveryi* to be used as non-mycorrhizal control plants (NMP). Three months after spore inoculation, mycorrhizal status was checked by microscopy methods (Gutiérrez et al., 2003) and 12 of the inoculated plants were subjected to drought stress. Soil moisture was maintained above 75 % for well-watered mycorrhizal plants (WWMP) and NMP but for drought-stressed mycorrhizal plants (DSMP), it was reduced to 40 % soil moisture and maintained until shoot water potential (Ψ_{shoot}) was less than -2 MPa. Shoot water potential (Ψ_{shoot}) was measured as follows: 5 cm-long plant apices were covered in dark for one hour, cut and immediately placed in a pressure chamber (Soil Moisture Equipment Co; Santa Barbara, CA, U.S.A.) according to Scholander et al. (1965). Once DSMP reached Ψ < -2 MPa, secondary and tertiary roots containing apical tips from six plants per treatment were rinsed to remove soil and harvested. They were immediately stained with tripan ink blue and observed under an Olympus BH2 microscope, to calculate mycorrhizal colonization, mycorrhizal intensity and intracellular colonization from six replicates per treatment (for detailed information, see **Appendix A: Supplementary protocols**). One hundred sections of secondary and tertiary root per sample were observed under the microscope and classified as "mycorrhizal" or "non-mycorrhizal" depending on the presence/absence of mycorrhizal structures of *T. claveryi*. The results were given as a percentage of the total sections observed. To calculate mycorrhization intensity, each mycorrhizal structure of *T. claveryi* observed was classified as 1 (less than 10 % of mycorrhizal structures observed in one segment), 2 (less than 50 %), 3 (more than 50 %) or 4 (more than 90 %), depending on the amount of

mycorrhiza observed in a single section, similarly as Derkowska et al. (2008). Then, the mycorrhization intensity was calculated as the weighted average divided by four. Each *T. claveryi* mycorrhizal colonization observed was also classified as "intercellular" or "intracellular", depending on whether it was forming a clear Hartig net ("intercellular") or the observed hyphae were clearly inside the root cells ("intracellular"). To support these observations, another portion of roots was observed under the stereo microscope and some mycorrhizal root morphotypes were selected and processed to embed them in spurr resin to make semi-thin sections of 0.5 μm, using an Ultramicrotome Leica UC6. Then, these sections were stained with toluidine blue and observed under an Olympus BH2 microscope. From three replicates per treatment, secondary and tertiary roots were immediately flash frozen in liquid nitrogen and stored at -80 °C for RNA extraction and transcriptome analysis.

4.2.5. Transcriptome analysis of *T. claveryi*

Total RNA was extracted from three biological replicates of *T. claveryi* free living mycelium (FLM) and from mycorrhizal root morphotypes of WWMP, DSMP and NMP with the same methodology as reported above. RNA sequencing was performed using 2 x 75 bp Illumina HiSeq^{TM} system after mRNA library construction by Lifesequencing SL (Valencia, Spain). Raw reads were analyzed using FastQC for quality (https://www.bioinformatics.babraham.ac.uk/projects/fastqc/) paired, trimmed and mapped to the *T. claveryi* reference transcripts (https://genome.jgi.doe.gov/mycocosm/home) using CLC genomics Workbench 11. For mapping, the minimum length fraction was 0.9, the minimum similarity fraction 0.9 and the maximum number of hits for a read was set to 10. The unique mapped reads number for each transcript was exported from CLC, normalized, and differential expressed genes with statistical significance (Bonferroni adjusted p < 0.05) were calculated among the conditions using DESeq2 (Love et al., 2014). The RNA-seq data were consistent according to the quality assessment (to asses quality control, see **Figures S1** and **S2** in **Appendix C: Supplementary Figures**), permitting our transcritomic analyses. Condition-specific highly differentially transcribed genes (fold-change > 4 or < -4, FDR <0.05) were identified using a set of custom R scripts from SHIN+GO pipeline (Miyauchi et al., 2016; 2017; 2018)..

4.2.6. Plant *de novo* co-assembly and transcriptome analysis

A *de novo* co-assembly was performed using sequencing reads from NMP, WWMP and DSMP samples using Megahit version 1.1.3 (Li et al., 2015). Transcripts from each condition (NMP, WWMP and DSMP) were mapped onto the contigs generated before with Bowtie2 version 2.3.0 (Langmead and Salzberg, 2012) and reads mapped onto the contigs were counted with SAMtools version 1.7 (Li et al., 2009). Only the contigs with more than 200 bases were selected for further steps and then they were annotated by blasting on NCBI-nr (Non-redundant NCBI database, March 2018 version) and JGI Mycocosm annotation data (July 2018 version) using DIAMOND version 0.9.19 (Buchfink et al., 2014) with the parameters (—more-sensitive --max-target-seqs 1 --max-hsps 1 --evalue 0.00001). Taxonomic annotations for each contig were those of the best hits obtained from NCBI or JGI databases when blast was performed.

The annotated contigs were further separated into three categories (plants, fungi, metazoa) according to the annotations and unknown contigs were removed. Contigs showing sequence coverage above 80 % with a known sequence in the NCBI or JGI databases and with average reads >5 combined from all conditions were selected for further analyses. A summary of the assembly and the contig selection process is shown in **Table 4.1**. Read counts were normalized and differential transcription levels of the contigs were calculated using DESeq2 (Love et al., 2014). Condition-specific highly transcribed and highly differentially transcribed genes were identified with a set of R scripts modified from SHIN+GO pipeline (Miyauchi et al., 2016; 2017; 2018).

Table 4.1. Summary of the number of contigs during the selection process for *de novo* assembly of plants, fungi and metazoans.

Contigs	Number of contigs	Contigs with > 200 bps, hits with sequence coverage with NCBI and/or JGI > 80%, and average > 5 reads
Total	135,404	27,346
Plant	65,209	19,695
Fungi	31,023	7,543
Metazoa	575	108

4.2.7.   Data availability

Full genomes, predicted genes and transcripts of *T. claveryi* T7 and *T. nivea* G3 can be found at JGI portal: https://genome.jgi.doe.gov/Tercla1/Tercla1.home.html and https://genome.jgi.doe.gov/Tirniv1/Tirniv1.home.html, respectively.

4.3.   Results

4.3.1.   Comparative genomics and phylogeny

The genomes of *Terfezia claveryi* and *Tirmania nivea* were sequenced and released in January 2017 and November 2018, respectively, to the JGI Mycocosm portal (https://genome.jgi.doe.gov/mycocosm/home). Phylogenomic analyses placed both *T. claveryi* and *T. nivea* in *Pezizaceae* family, within *Pezizales* order, and close to the other desert truffles, *T. boudieri* and *K. pfelii* (**Figure 4.1**). From a set of conserved fungal BUSCO genes, 83.11% and 86.50% were found in *T. claveryi* and *T. nivea* genomes, respectively, and around 96% of the RNA-seq reads mapped to gene repertoire (Info page, JGI Genome portal), indicating that the assembled genomes are capturing the majority of the coding genes. With genome sizes of 74.5 and 63.1 Mb, respectively, these genomes were similar in size to other *Pezizaceae* analyzed (70.0 Mb average) but significantly smaller than the genomes of ectomycorrhizal *Tuberaceae* (124.0 Mb average) (**Figure 4.1**). *T. claveryi* and *T. nivea* were predicted to contain 12,765 and 10,591 gene models, respectively, with an average gene content not significantly different from *Tuberaceae* (**Figure 4.1**).
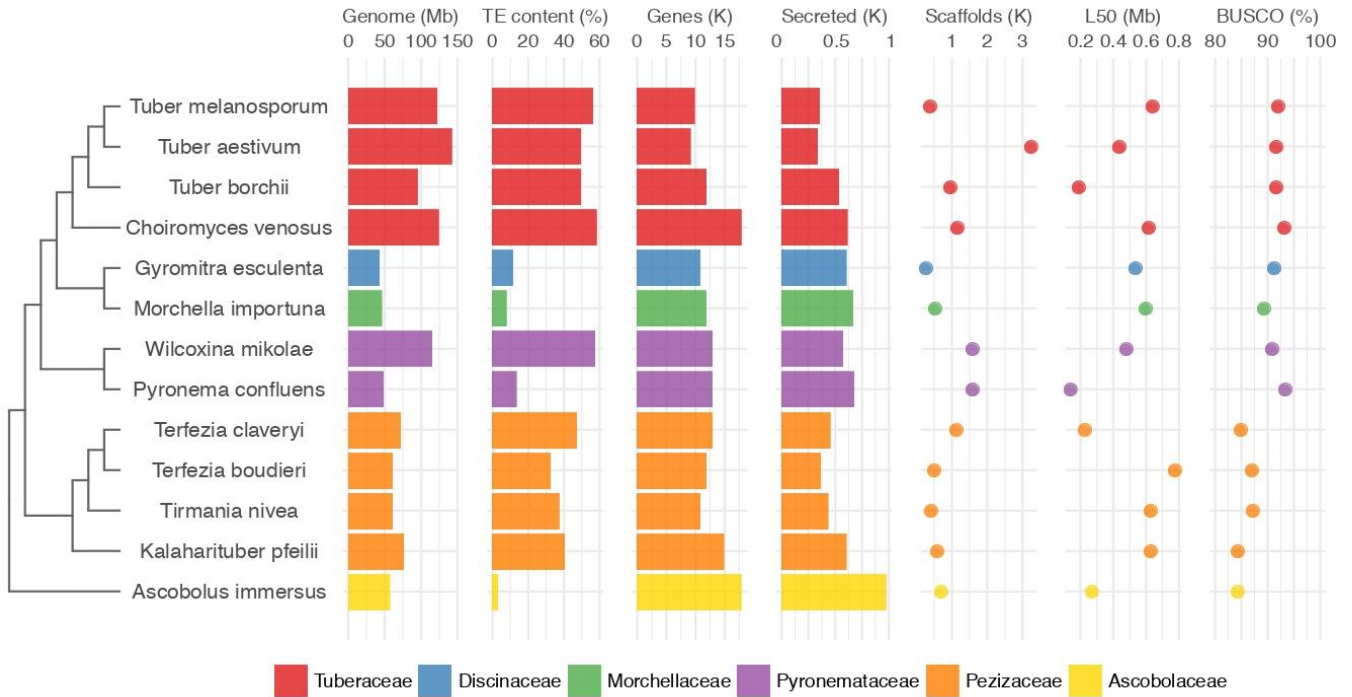
Figure 4.1. Phylogenomic tree and general features and statistics of the compared 13 Pezizomecetes genomes. Colors in the plots represent different taxonomic families. TE = Transposable element; L50 = the number of contigs whose summed length is the mean length of a scaffold; BUSCO = Benchmarking Universal Single-Copy Orthologs, a marker for genome completeness.

The genomes of ECM or EEM *Tuberaceae*, *Pezizaceae* and *Pyronemataceae* contained a higher proportion of transposable elements (TE) than non-mycorrhizal species of the same taxa: 49.8 Mb and 48% genome coverage on the average of the 9 symbiotic species considered *vs* 4.7 Mb and 9.5% genome coverage on the average of the 4 non-mycorrhizal species. *T claveryi* presented 48.3 % genome coverage of TE, which was the highest among *Pezizaceae*, while 38.3 % for *T. nivea* (**Figure 4.1**). Although all mycorrhizal genomes analyzed shared the high content of TE, it was significantly lower (28.4 Mb and 40.2% genome coverage) in *Pezizaceae* than in *Tuberaceae* (66.8 Mb and 54.1 % genome coverage) (**Figure 4.1**). Normally, there is a strong association between TE content and genome size, and these *Pezizaceae* have not been an exception (**Figure 4.2**).
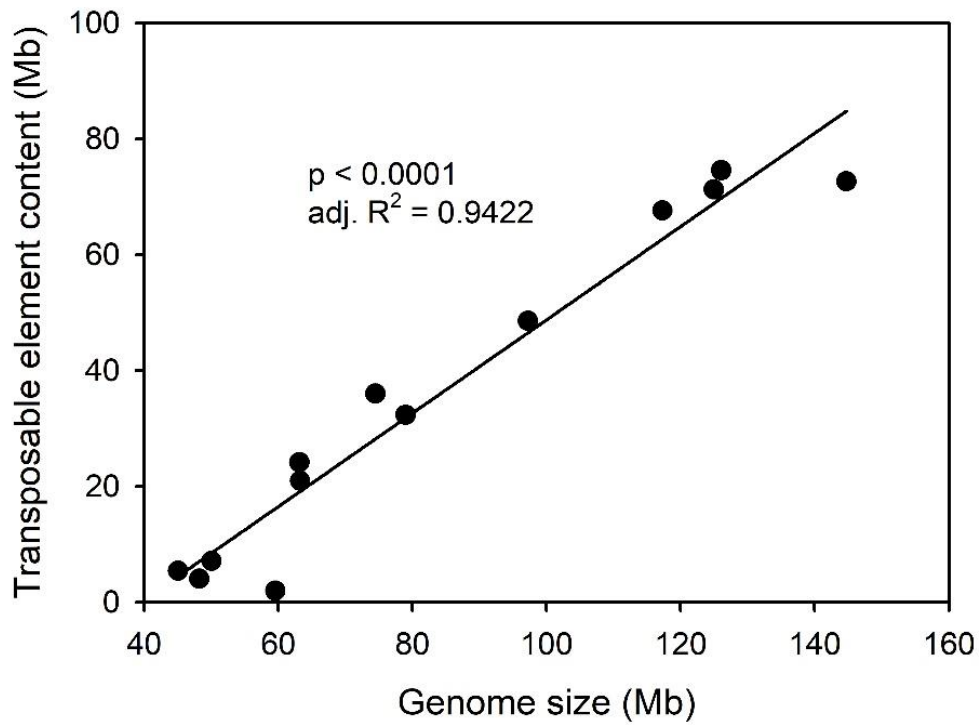
Figure 4.2. Correlation and linear regression analysis between the content of transposable elements and the genome size of the 13 genomes of *Pezizaceae* analyzed.

In terms of TE distribution, the LTR (Gypsy and Copia) and non-LTR (Tad1) transposons are distributed in the 13 fungi analyzed, while the rest (DNA transposons) were found almost exclusively in the mycorrhizal lifestyle of the 13 species studied (**Figure 4.3**).
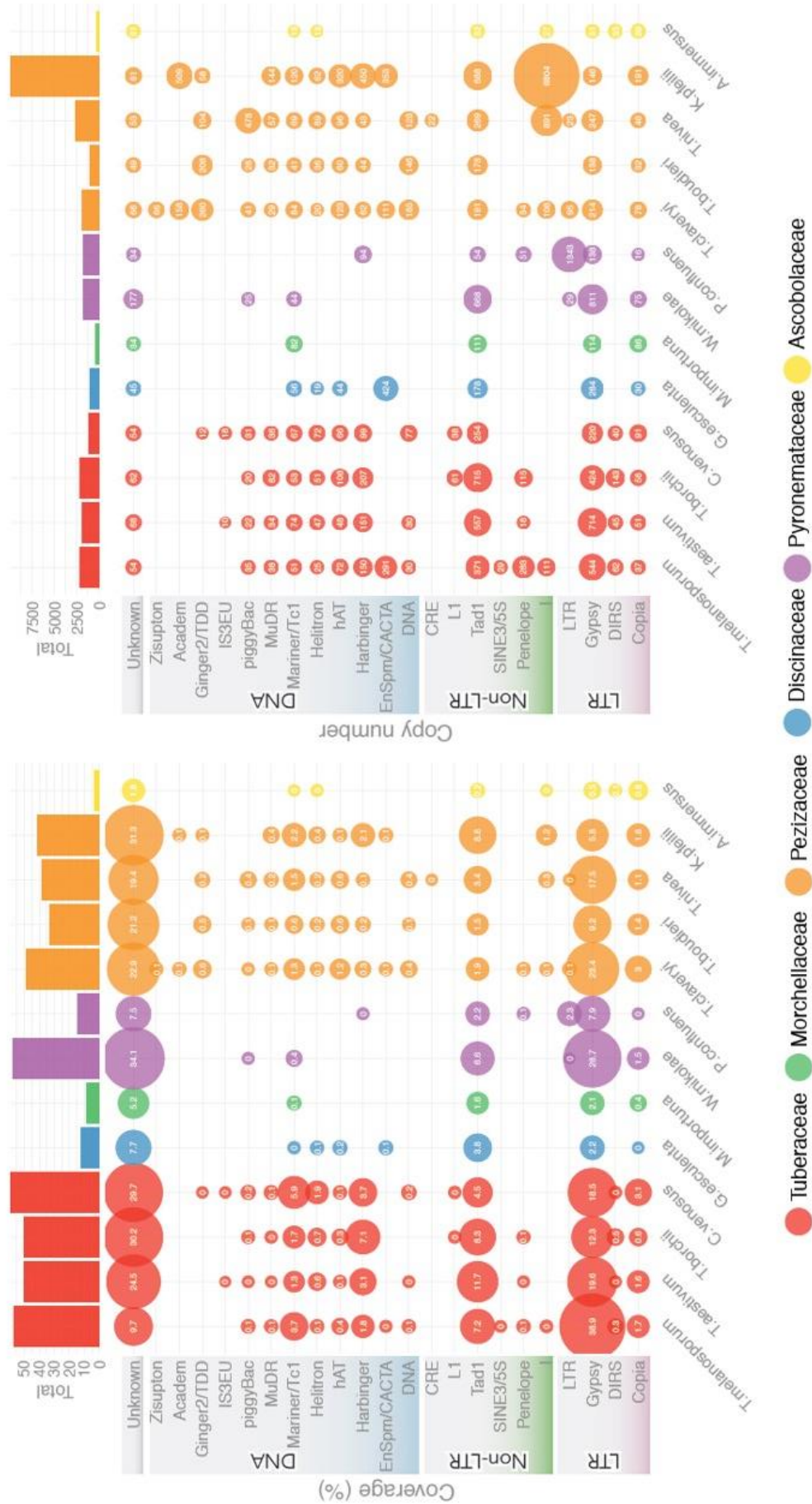
Figure 4.3. Transposable elements identified in 13 genomes. The bubble size is proportional to the coverage of each of the transposable elements (shown inside the bubbles). The bars at the top show the total coverage per genome. LTR = long terminal repeat retrotransposons; Non-LTR = non-long terminal repeat retrotransposons; DNA = DNA transposons; Repetitive/SAT = simple repeats; Unknown = unclassified repeated sequences.

The four desert truffles included in this analysis clustered together, and were separated from other *Tuberaceae* truffles or non-mycorrhizal fungi when a NMDS of total and secreted CAZymes was performed (**Figure 4.4**). The comparison of theoretically secreted enzymes among the 13 fungal genomes showed that *T. claveryi* and *T. nivea* genomes presented a number of total and secreted CAZymes and PCWDE similar to other mycorrhizal species, but remarkably lower than other saprotrophic species (**Figure 4.5**). *Pezizaceae* family, however, presented some differences with respect to (ECM) *Tuberaceae,* as the former possessed less MCWDE and a significantly lower number of genes targeting pectin and chitin (**Figure 4.5**).
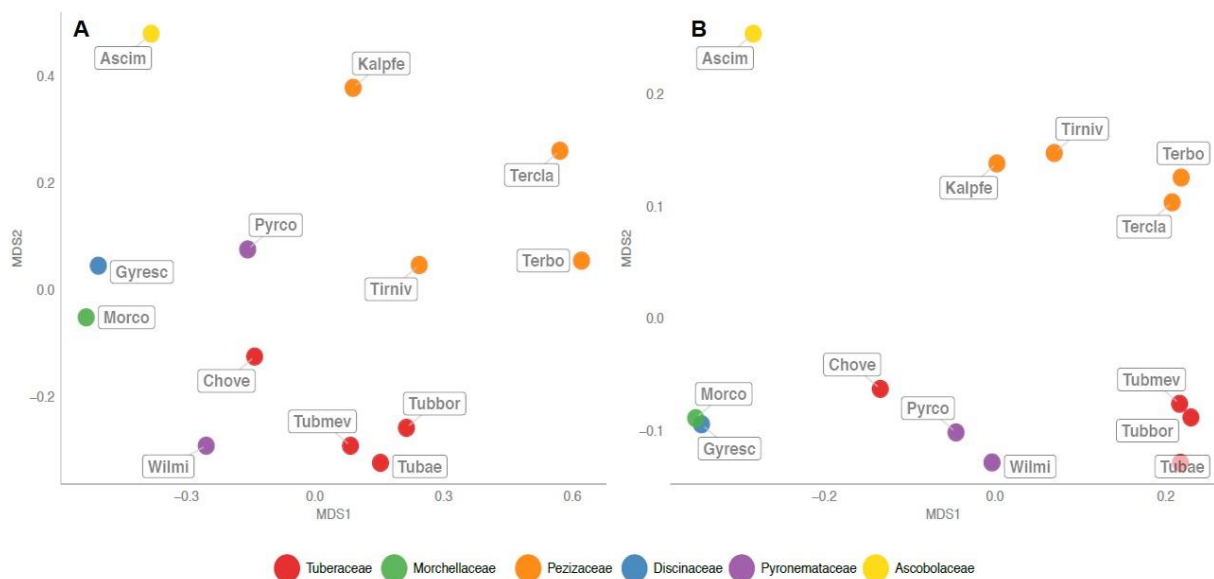
Figure 4.4. CAZyme based clusters of 13 fungi. Secreted CAZyme modules (**A**) and total CAZyme modules present in the genomes (**B**). The fungi are grouped according to taxonomic families and labelled with short JGI fungal IDs. Terbo = *Terfezia boudieri*; Kalpfe = *Kalahatituber pfeilii*; Tirniv = *Tirmania nivea*; Chove = *Choiromyces venosus*; Tubmev = *Tuber melanosporum*; Morco = *Morchella importuna*; Pyrco = *Pyronema confluens*; Tubbor = *Tuber borchii*; Tubae = *Tuber aestivum*; Wilmi = *Wilcoxina mikolae*; Gyresc = *Gyromitra esculenta*; Ascim = *Ascolobus immersus*.
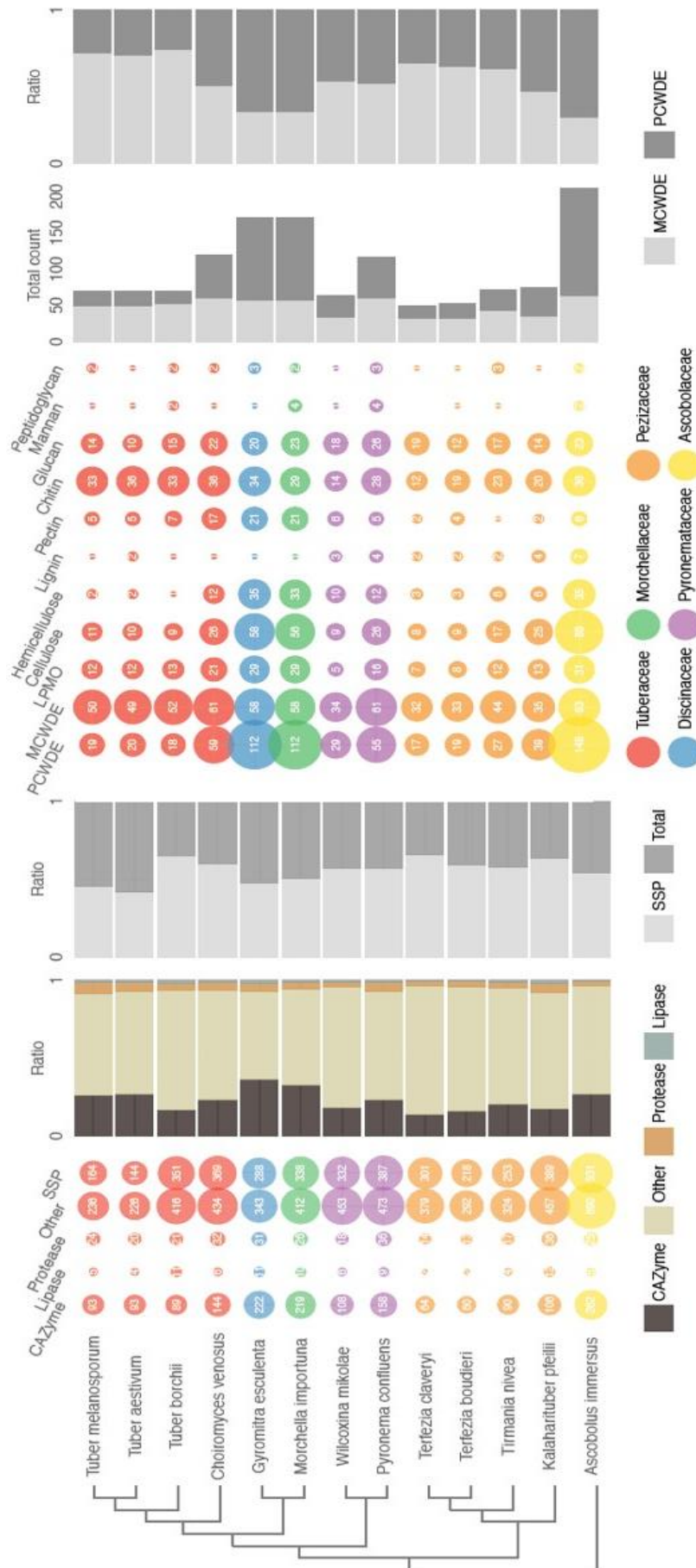
Figure 4.5. Theoretical secretomic profiles of thirteen genomes. Left bubble plot shows the number of secreted genes for CAZymes, lipases, proteases and others (*i.e.* all secreted proteins not in these first three groups). SSPs group refers to the number of small secreted proteins (< 300 aa). The size of bubbles corresponds to the number of genes. Colors in the plots represent different taxonomic families. Left bar plot represents the ratio of CAZymes, lipases, proteases, to all secreted proteins (left) and the ratio of SSPs among the entire secretome (right). Right bubble plot shows the number of plant cell wall degrading enzymes (PCWDE) and microbial cell wall degrading enzymes (MCWDE; fungal cell walls and bacterial membranes), including lytic polysaccharide monooxygenase (LPMO), substrate-specific enzymes for cellulose, hemicellulose, lignin, and pectin (plant cell walls); chitin, glucan, mannan (fungal cell walls); peptidoglycan (bacterial membranes). Right bar plot shows the total count of genes including PCWDE and MCWDE (left) and the ratio of PCWDE to MCWDE (right).

4.3.2.   Sexual reproduction in desert truffles

MAT genes were detected *in silico* in all the four desert truffles included in the study. The *MAT 1-1-1* gene was identified in *T. claveryi* (scaffold 39), *T. nivea* (scaffold 83) and *K. pfeilii* (scaffold 10), while *MAT 1-2-1* was present in *T. boudieri* (scaffold 37). The genomic regions flanking these genes were conserved across these species, with a putative DNA lyase (APN) in all these species, a SAM decarboxylase in *T. claveryi* and *T. boudieri*, whereas a putative cyclooxygenase (COX13) was found next to the *MAT 1-1-1* of *K. pfeilii.* (**Figure 4.6**). Moreover, a putative second *MAT* locus was identified in *K. pfeilii* (scaffold 14), harboring, in this case, a *MAT 1-2-1* gene. Although this gene showed the typical HMG domain, maintained the intron position characteristic of *MAT 1-2-1* genes (see **Figure S3** in **Appendix C: Supplementary Figures**), and clustered together with *Pezizaceae MAT* genes (see **Figure S4** in **Appendix C: Supplementary Figures**), none of the conserved genes flanking the *MAT* locus in the Ascomycetes were found in the surroundings of *K. pfeilii MAT 1-2-1* gene (**Figure 4.6**). Most of the key genes related to pheromone signaling were identified in the two reference genomes of *Pezizaceae* as per BLASTP (see **Table S2** in **Appendix B: Supplementary Tables**).
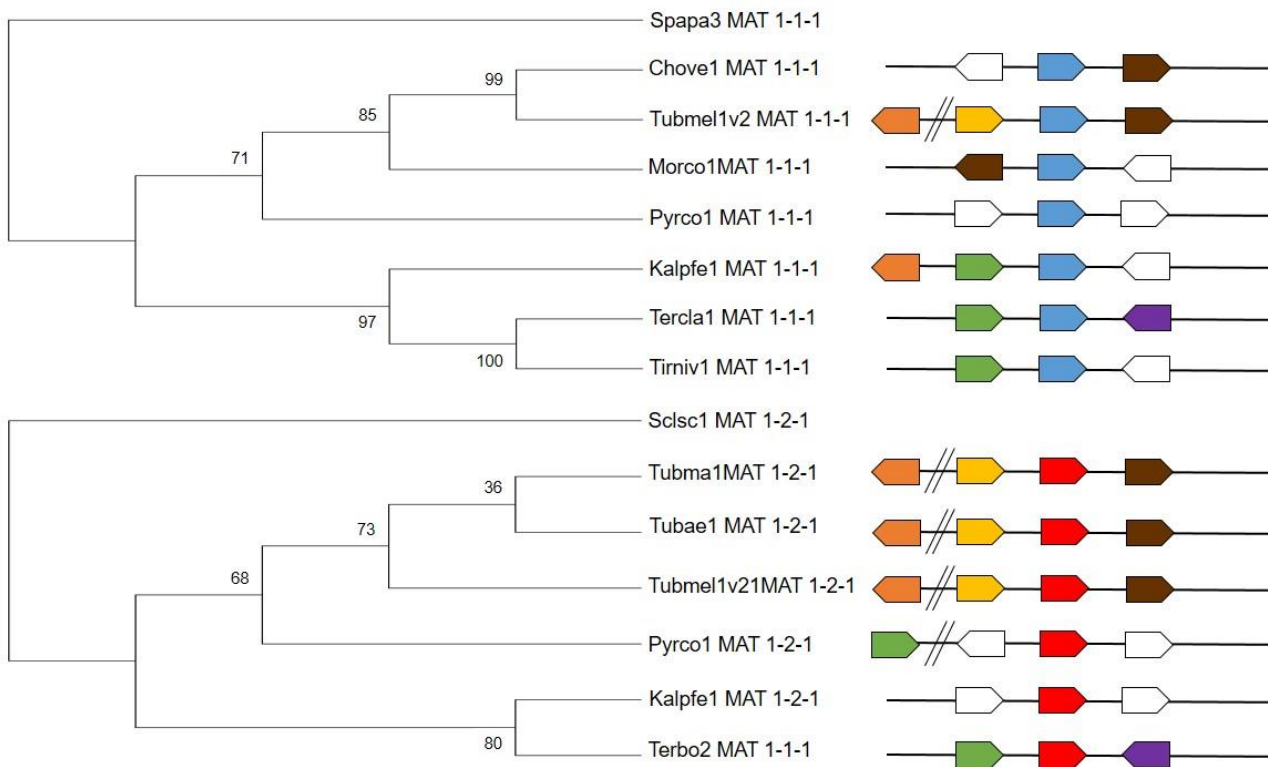
Figure 4.6 (previous page). Phylogenetic tree of *MAT* genes from desert truffles and schematic organization of the mating type loci. Phylogenetic tree was constructed by Maximum-Likelihood method. Colored arrows represent conserved genes among species. Blue = MAT 1-1-1; red = MAT 1-2-1; green = DNA lyase (APN); purple = SAM decarboxylase; orange = cyclooxigenase 13 (COX13); yellow = mitochondrial ribosomal protein of the small subunit (RSM22); brown = homolog to GSTUMT2000009628001 from *T. melanosporum*. Tercla1 = *Terfezia claveryi*; Terbo2 = *Terfezia boudieri*; Kalpfe1 = *Kalaharituber pfeilii*; Tirniv1 = *Tirmania nivea*; Chove1 = *Choiromyces venosus*; Tubmelv2 = *Tuber melanosporum*; Morco1 = *Morchella importuna*; Pyrcon1 = *Pyronema confluens*; Tubma1 = *Tuber magnatum*; Tubae1 = *Tuber aestivum*; Sclsc1 = *Sclerotinia sclerotiorum*; Spapa3 = *Spatasphora passalidarum*.

4.3.3. Desert truffle specific Pfam family domains gains and losses

From the top 100 Pfam family domains represented in all the 13 genomes analyzed, only two of them appeared to have experienced an expansion: WD domain-G-beta repeat, and 50 ribosome-binding GTPase domains (**Figure 4.7**). On the other hand, 18 families showed a constrained number of genes in desert truffles. It is worth noting the reduction of genes related to transport, such as the Major Facilitator Superfamily (MFS), sugar transporters, ABC transporters, or Mg^{2+} transporters (**Figure 4.7**) and the presence of only one aquaporin gene (AQP) in the four desert truffles *versus* at least two AQP genes in the genomes of non-desert truffle species (see **Table S3** in **Appendix B: Supplementary Tables**).

We also found several desert truffle-specific SSPs gene domains including AP complex (*T. claveryi, T. nivea* and *K. pfeilii*), CHAP domain (*T. claveryi* and *T. nivea*), HNH nuclease (*T. claveryi* and *T. nivea*), proteolipid membrane potential modulator (*T. claveryi* and *K. pfeilli*) and ricin B lectin domain (*T. claveryi, T. nivea* and *K. pfeilii*) that were not present in the rest of genomes analyzed (see **Figure S5** in **Appendix C: Supplementary Figures**).
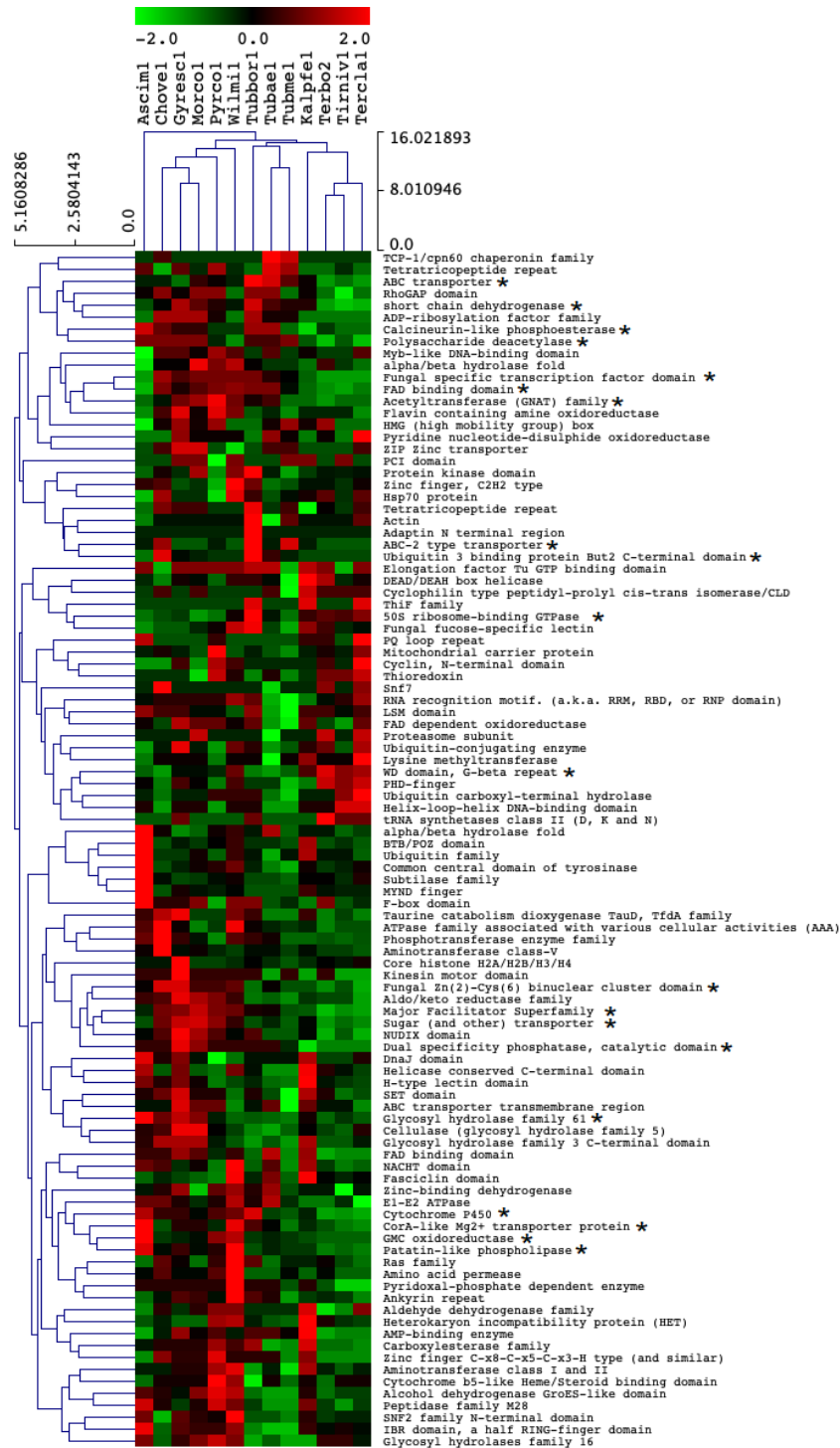
Figure 4.7. Top 100 Pfam families in desert truffles. The heatmap depicts a double hierarchical clustering of all the Pfam families in the 13 fungi analyzed. Frequency values are shown as z-scores, which are a measure of relative enrichment (red) and depletion (green). Significant enriched or depleted gene families (Mann-Whitney_Wilcoxon test, $p < 0.05$) in desert truffles are represented by an asterisk. Tercla 1= *Terfezia claveryi*; Terbo2 = *Terfezia boudieri*; Kalpfe1 = *Kalaharituber pfeilii*; Tirniv1 = *Tirmania nivea*; Chove1 = *Choiromyces venosus*; Tubme1 = *Tuber melanosporum*; Morco1 = *Morchella importuna*; Pyrco1 = *Pyronema confluens*; Tubbor1 = *Tuber borchii*; Tubae1 = *Tuber aestivum*; Wilmi1 = *Wilcoxina mikolae*; Gyresc1 = *Gyromitra esculenta*; Ascim1 = *Ascolobus immersus*.

4.3.4. *Terfezia claveryi* mycorrhiza induced genes

When comparing transcriptomic data from mycorrhizal tissue with data from free living mycelium, 752 genes were found to be upregulated (5.89 % of the total predicted genes, fold-change > 4, FDR <0.05), while 303 were found to be downregulated (2.37 % of the total predicted genes, fold-change < -4, FDR <0.05). Among highly upregulated genes of known function several oxidoreductases (multicopper oxidases, FAD dependent oxidoreductases, cytochrome P450, thioredoxin, cupredoxin…), several transcription factors, membrane transporters (aquaporin, auxin carrier, amino acid, ammonium, nitrate, sugar or sulphate transporters, among others) and amino acid metabolism enzymes (monophenol monooxygenase, L-amine oxidase, amidase…) were found (**Figure 4.8**).
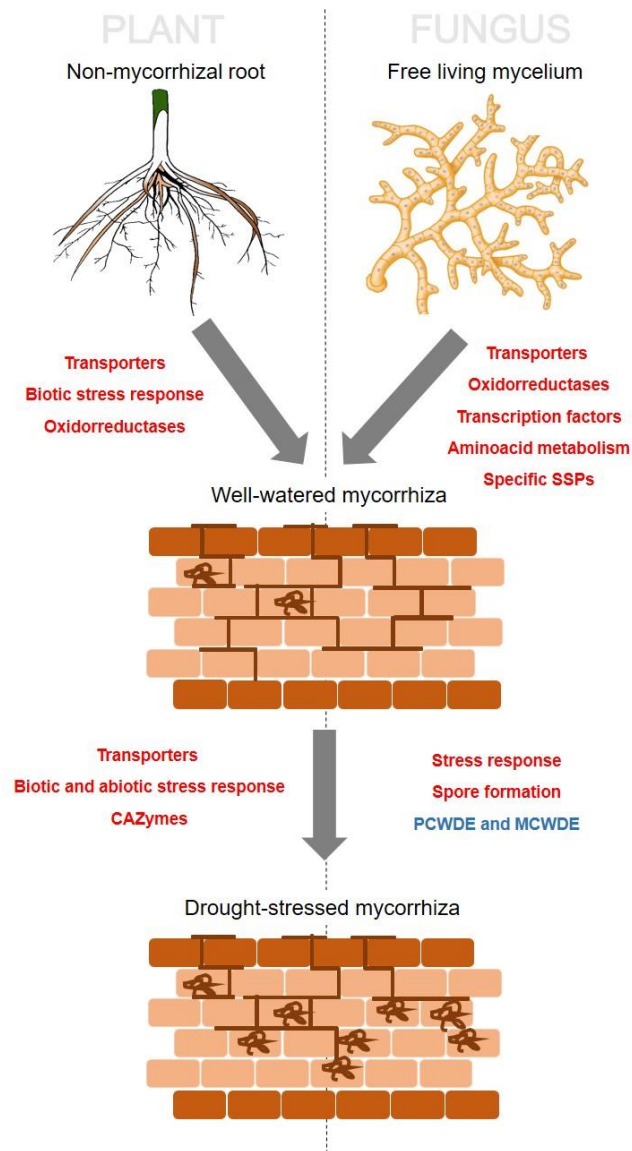
Figure 4.8. Schematic representation of highly upregulated (red) and downregulated (blue) gene groups in each condition assayed. The first arrows represent up or downregulated genes in well-watered mycorrhiza *vs* non-mycorrhizal plant (left) or *vs* free living mycelium (right). The second arrow represents up or downregulated genes in drought-stressed mycorrhiza *vs* well-watered mycorrhiza in the plant (left) or the fungus (right).

Approximately 33% of the *T. claveryi* genes upregulated in symbiosis were conserved among the 13 fungi analyzed (clusters VI and VII, **Figure 4.9**). In these clusters, CAZymes, metabolism and cellular process, and signaling genes were enriched in comparison to the whole genome (Fisher's exact test, $p < 0.05$). Almost 20% of the upregulated genes were specific to *T. claveryi*, finding no homology in any of the other 12 genomes (cluster V, **Figure 4.9**). The rest of the clusters (I to IV, **Figure 4.9**) contained genes shared by all or some of the desert truffles analyzed. SSPs were enriched in the

whole set of upregulated genes and in clusters I and II compared to the whole genome (Fisher's exact test, $p < 0.05$).
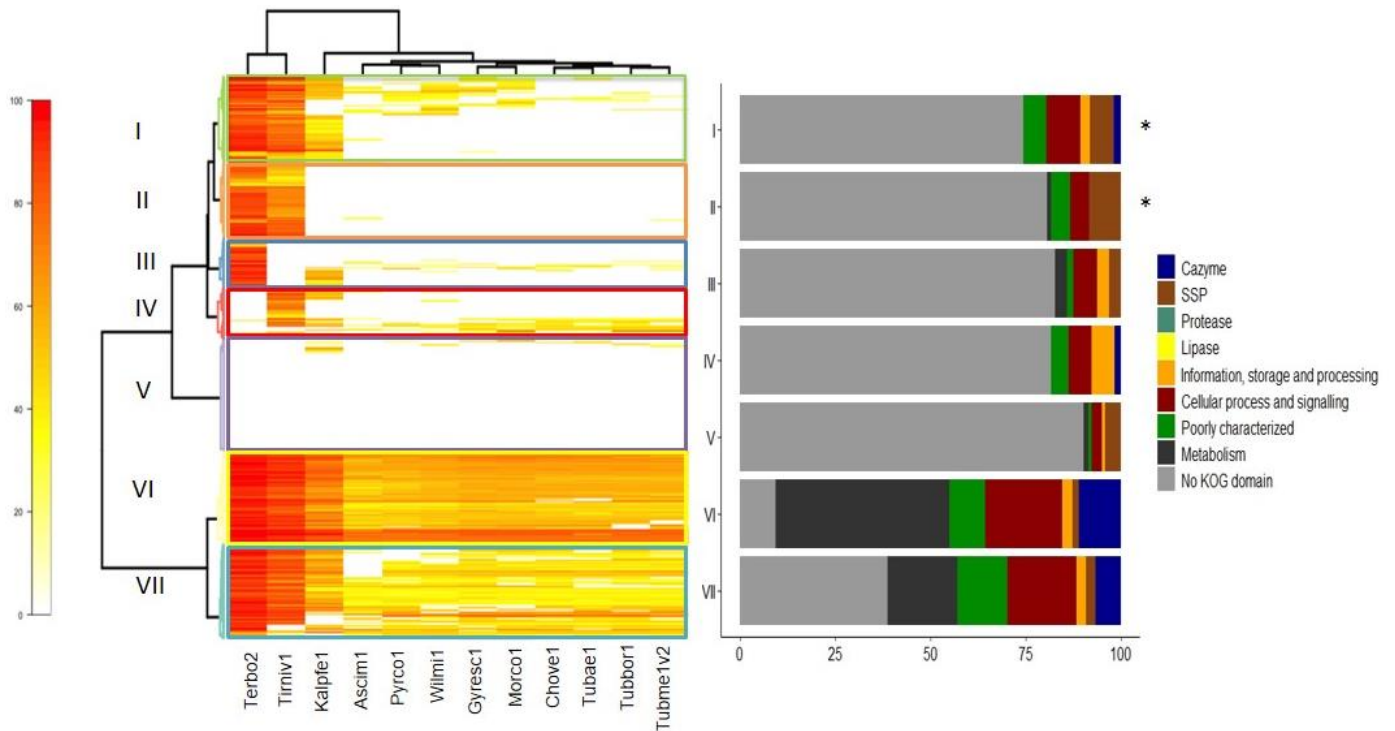
Figure 4.9. Sequence conservation and functional analysis of symbiosis induced transcripts. The heatmap depicts a double hierarchical clustering of the symbiosis-upregulated *Terfezia claveryi* genes (rows, fold-change > 4, FDR-corrected < 0.05). Symbiosis-induced genes were blasted (BLASTP) against the genomes of the thirteen genomes analyzed (see **Figure S6** in **Appendix C: Supplementary Figures** for downregulated genes). Homologues are coloured from yellow to red depending on the percentage of similarity. Clusters are numbered and highlighted with different colors. Right of the heatmap, the percentages of putative functional categories are given for each cluster as bar plots. Clusters significantly enriched in small secreted proteins (SSPs) are marked with an asterisk (Fisher's exact test $p < 0.05$); Terbo2 = *Terfezia boudieri*; Kalpfe1 = *Kalaharituber pfeilii*; Tirniv1 = *Tirmania nivea*; Chove1 = *Choiromyces venosus*; Tubme1v2 = *Tuber melanosporum*; Morco1 = *Morchella importuna*; Pyrco1 = *Pyronema confluens*; Tubbor1 = *Tuber borchii*; Tubae1 = *Tuber aestivum*; Wilmi1 = *Wilcoxina mikolae*; Gyresc1 = *Gyromitra esculenta*; Ascim1 = *Ascolobus immersus*.

The number of *T. claveryi* PCWDE genes upregulated in symbiosis shared with species forming ECM and AM was low. Moreover, while ECM *T. magnatum* or *L. bicolor* presented seven and six upregulated PCWDE genes, respectively, *T. claveryi* only two genes: an AA9, targeting cellulose/hemicelulose, and a CE8, targeting pectin (**Figure 4.10A**).

In addition to SSPs and PCWDE, in the mycorrhiza-induced gene set we also found several enzymes related to the metabolism of tryptophan, which is the main precursor of the auxin indole-3-acetic acid (IAA). This hormone is related, among other functions, to the "acid-growth theory" of plant cell wall remodeling. Two L-aminoacid oxygenases (E.C. 1.4.3.2; protein ID 281043 and 1227268), enzymes potentially responsible for the oxidative deamination of tryptophan to indole-3-piruvic acid (IPA), a precursor of IAA, were upregulated in symbiosis. Furthermore, an amidase (E.C. 3.5.1.4; ID 1102465), potentially responsible for the transformation of indole-3-acetadomide (IAM) to IAA was also upregulated in symbiosis. Also related to IAA, there was an auxin efflux carrier (ID 1084486) upregulated, not only during symbiosis, but also in mycorrhiza under drought stress. In addition, we have identified a fungal EXPN gene upregulated in *T. claveryi* symbiosis (ID 1083860), which was also related to the "acid-growth theory" of plant cell wall remodeling.
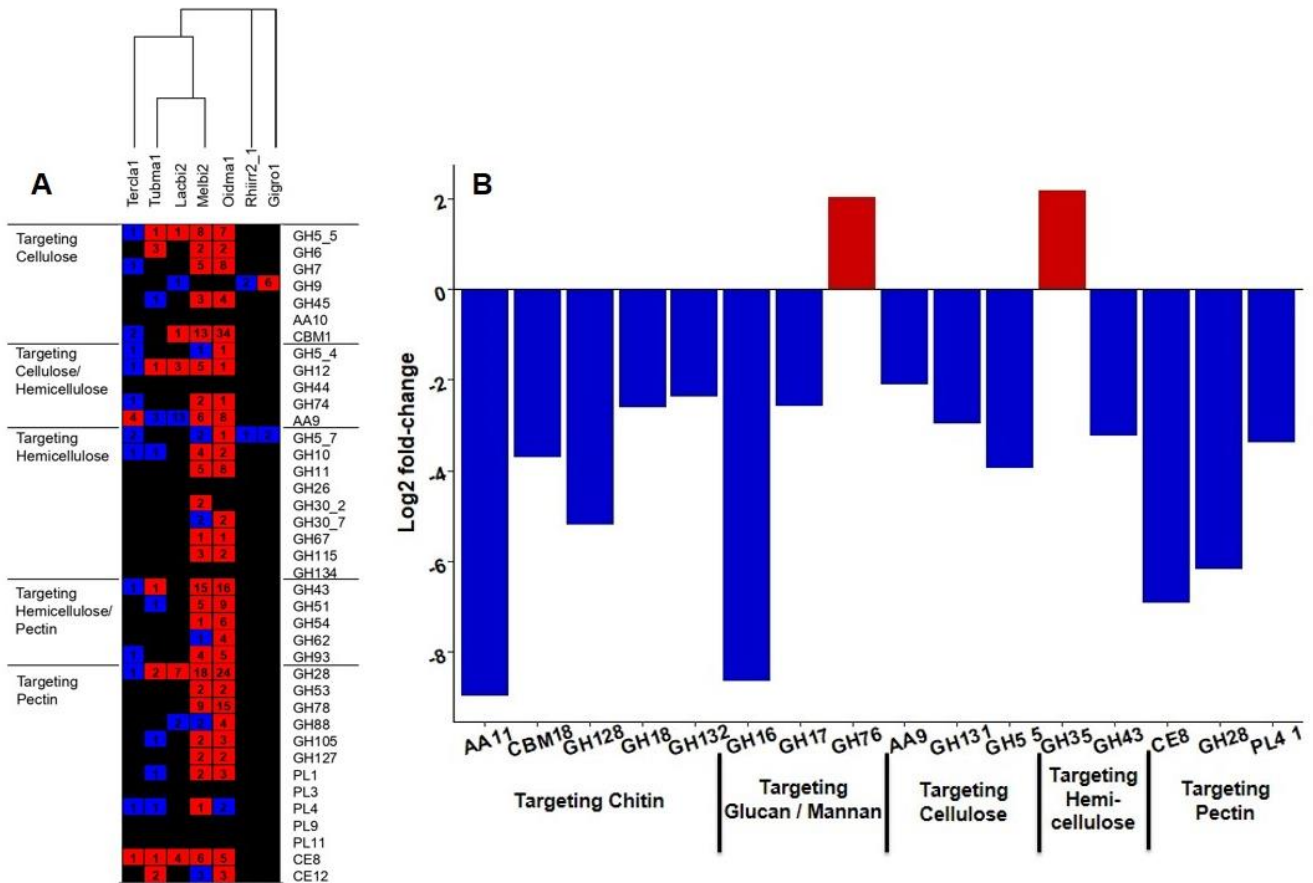
Figure 4.10. *Terfezia claveryi* **genes coding for plant cell wall degrading enzymes (PCWDE) and microbe cell wall degrading enzymes (MCWDE).** (**A**) Presence of genes encoding for different PCWDE in different mycorrhizal organisms. Species were clustered using the Jaccard method. Black = no gene in the genome; Blue = gene present in the genome; Green = gene present in the genome and at least one upregulated gene in symbiosis. Tercla1 = *Terfezia claveryi*; Tubma1 = *Tuber magnatum*; Lacbi2 = *Laccaria bicolor*; Rhiirr2_1 = *Rhizophagus irregularis*; Gigro1 = *Gigaspora rosea*; Melbi2 = *Meliniomyces bicolor*; Oidma1 = *Oidiodendrom mauis*. Transcriptomic data obtained from Kohler et al. (2015); Murat et al. (2018); Martino et al. (2018); Morin et al. (2019). (**B**) Regulation of *T. claveryi* PCWDE and MCWDE under drought stress. Red color represents upregulation and blue color, downregulation.

4.3.5. Fungal colonization and gene regulation under drought conditions

Mycorrhizal colonization of drought-stressed plants was both greater and more intense (**Table 4.2**) than in well-watered plants. In addition, a greater number of intracellular colonization, up to 41.91 % was observed in drought stressed mycorrhizal plants compared to well-watered mycorrhizal plants (2.73 %) (**Table 4.2**, **Figure 4.11**).

Table 4.2. Mycorrizhal colonization of *T. claveryi* x *H. almeriense* plants under different irrigation conditions. Mean ± standard error is represented for each variable. Data was submitted to Mann-Whitney-Wilcoxon test and different letters represent significant differences (p < 0.05).

	Mycorrhizal colonization (%)	Mycorrhizal intensisty (out of 4)	Intracellular colonization (%)
Well-watered	21.34 ± 4.83 a	1.52 ± 0.19 a	2.73 ± 1.88 a
Drought-stressed	45.37 ± 6.62 b	2.20 ± 0.24 b	41.91 ± 9.98 b

When comparing drought stressed to well-watered mycorrhizal plants 228 genes were upregulated, while 329 were downregulated (1.79 % and 2.58 %, fold-change > 4 or < -4, respectively, FDR < 0.05). Up to 26 genes with known function on stress response were upregulated, for instance genes coding for a catalase, a thioredoxin, cupredoxins, superoxide dismutases and several heat shock proteins. Two conidiation specific proteins, one sporulation and one anoctamin, genes known to be involved in spore formation, were also found to be upregulated under drought conditions (**Figure 4.8**).

When analyzing secreted CAZymes in drought conditions, a significant downregulation was found (Fisher's exact test, $p = 0.0007167$ for PCWDE and $p = 0.004683$ for FCWDE) compared to the whole genome set. Seven PCWDE targeting cellulose (AA9, GH131 and GH5_5), hemicellulose (GH43) and pectin (CE8, GH28 and PL4_1) and seven FCWDE targeting chitin (AA11, CBM18, GH128, GH18 and GH132), and glucan (GH16 and GH17) were downregulated during drought stress, while only a GH76 targeting mannan and a GH35 targeting hemicellulose were upregulated (**Figure 4.10B**).
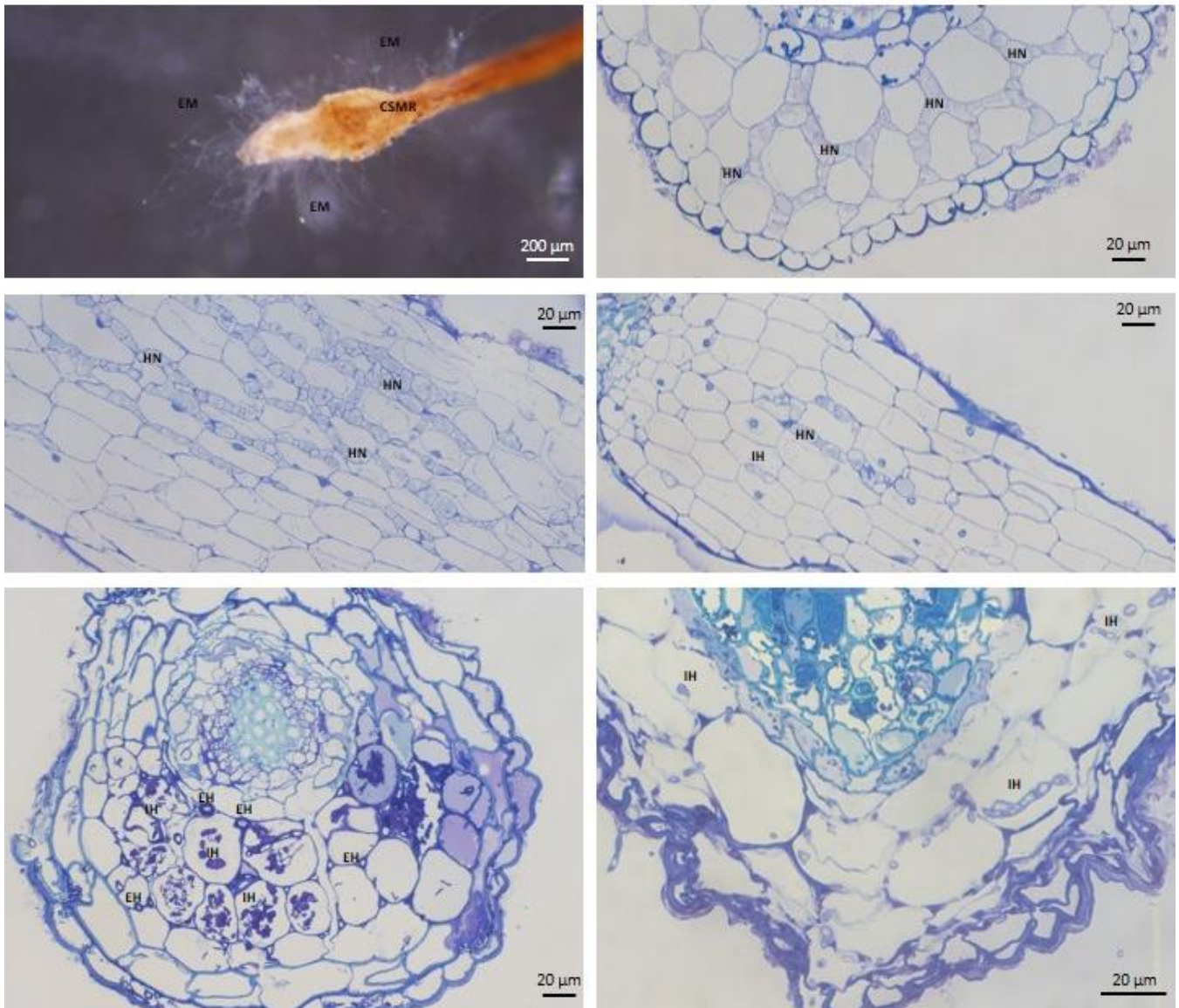
Figure 4.11. *Terfezia claveryi* **x** *Helianthemum almeriense* **mycorrhiza.** (**A**) Club shaped mycorrhizal root (CSMR), one of the four morphotypes described by Gutiérrez et al. (2003), with extraradical mycelium (EM). (**B**) Transversal section of a well-watered mycorrhiza; several hyphae forming Hartig net (HN) can be observed. (**C**) Longitudinal section of a well-watered mycorrhiza; several hyphae forming Hartig net (HN) can be observed. (**D**) Longitudinal section of a drought-stressed mycorrhiza; both hyphae forming Hartig net (HN) and intracellular hyphae (IH) can be observed. (**E**) Transversal section of a drought-stressed mycorrhiza; both intracellular hyphae (IH) forming clumps and extracellular hyphae (EH) can be observed. (**F**) Transversal section of a drought-stressed mycorrhiza with intracellular hyphae (IH).

4.3.6. Plant metatranscriptome

A total of 135,414 contigs were assembled and, after applying the selection criteria previously explained in Materials and Methods, a total of 27,346 contigs were selected for further transcriptomic analysis (**Table 4.1**). 72% of these contigs were from plant origin and more than 80% of the reads were either from *T. claveryi* or from plant origin in all the replicates from all the treatments (**Figure S7**, see **Appendix C: Supplementary Figures**). DSMP was the treatment with more reads from *T. claveryi* (21% *vs* 12% in WWMP and 0.4% in NMP) (**Table S5**, see **Appendix B: Supplementary Tables**). From the 19,696 plant contigs identified in the plant *de novo* assembly, 163 were upregulated when forming mycorrhiza with *T. claveryi* and 72 where downregulated (> 4 and < -4 fold-change, respectively; **Figure 4**). Among the upregulated genes, there were several ABC and MFS transporters, pathogen defense related proteins (such as thaumatin) and oxidoreductases (multicopper oxidases, cytochrome P450…).

H. almeriense mycorrhizal plants subjected to drought stress presented 255 plant genes upregulated and 611 downregulated (> 4 and < -4 fold-change, respectively; **Figure 4**) compared to well-watered mycorrhizal plants. Among the upregulated plant genes, several abiotic and biotic stress-response genes (heat-shock proteins, spermidine synthases, thaumatin…), transporters (sugar and aminoacid transporters, MFS…) and genes related to the carbohydrate metabolism (mainly glucosyl transferases and glucosyl hydrolases) were found.

4.4. Discussion

By comparing the genomes of *T. claveryi* and *T. nivea* with those of other 11 *Pezizomycetes* basic knowledge on the biology of desert truffles has been gained. The genomes of these two species are similar to each other and to those of other desert truffles and, although with some intriguing exceptions, to those of mycorrhizal species belonging to *Tuberaceae* and *Pyronemetaceae* families published so far (Martin et al., 2008, 2010; Kohler et al., 2015; Murat et al., 2018; Miyauchi et al., 2019). The expansion of genome size, normally accompanied with expansion on TE content, on orphan SSPs and a reduced set of PCWDE and CAZymes are among the features shared by the genomes of desert truffles with those of the other symbiotic species. Yet, although both their genome size

and TE content are significantly smaller than in *Tuberaceae*, a significant correlation between these variables is still maintained both in *T. claveryi* and *T. nivea* genomes, to reinforce the contention that genome expansion in mycorrhizal fungi is mainly due to repeated element proliferation (Murat et al., 2018). Likewise, the contraction of PCWDE and CAZymes in all desert truffles is a trait that typifies symbiotic ascomycetes (Kohler et al., 2015). By coupling morpho-anatomical observations of *T. claveryi* x *H. almeriense* mycorrhizae to transcriptomic data, desert truffles specific traits - related to the formation of ectoendomycorrhizae and the adaptation of these species to arid-semiarid environments - have been also identified.

4.4.1. The genomes of desert truffles unveil their reproductive modes

Due to the difficulty to mate desert truffles under controlled conditions, genome sequencing represents the only way to understand their reproductive mode. Firstly, a lack of MAT genes was reported in *T. boudieri* (Murat et al., 2018), but we have demonstrated that these genes are present in this and other desert truffles. The finding of only a single *MAT* gene (either *MAT1-1-1* or *MAT1.2.1*) in the sequenced strains of *T. claveryi*, *T. nivea* and *T. boudieri*, let us in fact argue that these fungi are heterothallic, similarly to *T. melanosporum* (Rubini et al., 2011) and to all *Tuberaceae* studied up to date (Murat et al., 2018). Although with different extent, all these desert truffles *MAT* genes are surrounded by genes such as *APN* and *COX13,* generally linked to the *MAT* locus of filamentous ascomycetes (Debuchy et al., 2010; Traeger et al., 2013; Murat et al., 2018) (**Figure 4.6**). Only in the sequenced strain of *K. pfeilli*, the two opposite *MAT* genes were likely found, suggesting that this species might self-fertilize. However, while the *K. pfeilli MAT1-1-1* gene is embedded in a genomic region that shares synteny with the other desert truffles, the putative *K. pfeilli MAT1-2-1* does not. Further studies are needed to understand whether this HMG containing gene serves as a functional *MAT1-2-1* gene in *K. pfeilli*. The characterization of *MAT* genes in the desert truffles will contribute to our understandings of the evolution and organization of the *MAT* locus within *Pezizomycetes*, and it will be also of pivotal importance for desert truffles cultivation. On this ground, we note that the genome-based disclosure of heterothallism in *Tuber melanosporum* has led to a profound reconsideration of strategies to manage productive

black truffle orchards (Rubini et al., 2011; Zampieri et al., 2012; Linde and Selmes, 2012; Murat et al., 2013; Rubini et al., 2014; Le Tacon et al., 2014).

4.4.2. Desert truffles specific genomic features.

Navarro-Ródenas et al. (2018) characterized a non-canonical ribosomal RNA (rRNA) on some desert truffles, including *T. claveryi, T. boudieri* and *T. nivea*, called "hidden-gap". Although its biological role remains unknown, some authors have related this event with mechanisms for dealing with stressful conditions (Nishimura et al., 2010; Azpurua et al., 2013; Nomura et al., 2016). Expansion of 50S ribosome-binding GTPase family in desert truffles may be related to this rare rRNA profile and somehow linked to adaptation to extreme environments. On the other side, genes related to transport such as MFS, ABC or sugar transporters, together with AQPs, seem to have experienced a reduction in these fungi (**Figure 4.7**). The same trend was found in the mutualistic endophyte *Piriformospora indica*, a fungal species well adapted to desert environments that is known to confer several benefits to its hosts under these conditions (Zuccaro et al., 2011). Therefore, the contraction in genes related to transport observed in desert truffles seems to respond to a conserved adaptive mechanism to optimize the hydraulic conductance in species living in water deficient environments. Likewise, the contraction of PCWDE and MCWDE genes is an expected outcome for species adapted to habitats poor in organic matter.

4.4.3. Mycorhizal - and drought - specific desert truffle traits

T. claveryi colonizes *H. almeriense* through exchanging structures strikingly different from those of ECM and with a remarkable level of plasticity (Gutierrez et al., 2003). Environmental conditions affect not only to the extent of root colonization but also to the ability of this fungus to colonize host roots, forming either inter or intra cellular structures. As previously observed (Navarro-Ródenas et al., 2013; Marques-Gálvez et al., 2019), drought stress triggers a greater *T. claveryi* mycorrhizal colonization level on *H. almeriense* roots. This anatomical observation is confirmed by the higher number of reads corresponding to *T. claveryi* found in drought stress *vs* well-watered mycorrhizal plants (**Table S4**, in **Appendix B: Supplementary Tables**). More intriguingly, under drought

we appreciated a shift in the mycorrhizal structures formed: while *T. claveryi* does not generally penetrate the host cells under control condition, under water deficient condition around 40% of the root cortex cells host *T. claveryi* hyphae (**Table 4.2**; **Figure 4.10**). Due to its ability to degrade the middle lamella, pectin targeting enzymes are thought to play a key role in the formation of the intercellular Hartig net (Veneault-Fourrey et al., 2014). The activity of these enzymes might be dispensable when the intracellular colonization is favored. Accordingly, we observed that among the enzymes that target pectin, only one (CE8) is upregulated in mycorrhizae with respect to *T. claveryi* free living mycelium, whereas both CE8 and other pectin targeting enzymes (*i.e.* GH28 and PL4_1) are downregulated in mycorrhizae under drought stress. Because under this condition the plant genes for carbohydrate metabolism are upregulated (**Figure 4.8**), it is conceivable that the mechanism of *T. claveryi* penetration into the *H. almeriense* roots could depend more on the plant than on the fungal symbiotic partner, as it occurs in AM associations (Tisserant et al., 2013). Additionally, the upregulation of genes related to auxin biosynthesis in the symbiotic stage and the upregulation of an auxin carrier under drought might function to remodel the plant cell wall to accommodate the fungal hyphae intracellularly.

Mutual recognition and the developing of symbiotic exchanging structures are processes that rely on a finely tuned exchange of signaling molecules between the partners, as it occurs in the symbiosis of plants with rhizobia and AM (Perret et al., 2000; Bonfante and Genre, 2015). Recent researches suggest that a combination of differential expression of fungal effectors genes actively counteract plant local defense responses and immunity (reviewed in van der Heijden et al., 2015). As an example, MiSSP7 is the effector, internalized within the plant cells, secreted by *L. bicolor* to colonize its hosts (Plett et al., 2011; 2014). Interestingly, among *T. claveryi* genes upregulated in symbiosis we detected SSPs with different levels of conservation within desert truffles. Along with SSPs shared by all desert truffles (*T. claveryi*, *T. boudieri, T. nivea* and *K. pfeilli*), there are others shared only by *T. claveryi* and its most closely related species (*T. boudieri, T. nivea*), and six specific only to *T. claveryi*. The presence of shared and species-specific SSPs upregulated in symbiosis along with the evidence that *T. claveryi*, *T. boudieri, T. nivea* are known to form mycorrhizal symbiosis with species belonging to the same host genus, *Helianthemum* (Moreno et al., 2014) led us to discuss the presence of a signalling mechanism between desert truffles and their hosts in which both shared and species-

specific SSPs are needed. According to this scenario, the effectors shared by these fungi might reflect the presence of a mechanism, conserved among desert truffles, to interact with their hosts. Future functional analysis would be needed in order to determine the involvement of these effectors in mycorrhiza formation, their specificity among different desert truffles and toward different host species.

In conclusion, although similar to other mycorrhizal genomes in general aspects, several singularities have been found in desert truffle genomes that can be a result of the adaptation to arid and semiarid environments. Among them, the expansion in gene families related to rRNA processing and the contraction in gene families related to water and metabolites transport. Moreover, we have found a relationship between the morphological response of mycorrhizal plants under drought stress and the transcriptomic profile of PCWDE in *T. claveryi*, with special attention to pectin degrading enzymes. These responses to drought stress could be considered an adaptation to arid environments. Future and deeper functional analyses should be carried out in order to improve our understanding on desert truffles and their relationship with the extreme environments they occupy.

References

Arenas F, Navarro-Ródenas A, Chávez D, Gutiérrez A, Pérez-Gilabert M, Morte A (2018) Mycelium of *Terfezia claveryi* as inoculum source to produce desert truffle mycorrhizal plants. Mycorrhiza 28(7):691-701. https://doi.org/10.1007/s00572-018-0867-3.

Auguie B (2017). egg: Extensions for 'ggplot2', to Align Plots, and Set Panel Sizes. https://cran.r-project.org/web/packages/egg/index.html.

Azpurua J, Ke Z, Chen IX, Zhang Q, Ermolenko DN, Zhang ZD., Gorbunova V, Seluanov A (2013) Naked mole-rat has increased translational fidelity compared with mouse, as well as a unique 28S ribosomal RNA cleavage. Proc. Natl. Acad. Sci. USA. 110:17350–17355. https://doi.org/10.1073/pnas.131347311.

Bonfante P, Genre A (2015). Arbuscular mycorrhizal dialogues: Do you speak "plantish" or "fungish"? Trends Plant Sci. 20(3):150–154. https://doi.org/10.1016/j.tplants.2014.12.002.

Bonifacio E, Morte A (2014). Soil properties. In: Kagan-Zur V, Roth-Bejerano N, Sitrit Y, Morte A, eds. Desert Truffles. Phylogeny, Physiology, Distribution and Domestication. Soil Biology, volume 38, Springer-Verlag, Berlin, Heidelberg pp. 57–67. https://doi.org/10.1007/978-3-642-40096-4_2.

Buchfink B, Xie C, Huson DH (2014) Fast and sensitive protein alignment using DIAMOND. Nat. Methods12(1):59–60. https://doi.org/10.1038/nmeth.3176.

Casacuberta E, González J (2013) The impact of transposable elements in environmental adaptation. Mol. Ecol. 22: 1503–1517. https://doi.org/10.1111/mec.12170.

Chang S, Puryear J, Cairney J (1993) A simple and efficient method for isolating RNA from pine trees. Plant Mol. Biol. Rep. 11(2):113–116. https://doi.org/10.1007/BF02670468.

Cruickshank, R (2000) Selection of conserved blocks from multiple alignments for their use in phylogenetic analysis. Mol. Biol. Evol. 17(4):540–552. https://doi.org/10.1093/oxfordjournals.molbev.a026334.

Debuchy R, Berteaux-Lecellier V, Silar P (2010) Mating systems and sexual morphogenesis in ascomycetes. In: Borkovich KA, Ebbloc DJ, eds. Cellular and Molecular Biology of Filamentous Fungi. American Society of Microbiology Press, Washington, DC pp. 501-535. https://doi.org/10.1128/9781555816636.ch33.

Derkowska E, Sas-Paszt L, Sumorok B, Szwonek E, Gluszek S (2008) The influence of mycorrhization and organic mulches on mycorrhizal frequency in apple and strawberry roots. J. Fruit Ornamental Plant Res. 16:227-242.

El-Gebali S, Mistry J, Bateman A, Eddy SR, Luciani A, Potter SC, et al. (2019) The Pfam protein families database in 2019. Nucleic Acids Res. 47(D1):D427-D432. https://doi.org/10.1093/nar/gky995.

Gouws A, De Wet T, Abdullah F, Hassan A, Honrubia M, Morte A (2014) Desert truffle researchin U.A.E. Abstract book of Second Symposium on Hypogeous Fungi in Mediterranean basin(HYPOGES2) & Fifth Congress *Tuber aestivum/uncinatum* European Scientific Group(TAUESG5), Université Mohammed V, Rabat (Morocco), 9–13 April 2014, p 17.

Grabherr MG, Haas BJ, Yassour M, Levin JZ, Thompson DA, Amit I, et al. (2011) Full-length transcriptome assembly from RNA-seq data without a reference genome. Nat. Biotechnol. 29(7):644-52. https://doi.org/10.1038/nbt.1883.

Grigoriev IV, Nikitin R, Haridas S, Kuo, A, Ohm R, Otillar R, et al. (2014) MycoCosm portal: Gearing up for 1000 fungal genomes. Nucleic Acids Res. 42(D1):699–704. https://doi.org/10.1093/nar/gkt1183.

Gutiérrez A, Morte A, Honrubia M (2003) Morphological characterization of the mycorrhiza formed by *Helianthemum almeriense* Pau with *Terfezia claveryi* Chatin and *Picoa lefebvrei* (Pat.) Maire. Mycorrhiza 13(6):299–307. https://doi.org/10.1007/s00572-003-0236-7.

Honrubia M, Gutiérrez A, Morte A (2001) Desert truffle plantation from southeast Spain. In: Edible Mycorrhizal Mushrooms and Their Cultivation: Proceedings of the Second International Conference on Edible Mycorrhizal Mushrooms. Christchurch, New Zealand, pp 3–5.

Kagan-Zur V, Roth-Bejerano N (2008) Desert truffles. Fungi 1 (Special Issue: Truffles) 1(3):32–37.

Kagan-Zur V, Roth-Bejerano N, Sitrit Y, Morte A (2014) Desert Truffles. Phylogeny, Physiology, Distribution and Domestication. Soil Biology, volume 38. Springer-Verlag, Berlin, Heidelberg. ISBN 978-3-642-40095-7.

Kalyaanamoorthy S, Minh BQ, Wong TK, von Haeseler A, Jermiin LS.(2017) ModelFinder: fast model selection for accurate phylogenetic estimates. Nat. Methods 14(6):587. https://doi.org/10.1038/nmeth.4285.

Katoh K, Standley DM (2013) MAFFT multiple sequence alignment software version 7: improvements in performance and usability. Mol. Biol. Evol. 30(4):772–780. https://doi.org/10.1093/molbev/mst010.

Kohler A, Kuo A, Nagy LG, Morin E, Barry KW, Buscot F, et al. (2015) Convergent losses of decay mechanisms and rapid turnover of symbiosis genes in mycorrhizal mutualists Nat. Gen. 47(4):410–415. https://doi.org/10.1038/ng.3223.

Kovács G, Trappe J (2014) Nomenclatural history and genealogies of desert truffle. In: Kagan-Zur V, Roth-Bejerano N, Sitrit Y, Morte A, eds. Desert Truffles. Phylogeny, Physiology, Distribution and Domestication. Soil Biology, volume 38. Springer-Verlag, Berlin, Heidelberg pp. 57–67. https://doi.org/10.1007/978-3-642-40096-4_2.

Kumar S, Stecher G, Li M, Knyaz C, Tamura K (2018) MEGA X: Molecular evolutionary genetics analysis across computing platforms. Mol. Biol. Evol. 35(6):1547–1549. https://doi.org/10.1093/molbev/msy096.

Kuo A, Bushnell B, Grigoriev, IV (2014) Fungal genomics: Sequencing and annotation. In: Grimm B, ed. Advances in Botanical Research (1st ed., Vol. 70). Elsevier Ltd pp. 1-52. https://doi.org/10.1016/B978-0-12-397940-7.00001-X.

Langmead B, Salzberg SL (2012) Fast gapped-read alignment with Bowtie 2. Nat. Methods 9(4):357–359. https://doi.org/10.1038/nmeth.1923.

Lavee H, Imeson AC, Sarah, P (1998) The impact of climate change on geomorphology and desertification along a Mediterranean-arid transect. Land Degrad. Dev. 9(5):407–422. https://doi.org/10.1002/(SICI)1099-145X(199809/10)9:5<407::AID-LDR302>3.0.CO;2-6

Le Tacon F, Marçais B, Courvoisier M, Murat C, Montpied P, Becker M (2014) Climatic variations explain annual fluctuations in French 'Périgord black truffle' wholesale markets but do not explain the decrease in 'black truffle' production over the last 48 years. Mycorrhiza 24 (1):115–125. https://doi.org/10.1007/s00572-014-0568-5.

Li H, Handsaker B, Wysoker A, Fennell T, Ruan J, Homer N, et al. (2009) The Sequence Alignment/Map format and SAMtools. Bioinformatics 25(16):2078–2079. https://doi.org/10.1093/bioinformatics/btp352.

Li D, Liu CM, Luo R, Sadakane K, Lam TW (2015) MEGAHIT: An ultra-fast single-node solution for large and complex metagenomics assembly *via* succinct de Bruijn graph. Bioinformatics 31(10):1674–1676. https://doi.org/10.1093/bioinformatics/btv033.

Linde, CC, Selmes H (2012) Genetic diversity and mating type distribution of *Tuber melanosporum* and their significance to truffle cultivation in artificially planted truffieres in Australia. Appl. Environ. Microbiol. 78(18):6534-6539. . https://doi.org/10.1128/AEM.01558-12.

Love MI, Huber W, Anders S (2014) Moderated estimation of fold-change and dispersion for RNA-seq data with DESeq2. Genome Biol. 15(12):550. https://doi.org/10.1186/s13059-014-0550-8.

Marqués-Gálvez JE, Morte A, Navarro-Ródenas A, García-Carmona F, Pérez-Gilabert M (2019) Purification and characterization of *Terfezia claveryi* TcCAT-1, a desert truffle catalase upregulated in mycorrhizal symbiosis. PloS One 14(7):e0219300. https://doi.org/10.1371/journal.pone.0219300.

Martin F, Aerts A, Ahrén D, Brun A, Danchin EGJ, Duchaussoy F, et al. (2008) The genome of *Laccaria bicolor* provides insights into mycorrhizal symbiosis. Nature 452(7183):88–92. https://doi.org/10.1038/nature06556.

Martin F, Kohler A, Murat C, Balestrini R, Coutinho PM, Jaillon O, et al. (2010) Périgord black truffle genome uncovers evolutionary origins and mechanisms of symbiosis Nature 464(7291): 1033–1038. https://doi.org/10.1038/nature08867.

Martino E, Morin E, Grelet GA, Kuo A, Kohler A, Daghino S, et al. (2018) Comparative genomics and transcriptomics depict ericoid mycorrhizal fungi as versatile saprotrophs and plant mutualists. New Phytol. 217(3):1213-1229. https://doi.org/10.1111/nph.14974.

Miyauchi S, Navarro D, Grigoriev IV, Lipzen A, Riley R, Chevret D, et al. (2016) Visual comparative omics of fungi for plant biomass deconstruction. Front. Microbiol. 7(AUG):1–10. https://doi.org/10.3389/fmicb.2016.01335.

Miyauchi S, Navarro D, Grisel S, Chevret D, Berrin JG, Rosso, MN. (2017). The integrative omics of white-rot fungus *Pycnoporus coccineus* reveals co-regulated CAZymes for orchestrated lignocellulose breakdown. PloS One 12(4):1–17. https://doi.org/10.1371/journal.pone.0175528.

Miyauchi S, Rancon A, Drula E, Hage H, Chaduli D, Favel A, et al. (2018). Integrative visual omics of the white-rot fungus *Polyporus brumalis* exposes the biotechnological potential of its oxidative enzymes for delignifying raw plant biomass. Biotechnol. Biofuels 11(1):1–14. https://doi.org/10.1186/s13068-018-1198-5.

Moreno G, Alvarado P, Manjón JL. (2014). Hypogeous desert fungi. In: Kagan-Zur V, Roth-Bejerano N, Sitrit Y, Morte A, eds. Desert Truffles. Phylogeny, Physiology, Distribution and Domestication. Soil Biology, volume 38. Springer-Verlag, Berlin, Heidelberg pp. 57–67. https://doi.org/10.1007/978-3-642-40096-4_1.

Morin E, Miyauchi S, San Clemente H, Chen ECH, Pelin A, de la Providencia, I, et al. (2019) Comparative genomics of *Rhizophagus irregularis*, *R. cerebriforme*, *R.diaphanus* and *Gigaspora rosea* highlights specific genetic features in Glomeromycotina. New Phytol. 222(3):1584–1598. https://doi.org/10.1111/nph.15687.

Morte A, Cano A, Honrubia M, Torres P (1994) *In vitro* mycorrhization of micropropagated *Helianthemun almeriense* plantlets with *Terfezia claveryi* (desert truffle). Agric. Sci. Finl. 3:309–314. https://doi.org/10.23986/afsci.72700.

Morte A, Lovisolo C, Schubert A (2000) Effect of drought stress on growth and water relations of the mycorrhizal association *Helianthemum almeriense-Terfezia claveryi*. Mycorrhiza 10(3):115–119. https://doi.org/10.1007/s005720000066.

Morte A, Honrubia M, Gutiérrez A (2008) Biotechnology and cultivation of desert truffles. In: Varma A, ed. Mycorrhiza. Springer Berlin Heidelberg pp. 467–483. https://doi.org/10.1007/978-3-540-78826-3_23.

Morte A, Navarro-Ródenas A, Nicolás E (2010) Physiological parameters of desert truffle mycorrhizal *Helianthemun almeriense* plants cultivated in orchards under water deficit conditions. Symbiosis 52(2–3):133–139. https://doi.org/10.1007/s13199-010-0080-4.

Morte A, Pérez-Gilabert M, Gutiérrez A, Arenas F, Marqués-Gálvez JE, Bordallo JJ, Rodríguez A, Berná LM, Lozano-Carrillo C, Navarro-Ródenas, A (2017) Basic and applied research for desert truffle cultivation. In: Varma A, Prasad R, Tuteja N, eds. Mycorrhiza-ecophysiology, secondary metabolites, nanomaterials. Springer International Publishing pp. 23–24. https://doi.org/10.1007/978-3-319-57849-1_2.

Murat C, Rubini A, Riccioni C, De la Varga, H, Akroume E, Belfiori B, et al. (2013) Fine-scale spatial genetic structure of the black truffle (*Tuber melanosporum*) investigated with neutral microsatellites and functional mating type genes. New Phytol. 199(1):176-187. https://doi.org/10.1111/nph.12264.

Murat C, Payen T, Noel B, Kuo A, Morin E, Chen J, et al. (2018) Pezizomycetes genomes reveal the molecular basis of ectomycorrhizal truffle lifestyle. Nat. Ecol. Evol. 2(12):1956–1965. https://doi.org/10.1038/s41559-018-0710-4.

Navarro-Ródenas A, Pérez-Gilabert M, Torrente P, Morte A (2012) The role of phosphorus in the ectendomycorrhiza *continuum* of desert truffle mycorrhizal plants. Mycorrhiza 22(7):565-575. https://doi.org/10.1007/s00572-012-0434-2.

Navarro-Ródenas A, Bárzana G, Nicolás E, Carra A, Schubert A, Morte A (2013) Expression analysis of aquaporins from desert truffle mycorrhizal symbiosis reveals a fine-tuned regulation under drought. Mol. Plant Microbe Interact. 26(9):1068–78. https://doi.org/10.1094/MPMI-07-12-0178-R.

Navarro-Ródenas A, Carra A, Morte A (2018) Identification of an alternative rRNA post-

transcriptional maturation of 26S rRNA in the Kingdom Fungi. Front. Microbiol. 9(MAY):1–8. https://doi.org/10.3389/fmicb.2018.00994.

Nguyen LT, Schmidt HA, von Haeseler A, Minh BQ (2014) IQ-TREE: a fast and effective stochastic algorithm for estimating maximum-likelihood phylogenies. Mol. Biol. Evol. 32(1):268-274. https://doi.org/10.1093/molbev/msu300.

Nishimura K, Ashida H, Ogawa T, Yokota A (2010) A DEAD box protein is required for formation of a hidden break in *Arabidopsis* chloroplast 23S rRNA. Plant J. 63:766–777. https://doi.org/10.1111/j.1365-313X.2010.04276.x.

Nomura T, Ito M, Kanamori M, Shigeno Y, Uchiumi T, Arai R, et al. (2016).Characterization of silk gland ribosomes from a bivoltine caddisfly, *Stenopsyche marmorata*: translational suppression of a silk protein in cold conditions. Biochem. Biophys. Res. Commun. 469:210–215. https://doi.org/10.1016/j.bbrc.2015.11.112.

Oksanen J, Blanchet FG, Friendly M, Kindt, P, Legendre P, McGlinn D, et al. (2016) Vegan: community ecology package. R version 3.2. 4. https://cran.r-project.org/web/packages/vegan/index.html.

Payen T, Murat C, Martin F (2016) Reconstructing the evolutionary history of gypsy retrotransposons in the Périgord black truffle (*Tuber melanosporum* Vittad.). Mycorrhiza 26(6):553–563. https://doi.org/10.1007/s00572-016-0692-5.

Pellegrin C, Morin E, Martin FM, Veneault-Fourrey C (2015) Comparative analysis of secretomes from ectomycorrhizal fungi with an emphasis on small-secreted proteins. Front. Microbiol. 6:1278. https://doi.org/10.3389/fmicb.2015.01278.

Perret X, Staehelin C, Broughton WJ (2000) Molecular basis of symbiotic promiscuity. Microbiol Mol. Biol. Rev.: MMBR. 64(1):180–201.

Plett JM, Kemppainen M, Kale SD, Kohler A, Legué V, Brun A, et al. (2011) A secreted effector protein of *Laccaria bicolor* is required for symbiosis development. Curr. Biol. 21(14):1197-1203. https://doi.org/10.1016/j.cub.2011.05.033.

Plett JM, Daguerre Y, Wittulsky S, Vayssieres A, Deveau A, Melton SJ, et al. (2014) Effector MiSSP7 of the mutualistic fungus *Laccaria bicolor* stabilizes the *Populus* JAZ6 protein and represses jasmonic acid (JA) responsive genes. Proc. Natl. Acad. Sci. USA. 111(22):8299–8304. https://doi.org/10.1073/pnas.1322671111.

Price AL, Jones NC, Pevzner PA (2005) *De novo* identification of repeat families in large genomes. Bioinformatics. 21(SUPPL1):351–358. https://doi.org/10.1093/bioinformatics/bti1018.

Raffaele S, Kamoun S (2012) Genome evolution in filamentous plant pathogens: why bigger can be better. Nat. Rev. Microbiol. 10:417–430. https://doi.org/10.1038/nrmicro2790.

Roth-Bejerano N, Navarro-Ródenas A, Gutiérrez A. (2014). Hypogeous desert fungi. In: Kagan-Zur V, Roth-Bejerano N, Sitrit Y, Morte A, eds. Desert Truffles. Phylogeny, Physiology, Distribution and Domestication. Soil Biology, volume 38. Springer-Verlag, Berlin, Heidelberg pp. 57–67. https://doi.org/10.1007/978-3-642-40096-4_5.

Rubini A, Belfiori B, Riccioni C, Tisserant E, Arcioni S, Martin F, Paolocci F (2011) Isolation and characterization of MAT genes in the symbiotic ascomycete *Tuber melanosporum*. New Phytol. 189(3):710–722. https://doi.org/10.1111/j.1469-8137.2010.03492.x.

Rubini A, Riccioni C, Belfiori B, Paolocci F (2014) Impact of the competition between mating types on the cultivation of Tuber melanosporum: Romeo and Juliet and the matter of space and time. Mycorrhiza 24(1):19-27. https://doi.org/10.1007/s00572-013-0551-6.

Schlesinger WH, Reynolds JF, Cunningham GL, Laura F, Jarrell WM, Virginia RA, et al. (1990) Biological feedbacks in global desertification conceptual models for desertification. Science 247(4946):1043–1048. https://doi.org/10.1126/science.247.4946.1043.

Scholander PF, Bradstreet ED, Hemmingsen EA,Hammel H (1965) Sap pressure in vascular plants. Science 148:339–346. https://doi.org/10.1126/science.148.3668.339.

Sima FA, Waterhouse RM, Ioannidis P, Kriventseva EV, Zdobnov EM (2015) BUSCO: Assessing genome assembly and annotation completeness with single-copy orthologs. Bioinformatics 31(19):3210–3212. https://doi.org/10.1093/bioinformatics/btv351.

Slama A, Fortas Z, Boudabous A, Neffati, M (2010) Cultivation of an edible desert truffle (*Terfezia boudieri* Chatin). Afr J Microbiol Res. 4(22): 2350–2356.

Stamatakis, A (2006) RAxML-VI-HPC: Maximum Likelihood-based phylogenetic analyses with thousands of taxa and mixed models. Bioinformatics 22(21):2688–2690. https://doi.org/10.1093/bioinformatics/btl446.

Tisserant E, Malbreil M, Kuo A, Kohler A, Symeonidi A, Balestrini R, et al. (2013) Genome of an arbuscular mycorrhizal fungus provides insight into the oldest plant symbiosis. Proc. Natl. Acad. Sci. USA. 110(50):20117-20122. https://doi.org/10.1073/pnas.1313452110.

Traeger S, Altegoer F, Freitag M, Gabaldon T, Kempken F, Kumar A, et al. (2013) The genome and development-dependent transcriptomes of *Pyronema confluens*: A window into fungal evolution. PLoS Genetics 9(9). https://doi.org/10.1371/journal.pgen.1003820.

Trappe JM, Claridge AW, Arora D, Smit WA (2008) Desert truffles of the African Kalahari: ecology, ethnomycology, and taxonomy. Econ. Bot. 62(3):521. https://doi.org/10.1007/s12231-008-9027-6.

United Nations Educational, Scientific and Cultural Organization (UNESCO) (1979) Map of the world distribution of arid regions: map at scale 1:25,000,000 with explanatory note. MAB Technical Notes 7, UNESCO, Paris.

Veneault-Fourrey C, Commun C, Kohler A, Morin E, Balestrini R, Plett J, et al. (2014) Genomic and transcriptomic analysis of *Laccaria bicolor* CAZome reveals insights into polysaccharides remodelling during symbiosis establishment. Fungal Genet. Biol. 72:168–181. https://doi.org/10.1016/j.fgb.2014.08.007.

Wattam AR, Abraham D, Dalay O, Disz TL, Driscoll T, Gabbard JL, et al. (2014) PATRIC, the bacterial bioinformatics database and analysis resource. Nucleic Acids Res. 42(D1):581–591. https://doi.org/10.1093/nar/gkt1099.

Wickham H (2009) GGplot2: elegant graphics for data analysis. Springer New York.

Yu TE, Egger KN, Peterson LR (2001) Ectendomycorrhizal associations - Characteristics and functions. Mycorrhiza 11(4):167–177. https://doi.org/10.1007/s005720100110.

Yu G, Smith DK, Zhu H, Guan Y, Lam TTY (2017) GGtree: an R package for visualization and annotation of phylogenetic trees with their covariates and other associated data. Methods Ecol. Evol. 8(1):28–36. https://doi.org/10.1111/2041-210X.12628.

Zampieri E, Rizzello R, Bonfante P, Mello A (2012) The detection of mating type genes of *Tuber melanosporum* in productive and non productive soils. Appl. Soil. Ecol. 57:9-15. https://doi.org/10.1016/j.apsoil.2012.02.013.

Zaretsky M, Kagan-Zur V, Mills D, Roth-Bejerano N (2006a) Analysis of mycorrhizal associations formed by *Cistus incanus* transformed root clones with *Terfezia boudieri* isolates. Plant Cell Rep. 25(1):62–70. https://doi.org/10.1007/s00299-005-0035-z.

Zaretsky M, Sitrit Y, Mills D, Roth-Bejerano N, Kagan-Zur V (2006b) Differential expression of fungal genes at preinfection and mycorrhiza establishment between *Terfezia boudieri* isolates and *Cistus incanus* hairy root clones. New Phytol. 171(4):837–846. https://doi.org/10.1111/j.1469-8137.2006.01791.x.

Zuccaro A, Lahrmann, U, Güldener U, Langen G, Pfiffi S, Biedenkopf D,et al. (2011) Endophytic life strategies decoded by genome and transcriptome analyses of the mutualistic root symbiont *Piriformospora indica*. PLoS Pathogens. 7(10). https://doi.org/10.1371/journal.ppat.1002290.

CHAPTER V

The crop of desert truffle depends on agroclimatic parameters during two key annual periods

5.1. Introduction

During the last decades great efforts have been made to domesticate diverse species of edible mycorrhizal fungi such as saffron milk caps, matsutake, boletus, black truffles or desert truffles (Hall et al., 2003). However, compared saprophytic fungi, the **cultivation of mycorrhizal fungi** continues to be more challenging and fewer species are cultivated. One of the main difficulties for their cultivation is the difficulty involved in the optimization and stabilization of the fruiting bodies crop over time (Morte et al., 2012).

Desert truffles are edible hypogeous fungi of the *Pezizaceae* family (*Pezizales*, *Ascomycetes*), and these mycorrhizal fungi have been used as food for thousands of years in countries with arid or semiarid climates (Volpato et al., 2013). During recent years, these fungal species and their host mycorrhizal plants have become an alternative agricultural crop (**Figure 5.1A**) in semiarid areas of the Iberian Peninsula due to their appreciated edible fruiting bodies (**Figure 5.1B**) and the low water requirements for cultivation (Morte et al., 2010; 2012; 2017). The first desert truffle to be cultivated was ***Terfezia claveryi*** in symbiosis with ***Helianthemum almeriense*** in the southeast of Spain (Honrubia et al., 2001; Morte et al., 2008). *T. claveryi* fructification usually occurs 2-3 years after plantation, depending on site suitability, season and framework of the plantation, as well as management practices, mostly irrigation and weed elimination (Morte et al., 2017). In these plantations, carpophores fructified yearly and production increased over time, with an average production of 350-400 kg per ha and year (Morte et al., 2008; 2012; 2017). However, annual production is erratic (Morte et al., 2012) and there is a demand for management knowledge to minimize large interannual fluctuations. For the proper management of *T. claveryi* plantations, it is key to identify the biotic and abiotic factors that could explain this variability (Navarro-Ródenas et al., 2016).

The host plant *H. almeriense* presents the typical phenology of summer deciduous plants (Flexas et al., 2014) with a maximum of photosynthetic activity during the winter (Dec-Jan), but that descends progressively as the plants approach to spring (fructification season) and summer (dehiscence of the leaves) (Navarro-Ródenas et al., 2015; Marqués-Gálvez et al., 2016). The delay time between the phenology of the plant

and the fungus causes several moments during the year when the environmental conditions could be decisive in their interaction.

Figure 5.1. Desert truffle cultivation. (**A**) Desert truffle plantation of *H. almeriense* x *T. claveryi* in the spring of the second year after plantation. (**B**) Detail of two fruiting bodies of T. claveryi collected in the plantation.

Agroclimatic parameters, such as precipitation or temperature determine the annual production of other mycorrhizal fungi, especially *Basidiomycota*, before or during the fruiting season (Martínez-Peña et al., 2012). However, unlike the fruiting bodies of *Basidiomycota* mycorrhizal fungi whose development takes place in few days (Teramoto et al., 2012; Xu et al., 2016), in the case of *Ascomycota* such as *Tuber* and *Terfezia* their development is slower and usually takes several months (Olivier et al., 2012; Le Tacon et al., 2014). Therefore, it is expected that long-term environmental factors may influence their development, as already observed in black truffle (Baragatti et al., 2019).

To date, there is limited knowledge on the environmental factors directly related to desert truffle fructification, with the exception of some hunches gathered from truffle collectors. In general, truffles show up more frequently during March-April, and according to desert truffle pickers, their production is affected by rain (97.8 %) and soil type (62.2 %) (Mehmet, 2017). Around 80 % of the pickers think that winter showers are an important factor that enables the truffle to reach a good size (Mehmet, 2017). However, spring showers or spring temperatures were important for 9.1 % and 25 % of the interviewed pickers, respectively (Mehmet, 2017). Bradai et al. (2015) found that the natural production of desert truffle was highly related to the accumulated precipitations

from October–December, when the rainfall determines the development of truffles after the dry period (summer) (Mandeel and Al-Laith, 2007; Bradai et al., 2014). Morte et al. (2012) observed a statistical correlation, according to the Pearson's test, between the amount of precipitations during autumn (September, October, and November) of one year and the yield of *T. claveryi* in the spring of the following year. Honrubia et al. (2014) recommended that irrigation should be provided at the end of summer/beginning of autumn and, based on their own experience, if the dry conditions continue, an extra irrigation of 50–80 L m^{-2} at the beginning of the fructification season could greatly improve the crop.

Although most studies related to the production of desert truffle point to the sole importance of precipitation, a systematic study has not yet been carried out to characterize whether other important agroclimatic parameters such as evapotranspiration (ET0), soil moisture, relative air humidity % (RH) or air vapour pressure deficit (VPD) can have an impact on desert truffle production, in the same way as in other crops (Ben-Gal et al., 2009). The aim of this study is to determine whether precipitation or any other related agroclimatic parameter had an effect on the productivity of a desert truffle orchard over 15 years of cultivation, and to know the critical periods of the year when those agroclimatic parameters determine the truffle yield. This knowledge is essential to develop **management models** and establish **threshold values of certain parameters**, which could help to maintain the annual yield of desert truffle stable over the years in agricultural plantations. Several agroclimatic parameters may vary in intensity, time and duration over a year of desert truffle fructifications, therefore, we hypothesize that there are optimal ranges in which desert truffle yield is sensitive to precipitation, ET0, soil moisture, VPD, RH and related parameters.

5.2. Materials and methods

5.2.1. Experimental site

The plantation was located in Zarzadilla de Totana, Lorca, Murcia (37°52'15.5"N 1°42'10.5"W) at an altitude of 870 m a.s.l. The area belongs to the biogeographic province Castellano-Maestrazgo-Manchega, subsector Manchego-

Espuñense, with a Mesomediterranean calid thermotipe, semiarid ombrotipe with annual precipitation of 289±106 mm/year (Alcaraz et al., 2008).

In May 1999, the experimental plantation with 60 *H. almeriense* plants inoculated with *T. claveryi* was established (Gutiérrez, 2001). At the time of planting, the mycorrhizal seedlings showed a percentage of mycorrhization higher than 90% (Gutiérrez, 2001). The plantation frame was 0.5x0.5m in a total area of 20 m^2. To promote the correct establishment of plants, during the first three months mycorrhized plants were irrigated with 15 L m^{-2}, every 15 days, until August 1999. In August and January 1999-2000, 50 L m^{-2} were supplied in each irrigation time. During the harvest time (March - May), a search for the characteristic soil cracks near the stems of adult *H. almeriense* plants was carried out. During the spring of 2001, the first desert truffles were harvested. After the first fructifications took place, no more artificial irrigation was applied and the orchard developed only with the natural precipitation. From 2001 to 2015, all harvested truffles were weighed and the total production was expressed as fresh weight per hectare (kg per ha).

5.2.2. Agroclimatic parameters and calculations

Daily agroclimatic data were collected from the nearest meteorological station, located in La Paca (Lorca, Spain IMIDA LO41, http://siam.imida.es) (**Table 5.1**). In 2010, a MiniMet automatic weather station (Skye Instruments Limited, Wales, UK) was installed close to the plantation and its data were used as a control to check the variations between both stations. **Aridity index** (AI) was calculated as precipitation divided by evotranspiration of reference (ET0), in 10 days periods, according to Barrow (1992). **Soil water potential** and **soil water potential anomaly** were retrieved from the European Drought Observatory (EDO) (http://edo.jrc.ec.europa.eu) in 10-day periods. Soil water potential from EDO is in pF units, which can easily be converted in kPa according to the formula: pF=Log10 - (10 * kPa) (Schachtschabel et al., 1976).

Each agroclimatic parameter was recalculated for 10 days periods having, in the end, 36 data per parameter and year. Parameters collected from La Paca agroclimatic station and those from the Minimet, located in the plantation, did not differ substantially during the overlapping time (2010-2015). The period of the year that was associated with

each truffle production data was considered according to the phenology of truffle production, since no truffles were collected after June 1st, and for this reason, each productive year begins on June 1st from the year before the occurrence of the fructifications (*e.g.* truffles produced during 2002 would be associated with agroclimatic data from June 1st, 2001 to May 31st, 2002).

Table 5.1. Selected agroclimatic parameters considered in the truffle production modelling. IMIDA (Instituto Murciano de Investigación y Desarrollo Agrario y Alimentario) LO41 refers to data collected from one of the IMIDA's meteorological stations located in La Paca (Murcia, Spain). EDO data was retrieved from the European Drought Observatory in 10 days periods. SMS stands for simple moving sum and SMA for simple moving average.

Parameter	Source	Unit	Abbreviation	Calculation	Optimal elapse time
Aridity index	Calculation	Adimensional	AI	SMS	50 days
Dewpoint	IMIDA LO41	ºC	DP	SMA	No significant
Evapotranspiration (FAO)	IMIDA LO41	mm	ET0	SMS	60 days
Hour below 0 ºC	IMIDA LO41	hr	HB0	SMS	No significant
Mean temperature	IMIDA LO41	ºC	Tº	SMA	50 days
Mean relative humidity	IMIDA LO41	%	HR	SMA	60 days
Precipitation	IMIDA LO41	mm	PREC	SMS	50 days
Soil moisture	EDO	pF	SoMo	SMA	50 days
Soil moisture anomaly	EDO	sd	SoMoA	SMA	20 days
Vapor Pressure Deficit	IMIDA LO41	kPa	VPD	SMA	60 days

5.2.2.1. *Simple moving sum (SMS) and simple moving average (SMA)*

SMS and SMA are calculations applied to time series in order to smooth out short-term fluctuations and highlight longer-term trends or cycles (Johnston et al., 1999). For each agroclimatic parameter, the simple moving average (SMA) or the moving sum (SMS) were calculated (**Table 5.1**) in periods of 10, 20, 30, 40, 50, 60 and 70 days, turning the initial data set of 36 values into 252 values per parameter and year.

5.2.2.2. *Pearson correlation analysis and heatmap*

To infer which meteorological parameters have an effect on desert truffle cultivation, Pearson correlation tests ($p > 0.05$) were performed between SMA and SMS of the different parameters and annual truffle production (kg per ha). Therefore, for each parameter, 7 different sets of Pearson's correlations were calculated between the SMA or SMA values, as appropriate, and the truffle production values. Finally, the set of SMA or SMS data that showed the highest number of significant correlations with desert truffle production was selected. By using this rule, by which the largest number of significant correlations is selected, it is possible to maximize which period of the year is relevant for a given parameter, for desert truffle production. The optimal SMS and SMA values of the agroclimatic parameters that present any correlation with desert truffle production (**Table 5.1**) were then represented on a heatmap, where the optimal periods of each parameter were grouped depending on whether they correlated positively or negatively with desert truffle yield.

5.2.2.3. *Agroclimatic parameter comparison*

To find out the trend in the production of desert truffles over the 15 years of this study, the cumulative average of truffle production was calculated. This value was then used to establish two groups, defined by their **low productive (L)** or **high productive (H) years**, compared to the accumulated mean for the period 2000-2015. Two groups, L and H, were produced for the optimal SMS and SMA values of each meteorological parameter. The values of each group L and H were compared with each other (Mann–Whitney U test) to identify which periods of the year showed significant differences in desert truffle production for each meteorological parameter.

5.2.2.4. *Classification and regression trees*

Classification and regression trees (C&RT) are nonparametric and nonlinear methods that determine, *via* tree-building algorithms, a set of "if-then" logical (split) conditions that allow accurate prediction or classification of cases. C&RT are methods that deliver models that meet both explanatory and predictive goals. Two of the strengths of these methods are the simple graphical representation based on trees and the compact format of the natural language rules (Breiman and Ihaka, 1984). C&RT were calculated

to predict the optimal SMA and SMS values of each meteorological parameter with an impact on desert truffle production. For each newly created sub-node, a minimum size for a child-node of n=3 cases was used as stop criteria. Then, the values predicted by the regression tree were evaluated by computing the Root Mean Square Error (RMSE) between the observed desert truffle production and the predicted values. RMSE quantifies how different a set of values is, where the lower an RMSE value (kg per ha), the closer the predicted and observed values will be.

5.2.3. Software packages

Descriptive statistics, Pearson correlations, heatmap and Mann–Whitney U test were calculated with XLSTAT 2018 (Adinsoft, 2018). The comparison charts of agroclimatic parameters (L and H agroclimatic parameter comparison graphs) were created with Rapidminer v.9.3.

5.3. Results

5.3.1. Desert truffle production

Once the plantation was established, it took 2 years before the first *T. claveryi* fruiting event occurred, during the spring of 2001. In the following years, the plantation increased its cumulative average production, almost linearly, until 2009 (**Figure 5.2**), when it reached a cumulative average production of 379 kg per ha and remained almost constant with a standard deviation of ±14 kg per ha throughout the rest of the years. The average desert truffle yield was 355 kg per ha after 15 years. The stability of the average accumulated production indicated that, after 10 years of sampling, the accumulated average fluctuated less than 4% and, therefore, we could consider that the minimum sample size was adequate. However, annual production showed great interannual fluctuation with a standard deviation of ±318 kg per ha. After the first fructification, two years following plantation (2001), only in three years the production was zero (2014) or less than 2 kg per ha (2005, 2006). The greatest harvest was 2009 with 1,069 kg per ha. Despite the high standard deviation, according to the Grubbs test, no production value should be considered as outlier (Grubbs, 1950).
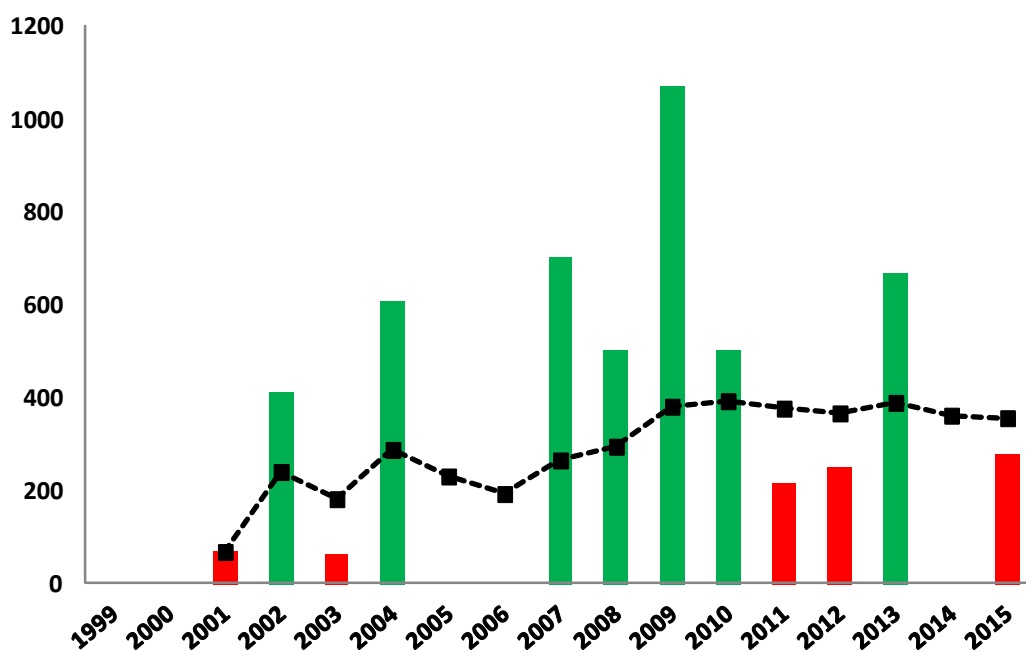
Figure 5.2. Variation of the interannual production of desert truffle (kg per ha) from 2001 to 2015. Dashed line represents the cumulative average desert truffle production. Bars represent the total annual fructifications of ascocarps per year; red bars are the years when the yields fell below the annual mean (kg per ha/year) and are classified as low crop years (L); green bars are those when the yields were above the annual mean (kg per ha and year) and classified as high crop years (H). There are no bar when the crop was zero (2014) or less than 2 kg per ha (2005, 2006).

5.3.2. Pearson correlations and heatmap

From the initial group of agroclimatic parameters, eight out of ten parameters showed significant Pearson correlations with *T. claveryi* production (**Table 5.1**) (AI, ET0, mean temperature, mean relative humidity, precipitation, soil water potential, soil water potential anomaly and VPD). The SMS of precipitation (mm) over a period of 40 days showed the highest number of significant Pearson correlations ($p > 0.05$) with desert truffle production. The significant SMS for ET0 (mm) was for 60 days. The significant SMAs were 50 days for AI, 60 days for RH (%), 60 days for VPD (kPa), 50 days for temperature (ºC), 50 days for soil moisture (pF) and 20 days for soil moisture anomaly (sd) (**Figure 5.3**).

According to the heatmap (**Figure 5.3**), it is possible to explain the high interannual variability in desert truffle production, in relation to the variation of eight of the ten agroclimatic parameters analyzed in certain seasons. The parameters AI and

precipitation were positively correlated with the truffle production during autumn prior to the fructification and slightly during the current spring, while RH was correlated only at the beginning of the autumn. The parameters VPD, ET0 and soil moisture were negatively correlated with truffle production during autumn and spring, while the temperature was correlated only at the end of spring. Only soil moisture anomaly showed a significant positive correlation with truffle production from the beginning of autumn until the end of May steadily (**Figure 5.3**)
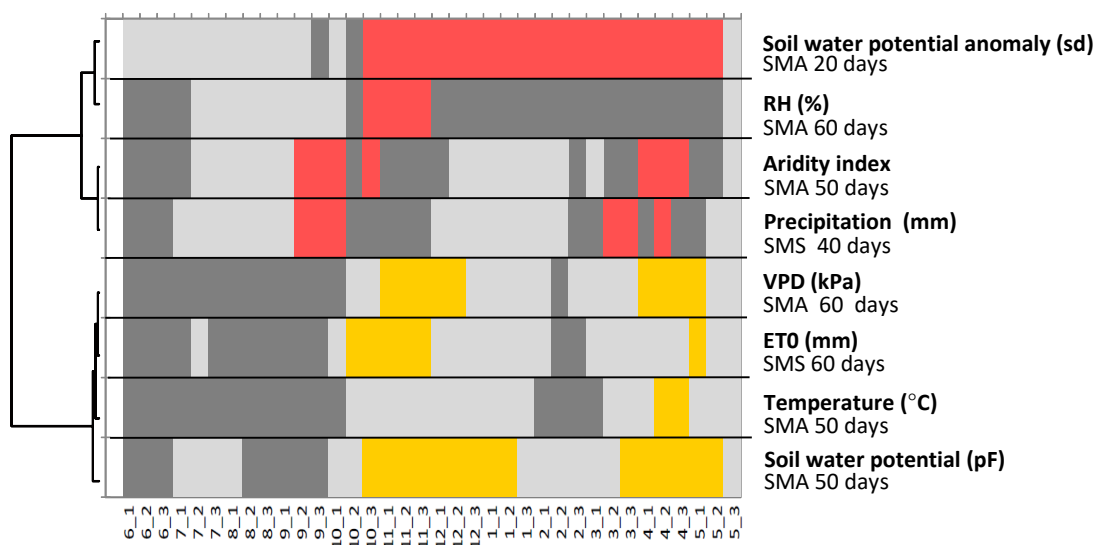
Figure 5.3. Heatmap grouping the significant ($p < 0.05$) positive (red) and negative (yellow) Pearson correlations among the agroclimatic parameters and the truffle production in ten day periods. The dark and light grey indicate no statistically significant Pearson correlations. The average (SMA) or cumulative (SMS) period (days) used to calculate the Pearson correlations are given under the name of each meteorological parameter. The SMA or SMS period is that showing the highest number of significant correlations. On the abscissa axis: periods of the year are represented by month numbers and each month is divided into ten-day sub-periods.

5.3.3. Annual agroclimatic parameter profiles

Comparisons of the annual profile of each agroclimatic parameter between H and L years allowed to identify which periods of the year are key to define a year as a H or L year (**Figure 5.4**).
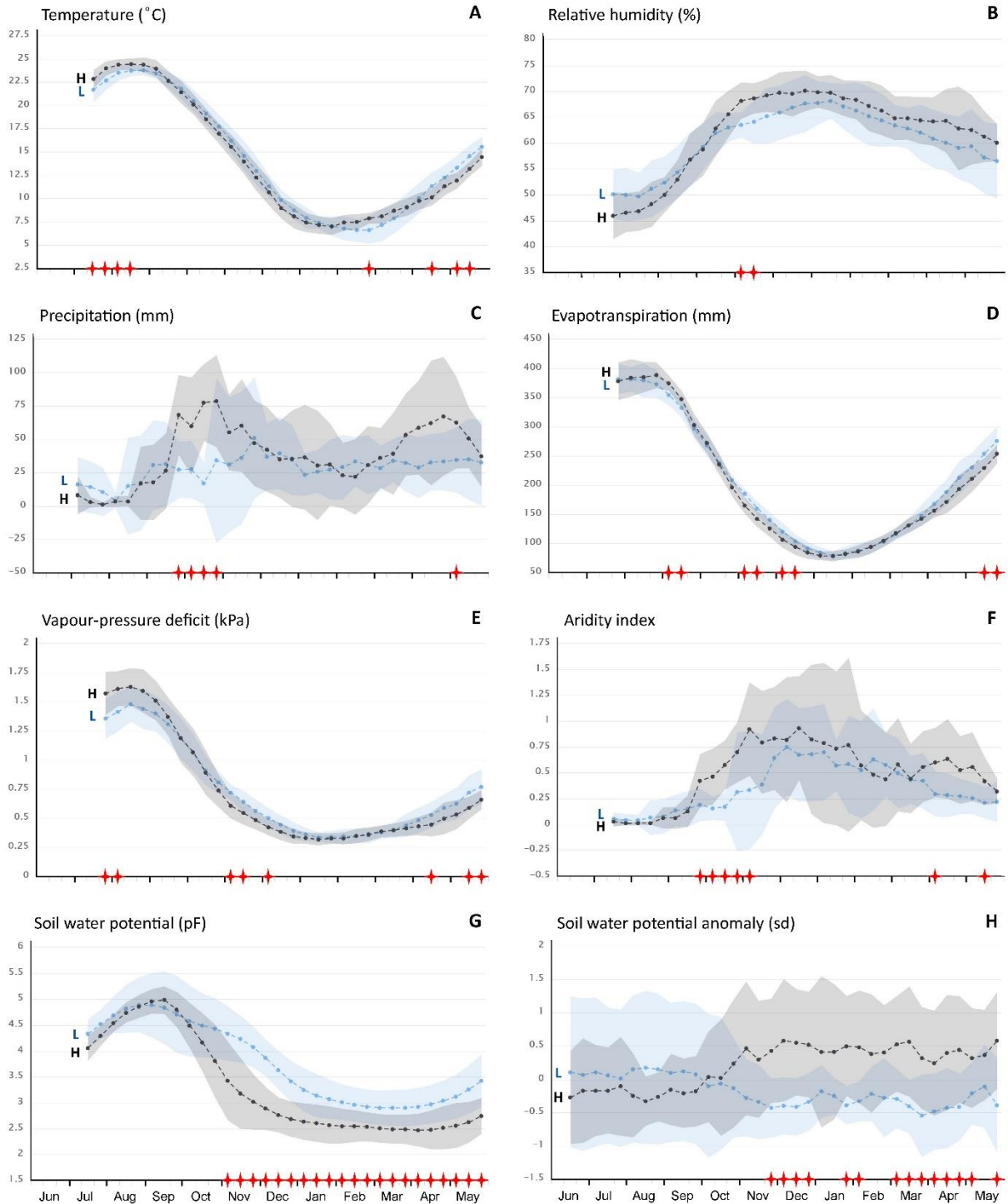
Figure 5.4. Annual agroclimatic parameter profile showing the mean value (dashed line with circles) and standard deviation (coloured shadow) of the different agroclimatic parameters represented for high productive years (H, black colour) and low productive years (L, blue colour). The plotting of the different parameters starts at different dates due to the different SMA or SMS calculated for each one. The axis of abscissa shows the months of the year distributed in periods of 10 days and the significantly different values between L and H productions are marked with a red star where it corresponds, as a result of the Mann–Whitney U test ($p < 0.1$).

When comparing H and L years, in general, the autumn before *T. claveryi* fructification and spring (just before or coinciding with fructification) turned out to be the periods of the year with the highest number of agroclimatic parameters with significant differences (**Figure 5.4**). AI, precipitation, VPD, RH and ET only showed significant differences during these periods, while soil moisture and soil moisture anomaly showed the highest number of significant differences throughout the whole period from autumn to the end of spring, including winter (**Figure 5.4**). Summer was the only period in which no significant differences were found for any agroclimatic parameter studied (**Figure 5.4**).

Taking precipitation profiles (**Figure 5.4C**) as an example, it is possible to identify two periods, during summer and winter, where average of precipitation between L and H years overlapped and no significant differences were found. However, during autumn and, weaker, in spring, the average of precipitation between L and H years became significantly different. Differences in precipitation during those significant periods would explain the differences in production between years.

5.3.4. Classification and regression trees

Among the regression models calculated with C&RT, those corresponding to the parameters ET0 (**Figure 5.5A**), precipitation (**Figure 5.5B**), AI (**Figure 5.5C**) and soil moisture (**Figure 5.5D**) showed the lowest RMSE values. The C&RTs established the ranges for the different agroclimatic parameters to which *T. claveryi* production was more sensitive. Precipitation and AI sorted the data into four son nodes, meaning that the parameters were classified with a higher resolution. Using the AI (**Figure 5.5C**) parameter as an indicator of the maximum desert truffle productivity, the tree defined two key periods, from September 30 to November 10 (0.3-1.7) and from March 30 to May 10 (0.5-1). In case of precipitation (**Figure 5.5B**), the two periods were from September 10 to October 20 (26.9-115.4 mm) and from March 20 to April 30 (70.2-123.4 mm). For example, the sum of precipitation during the 50 days before October 20th should be at least 26.9 mm (**Figure 5.5B**). In addition, the decision trees informed us about different alternative scenarios that could lead to similar productions. For example, if the sum of precipitations during the 50 days prior to October 20th is less than 26.9 mm, the expected

production should not exceed 89.1 kg per ha, but if during the 40 days prior to April 10th the sum of precipitations reaches more than 30 mm, the yield could be between 89.1 and 156 kg per ha (**Figure 5.5B**). In the case of ET0, the period with the highest truffle productivity belongs to the range of dates from September 30 to November 20 (120.2-141.7 mm) (**Figure 5.5A**). Using the soil moisture parameter, the tree defined one key period, from November 10th to December 20th (2.3-3 pF) (**Figure 5.5D**).
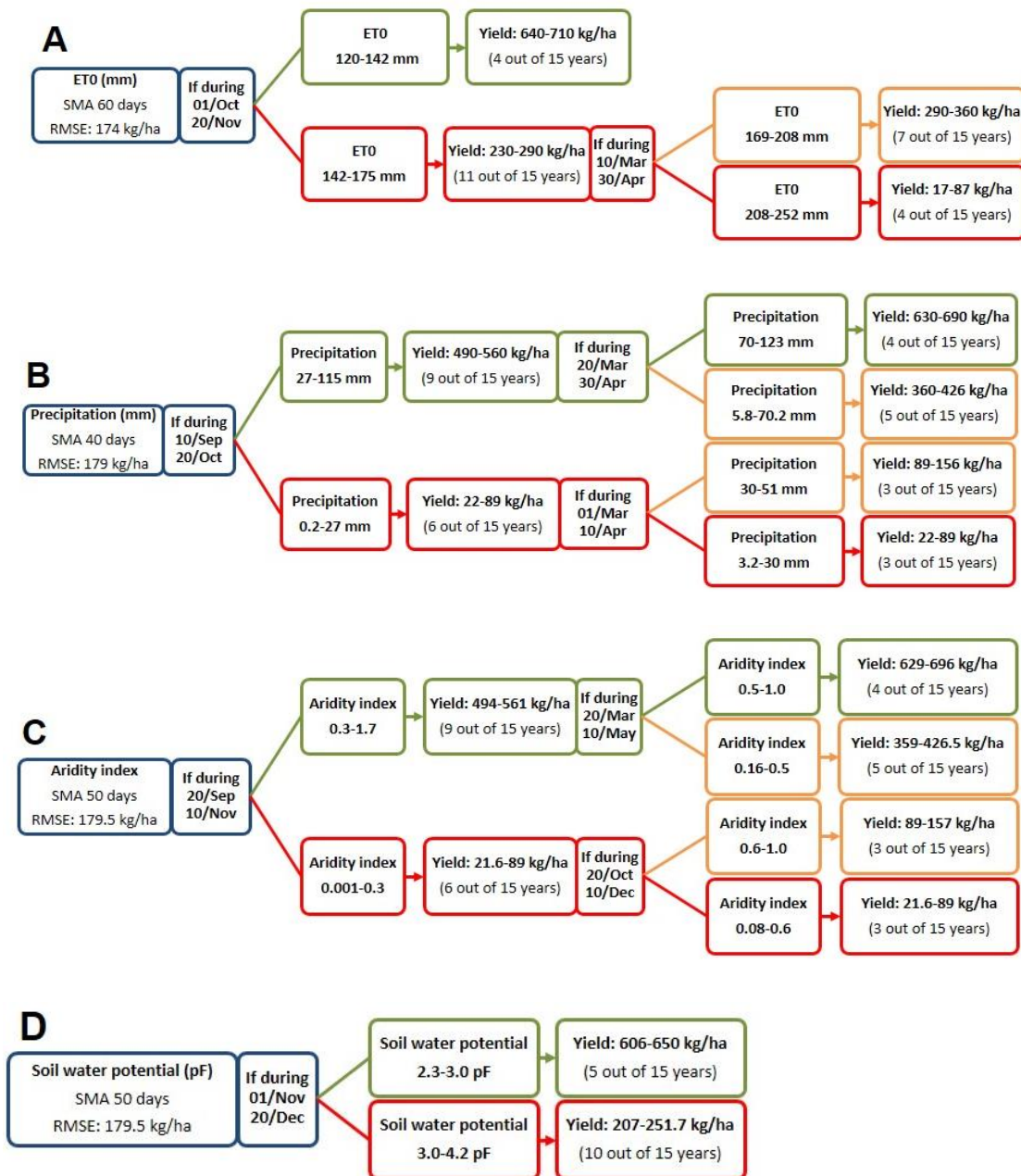
Figure 5.5 (previous page). **Classification and regression tree analysis of the different agroclimatic parameters.** The first box on the left (blue) shows the optimal SMA or SMS values derived from the heatmap (**Figure 2**) and used to calculate the C&RT. The same box includes the RMSE value calculated between the observed and the predicted truffle crop. The following box to the right shows the dates predicted by the C&RT with the greater impact on the truffle crop. The two nodes on the right show the range of the predicted values of the different agroclimatic parameters, the desert truffle crop ranges and the number of years included in each son node. Green nodes show the optimal scenario, orange nodes show the suboptimal scenarios and red nodes show the undesirable scenario. (**A**) ET0. (**B**) Precipitation. (**C**) Aridity index. (**D**) Soil water potential.

5.4.   Discussion

According to our hypothesis, our results point to a seasonal influence of the different agroclimatic parameters in the production of *T. claveryi* desert truffles. We could consider the beginning of the desert truffle year on June 1st. During summer (Jun-Aug), *H. almeriense* plants remain vegetative and photosynthetically inactive and mycorrhizal structures are almost undetectable (Morte et al., 2010; Navarro-Ródenas et al., 2015). According to the heatmap (**Figure 5.3**), annual profiles (**Figure 5.4**) and C&RTs (**Figure 5.5**), this time seems be unimportant for the future truffle crops since no significant correlations were observed and only the temperature and the VPD showed significant but slight changes (**Figure 5.4A**; **5.4E**), whereby the stressful condition seems to favour the desert truffle yield. *H. almeriense* is a summer deciduous plant but if the conditions are not dry enough the plant does not lose its leaves, which could eventually result in plant death (Morte et al., 2010). Therefore, in general, climatic parameters, particularly drought conditions in summer, are not critical for desert truffle, contrary to what happens in other close species such as black truffle (Le Tacon et al., 1982; 2014; Büntgen et al., 2012; 2019; Baragatti et al., 2019). This could be due to the different fruiting season and to the difference in the phenology of the host plants, since *H. almeriense* is a summer deciduous plant, while *Quercus* species are perennial or winter deciduous plants.

Autumn (Sep, Oct and Nov) seems to be a key season for the truffle production. All agroclimatic parameters, with the exception of temperature, showed significantly correlations with truffle yield (**Figure 5.3**). According to the heatmap, RH, precipitation and AI are the parameters most strongly related to production (**Figure 5.3**), and comparing annual profiles, precipitation and AI between L and H years are statistically differents (**Figure 5.4C; 5.4F**). In this season, a window of approximately 50 days opens

(from Sept 10th to Oct 3th), during which the accumulated rainfall around 80 l/m^2, would give rise to a H year (**Figure 5.5B**). However, if the accumulated rainfall in this window were less than 26 L m^{-2}, that years´s production would be severely affected and a yield of less than 89 kg per ha would be expected (**Figure 5.5B**). In any case, the final effectiveness of the rain during the autumn can be affected by other parameters such as ET0 (**Figure 5.3**), since if the rains are abundant enough, but the ET0 is high, this water will not be available to the plants for a suitable period of time. As a combination of these two parameters, the AI was calculated and it turned out to be the agroclimatic parameter with the most significant differences (5) between H and L years, in autumn (**Figure 5.4F**). The high dependence on agroclimatic parameters over time corroborates the hypothesis regarding the early formation of truffle primordia in autumn (Bordallo, 2007; Pacioni et al., 2014). Moreover, the correlation between soil water potential and desert truffle yield, the correlation that covered more period of time (**Figure 5.3**), is also evident at the end of autumn (**Figure 5.3G**).

During winter (Dec, Jan, Feb), the host plant presents the maximum gas exchange activity and the maximum amount of mycorrhizal roots (Marqués-Gálvez et al., 2016), but few and weak correlations were found with the parameters studied. The only parameter in which significant differences were detected between the H and L years was the temperature between January 11th and February 31st, although this difference was less than 1ºC. During winter, the parameter with most correlations throughout the entire season was the soil water potential (**Figure 5.3**). Morte et al. (2010) and Navarro-Ródenas et al. (2013) observed a decrease in gas exchange parameters in drought conditions, so that high soil moisture could facilitate the production of photoassimilates that could later be derived for the formation of desert truffles.

Spring (Mar, Apr and May) comprises the months when *T. claveryi* usually fructifies, although the beginning of the fruiting period can differ widely from one year to another. As expected, in spring there were several agroclimatic parameters that correlated significantly with the production of truffles. However, the number of significant correlations was lower, both in number and intensity, than the observed in other seasons more distant from the time of fruiting events (**Figure 5.3**). Once more, the spring rainfall, ET0 and AI appear to be important and significantly different profiles were observed between H and L years (**Figure 5.4**). In fact, spring precipitation could complement autumn rainfalls when not sufficient and even partially correct the yield if

rainfalls were not abundant (**Figure 5.5**). During spring, photosynthesis progressively decreases as plants approach summer (Navarro-Ródenas et al., 2015). This reduction in host plant photosynthesis may be the factor that triggers the fruiting of *T. claveryi*. As Pacioni et al. (2014) pointed out, most of the changes that stimulate fruiting body formation negatively affect the growth of the mycelium, and therefore the less favourable conditions for the mycelial growth would favour the formation of fruiting bodies. In spring, another group of related agroclimatic parameters are temperature and VPD, which are negatively correlated. It seems that mild temperatures and, consequently, mild VPD could increase the desert truffle yield. Some authors have previously reported a decrease in photosynthesis if the atmospheric demand (VPD) reaches certain values and increases the leaf senescence and fall, so high VPD values during the fruiting stage could cause a premature end of fruiting period with the consequent decrease in yield (Morte et al., 2010; León-Sánchez et al., 2016; Marqués-Gálvez et al., 2016). The third and the most clearly correlated agroclimatic parameter was soil water potential. Indeed, this parameter showed a close correlation from the end of autumn, during winter and to the end of spring. The growth of the mycelium of *T. claveryi* is improved by moderate drought stress (Navarro-Ródenas et al., 2012) but, like other hypogeus ascocarps, fruiting bodies also develop over several months and developing truffles are susceptible to desiccation. Therefore, adequate soil moisture needs to be maintained throughout the production season (Bruhn and Hall, 2011) and the implementation of soil water potential sensors in future desert truffle plantations could help to manage them properly.

5.4.1. Management proposal

As a summary, we propose four different models to manage desert truffle plantations of *T. claveryi* in *H. almeriense* plants in a semiarid Mediterranean climate, depending on the resources and facilities available in the plantations:

1) **Based on the aridity index and the decision tree** (**Figure 5.5C**): The ET0 should be monitored during the 50 days prior to October the 10th and irrigation applied in order to maintain the AI at least above the threshold of 0.35 (**Table 5.2**) and during the 50 days prior to May the 10th, at least, above the AI threshold of 0.50 (**Table 5.2**). ET0 and precipitation values

can be obtained from a weather station located on the plantation or from the nearest official weather station.

2) **Based on soil water potential and annual profile** (**Figure 5.4G**): Irrigation should be carefully controlled from November 10th in order to maintain the soil water potential (pF) always below the average value of L years and as close as possible to the average value of H years according to the values in **Figure 5.4G**. The pF values should be measured using field probes such as MPS-2 or MPS-6 Dielectric Water Potential Sensors (Decagon Devices, Inc. Pullman WA) or similar probes, which are able to register the range of data observed in our study.

3) **Based on a combination of aridity index and soil moisture**: Irrigation should be monitored and applied during autumn (50 days before October 10th) to maintain the aridity index above the threshold. Soil water potential should not be allowed to surpass those of L year values from November to May. In spring (50 days before May 10th), irrigation should be decided on the basis of the aridity index or soil water potential and irrigation should only be applied when either of these two parameters reaches its critical value.

4) **Based on soil water potential anomaly and annual profiles** (**Figure 5.4H**): Irrigation should be monitored from November the 10th in order to maintain the soil water potential anomaly always below the average value of L years and as close as possible to the average value of H years according to the values in **Figure 5.4H**. The soil water potential anomaly values can be checked in the European Drought Observatory website (EDO, http://edo.jrc.ec.europa.eu).

Table 5.2. Management proposal based on the aridity index (AI) threshold. (**A**): represents the ET0 and precipitation averages of the three lowest production years and the irrigation proposed. (**B**): represents the ET0 and precipitation averages of the three highest production years and the irrigation proposed.

(A) Periods	ET0	Precipitation	AI	AI threshold	Required water*	Irrigation**
Sep21-30	36.7	1.2	0.033	0.35	12.85	11.65
Oct01-10	31.1	2.2	0.0708	0.35	10.89	8.60
Oct11-20	28.8	1.5	0.0503	0.35	10.08	8.58
Oct21-30	29.5	2.0	0.0662	0.35	10.33	8.33
Nov01-10	22.3	1.2	0.0538	0.35	7.81	6.61
Mar21-30	31.2	7.0	0.2238	0.50	15.60	8.6
Apr01-10	35.4	4.3	0.1223	0.50	17.70	13.40
Apr11-20	33.8	6.7	0.1969	0.50	16.90	10.2
Apr21-30	48.1	9.5	0.1963	0.50	24.05	15.05
May01-10	34.1	11.9	0.3496	0.50	17.05	5.15
Total		**47.5**			**143.26**	**96.17**
(B) Periods	**ET0**	**Precipitation**	**AI**	**AI threshold**	**Required water**	**Irrigation**
Sep21-30	31.7	47.3	1.4936	0.35	11.09	-
Oct01-10	32.0	8.0	0.2504	0.35	11.2	3.2
Oct11-20	24.1	16.5	0.6872	0.35	8.44	-
Oct21-30	21.2	19.5	0.8968	0.35	7.35	-
Nov01-10	13.7	28.2	2.0574	0.35	4.79	-
Mar21-30	33.1	34.0	1.0268	0.50	16.55	-
Apr01-10	35.5	13.9	0.3932	0.50	17.75	3.85
Apr11-20	40.7	21.8	0.5361	0.50	20.35	-
Apr21-30	45.4	18.9	0.4166	0.50	22.70	3.8
May01-10	52.0	5.8	0.1110	0.50	26	20.2
Total		**213.9**			**146.22**	**31.05**

*$RW_p = AI_t \cdot ET0_p$; **$I_p = RW_p - P_p$; Where RW is Required Water, AI_t is the aridity index threshold, $ET0_p$ is the Evotranspitarion during the period, I_p is the irrigation during the periods, P_p is the Precipitation during the periods.

All these models must be carefully adjusted to each cultivation site, taking into account other environmental factors that could modulate the final result, such as type of soil, slope, altitude, orientation, etc.

In conclusion, our results show for the first time that annual crop yields of *T. claveryi* are mainly affected by agroclimatic parameters during the autumn and spring months in a semiarid climate. Moreover, the aridity index and soil water potential are the agroclimatic parameters that most determine the annual desert truffle crop. Agroclimatic parameters play a role long before the fruiting season of desert truffles, contrary to what

happens with other edible mycorrhizal mushrooms. The key agroclimatic parameters can be controlled by applying irrigation in the field, at the identified times of autumn and spring, and thus allow maximizing desert truffle crop.

References

Addinsoft (2018) XLSTAT. Extensión de análisis estadístico para Microsoft Excel. Software.

Alcaraz F, Barreña J, Clemente M, González-Garnés J, Rivera D, Ríos S (2008) Manual de interpretación de los hábitats naturales y seminaturales de la Región de Murcia. Tomo 1: Hábitats y Sistemas de Hábitats. Murcia: Dirección General del Medio Natural, Consejería de Desarrollo Sostenible y Ordenación del Territorio, Región de Murcia

Ben-Gal A, Agam N, Alchanatis V, Cohen Y, Yermiyahu U, Zipori I, Presnov, E, Sprintsin M, Dag, A (2009) Evaluating water stress in irrigated olives: Correlation of soil water status, tree water status, and thermal imagery. Irrig. Sci. 27:367–376. https://doi.org/10.1007/s00271-009-0150-7.

Baragattil M, Grollemund PM, Montpied P, Dupouey JL, Gravier J, Murat C, Le Tacon F (2019) Influence of annual climatic variations, climate changes, and sociological factors on the production of the Périgord black truffle (*Tuber melanosporum* Vittad.) from 1903–1904 to 1988–1989 in the Vaucluse (France). Mycorrhiza 29:113–125. https://doi.org/10.1007/s00572-018-0877-1.

Barrow CJ (1992) World Atlas of Desertification (United nations Encironment Program). In: Middleton N, Thomas DSG, eds. Edward Arnold, London.

Bordallo JJ (2007) Estudio del Ciclo Biológico de *Terfezia claveryi* Chatin. Memoria de Suficiencia Investigadora del Programa de Doctorado de Biología Vegetal, Universidad de Murcia, Spain.

Bradai L, Bissati S, Chenchouni H (2014) Desert truffles of the North Algerian Sahara: Diversity and bioecology. Emir. J. Food Agric. 26(5):425-435. https://doi:org/10.9755/ejfa.v26i5.16520.

Bradai L, Bissati S, Chenchouni H, Amrani K (2015) Effects of climate on the productivity of desert truffles beneath hyper-arid conditions. Int. J. Biometeorol. 59(7):907-915. https://doi.org/10.1007/s00484-014-0891-8.

Breiman L, Ihaka R (1984) Nonlinear Discriminant Analysis *via* Scaling and ACE. Department of Statistics, University of California.

Bruhn J, Hall M (2011) Agroforestry in Action. Burgundy black truffle cultivation in an agroforestry practice. Conference Proceedings.

Büntgen U, Egli S, Camarero JJ, Fischer EM, Stobbe U, Kauserud H, Tegel W, Sproll L, Stenseth NC (2012) Drought-induced decline in Mediterranean truffle harvest. Nat. Clim. Change 2(12):827–829. https://doi.org/10.1038/nclimate1733.

Büntgen U, Oliach D, Martínez-Peña F, Latorre J, Egli S, Krusic P J (2019) Black truffle winter production depends on Mediterranean summer precipitation. Environ. Res. Lett. 14(7):074004. https://doi.org/10.1088/1748-9326/ab1880.

Flexas J, Diaz-Espejo A, Gago J, Gallé A, Galmés J, Gulías J, Medrano H (2014) Photosynthetic limitations in Mediterranean plants: A review. Environ. Exp. Bot. 103:12-23. https://doi.org/10.1016/j.envexpbot.2013.09.002.

Grubbs FE (1950) Sample criteria for testing outlying observations. Ann. Math. Stat. 21(1):27-58.

Gutiérrez A (2001) Caracterización, Micorrización y Cultivo en Campo de las Trufas del Desierto. Dissertation, University of Murcia, Murcia, Spain.

Hall IR, Yun W, Amicucci A (2003) Cultivation of edible ectomycorrhizal mushrooms. Trends Biotechnol. 21(10):433-438. https://doi.org/10.1016/S0167-7799(03)00204-X.

Honrubia M, Andrino A, Morte A (2014) Preparation and maintenance of both man-planted and wild plots. In: Kagan-Zur V, Roth-Bejerano N, Sitrit Y, Morte A, eds. Desert Truffles: Phylogeny, Physiology, Distribution and Domestication. Springer Berlin Heidelberg pp. 367-387. https://doi.org/10.1007/978-3-642-40096-4_22.

Johnston FR, Boyland JE, Meadows M, Shale E (1999) Some properties of a simple moving average when applied to forecasting a time series. J. Oper. Res. Soc. 50(12):1267-1271. https://doi.org/10.1057/palgrave.jors.2600823.

Le Tacon F, Delmas J, Gleyze R, Bouchard D (1982) Effect of soil water regime and fertilization on fructification of the black truffle of Perigord (*Tuber melanosporum* Vitt.) in south east of France. Acta Oecol. Oecol. Appl. 3(4):291-306.

Le Tacon F, Marçais B, Courvoisier M, Murat C, Montpied P, Becker M (2014) Climatic variations explain annual fluctuations in French 'Périgord black truffle' wholesale markets but do not explain the decrease in 'black truffle' production over the last 48 years. Mycorrhiza 24(1):115–125. https://doi.org/10.1007/s00572-014-0568-5.

León-Sánchez L, Nicolás E, Nortes PA, Maestre FT, Querejeta JI (2016) Photosynthesis and growth reduction with warming are driven by nonstomatal limitations in a Mediterranean semiarid shrub. Ecol. Evol. 6(9):2725-2738. https://doi.org/10.1002/ece3.2074.

Mandeel QA, Al-Laith AAA (2007) Ethnomycological aspects of the desert truffle among native Bahraini and non-Bahraini peoples of the Kingdom of Bahrain. J. Ethnopharmacol. 110(1):118-129. https://doi.org/10.1016/j.jep.2006.09.014.

Marqués-Gálvez J, Navarro-Ródenas A, Nicolás E, Morte A (2016) Combined effect of vapour pressure deficit and irrigation on desert truffle mycorrhizal plants. VIII International Workshop on Edible Mycorrhizal Mushroom. Cahors, France.

Mehmet A (2017) Ethnomycological aspects of traditional usage and indigenous knowledge about the arid-semi arid truffles consumed by the residents of the Eastern Anatolia Region of Turkey. Gazi Univ. J. Sci. 30(4):57-70.

Morte A, Navarro-Ródenas A, Nicolás E (2010) Physiological parameters of desert truffle mycorrhizal *Helianthemun almeriense* plants cultivated in orchards under water deficit conditions. Symbiosis 52 (2–3): 133–139. https://doi.org/10.1007/s13199-010-0080-4.

Morte A, Andrino A, Honrubia M, Navarro-Ródenas A (2012) *Terfezia* cultivation in arid and semiarid soils. In: Zambonelli A, Bonito GM, eds. Edible Ectomycorrhizal Mushrooms: Current Knowledge and Future Prospects. Berlin, Heidelberg: Springer Berlin Heidelberg pp. 241-263. https://doi.org/10.1007/978-3-642-33823-6_14.

Morte A, Pérez-Gilabert M, Gutiérrez A, Arenas F, Marqués-Gálvez JE, Bordallo JJ, Rodríguez A, Berná LM, Lozano-Carrillo C, Navarro-Ródenas A (2017) Basic and applied research for desert truffle cultivation. In: Varma A, Prasad R, Tuteja N, eds. Mycorrhiza-Ecophysiology, Secondary Metabolites, Nanomaterials. Springer International Publishing pp. 23-42. https://doi.org/10.1007/978-3-319-57849-1_2.

Navarro-Ródenas A, Bárzana G, Nicolás E, Carra A, Schubert A, Morte A (2013) Expression analysis of aquaporins from desert truffle mycorrhizal symbiosis reveals a fine-tuned regulation under drought. Mol. Plant-Microbe Interact. 26(9):1068-1078. https://doi.org/10.1094/MPMI-07-12-0178-R.

Navarro-Ródenas A, Nicolas E, Morte A (2015) Effect of irrigation on desert truffle mycorrhizal plants in field. XXI Reunión de la Sociedad Española de Fisiologia Vegetal. Toledo, Spain.

Navarro-Ródenas A, Berná LM, Lozano-Carrillo C, Andrino A, Morte A (2016) Beneficial native bacteria improve survival and mycorrhization of desert truffle mycorrhizal plants in nursery conditions. Mycorrhiza 26(7):769-779. https://doi.org/10.1007/s00572-016-0711-6.

Navarro-Ródenas A, Ruíz-Lozano JM, Kaldenhoff R, Morte A (2012) The aquaporin TcAQP1 of the desert truffle *Terfezia claveryi* is a membrane pore for water and CO_2 transport. Mol. Plant-Microbe Interact. 25(2):259-266. https://doi.org/10.1094/MPMI-07-11-0190.

Olivier JPM, Savignac JC, Sourzat P (2012) Truffe et Trufficulture. FANLAC Editions. Périgueux, France.

Pacioni G, Leonardi M, Di Carlo P, Ranalli D, Zinni A, De Laurentiis G (2014) Instrumental monitoring of the birth and development of truffles in a *Tuber melanosporum* orchard. Mycorrhiza 24(1):65-72. https://doi.org/10.1007/s00572-014-0561-z.

Schachtschabel P, Blume HP, Brümmer G, Hartge KH, Schwertmann U (1976) Lehrbuch der bodenkunde. F. Enke.

Teramoto M, Wu B, Hogetsu T (2012) Transfer of 14C-photosynthate to the sporocarp of an ectomycorrhizal fungus *Laccaria amethystina*. Mycorrhiza 22(3):219-225. https://doi.org/10.1007/s00572-011-0395-x.

Volpato G, Rossi D, Dentoni D (2013) A reward for patience and suffering: Ethnomycology and commodification of desert truffles among Sahrawi refugees and nomads of Western Sahara. Econ. Bot. 67(2):147-160. https://doi.org/10.1007/s12231-013-9234-7.

Xu H, Navarro-Ródenas A, Cooke JEK, Zwiazek JJ (2016) Transcript profiling of aquaporins during basidiocarp development in *Laccaria bicolor* ectomycorrhizal with *Picea glauca*. Mycorrhiza 26(1):19-31. https://doi.org/10.1007/s00572-015-0643-6.

Spring stomatal response to vapor pressure deficit as a marker for desert truffle cultivation

6.1. Introduction

Helianthemum almeriense Pau is a drought-deciduous Mediterranean perennial shrub belonging to Cistaceae family. It usually appears in open dry, stony, limestone, mica or marl places with gypsum or sandy soils, at altitudes between 0 to 500 m. Its habitat is the southeast semiarid regions of Iberian Peninsula, although it can also be found in the north of Morocco (Morte and Honrubia, 1997).

Apart from its ecological value, the emergence of the cultivation of the desert truffle ***Terfezia claveryi*** Chatin (*Pezizaceae*, *Ascomycota*) during the last 20 years has conferred an important economic and commercial value to *H. almeriense*, since it is used as the host of this mycorrhizal edible fungus (Morte et al., 2008; 2017). Desert truffles are represented by several genera of edible hypogeus ascomycetes that are adapted to extreme conditions on arid and semiarid areas (Kovács and Trappe, 2014). Among these, *Terfezia* genus and particularly the species *T. claveryi* is one of the most studied and appreciated members, mainly because of its nutritional value (Murcia et al., 2002), and the possibility of its cultivation (Kagan-Zur and Roth-Bejerano, 2008; Morte et al., 2008). It was the first desert truffle to be cultivated (Honrubia et al., 2001; Morte et al., 2008) and, since 1999, several orchards have been established to produce *T. claveryi* ascocarps using *H. almeriense* as a host plant.

Desert truffle fructification usually occurs after 2-3 years of plantation and happens annually since then, reaching average productions of 350-400 kg per ha after 6-7 years, although with a high fluctuation in interannual production (Morte et al., 2017). Site suitability, season and framework of the plantation, management practices (Morte et al., 2017), biotic factors (Navarro-Ródenas et al., 2016), as well as agroclimatic parameters (Morte et al., 2012; Andrino et al., 2019), are the major limiting factors to obtain high and stable productions. With regard to agroclimatic parameters, precipitations during autumn, soil water potential from fall to spring (including winter) and precipitations plus temperature and vapor pressure deficit (VPD) in spring, are the major candidates to explain the interannual variations in *T. claveryi* production in Mediterranean orchards (Morte et al., 2012; Andrino et al., 2019). Moreover, based on interviews with desert truffles gatherers and farmers (known as "turmicultores"), another factor that also varies widely between years and that is related to the total production are the start and end dates of the collection season. The most common dates for desert truffle collection

are from February to May, but the first fructifications can occur as early as in December and the last fructifications as late as in June. Most gatherers and "turmicultores" indicated that, during this period, mild temperatures together with some soil moisture are needed for fructifications, and that they co-occur with some phenological changes of the plant: *i.e.* the start of the fructification coincides with the blooming, while the end is related to flower disappearance and leaf senescence. In addition, in **Chapter V** we found that mainly soil water potential and VPD are the most important factors that determine the production of desert truffle during spring.

Phenology is defined as the study of periodic events in the life cycles of living beings, as influenced by the environment. The annual phenology of *H. almeriense* desert truffle plant is the typical of other Mediterranean summer-deciduous or semi-deciduous shrubs (Nilsen and Muller, 1981; Haase et al., 2000; Gulías et al., 2009) and consists of a vegetative period that lasts from autumn (bud breaking) to spring, blooming events that start at the end of winter and finish in spring and leaf senescence at the end of spring. Maximum photosynthesis is found in winter. Mycorrhizal colonization in the field is mainly intracellular at above 40% of mycorrhization average, except for summer, when few signs of mycorrhiza are found (Gutiérrez et al., 2003; Morte et al., 2010; Navarro-Ródenas et al., 2015). **Spring** phenology of plants is closely related to climate change, (Badeck et al., 2004; Cleland et al., 2007) especially for Mediterranean shrubs (Bernal et al., 2010; León-Sánchez et al., 2018). In fact, the climate change is already causing spring to occur earlier (Corell, 2005), and the forecasted changes for the Mediterranean regions point to increases in temperature and **VPD** and to a lower availability of soil moisture (NOAA, 2015). It is, thus, necessary to provide new insights in the spring phenology of crops such as desert truffles, which are a good alternative for arid and semiarid areas.

We hypothesize that throughout the spring, there should be a generalized switch in most of the parameters of the plant. This phenological switch must be explained by one or several environmental parameters that also change throughout the spring. If the plant phenology is related in some way to desert truffle production, the environmental values that cause this phenological switch should also be able to explain the differences in desert truffle yield. The aim of the present work is to characterize the responses of the desert truffle plant *H. almeriense* to the environment changes in spring. This work is focused on the search for morpho-physio-molecular parameters that could help us to track easily the changes in phenology that may be related to desert truffle yield. To achieve this

goal, the leaf anatomy, water relations, gas-exchange and the expression of leaf Rubisco and aquaporin (AQP) have been analyzed. The increase of knowledge in these relationships could lead us to understand the biology of this Mediterranean shrub and, ultimately, to understand the dynamics of desert truffle production.

6.2. Materials and methods

Two different assays have been carried out in order to get the following objectives:

- **Assay 1** (spring 2016): to detect and characterize the phenological switch from early to late spring in mycorrhizal desert truffle plants,
- **Assay 2** (springs 2017 and 2018): to modify this phenological swicth, by reducing VPD with shadowing devices, in order to extend the truffle producing season.

These assays were performed in two different *H. almeriense* x *T. claveryi* orchards, where site, the year of plantation, irrigation, number of mycorrhizal plants and plantation frame were different for each of them, as detailed below.

6.2.1. Assay 1: Spring 2016

6.2.1.1. Experimental site and procedure

The experimental *H. almeriense* x *T. claveryi* site used in Assay 1 was located in Espinardo, Murcia (Spain) (38°01'20"N 1°10'00"W) at an altitude of 91 m. In May 2008, 40 mycorrhizal plants inoculated with *T. claveryi,* as explained in Morte et al. (2008), were transplanted at 1 x 1 m of distance one to another in a square pattern and were well-irrigated until February 2009 in order to ensure the proper establishment and initial development of the plants. Temperature (ºC), relative humidity (%) , VPD (kPa), radiation (W m^{-2}) and rainfall (mm) data were collected from an automatic weather station (Campbell Scientific Ltd, Shepshed, UK) sited on the experimental plot. Soil water potential (Ψ_{soil} expressed in kPa) was monitored using Watermark sensors (Irrometer, Spain) located in four different spots of the orchard. Temperature and VPD surrounding

the leaf were measured using a portable photosynthesis system (LI-6400, Li-Cor, Inc., Lincoln, NE, USA) simultaneously to the estimation of gas-exchange parameters.

Gas-exchange parameters, shoot water potential at midday (Ψ_{md}), leaf mass per area (LMA) and AQP and Rubisco gene expression were monitored during the spring of 2016 (April to June). Taking into account the large differences in meteorological conditions throughout the spring, and based on stomatal conductance (g_s) and Ψ_{md} regressions with VPD_{air} and Ψ_{soil}, respectively, threshold values of VPD_{air} and Ψ_{soil} were established, and spring season was divided between the first and second half of spring. For the experimental period, all data collected before May 8th were considered to belong to early spring, while after May 9th belonged to late spring. No irrigation was applied to the experimental site during the period of study.

6.2.1.2. *Gas-exchange parameters and shoot water potential at midday (Ψ_{md})*

Net assimilation rate (A_N), g_s, transpiration rate (E) and intracellular carbon (C_i), were estimated during twelve weeks from April to June 2016, every two days, in six plants. They were measured in the morning from 09.00 am to 13.00 pm and then in the afternoon from 14.00 pm to 19.00 pm. Leaf gas exchange was estimated with a portable photosynthesis system (LI-6400xt, Li-Cor, Inc., Lincoln, NE, USA), on fully expanded leaves that were placed in a 2 cm^2 leaf cuvette. Due to the small leaves of this species, two to three of them were placed carefully in the cuvette and after the measurements, they were collected to measure their area using an Olympus SHZ stereomicroscope coupled to an Olympus DP73 camera. Area calculation was made using the image analysis software cellSens v1.14 (Olympus, Japan). Intrinsic water use efficiency ($_iWUE$) was calculated as the ratio between A_N and g_s. Measurements were taken at an air flow of 200 µmol s^{-1}, a controlled CO_2 concentration of 390 µmol s^{-1} achieved using the injection system and compressed CO_2 cylinders, at saturating light or PPDF (photosynthetic photon flux density) of 1500 µmol m^{-2} s^{-1} (Morte et al., 2010) and at ambient air temperature and relative humidity. Throughout the same week, measurements were taken at different times to obtain data from all the different time periods and, therefore, to obtain a weekly diurnal pattern of gas-exchange parameters.

For Ψ_{md} measurements, five cm-long plant apices from the same six plants, that were used to measure gas-exchange parameters, were cut at noon and immediately placed in a pressure chamber (Soil Moisture Equipment Co; Santa Barbara, CA, U.S.A.) according to Scholander et al. (1965).

6.2.1.3. Leaf mass per area (LMA)

Once every two weeks, three leaves per plant from the second and third node from the apex, from six plants, were cut and their area without petiole was measured as explained in **Section 6.2.1.2**. Afterwards, leaves were dried at 60 ° C for 72h and their dry weights were measured. LMA is the ratio of dry weight per area (g m^{-2}).

6.2.1.4. RNA extraction and quantitative real-time PCR

Once per week in the morning and once in the afternoon, after gas-exchange measurements, leaves from six plants were collected and immediately frozen in liquid nitrogen. 100 mg of frozen leaf material was homogenized in liquid nitrogen with the help of mortar and pestle. RNA was extracted with the CTAB method according to Chang et al. (1993). cDNA was synthetized by Reverse-Transcription Polymerase Chain Reaction (RT-PCR) from 0.5 µg of total RNA from each sample using QuantiTect Reverse Transcription Kit (Qiagen, Hilden, Germany), following manufacturer´s instructions (for detailed protocol, see **Appendix A: supplementary protocols**).

Expression of five *H. almeriense* AQPs (*HaPIP1.1*, *HaPIP1.2*, *HaPIP2.1*, *HaPIP2.2*, and *HaTIP1.1*) previously characterized (Navarro-Ródenas et al., 2013) and *H. almeriense* ribulose-1,5-bisphosphate carboxylase/oxygenase large subunit (*HarbcL*) was studied by real-time PCR using a QuantStudioTM 5 Flex (Applied Biosystems, Foster City, California, USA). Primers described in Navarro-Ródenas et al. (2013) were used for the five *H. almeriense* AQPs. Primers used for quantification of *HarbcL* were designed for this study using *H. almeriense rbcL* gene sequence deposited in GenBank (FJ492025.1) by Guzmán and Vargas (2009). *HarbcL* primers (**Table 6.1**) were designed using http://www.idtdna.com and tested to prove its specificity and efficiency. Each 15 µl of reaction medium contained 1.5 µl of 1:10 cDNA template, 0.11 µl of primer mix 5

μM each and 7.5 μl of SyBR Green Master Mix (Applied biosystems, Foster City, California, USA). The PCR program consisted of 10 min incubation at 95 °C, followed by 40 cycles of 15s at 95 °C and 1 min at 60 °C, where the fluorescence signal was measured (for detailed protocol, see **Appendix A: supplementary protocols**).

The efficiency of the primer sets was evaluated by performing real-time PCR on several dilutions of cDNA. Real-time PCR threshold cycle (Ct) was determined in triplicate. $2^{-\Delta\Delta Ct}$ method was used to evaluate the expression of each gene (Livak and Schmittgen, 2001) normalizing gene expression to the geometric mean of *H. almeriense ATP synthase* (AF035907.1, GenBank) and *H. almeriense 18S* (Navarro-Ródenas et al., 2013) levels (**Table 6.1**). These genes have been confirmed as suitable reference genes under different conditions using and geNorm, included in qbase+ software, version 3.0 (Biogazelle, Zwijnaarde, Belgium (www.qbaseplus.com). Real-time qPCR experiments were carried out in six separate biological samples and non-template controls were performed in all reactions.

Table 6.1. List of primers used for qPCR analysis. F = forward; R = reverse.

Name	Sequence	Source
HaPIP1.1 F	5′-GATGGGTGATGATGATGAAGC-3′	Navarro-Ródenas et al. (2013)
HaPIP1.1 R	5′-AGAAGGCGCATGGATAGAAG-3′	Navarro-Ródenas et al. (2013)
HaPIP1.2 F	5′-TCAGGACCGTTGATTTGATG-3′	Navarro-Ródenas et al. (2013)
HaPIP1.2 R	5′-CATCATGTAGGGCCCACTTAC-3′	Navarro-Ródenas et al. (2013)
HaPIP2.1 F	5′-TGCCTTTGTGTGTATGATGAAG-3′	Navarro-Ródenas et al. (2013)
HaPIP2.1 R	5′-TGATACAAGCCACCACCAGA-3′	Navarro-Ródenas et al. (2013)
HaPIP2.2 F	5′-TGCCCAAATGTAGCATTATCC-3′	Navarro-Ródenas et al. (2013)
HaPIP2.2 R	5′-GAGAGGAAATGAACTTCACATT-3′	Navarro-Ródenas et al. (2013)
HaTIP1.1 F	5′-TAGTAACTCCGGCCATGAGC-3′	Navarro-Ródenas et al. (2013)
HaTIP1.1 R	5′-CACAATAACAACAACTCCCA-3′	Navarro-Ródenas et al. (2013)
HarbcL F	5′-CTACGCGGTGGACTTGATTT-3′	*De novo*
HarbcL R	5′-TCGCTTCGGCACAGAATAAG-3′	*De novo*
HaATPsyn F	5′-GTATCCGTATTTGCCGGAGTAG-3′	*De novo*
HaATPsyn R	5′-ACCGTAGACTAGAGCCACTT-3′	*De novo*
Ha18S F	5′-CCTGCGGCTTAATTTGACTC-3′	Navarro-Ródenas et al. (2013)
Ha18S R	5′-AACTAAGAACGGCCATGCAC-3′	Navarro-Ródenas et al. (2013)

6.2.1.5. Relation between desert truffle yield and VPD

From spring 2001 to spring 2019, all truffles harvested from an experimental site located in Zarzadilla de Totana, Lorca Murcia, Spain (37°52'15.5"N 1°42'10.5"W) at an altitude of 870 m (more details in Andrino et al. 2019), were weighed and total production was expressed as fresh weight per hectare (kg per ha). These data were analyzed together with environmental data collected from the nearest meteorological station located in La Paca (Lorca, Spain IMIDA LO41, http://siam.imida.es). In order to highlight long-term trends and to identify the day of the year in which the VPD stably reaches a certain threshold of VPD (DOY_{VPDt}), the simple moving sum of seven days for VPD was calculated.

6.2.2. Assay 2: Spring 2017-2018

6.2.2.1. Experimental site and procedure

The experimental *H. almeriense* x *T. claveryi* site used in this assay was located in "Finca Torrecillas", Corvera, Murcia (Spain) (37°50'54.8"N 1°11'20.1"W) at an altitude of 291 m. In autumm 2015, 400 mycorrhizal plants inoculated with *T. claveryi,* as explained in Morte et al. (2008), were transplanted at 1 x 0.75 m of distance one to another within the same row. Plants were disposed in rows of three, separated by a passage of 1.5 m of distance between rows (**Figure S8** in **Appendix C: Supplementary Figures**). The first fructifications occurred in spring 2017. The experimental assay was carried out in spring 2017 (from March 1st to July 15th) and spring 2018 (from March 1st to May 30th). From the total 400 mycorrhizal plants, only 216, placed in the center of the orchard, were selected for the assay. These 216 plants were divided into groups of 9, and each group was considered as our experimental unit, resulting in a total of 24 groups of plants. An irrigation treatment given to half of the groups consisted of a weekly irrigation of approximately 2L per plant, while the other half were not irrigated. In addition, half of the plants of each irrigation treatment were covered with a shadowing device of 1.5 x 1.5 m that was constructed surrounding the group of plants with agricultural mesh, as shown in **Figure 6.1**. The location of the shadow treatments was randomly selected while for the irrigation treatments randomization was not possible due to technical limitations of the orchard. Therefore, the first two rows and a half were irrigated, but not the rest (for details

see **Figure S8** in **Appendix C: Supplementary Figures**). In total, we had 4 different treatments with 6 repetitions each: control (no irrigation, no shadowing), irrigation (irrigation, no shadowing), shadowing (no irrigation, shadowing) and irrigation + shadowing (irrigation and shadowing).

Figure 6.1. Shadowing devices at the experimental site "Finca Torrecillas" during the spring of 2018.

Environmental temperature (ºC), relative humidity (%), VPD (kPa), radiation (W m^{-2}) and rainfall (mm) data were collected from the nearest meteorological station located in Corvera (Corvera, Spain IMIDA CA21, http://siam.imida.es). Soil water potential (Ψ_{soil} expressed in kPa) was monitored using Watermark sensors (Irrometer, Spain) located in four different spots of the orchard. Environmental parameters near the plant were measured with HOBO U12 temperature/relative/humidity/light loggers (Onset computer corporation, MA, USA). Two different loggers were placed in the experimental site, one of them under a shadowing device and the other in a control treatmetent.

6.2.2.2. *Gas-exchange measurements*

Gas-exchange measurements were performed as explained in **Section 6.2.1.2**. During the experimental time, the measurements were made twice per week in the morning from 9.00 to 13.00, intercalating different treatments so that the measurements were not affected by the time of the day. From the group of nine plants that were

considered our experimental unit, the plant situated in the center was selected for the measurement, which was made in two different shoots from each experimental unit.

6.2.2.3. *Desert truffle production*

During the experimental period, all the harvested desert truffles were weighted, the fructification site was annotated, and the number of desert truffles, the total production and the weight per unit were calculated.

6.2.3.   Statistical analysis

Student's t test, analysis of variance ANOVA, Tuckey's post-hoc tests and Pearson´s correlation analysis were performed using R programming language with Rstudio software v1.1.456. Data plotting, regression analysis and model fitting was carried out using Sigmaplot v 10.0 (Systat Software, UK).

To visualize the dissimilarities between groups of plants in Assay 1 (early and late spring) and Assay 2 (control, irrigation, shadowing and irrigation + shadowing), two-dimensional principal coordinate analyses (PCoA) calculated on a Euclidean dissimilarity matrixof plant physiological parameters were performed. To confirm the effect of the factors, permutational multivariate analysis (perMANOVA) and analysis of similarities (ANOSIM) were conducted on the same Euclidean matrix, using the adonis function of the vegan package (Oksanen et al., 2007), and 999 permutations.

6.3. Results

6.3.1. Assay 1

6.3.1.1 Gas-exchange parameters, Ψ_{md} and LMA responses
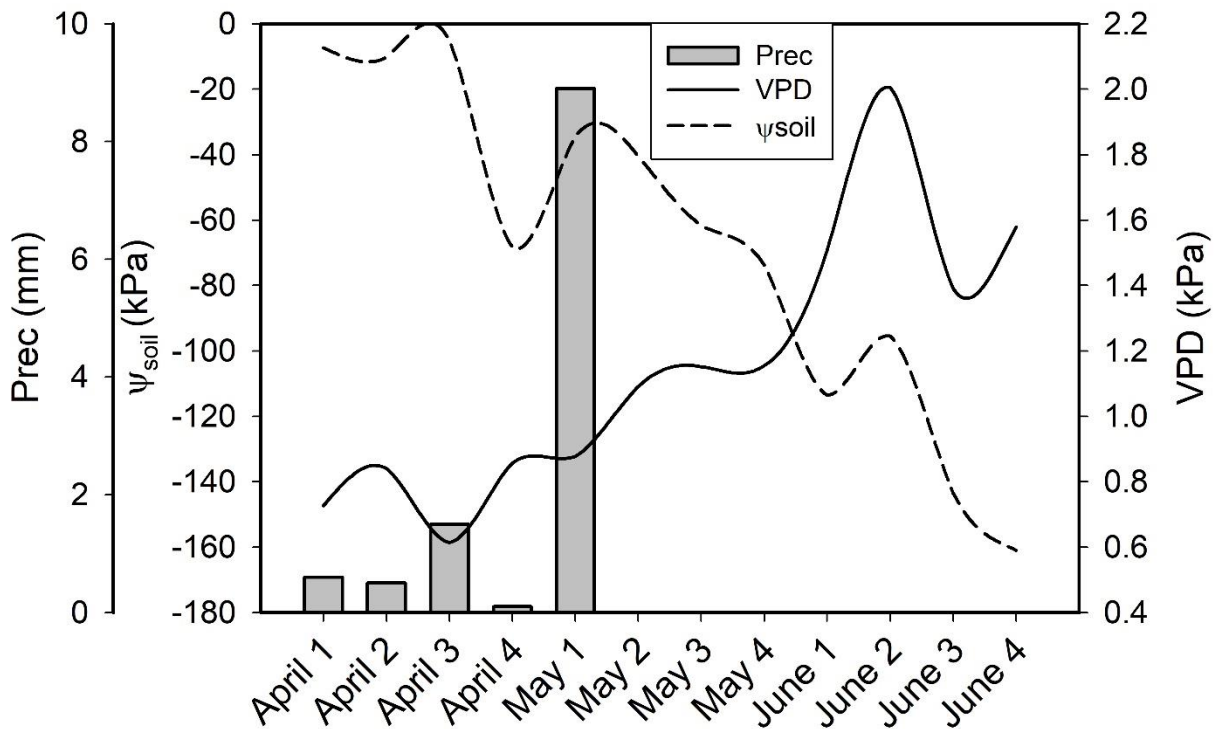
Figure 6.2. Vapor pressure deficit (VPD), soil water potential (Ψsoil) and precipitations evolution during spring 2016.

VPD, radiation and precipitation profiles from the spring 2016 were typical of Mediterranean regions, with a characteristic increase in average air VPD during spring. Precipitations were scarce during the study period, having minimum values in late spring and at the beginning the start of summer (**Figure 6.2**). When analyzing Pearson's correlation table between environmental and plant parameters, several correlations appeared, being g_s the gas-exchange parameter with stronger correlations with environmental parameters during spring (**Figure 6.3**). Correlations coefficients between g_s and VPD_{air} (-0.63, $p < 0.001$) and VPD_{leaf} (-0.88, $p < 0.001$), were higher than those with Ψ_{soil} (0.53, $p < 0.01$). Ψ_{md} showed its main correlation with Ψ_{soil} (0.82, $p < 0.001$), while no correlations were found with VPD_{air} (-0.44, no significance) (**Figure 6.3**).
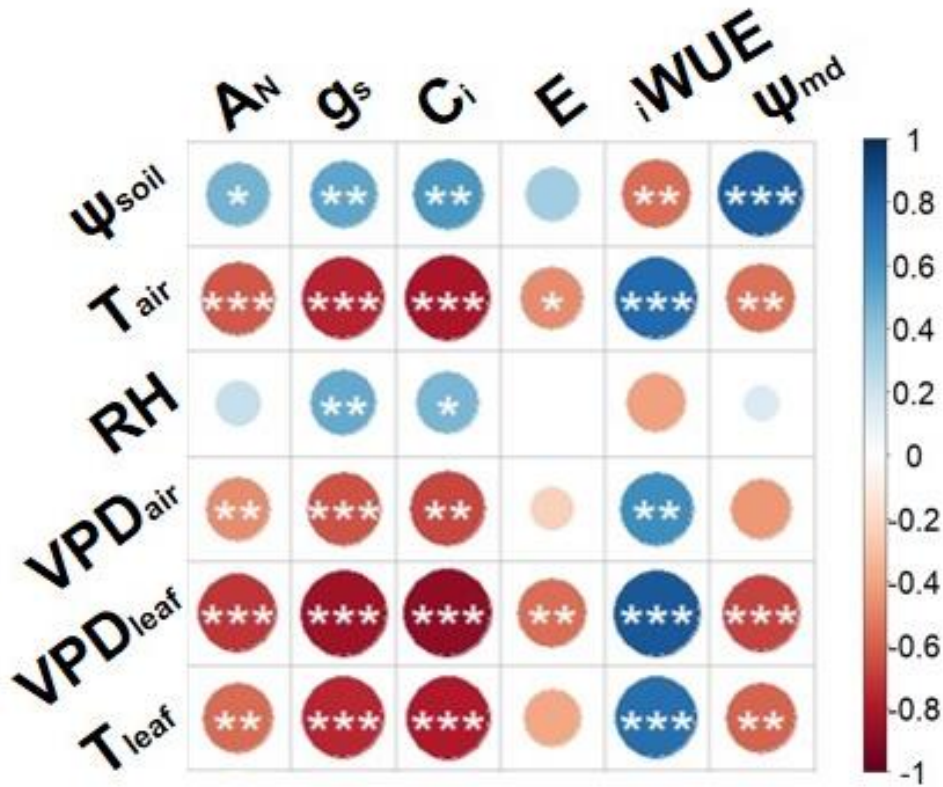
Figure 6.3. Pearson's correlation table between plant and environmental parameters in spring 2016. Different colors represent positive (blue) or negative correlations (red) and color intensity represents Pearson's correlation coefficient. Asterisks indicate statistical correlations. * = $p \leq 0.05$; ** = $p \leq 0.01$ and *** = $p \leq 0.001$.

Figures 6.4A and **6.4B** show gs and Ψ_{md} regressions with VPD_{air} and Ψ_{soil}, respectively. In both cases, a sigmoid regression following **Equation 6.1** proved to be the best fit. For both regressions, points where gs or Ψ_{md} starts a linear decrease, another where it achieves its minimum and the inflection point can be estimated thanks to the sigmoid fit. At a range of week average VPD_{air} between 0.8 and 1.1 kPa, a sudden linear decrease of stomatal conductance occurred from 0.25 to 0.03 mol m^{-2} s^{-1}, and an inflection point of 0.93 kPa was calculated (**Figure 6.4A**). A similar behavior was observed with Ψ_{md}, as at Ψ_{soil} between -50 and -80 kPa approximately, Ψ_{md} experimented a sudden linear decrease from -1,4 MPa to -2,4 MPa, with an inflection point at -65 kPa (**Figure 6.4B**). The inflection points were used to establish threshold values of VPD and Ψ_{soil} and to separate the data into two groups: early and late spring.

$$f = \frac{yo + a}{\left(1 + \exp\left(-\frac{x - xo}{b}\right)\right)}$$

Equation 6.1. Sigmoid regression from gs vs VPD_{air} and Ψ_{md} vs Ψ_{soil}.
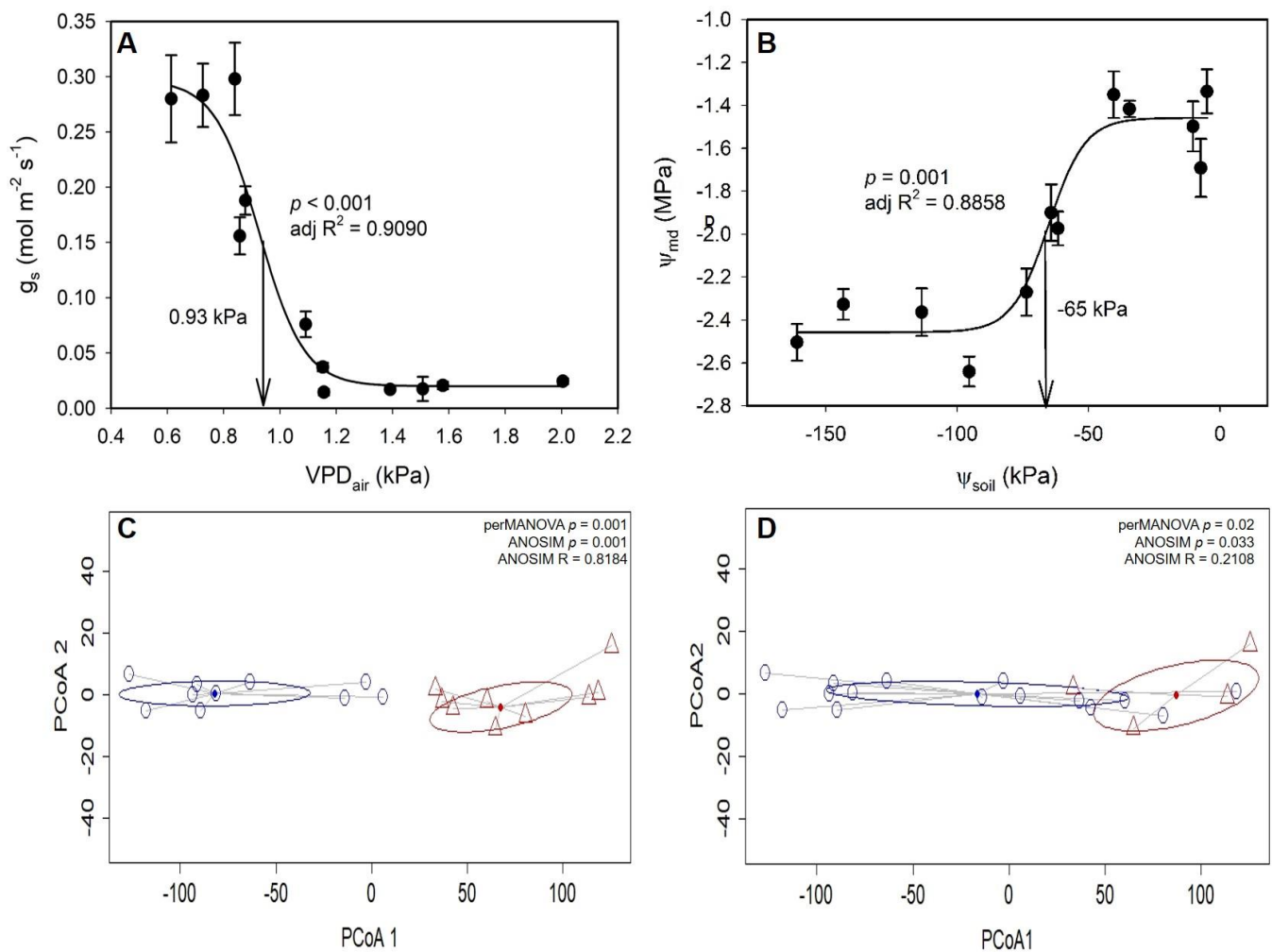
Figure 6.4. Threshold values of VPD and soil water potential (Ψ_{soil}), their relationship with stomatal conductance (g_s) and midday shoot potential (Ψ_{md}), respectively, and ordination of the data according to principal coordinate analysis. Each point represents the average of a week of measurements. (**A**) Sigmoid regression between gs and VPDair. (**B**) Sigmoid regression between Ψ_{md} and Ψ_{soil}. (**C**) and (**D**) Principal coordinate analysis (PCoA) of *H. almeriense* morpho-physio-molecular variables separating the points into early (blue circles) and late (red triangles) spring according to VPD threshold (**C**) or Ψ_{soil} threshold (**D**). Ellipses were drawn according to the standard deviation and perMANOVA and ANOSIM tests were performed using the same Euclidean dissimilarity matrix used for PCoA.

In order to reveal which parameter explained the most the overall differences in plant performance throughout the spring, we performed PCoA and perMANOVA analyses grouping the data based on VPD threshold (VPDt) (**Figure 6.4C**) or on Ψ_{soil} threshold (**Figure 6.4D**), respectively. For both cases, the two groups of data were significantly different, revealing a significant generalized switch in plant performance between early and late spring. In the case of VPDt based perMANOVA (**Figure 6.4C**),

better significance levels, ANOSIM values and no overlapping dispersion ellipses were found compared to Ψ_{soil} threshold based perMANOVA (**Figure 6.4D**) and, for the following analyses, we used this threshold (VPD = 0.95 kPa) to differentiate between early and late spring measurements. When comparing A_N, g_s, E, $_iWUE$, Ψ_{md} and LMA average values between early and late spring, all the parameters were different (**Table 6.2**) and the A_N and g_s dairy dynamics also changed (**Figure 6.5**).

Table 6.2. Plant parameters in early and late spring 2016. Mean of An, gs, E, iWUE, Ψ_{md}, and LMA ± standard error are represented. Different letters represent significant differences according to Student's t-test ($p < 0.05$).

	A_N (µmol m^{-2} s^{-1})	g_s (mol m^{-2} s^{-1})	E (mmol m^{-2} s^{-1})	$_iWUE$ (µmol mol^{-1})	Ψ_{md} (MPa)	LMA (g m^{-2})
Early Spring	6.99±0.64a	0.133±0.020a	3.04±0.29a	70.64±7.72a	-1.65±0.07a	170.11±7.24a
Late Spring	3.14±0.54b	0.023±0.003b	1.21±0.19b	134.26±9.45b	-2.37±0.08b	244.48±9.64b
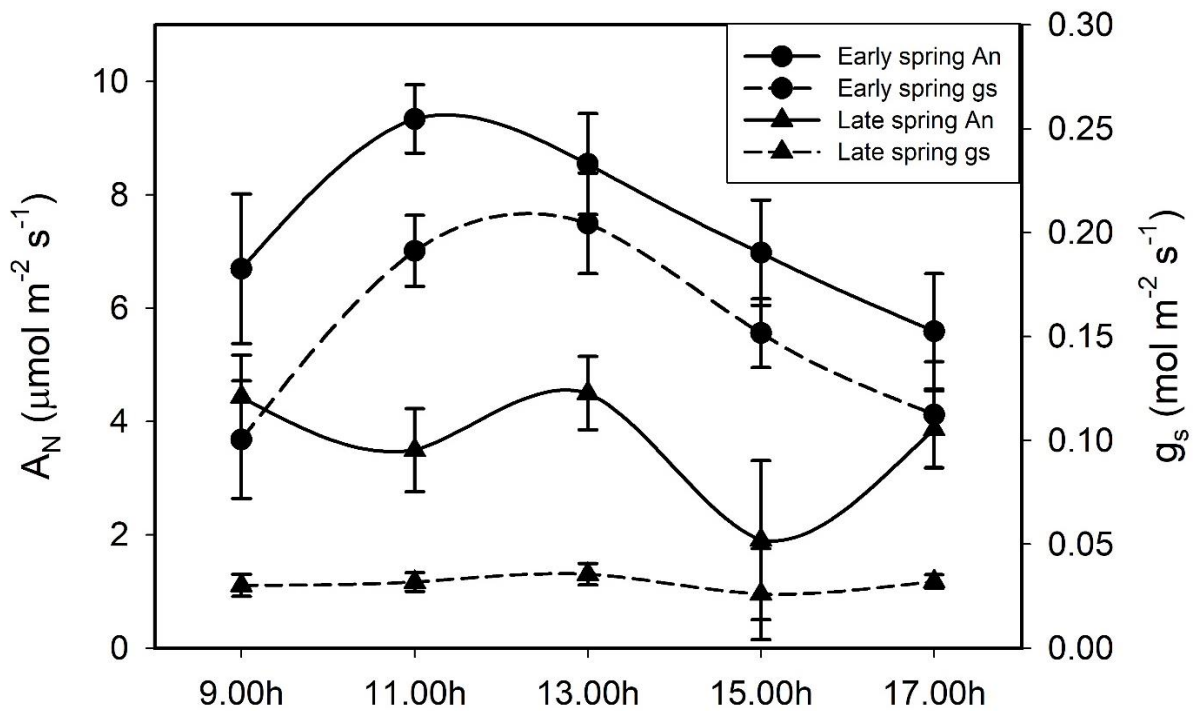
Figure 6.5. ***H. almeriense* net assimilation and stomatal conductance diurnal patterns in early and late spring.** Each point represents the average for a certain time lapse in early (circles) and late (triangles) spring and bars represent standard error.

6.3.1.2.   *Rubisco and AQP gene expression profiles*

The expression profile of *HarbcL* over time changed from early to late spring in a similar way to the rest of parameters studied. A decrease in the expression level of *HarbcL* from early to late spring was observed, finding its minimum during the first week of June, when it had a 6-fold downregulation, compared to the start of the study (**Figure 6.6A**). *HarbcL* and stomatal conductance showed almost parallel patterns during this period, as it is shown in Figure 6.6A. Their relationship was adjusted to an exponential regression following **Equation 6.2**, with an adjusted r^2 of 0.88 (**Figure 6.6B**).

$$f = yo + a * (1 - \exp(-b * x))$$

Equation 6.2. Exponential fit from *HarbcL* relationship with gs.
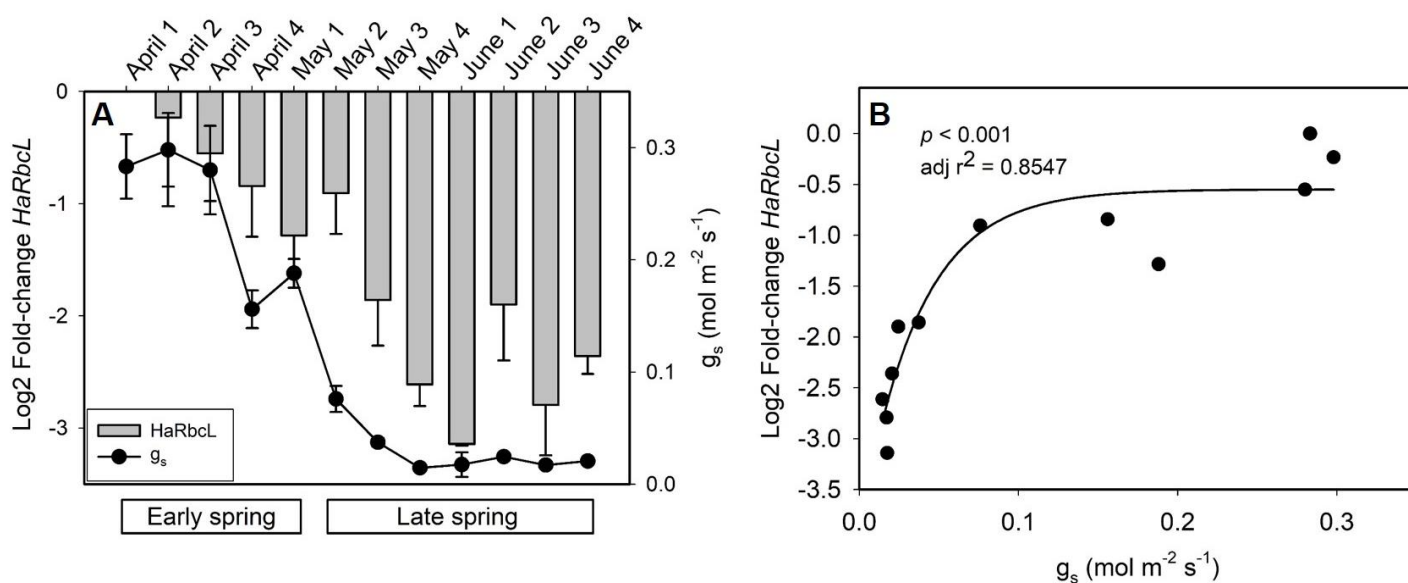
Figure 6.6. Rubisco expression relationship with vapor pressure deficit (VPD) and stomatal conductance (gs). (A) gs values and Harbcl expression levels expressed as log2 fold-change during the course of spring 2016, where 1, 2, 3, 4 are respectively the first, second, third and fourth weeks in a month. **(B)** Exponential relationship between gs and *HarbcL* expression levels, each point represents the average of a week of measurements.

The expression pattern of four plasma intrinsic proteins (PIPs) and one tonoplastic intrinsic protein (TIP) was studied along spring 2016. Almost no correlation was found between the expression pattern of all the AQPs analyzed and the rest of the parameters studied. When data from the beginning and end of spring were compared separately, no significant differences were observed when a Student's t test was carried out, however, several Pearson's correlations appeared. No correlations were observed in early spring, but all four *HaPIPs* were significantly correlated with environmental (VPD$_{leaf}$) and physiological (Ψ_{md}) parameters during late spring. The increase in VPD in late spring resulted in *HaPIP1.1* and *HaPIP2.1* upregulation (**Figures 6.7A**; **6.7C**) and *HaPIP1.2* and *HaPIP2.2* downregulation (**Figures 6.7B**; **6.7D**). *HaTIP1.1* showed no correlation with any parameter neither in early nor in late spring. *HaPIP1.1* and *HaPIP2.1* on the one hand, and *HaPIP1.2* and *HaPIP2.2* on the other, seemed to respond to the increase in VPD observed in spring as different clusters, and when their expressions were studied against each other, they showed linear regressions with adjusted r^2 higher than 0.62 in all the cases (**Figure 6.8**).
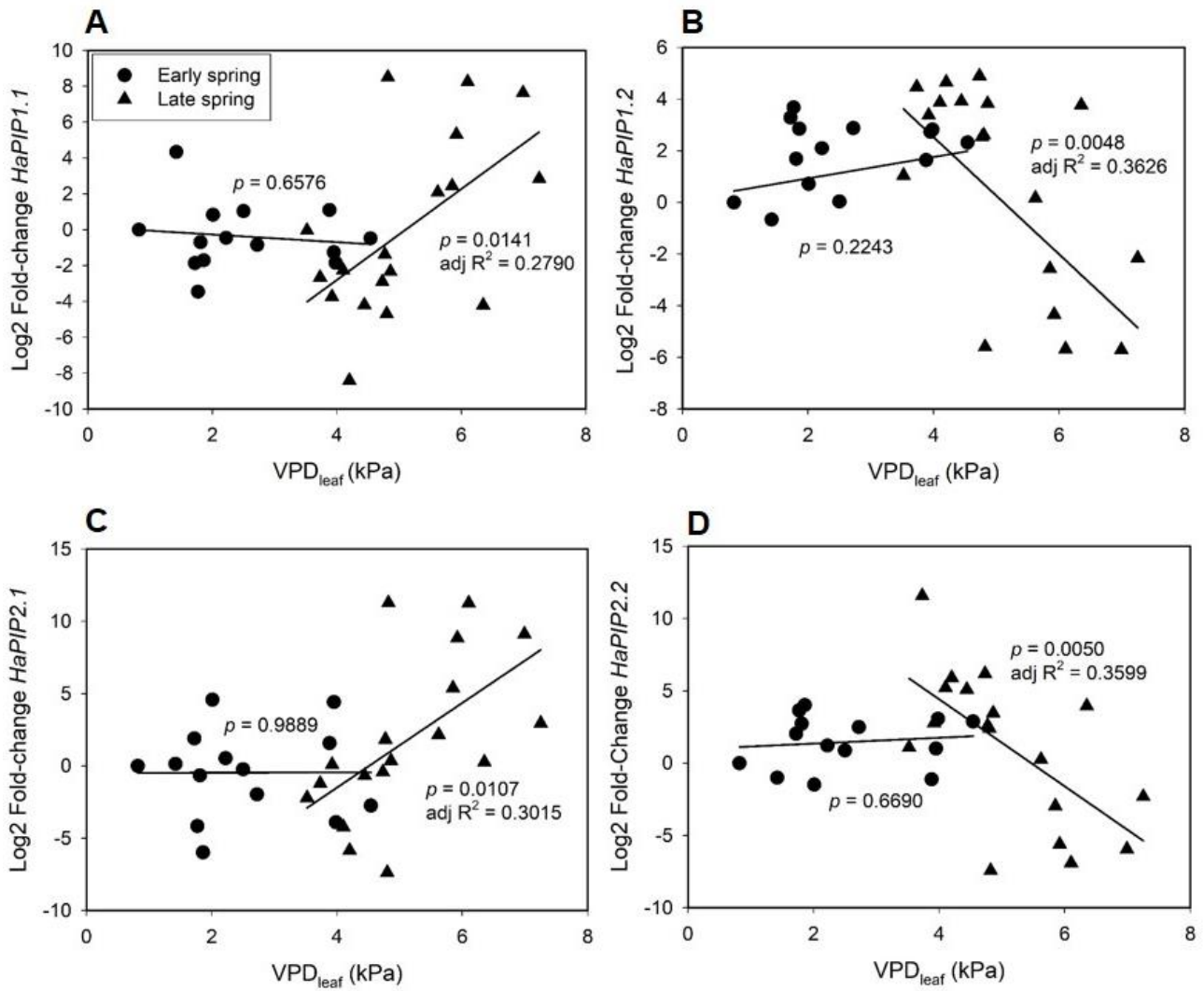
Figure 6.7. Relationship and linear regression between VPD and *HaPIP1.1* (A), *HaPIP1.2* (B), *HaPIP2.1* (C) and *HaPIP 2.2* (D) expressions in early and late spring 2016.
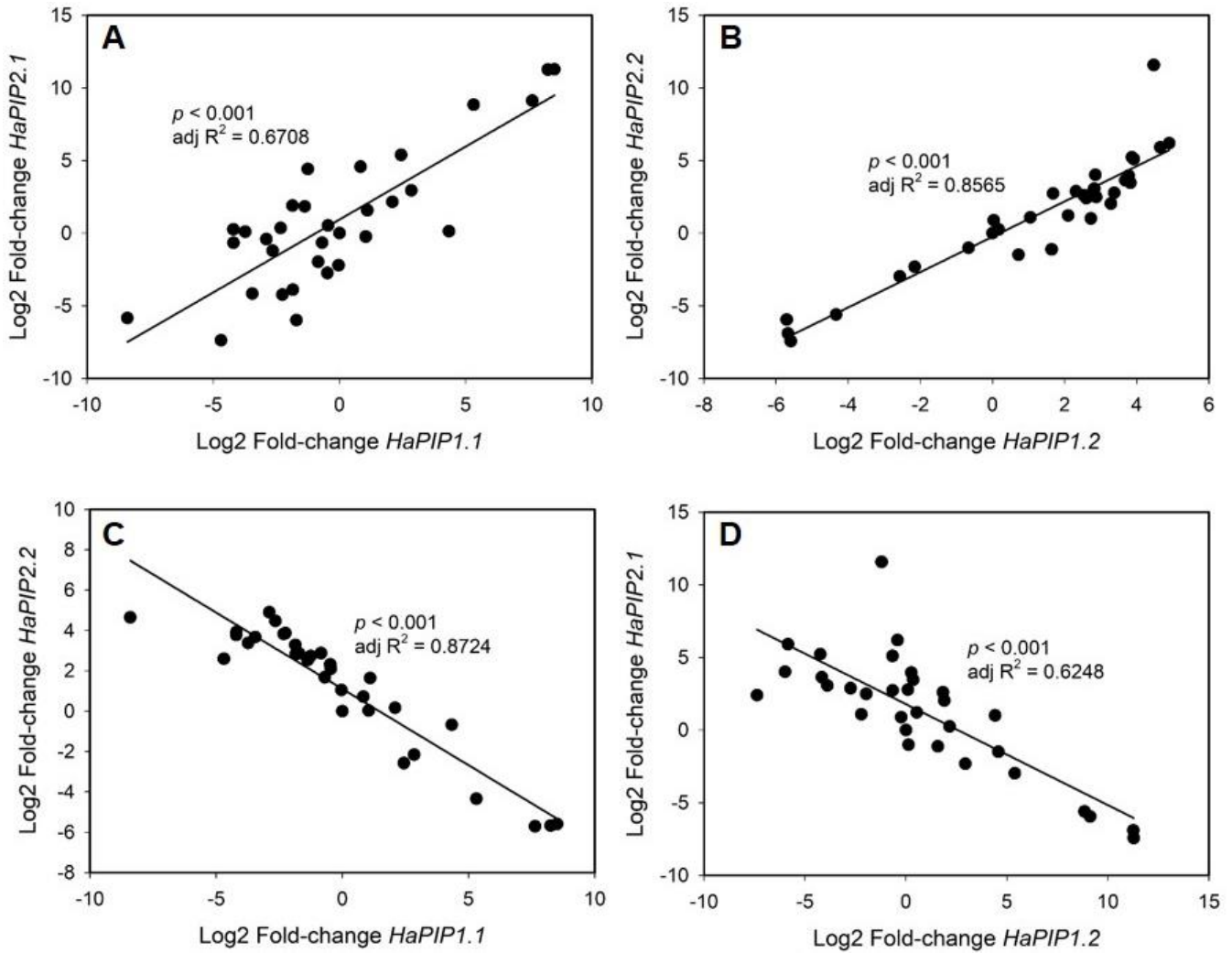
Figure 6.8. Expression of the studied leaf HaPIPs and correlation among themselves in spring 2016. (A) HaPIP1.1 *vs* HaPIP 2.1. **(B)** HaPIP1.2 *vs* HaPIP2.2. **(C)** HaPIP1.1 *vs* HaPIP2.2. **(D)** HaPIP1.2 *vs* HaPIP2.1.

6.3.1.3. Desert truffle production correlation to VPDt

Figure 6.4A allowed us to establish a VPD threshold point (VPDt) of 0.93 kPa that we used as a marker for the general switch that occurs between early and late spring. A correlation analysis was performed between desert truffle production and the day of the year (DOY) at which VPDt was stably reached (DOY$_{VPDt}$). A significant positive correlation was found between DOY$_{VPDt}$ and truffle production (**Figure 6.9**) and the years in which production was below average showed a significant earlier DOY$_{VPDt}$ (April 30th) than years with a production above average (May 19th) when a Student's t test was performed.
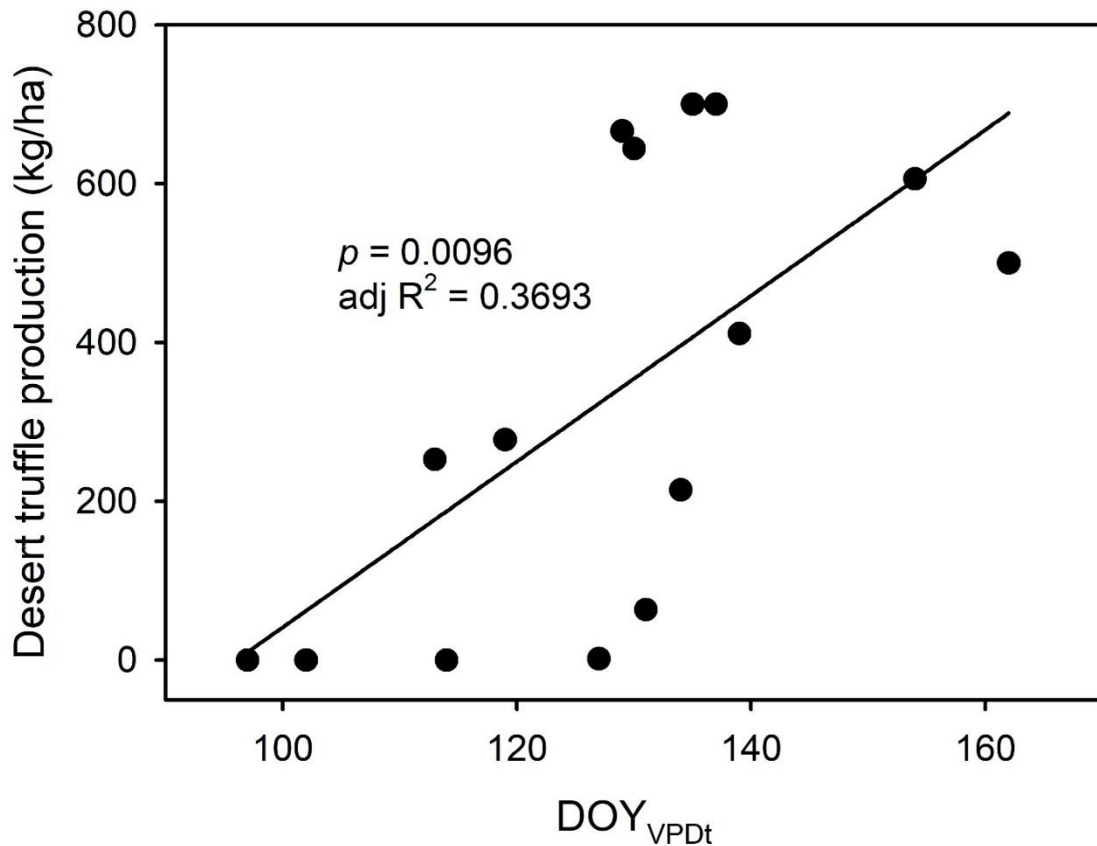
Figure 6.9. Desert truffle production from 2001 to 2019 compared to the day of the year when a stably vapor pressure deficit (VPD) threshold of 0.93 kPa is reached.

6.3.2. Assay 2

6.3.2.1. *Shadowing device*

The objective of the shadowing devices were to buffer the increase in VPD characteristic of Mediterranean springs. In order to check their effectiveness, temperature, relative humidity, VPD and light intensity were measured inside and outside the shadowing devices (**Table 6.3**). The shadowing device decreased the temperature and increased the relative humidity, so that the VPD decreased up to an 18% in the shadowing treatments during the experimental period. Furthermore, this decrease was greater as the summer approached, *i.e.* in March 2017, only a 10% decrease in VPD was achieved, while a 20% decrease was achieved in June of the same year. Moreover, the shadowing devices also hindered the solar radiation, subtracting between 55 and 60 % of the total radiation and around 35% of the photosynthetic active radiation (PAR).

Table 6.3. Comparison of temperature, relative humidity, vapor pressure deficit (VPD) and radiation between control and shadowing treatments. (A) Total differences for each environmental parameter in 2017 and 2018. **(B)** Month to month differences for each environmental parameter in 2017 and 2018. The numbers represent the percentage of the shadowing treatment with respect to the control.

A

	T (ºC)	HR (%)	VPD (kPa)	RAD (lum m^{-2})	PAR (PPDF)
2017					
Control	22.86 ± 5.82 a	47.48 ± 8.55 a	1.93 ± 0.87 a	8,375 ± 2,519 a	826 ± 148 a
Shadow	21.36 ± 5.33 a	50.47 ± 10.76 b	1.61 ± 0.74 b	3,828 ± 1,447 b	535 ± 62 b
Diff	-6.56 %	+6.30 %	-16.58 %	-54.29 %	-35.23 %
2018					
Control	21.14± 5.05 a	51.37 ± 11.30 a	1.29 ± 0.53 a	10,836 ± 1859 a	827 ± 161 a
Shadow	19.17 ± 3.70 b	54.50 ± 11.08 b	1.05 ± 0.39 b	4,119 ± 802 b	513 ± 116 b
Diff	-9.32 %	+6.09 %	-18.6%	-62.00 %	-37.97 %

B

	% T	% HR	% VPD	% RAD	% RAD PAR
2017					
March	94.61 ± 0.81 a	100.73 ± 1.12 a	90.52 ± 1.25 a	50.08 ± 1.17 a	89.15 ± 1.09 a
April	93.22 ± 0.70 a	104.38 ± 0.76 a	79.15 ± 1.98 b	53.67 ± 1.42 a	59.55 ± 0.92 b
May	94.90 ± 0.22 a	98.70 ± 0.43 b	87.35 ± 0.69 a	52.09 ± 1.84 a	51.67 ± 1.97 b
June	92.59 ± 0.29 a	106.95 ± 0.74 a	80.77 ± 0.72 b	70.72 ± 2.57 b	63.54 ± 0.44 b
2018					
March	94.40 ± 0.92 a	101.75 ± 1.84 a	95.89 ± 2.75 a	43.84 ± 2.12 a	66.6 ± 4.12 a
April	90.94 ± 0.52 b	106.69 ± 0.80 b	84.31 ± 1.11 b	40.42 ± 1.18 a	68.85 ± 1.20 a
May	90.14 ± 0.34 b	106.73 ± 0.70 b	81.77 ± 1.06 b	37.54 ± 0.84 a	58.86 ± 1.81 a

6.3.2.2. Gas-exchange parameters

When the PCoA and the permANOVA were performed, no differences were found between any of the different treatments in any of the months of each year, indicating that the treatments had no influence on the gas-exchange parameters of the plant at any moment (**Figure 6.10**).
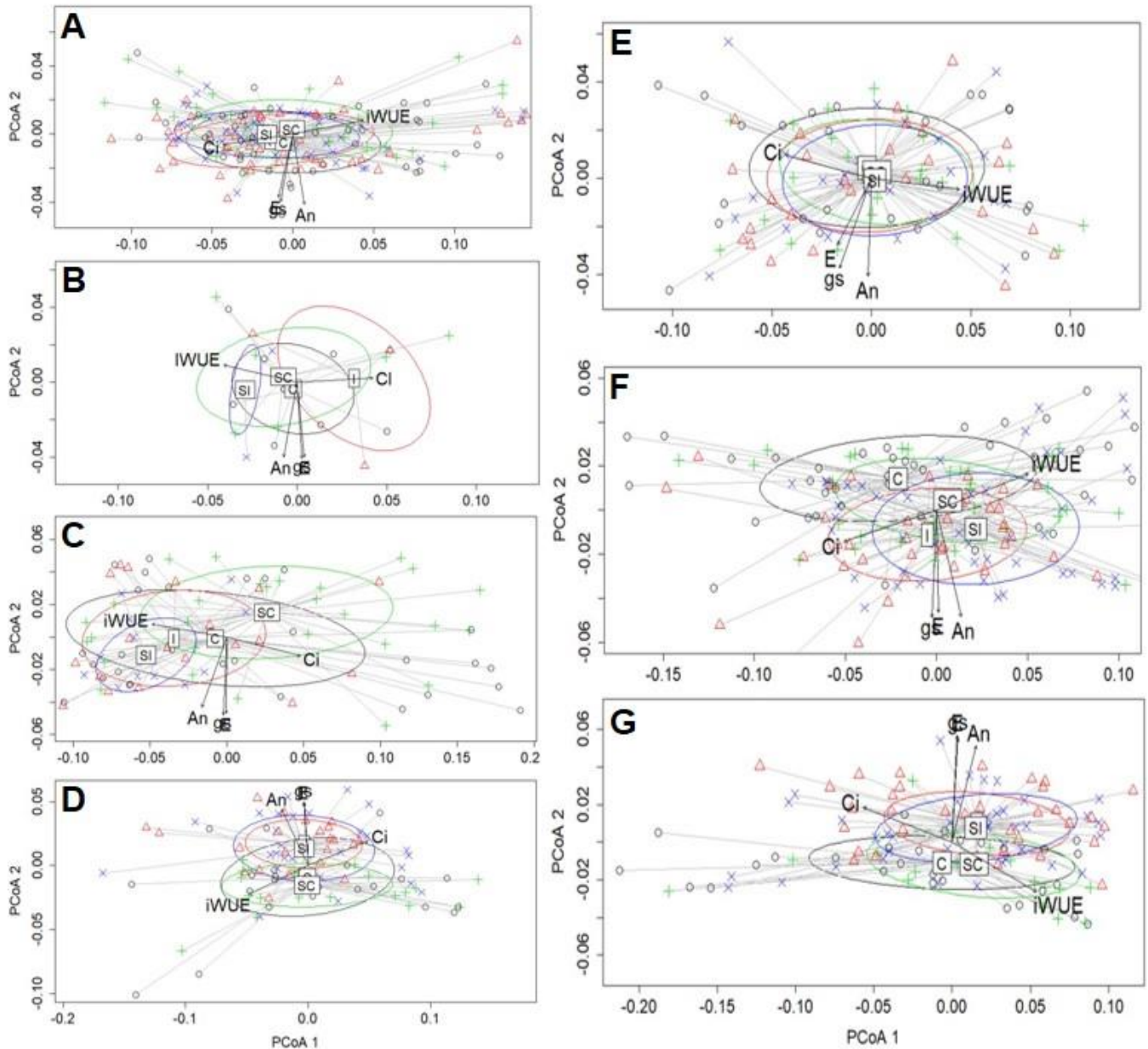
Figure 6.10. Principal coordinate analysis of plant gas-exchange parameters in Assay 2, springs 2017-2018. (A) March 2017. **(B)** April 2017. **(C)** May 2017. **(D)** June 2017. **(E)** March 2018. **(F)** April 2018. **(G)** May 2018. No statistical differences were found for any of the months when a permANOVA was performed. C= control; SC = shadowing control; I= irrigation; SI = shadowing irrigation

6.3.2.3. *Desert truffle production*

Regarding the production of desert truffles, there were no differences between the treatments when a Chi-square test was performed. However, in both years the most productive area was the irrigated one and the production in the irrigated and the shadowing + irrigation areas were two-fold higher than the non-irrigated areas (**Table**

6.4). Furthermore, in terms of total production, it was higher in 2017 (238 kg per hectar) than in 2018 (151 kg per hectar), coinciding with the later DOY$_{VPDt}$ of this year (**Figure 6.11**).

Table 6.4. Desert truffle production in the experimental area during the years 2017-2018 of the study of Assay 2. C= Control; SC = Shadowing control; I = Irrigation; SI = Shadowing irrigation.

Year	Treatment	Units	FW (g)	g / truffle
	C	3	245	81.7
	SC	2	185	92.5
2017	I	4	495	123.8
	SI	6	360	60.0
	Total	**15**	**1285**	-
	C	3	195	65.0
	SC	1	70	70.0
2018	I	5	320	64.0
	SI	3	230	76.7
	Total	**12**	**815**	-
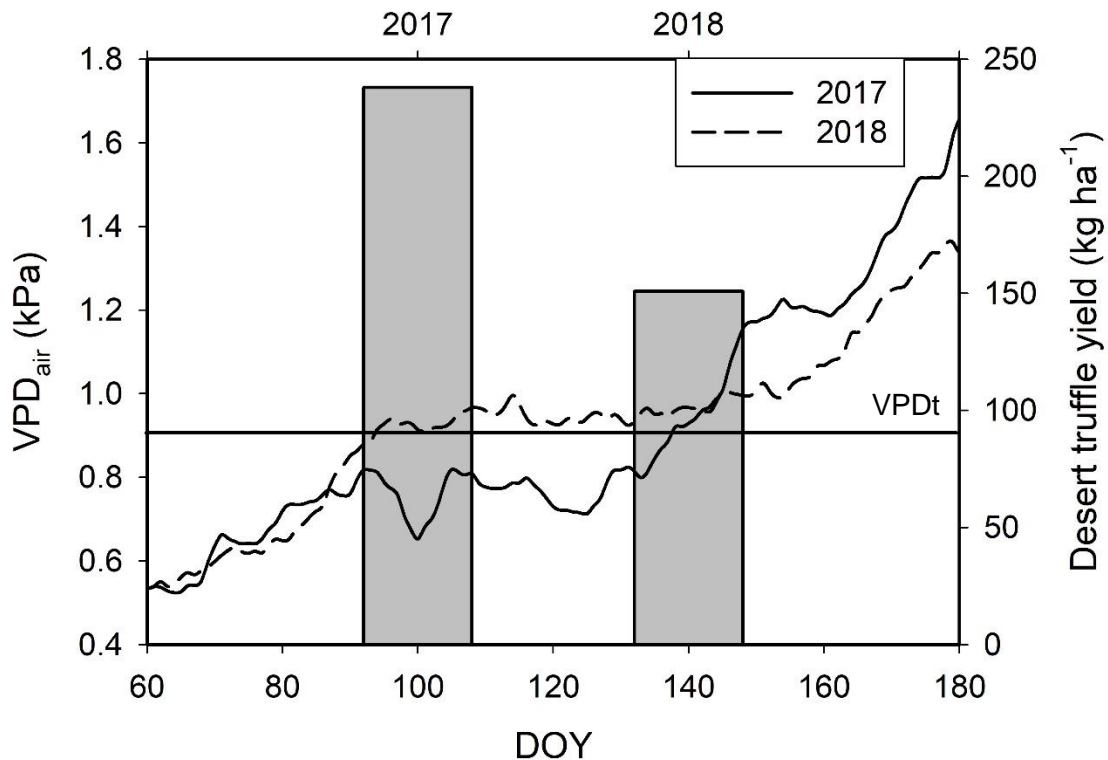
Figure 6.11. Desert truffle yield and VPD conditions of the experimental field during the springs of 2017 and 2018. DOY = day of the year, starting January 1st.

6.4. Discussion

Desert truffle *T. claveryi* cultivation was started in 1999 as a result of several years of research (Morte et al., 2008; 2017). Since then, its cultivation has grown exponentially and nowadays, *T. claveryi* cultivation is becoming an economical resource at regional, national and international level (Morte et al., 2017; Oliach et al., 2019). All these years of *H. almeriense* x *T. claveryi* association has led to a general knowledge about its phenology (Navarro-Ródenas et al., 2015; Morte et al., 2010; 2017) but there was a lack of detailed information about morpho-physio-molecular responses of the mycorrhizal plants during the spring, a key period of time for *H. almeriense* phenology and desert truffle fructification.

Mediterranean springs represent the start of the dry season: temperature increases, relative humidity decreases and, consequently VPD increases. Furthermore, rainfalls are scarce during this season, resulting in low soil water availability. The results of the correlation analysis (**Figure 6.3**), as well as the regressions (**Figure 6.4 A; 6.4B)** statistically demonstrate that most of changes in physiological parameters can be explained by VPD and Ψ_{soil}, and therefore, these environmental parameters and their complex interactions, determine the responses of the to water-stress, as occurs in most Mediterranean plants in the dry season (Flexas et al. 2014). More importantly, we proved that, in this species, a generalized phenological switch occurs during spring and that the VPD is the main factor determining it, since the switch in plant parameters is better explained by VPD ($p = 0.001$) than by Ψ_{soil} ($p = 0.02$) (**Figure 6.4C; 6.4D**).

With regard to LMA, the majority of deciduous and evergreen shrubs adapted to arid and semiarid conditions are considered as high-LMA species and, therefore, possess a conservative strategy (Poorter et al., 2009). The LMA increase in *H. almeriense* during spring (**Table 6.2**) could be considered a response to drought and can play a role in the adaptation of this species to arid ecosystems, since it has been proved that a decrease in water availability normally results in increases in LMA (Poorter et al., 2009). In several plant species, water-stress is also known to induce a decrease in Rubisco activity (Boyer, 1976; Lawlor 1995; Flexas et al., 2006a; Abdallah et al., 2018); the mechanism of these decreases can vary from biochemical regulation to a direct regulation of Rubisco genes or indirectly, *via* regulation of Rubisco inhibitors (Flexas et al., 2006a; Parry et al., 2008). The transcriptional repression of *HarbcL* during the study period was

highly correlated to stomatal closure (**Figure 6.5**), reinforcing the idea of stomatal closure as the triggering event for the downregulation of Rubisco through a decrease in the concentration of CO_2 in the chloroplast (Flexas et al., 2006a; 2006b), especially in Mediterranean species (Galmés et al., 2011). Normally, AQPs expression response to water-stress is difficult to analyze, since induction can be a way of increasing hydraulic conductance under stress conditions but repression could also be a way to minimize water loss (Alexandersson et al., 2005). The absence of correlations of AQP expression levels with VPD and Ψ_{md} in early spring and the subsequent later appearance of these correlations when environmental conditions become more stressful (**Figure 6.6**) implies a fine-tune regulation (Lovisolo et al., 2007) of *H. almeriense* leaf AQPs, confirming in field conditions what was previously described in nursery conditions by Navarro-Ródenas et al. (2013). Only in late spring, *HaPIP1.1* and *HaPIP2*.1 increased its expression with VPD increase, while *HaPIP1.2* and *HaPIP2.1* were repressed when VPD increased. This means that AQP are differentially regulated only in water restrictive conditions. Furthermore, it has been proved that *HaPIP1.1* increases CO_2 permeability (Navarro-Ródenas et al., 2013), so its induction in response to the increase in VPD could also be a way of facilitating the path of CO_2 through the mesophyll, therefore maximizing photosynthesis with reduced stomatal conductance. The co-expression of *HaPIP1.1* with *HaPIP2.1* and *HaPIP1.2* with *HaPIP2.2*, respectively (**Figure 6.8**), could be an indicative of *PIP1-PIP2* heteromerization process that has been proposed to be necessary to their correct function (Yaneff et al., 2014; Bienert et al., 2018). It is also important to note that only five AQPs were analyzed within a family that presumably counts with more than thirty members, so in order to fully understand the AQP response of the plant during spring, more AQPs should be identified and studied.

From all the gas-exchange parameters studied, we focused on the relationship of stomatal conductance with VPD in order to identify environmental and physiological markers that revealed the generalized phenological switch that *H. almeriense* plants experienced. Stomatal conductance showed a strong correlation with VPD (**Figure 6.2**), even stronger than with Ψ_{soil}, suggesting a major importance of VPD in stomatal closure regulation of *H. almeriense*, as reported for several species (Ohsumi et al., 2008; Aliniaeifard and Van Meeteren 2013). Moreover, the response of g_s to the average VPD_{air} was adjusted to a sigmoidal curve (**Figure 6.3A**), which is similar to that found in different gravepine cultivars (*Vitis vinifera*) (Prieto et al., 2010), consisting of a maximum

g_s at mild VPDs and a threshold value determining a linear decrease in g_s, until reaching a minimum value. Using the inflection point calculated in the sigmoidal adjustment from **Figure 6.3A,** we determined an average VPD threshold of 0.93 kPa. In order to prove that desert truffle production is related to the generalized phenological switch, we compared desert truffle production from a 20-year-old orchard with the day of the year at which VPD stably reached this threshold (DOY_{VPDt}). These regression analyses statistically demonstrate that this value (DOY_{VPDt}) explains part of the interannual differences in the production of desert truffle (production) previously discussed in **Chapter V**, and agree with the idea hinted by desert truffle gatherers and farmers who affirm that the years with early summers (early DOY_{VPDt}) are below average years in terms of total truffle yield production.

In order to test this hypothesis in field, we conducted Assay 2, which consisted of applying a basic shadowing device to dampen the increase in VPD that occurs in spring, so the DOY_{VPDt} would occur later. This objective was achieved since the VPD was reduced by 16-18 %, this decrease being greater, the higher the VPD was (**Table 6.3**). However, when the plant gas-exchange parameters and the truffle production were analyzed, this decrease in the VPD, did not translate into differences in the parameters of gas-exchange parameters or in the general plant phenology and desert truffle production (**Figure 6.10; Table 6.4**). The reason to this phenomenon could be the radiation subtracted by the shadowing device. It is widely known that light is an important factor for all the gas-exchange parameters (Walters et al., 2005), and, therefore, the hypothetical improvements caused by the decrease in VPD and irrigation are probably countered by the lack of radiation, especially PAR. Moreover, *H. almeriense* is a heliophilic plant, with a saturation light of photosynthesis around 2000 $\mu mol m^{-2} s^{-1}$ (Morte et al., 2010), meaning that a decrease in radiation will have a high impact on the photosynthetic levels of the plant. The inability to achieve better gas-exchange parameters and a delayed phenology is the probable cause of the lack of differences in desert truffle production between treatments (**Table 6.4**), although an interesting trend was revealed, since the irrigation treatments yielded two-fold more desert truffles and, hence, a greater productivity. Moreover, the differences in total yield between both years also point to the importance to the DOY_{VPDt} as a factor determining desert truffle production (**Figure 6.11**).

In conclusion, mycorrhizal *H. almeriense* desert truffle plants present physiological, morphological and molecular responses to the environmental transition from spring to summer, showing a clear phenological switch. By using VPD-g_s relationship as a marker of the phenological state of the plant, the interannual fluctuations in desert plant production can be partially explained. This marker can be further used as a tool for plantation design (selecting potential places with historically late DOY_{VPDt}), plantation diagnosis, and will allow future basic and applied research to fully understand the relationship between plant phenology and desert truffle production. Furthermore, the first trial of a simple and accessible device to buffer the VPD increase in spring and to relate it to desert truffle production is also reported. This, and the next to come assays, will suppose a great step for desert truffle plantation management.

References

Abdallah MB, Dalila T, Antonella P, Elena DZ, Mauro S, Andrea S, et al. (2018) Unraveling physiological, biochemical and molecular mechanisms involved in olive (*Olea europaea* L. Cv. Chétoui) tolerance to drought and salt stresses. J. Plant. Physiol. 220(November 2017):83–95. https://doi.org/10.1016/j.jplph.2017.10.009.

Alexandersson E, Fraysse L, Sjövall-Larsen S, Gustavsson S, Fellert M, Karlsson M, Johanson U, Kjellbom P (2005) Whole gene family expression and drought stress regulation of aquaporins. Plant Mol. Biol. 59(3):469–84. https://doi.org/10.1007/s11103-005-0352-1.

Aliniaeifard S, Uulke VM (2013) Can prolonged exposure to low VPD disturb the ABA signalling in stomatal guard cells? J. Exp. Bot. 64(12):3551–66. https://doi.org/10.1093/jxb/ert192.

Andrino A, Navarro-Ródenas A, Marqués-Gálvez JE, Morte A (2019) The crop of desert truffle depends on agroclimatic parameters during two key annual perios. *In press: Agronomy for Sustainable Development.*

Badeck FW, Bondeau A, Böttcher K, Doktor D, Lucht W, Schaber J, Sitch S (2004) Responses of spring phenology to climate change. New Phytol. 162(2):295–309. https://doi.org/10.1111/j.1469-8137.2004.01059.x.

Bernal M, Estiarte M, Peñuelas J (2010) Drought advances spring growth phenology of the Mediterranean shrub *Erica multiflora*. Plant Biol. 13(2):252–57. https://doi.org/10.1111/j.1438-8677.2010.00358.x.

Bienert MD, Diehn TA, Richet N, Chaumont F, Bienert GP (2018) Heterotetramerization of plant PIP1 and PIP2 aquaporins is an evolutionary ancient feature to guide PIP1 plasma membrane localization and function. Front. Plant Sci. 9:382. https://doi.org/10.3389/fpls.2018.00382.

Boyer JS (1976) Photosynthesis at low water potentials. Phil. Trans. R. Soc. Lond. B. 273(927): 501–512.

Chang S, Puryear J, Cairney J (1993) A simple and efficient method for isolating RNA from pine trees. Plant Mol. Biol. Reports 11(2):113–116. https://doi.org/10.1007/BF02670468.

Cleland E, Chuine I, Menzel A, Mooney H, Schwartz M (2007) Shifting plant phenology in response to global change. Trends Ecol. Evol. 22(7):357–65. https://doi.org/10.1016/j.tree.2007.04.003.

Corell R (2005) Arctic climate impact assessment. Bulletin of the American Meteorological Society. 86(6):860.

Flexas J, Ribas-Carbó M, Bota J, Galmés J, Henkle M, Martínez-Cañellas S, Medrano H (2006a) Decreased Rubisco activity during water stress is not induced by decreased relative water content but related to conditions of low stomatal conductance and chloroplast CO_2 concentration. New Phytol. 172(1):73–82. https://doi.org/10.1111/j.1469-8137.2006.01794.x.

Flexas J, Bota J, Galmés J, Medrano H, Ribas-Carbó M (2006b) Keeping a positive carbon balance under adverse conditions: responses of photosynthesis and respiration to water stress. Physiol. Plant. 127:343–52. https://doi.org/10.1111/j.1399-3054.2005.00621.x.

Flexas J, Diaz-Espejo A, Gago J, Gallé A, Galmés J, Gulías J, Medrano H (2014) Photosynthetic limitations in Mediterranean plants: A review. Environ. Exp. Bot. 103:12-23. https://doi.org/10.1016/j.envexpbot.2013.09.002.

Galmés J, Ribas-Carbó M, Medrano H, Flexas J (2011) Rubisco activity in mediterranean species is regulated by the chloroplastic CO_2 concentration under water stress. J. Exp. Bot. 62(2):653–65. https://doi.org/10.1093/jxb/erq303.

Gulías J, Cifre J, Jonasson S, Medrano H, Flexas J (2009) Seasonal and interannual variations of gas exchange in thirteen woody species along a climatic gradient in the mediterranean island of Mallorca. Flora-Morphol, Distrib, Funct Ecol Plants. 204(3):169–81. https://doi.org/10.1016/j.flora.2008.01.011.

Gutiérrez A, Morte A, Honrubia M (2003) Morphological characterization of the mycorrhiza formed by *Helianthemum almeriense* Pau with *Terfezia claveryi* Chatin and *Picoa lefebvrei* (Pat.) Maire. Mycorrhiza 13(6):299–307. https://doi.org/10.1007/s00572-003-0236-7.

Guzmán B, Vargas P (2009) Historical biogeography and character evolution of Cistaceae (Malvales) based on analysis of plastid RbcL and TrnL-TrnF sequences. Org. Diversity Evol. 9(2):83–99. https://doi.org/10.1016/j.ode.2009.01.001.

Haase P, Pugnaire FI, Clark SC, Incoll LD (2000). Photosynthetic rate and canopy development in the drought-deciduous shrub *Anthyllis cytisoides*. J Arid Environ. 46(1):79–91. https://doi.org/10.1006/jare.2000.0657.

Honrubia M, Gutiérrez A, Morte A (2001) Desert truffle plantation from southeast Spain. In: Edible Mycorrhizal Mushrooms and Their Cultivation: Proceedings of the Second International Conference on Edible Mycorrhizal Mushrooms. Christchurch, New Zealand. pp 3–5.

Jones HG (1998) Stomatal control of photosynthesis and transpiration. J Exp Bot. 49(Special):387–98. https://doi.org/10.1093/jxb/49.Special_Issue.387.

Kagan-Zur V, Roth-Bejerano N (2008) Desert Truffles. Fungi 1 (Special Issue: Truffles) 1:32–37.

Kovács G, Trappe J (2014) Nomenclatural history and genealogies of desert truffle. In: Kagan-Zur V, Roth-Bejerano N, Sitrit Y, Morte A, eds. Desert Truffles. Phylogeny, Physiology, Distribution and Domestication. Soil Biology, volume 38. Springer-Verlag, Berlin, Heidelberg pp. 57–67. https://doi.org/10.1007/978-3-642-40096-4_2.

Lawlor DW (1995) The effects of water deficit on photosynthesis. In: Smirnoff N, ed. Environment and Plant Metabolism. Flexibility and Acclimation. Oxford, UK: BIOS Scientific Publishers pp. 129–160.

León-Sánchez L, Nicolás E, Goberna M, Prieto I, Maestre FT, Querejeta JI (2018) Poor plant performance under simulated climate change is linked to mycorrhizal responses in a semiarid shrubland. J. Ecol. 00(1):1–17. https://doi.org/10.1111/1365-2745.12888.

Livak KJ, Schmittgen TD (2001) Analysis of relative gene expression data using real-time quantitative PCR and the 2-$\Delta\Delta CT$ method. Methods 25(4):402–408. https://doi.org/10.1006/meth.2001.1262.

Lovisolo C, Secchi F, Nardini A, Salleo S, Buffa R, Schubert A (2007) Expression of PIP1 and PIP2 aquaporins is enhanced in olive dwarf genotypes and is related to root and leaf hydraulic conductance. Physiol. Plant. 130:543-551. https://doi.org/10.1111/j.1399-3054.2007.00902.x

Morte A, Honrubia M (1997) Micropropagation of *Helianthemum almeriense*. In: Bajaj YPS, ed. Biotechnology in Agriculture and Foresty, Vol 40, High-Tech and Micropropagation VI. Springer-Verlag Berlin Heidelberg pp 163–77.

Morte A, Honrubia M, Gutiérrez A (2008) Biotechnology and cultivation of desert truffles. In: Varma A, ed. Mycorrhiza. Springer Berlin Heidelberg pp. 467–483. https://doi.org/10.1007/978-3-540-78826-3_23.

Morte A, Navarro-Ródenas A, Nicolás E (2010) Physiological parameters of desert truffle mycorrhizal *Helianthemun almeriense* plants cultivated in orchards under water deficit conditions. Symbiosis 52(2–3):133–139. https://doi.org/10.1007/s13199-010-0080-4.

Morte A, Andrino A, Honrubia M, Navarro-Ródenas A (2012) Terfezia cultivation in arid and semiarid soils. In: Zambonelli A, Bonito GM, eds. Edible Ectomycorrhizal Mushrooms: Current Knowledge and Future Prospects. Springer-Verlag, Berlin Heidelberg pp. 241–263. https://doi.org/10.1007/978-3-642-33823-6_14.

Morte A, Pérez-Gilabert M, Gutiérrez A, Arenas F, Marqués-Gálvez JE, Bordallo JJ, Rodríguez A, Berná LM, Lozano-Carrillo C, Navarro-Ródenas, A (2017) Basic and pplied research for desert truffle cultivation. In: Varma A, Prasad R, Tuteja N, eds. Mycorrhiza-Ecophysiology, Secondary Metabolites, Nanomaterials. Springer International Publishing pp. 23–24. https://doi.org/10.1007/978-3-319-57849-1_2.

Murcia MA, Martíne-Tomé M, Jiménez AM, Vera AM, Honrubia M, Parras P (2002) Antioxidant activity of edible fungi (truffles and mushrooms): losses during industrial processing. J. Food Prot. 65(10):1614–22. https://doi.org/10.4315/0362-028x-65.10.1614.

Navarro-Ródenas A, Bárzana G, Nicolás E, Carra A, Schubert A, Morte A (2013) Expression analysis of aquaporins from desert truffle mycorrhizal symbiosis reveals a fine-tuned regulation under drought. Mol. Plant Microbe Interact. 26(9):1068–78. https://doi.org/10.1094/MPMI-07-12-0178-R.

Navarro-Ródenas A, Nicolás E, Morte A (2015) Effect of irrigation on desert truffle mycorrhizal plants in field. XXI Reunión de la Sociedad Española de Fisiología Vegetal, Toledo, Spain.

Navarro-Ródenas A, Berná LM, Lozano-Carrillo C, Andrino A, Morte A (2016) Beneficial native bacteria improve survival and mycorrhization of desert truffle mycorrhizal plants in nursery conditions. Mycorrhiza 26(7):769–79. https://doi.org/10.1007/s00572-016-0711-6.

Nilsen ET, Muller WH (1981) Phenology of the drought-deciduous shrub *Lotus scoparius*: climatic controls and adaptive significance. Ecol. Monogr. 51(3):323–41. https://doi.org/10.2307/2937277.

NOAA (2015). National Centers for Environmental Information, State of the Climate: Global Analysis for May, June and July 2015. https://www.ncdc.noaa.gov/sotc/global/201507.

Ohsumi A, Hamasaki A, Nakagawa H, Homma K, Horie T, Shiraiwa T (2008) Response of leaf photosynthesis to vapor pressure difference in rice (*Oryza sativa* L) varieties in relation to stomatal and leaf internal conductance. Plant Prod. Sci. 11(2):184–91. https://doi.org/10.1626/pps.11.184.

Oksanen J, Kindt R, Legendre P, O'Hara B, Stevens MMH, Oksanen MJ, Suggests MASS. (2007). The vegan package. Community ecology package. 10:631-637.

Oliach D, et al. 2019 Las trufas y las turmas. In: SG Mariola, C Rafael and BJ Antonio, eds. Los Productos Forestales no Madereros en España: Del Monte A La Industria. Monografías INIA: Serie Forestal(Madrid: Ministerio de EconomíaIndustria y Competitividad)

Parry MAJ, Keys AJ, Madgwick PJ, Carmo-Silva AE, Andralojc PJ (2008) Rubisco regulation: a role for inhibitors. J. Exp. Bot. 59(7):1569–80. https://doi.org/10.1093/jxb/ern084.

Poorter H, Niinemets U, Poorter L, Wright I, Villar R (2009) Causes and consequences of variation in leaf mass per area (LMA): a meta-analysis. New Phytol 182(3):565–88. http://dx.doi.org/10.1111/j.1469-8137.2009.02830.x.

Prieto JA, Lebon E, Ojeda H (2010) Stomatal behavior of different grapevine cultivars in response to soil water status and air water vapor pressure deficit. J. Int. Sci. Vigne Vin 44(1):9–20. https://doi.org/10.20870/oeno-one.2010.44.1.1459.

Scholander PF, Bradstreet ED, Hemmingsen EA, Hammel HT (1965) Sap pressure in vascular plants. Science 148(3668):339–346. https://doi.org/10.1126/science.148.3668.339.

Walters RG (2005) Towards an understanding of photosynthetic acclimation. J. Exp. Bot. 56(411):435-447. https://doi.org/10.1093/jxb/eri060.

Yaneff A, Sigaut L, Marquez M, Alleva K, Pietrasanta LI, Amodeo G (2014) Heteromerization of PIP aquaporins affects their intrinsic permeability. Proc. Natl. Acad. Sci. USA 111(1):231–36. https://doi.org/10.1073/pnas.1316537111.

Elevated atmospheric CO$_2$ modifies desert truffle mycorrhizal plant flowering and response to water-stress

7.1. Introduction

Atmospheric concentration of carbon dioxide (CO$_2$) have historically fluctuated on planet Earth between 200 and 280 ppm. However, since the Industrial Revolution, this value has been increasing and has reached values of 400 ppm in the current days and will probably increase up to values between 700 and 800 ppm over the next 50 years, depending on anthropogenic emissions and global policies (IPCC, 2018). This increase in atmospheric CO$_2$ concentration will probably be accompanied by increases in average global temperatures and will cause shorter, less frequent and less widespread precipitation eventswhich will result in expansion of drylands (Schlesinger et al., 1990; Huang et al., 2016).

It is known that all these predicted changes will affect the physiology of plants in different ways. Water-stress negatively affects the gas-exchange parameters of plants, such as the net assimilation rate (A$_N$), stomatal conductance (g$_s$) and mesophyll conductance (g$_m$), although to a different extent, and also depending on plant species (Bartels and Sunkar, 2005; Chaves et al., 2009; Flexas et al., 2012). Temperature also affects A$_N$, since high temperatures decrease total carbon gain, by promoting photorespiration rather than photosynthesis, mainly due to decreases in affinity of Rubisco for CO$_2$ (Crafts-Brandner and Salvucci, 2000). Moreover, supra-optimal temperatures also affect mesophyll conductance (Lambers, 2008) and disrupt the proper functioning of the Calvin-cycle (Pastenes and Horton, 1996).

On the other hand, normally, the increase in the concentration of CO$_2$ in the atmosphere affects the plants positively, although great differences can be observed depending on the plant species. Some of the general effects of high concentration of CO$_2$ on the parameters of gas exchange of the plant are decreases in gs, increases in A$_N$ and intrinsic water use efficiency ($_i$WUE) and from no effects to decreases in the maximum carboxylation rate of the Rubisco (V$_{cmax}$) or the maximum rate of electron transport (J$_{max}$) (Ainsworth and Rogers, 2007). The combined effect of CO$_2$ increases and warmer and/or drought conditions has not been studied in depth, since historically, the effects of these different factors have been analyzed separately. The combination of all these factors must be taken into account, since the increased use of water by plants under a rising CO$_2$ atmosphere could reduce predictions of future global warming and drought stress due to climatic change (Swann et al., 2016). Studies such as that carried out by Robredo et al.

(2011) stating that elevated CO_2 improves nitrogen metabolism by increasing photosynthesis and mitigating water-stress, or by Rodrigues et al. (2016) in coffee crops, which concluded that the elevated atmospheric concentration of CO_2 mitigates the negative impact of supra-optimal temperatures, support this idea.

Excess carbon generally results in accumulation of starch and sugar, and it is known that roots are the main organs for starch storage (Loescher et al., 1990; Verdaguer and Ojeda, 2002). It is, then, expectable that the climatic change will also affect the relationship between plants and mycorrhiza. Alberton et al. (2005) reviewed the effects of high atmospheric CO_2 concentration on mycorrhizal systems concluding that, without any other stressful condition, positive responses could be expected in general terms, both for plants and fungi. To sum up, all the changes related to climatic change are expected to alter plant physiology, as well as crop yields, and the positive effects caused by the CO_2 enriched atmosphere may be countered by the negative effects caused mainly by high temperatures and drought (DaMatta et al., 2010).

Desert truffles are a group of edible mycorrhizal fungi that grow in arid and semiarid environments (Kovács and Trappe, 2014). Because of its great flavor, nutritional and antioxidant properties (Murcia et al., 2002; 2003) and because it is cultivable (Honrubia et al., 2001; Morte et al., 2008), *Terfezia claveryi* Chatin is one of the best known and appreciated desert truffles. From the last 20 years, *T. claveryi* cultivation using *Helianthemum almeriense* Pau as host plant has expanded gradually and it is currently considered an alternative crop for arid and semiarid regions (Morte et al., 2017). Furthermore, its adaptation to drylands makes it a crop with a great future, as the potential areas for its cultivation are expected to increase due to climatic change (Schlesinger et al., 1990; Lavee et al., 1998; Huang et al., 2016). According to desert truffle farmers and gatherers, plant phenology plays a crucial role in desert truffle yields, since fungal fructification season usually coincides with flower appearance and it is a deciduous summer plant. Since another of the predicted changes related to climatic change is the advancement of the spring (Badeck et al., 2004; Corell et al., 2005; Cleland et al., 2007), it is important to study how the phenology of *H. almeriense*, especially flowering, will be affected by increases in atmospheric CO_2 concentrations. Although several studies have been carried out on desert truffle plants to understand their physiological and molecular responses to water-stress (Morte et al., 2000; 2010; Navarro-Ródenas et al., 2012; 2013;

Marqués-Gálvez et al., 2019), the effect of a higher concentration of atmospheric CO$_2$ together with water-stress and warming has not yet been assayed.

To the best of our knowledge, the only approach to how the climatic change will affect a similar plant species is the experiments carried out by León-Sánchez et al. (2016; 2018), with *Helianthemum squamatum*. In a manipulative field study, the authors concluded that the combination of warming and reduced irrigation causes decreases in A$_N$ and $_i$WUE, advanced plant phenology and affected mycorrhizal population. Nonetheless, the authors did not take into account how the forecasted increase in atmospheric CO$_2$ concentration will combine with all the predicted changes.

Therefore, the aim of the present work is to study the combined effect of progressive warming and drought, together with the high concentrations of atmospheric CO$_2$ concentrations in *H. almeriense* mycorrhizal plants. For this purpose, we have studied those effects in four different scenarios that mimic four environmental stages in the transition from winter to summer. We hypothesize that the negative effects on *T. claveryi* x *H. almeriense* plants caused by the increase in drought and VPD will be attenuated due to increased atmospheric CO$_2$ concentrations. At the same time, we hypothesize that excess carbon assimilation will result in into a higher sugar content in roots that could be related to increased mycorrhization and further affect desert truffle fructifications.

7.2. Materials and methods

7.2.1. Biological material and experimental procedure

H. almeriense seeds were collected in Zarzadilla de Totana, Lorca, Murcia and germinated according to Morte et al. (2008). Two months after germination, plants were transferred to bigger 230 cc pots, and inoculated with approximately 10^5 *Terfezia claveryi* mature spores, extracted from truffles collected at the same place, which were previously mixed with the new substrate (Morte et al., 2008). After 3 months, a total of 72 mycorrhizal plants were transferred to 24 clay-pots of 12,000 cc (3 plants per pot). Pots containing eight-moth-old mycorrhizal plants were placed in two different growth chambers (36 plants in each chamber) located at "Servicio de Experimentación

Agroforestal" in the University of Murcia (**Figure 7.1**). Temperature (ºC), relative humidity (%), light intensity (lux), photoperiod and CO_2 concentration were controlled in both chambers. Two different treatments were established: "control chamber" (CC) maintained at a CO_2 concentration of 400 ppm during the whole experimental period and "high CO_2 concentration chamber" (HC) maintained at a CO_2 concentration of 800 ppm. For both treatments, different scenarios with different environmental conditions were assayed. We matched these conditions with the transition from winter to summer by mimicking temperature, relative humidity, vapour pressure deficit (VPD), photoperiod and soil water potential (Ψ_{soil}) from January (winter), March (early spring), May (late spring) and July (summer). Environmental data were retrieved from a meteorological station located in La Alberca (Lorca, Spain IMIDA MU62, http://siam.imida.es) from 1999 to 2017 (**Table 7.1**, for detailed environmental design of the chambers see **Table S5** in **Appendix B: Supplementary Tables**). Environmental parameters were automatically controlled, equally for both chambers and registered using SCADA system. At first, mycorrhizal plants were maintained in winter conditions for two weeks, for acclimation purpose. After that, the assay started by maintaining the conditions showed in **Table 7.1** for three weeks each season. All the measurements were made in the same mycorrhizal plants, on the morning of the last day of the third week of the season and during the same day, except for A/Ci curves that were made on two consecutive days due to time constraints. Ψ_{soil} was measured every day with a portable data logger from Watermark tensiometers (Irrometer; Riverside, CA, USA) and irrigation was applied according to the measurements made in order to maintain the values from **Table 7.1** for each season
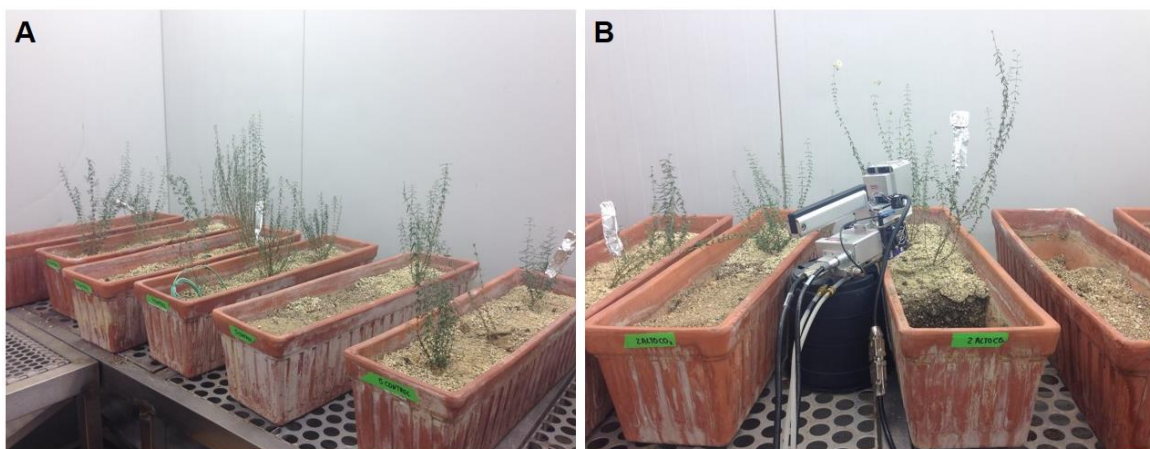
Figure 7.1 (previous page). ***H. almeriense* mycorrhizal plants during the course of the experiment. (A)** Detail of the growth chamber with control *H. almeriense* mycorrhizal plants in clay-pots. **(B)** Gas exchange measurements during summer in high CO_2 plants.

Table 7.1. Environmental data for each treatment and seasonal condition.

	CONTROL CHAMBER (CC)	HIGH [CO$_2$] CHAMBER (HC)
SCENARIO 1: WINTER		
Mean temperature (ºC)	12.64	12.64
Relative humidity (%)	60	60
Mean VPD (kPa)	0.61	0.61
Photoperiod (light/darkness)	10/14	10/14
Average Ψ_{soil} (MPa)	-14.33	-19.33
[CO$_2$] (ppm)	400	800
SCENARIO 2: EARLY SPRING		
Mean temperature (ºC)	14.47	14.47
Relative humidity (%)	60	60
Mean VPD (kPa)	0.80	0.80
Photoperiod (light/darkness)	12/12	12/12
Average Ψ_{soil} (MPa)	-70.44	-53.22
[CO$_2$] (ppm)	400	800
SCENARIO 3: LATE SPRING		
Mean temperature (ºC)	20.95	20.95
Relative humidity (%)	50	50
Mean VPD (kPa)	1.38	1.38
Photoperiod (light/darkness)	14/10	14/10
Average Ψ_{soil} (MPa)	-103.66	-107.57
[CO$_2$] (ppm)	400	800
SCENARIO 4: SUMMER		
Mean temperature (ºC)	27.28	27.28
Relative humidity (%)	50	50
Mean VPD (kPa)	2.04	2.04
Photoperiod (light/darkness)	14/10	14/10
Average Ψ_{soil} (MPa)	-160.4	-160.66
[CO$_2$] (ppm)	400	800

7.2.2. Plant biomass

The entire plant was collected and its aerial part of the plant was separated from the root system. The total dry weight (72h at 60ºC) of the aerial part from each plant was measured in six plants from each chamber, once every season (winter, early spring, late spring and summer). In addition, flower buds and number of flowers per plant were counted in both chambers during the course of the experiment. The root system was separated into two parts for different measurements: fungal colonization and sugars determination.

7.2.3. Leaf morphology and chlorophyll content

For the morphological determinations of the leaves, three leaves were cut per plant from the second and third node from the apex, of six plants per treatment and season and their areas without petiole were measured using image software, ImageJ (https://imagej.net). Then, the leaves were dried at 60 ºC for 72h and their dry weights were measured. Leaf mass per area (LMA) was calculated as the dry weight per area ratio (g m^{-2}). In addition, a non-destructive determination method (Morte and Andrino, 2014) with the help of a SPAD-502 (MINOLTA, Japan) device was used to estimate the total leaf chlorophyll concentration (mg g^{-1}) using in three leaves from each plant and six plants per season and treatment.

7.2.4. Shoot water potential

Shoot water potential (Ψ_{shoot}) was measured in six plants per season and treatment. To this aim, 5-cm-long plant apices were covered with alumminium foil in dark one hour before the measurement, cut and immediately placed in a pressure chamber (Soil Moisture Equipment Co; Santa Barbara, CA, U.S.A.) according to Scholander et al. (1965).

7.2.5. Sugar determination

Free sugars and starch content were determined in roots obtained from six plants per chamber and season, following the protocol of Knudsen (1997). Briefly, roots were pulverized in liquid nitrogen with the help of a pestle and a mortar. 100 mg of pulverized roots were incubated twice in 1 mL 80 % ethanol at 80 ºC for five minutes, cthen centrifuged and the collected supernatant was subsequently used to determine free sugars. Root pellets were rinsed and incubated in 0.1M pH 5.0 acetate buffer with 100 µL of a thermostable α-amylase (53,7 U mg^{-1} from *Bacillus licheniformis*, Sigma Aldrich, San Luis, MO, USA) at 100ºC for one hour in a thermostatic bath. After that, the thermostatic bath was cooled down to 60 ºC, and 200 µL of amyloglucosidase (3260 U mL^{-1}, from "starch assay reagent", Sigma Aldrich; San Luis, MO, USA) was added. The solution was incubated at 60 ºC for two hours, and then the enzyme was inactivated by heating at 100 ºC for fifteen minutes. The free sugars of the supernatant and starch were

determined as glucose equivalents using the glucose oxidase method (Trinder 1969; Lott and Turner 1975) with the QCA sugar determination kit (Química Clínica Aplicada SA, Spain), following manufacturer's instructions. The reaction product was measured at 505 nm in a Shimadzu UV-1700 spectrophotometer (Shimadzu Corporation, Kyoto, Japan) and the resulting data were compared with those of the glucose standard.

7.2.6. Fungal colonization

Total fungal colonization was measured in six plants per chamber and season under an Olympus BH2 microscope, after staining their roots with trypan blue as described in Gutiérrez et al. (2003) (for detailed protocol see **Appendix A: Supplementary protocols**). To calculate the mycorrhization status, 100 secondary and tertiary root sections per sample were observed under the microscope and classified as "mycorrhizal" or "non-mycorrhizal" depending on the presence/absence of *T. claveryi* mycorrizal structures.

7.2.7. Leaf gas exchange and chlorophyll fluorescence measurements

Leaf gas exchange parameters were estimated simultaneously with chlorophyll fluorescence measurements using a portable photosynthesis system (LI-6400, Li-Cor, Inc., Lincoln, NE, USA) equipped with an integrated fluorescence chamber head (Li-6400–40; Li-Cor). Six CO₂ response curves (A_N-C_i curves) of *H. almeriense* leaves, placed in a 2 cm² leaf cuvette, were obtained, once for each treatment and in each season, Due to the small foliar area of this species, several fully expanded leaves were carefully placed in the cuvette and after the measurements they were later collected to measure their area using the image analysis software Image J (www.imagej.com). Measurements were taken at an air flow of 200 μmol s⁻¹, in light-adapted mature leaves at a CO₂ concentration surrounding the shoot (C_a) of 400 μmol⁻¹ for CC plants and 800 μmol⁻¹ for HC plants, and a saturating PPFD (Photosynthetic photon flux density) of 1500 μmol m⁻² s⁻¹. Once the steady-state gas exchange rate was reached under these conditions, net assimilation rate (A_N), transpiration (E), stomatal conductance (g_s) and the effective

quantum yield of photosystem II (PSII) were estimated. Intrinsic water use efficiency (iWUE) was calculated as the ratio between A_N and g_s. Afterwards, C_a was gradually reduced down to 50 µmol mol⁻¹. After completion of measurements at low C_a, it was increased again to 400 or 800 µmol mol⁻¹. Then, C_a was increased stepwise to 1800 µmol mol⁻¹. Leakage of CO_2 in and out of the cuvette was determined for the same range of CO_2 concentrations with a photosynthetically inactive leaf (obtained by heating the leaf until no variable chlorophyll fluorescence was observed) and used to correct measured leaf fluxes (Flexas et al., 2007). The effective photochemical efficiency of photosystem II (ΦPSII) was measured simultaneously with A_N and g_s. For ΦPSII, the steady-state fluorescence (F_S) and the maximum fluorescence during a light-saturating pulse of $\sim$8000 µmol m⁻² s−1 (F`$_M$) were estimated, and ΦPSII was calculated as (F`$_M$ - F_S)/F`$_M$ following the procedures of Genty et al. (1989). The photosynthetic electron transport rate (J_{flu}) was then calculated according to Krall and Edwards (1992), multiplying ΦPSII by PPFD, by the leaf absorptance (the ratio of the absorbed to the incident radiant power) and by 0.5 (because we assumed an equal partitioning of absorbed quanta between photosystems I and II). The actual leaf absorptance was measured simultaneously with the portable photosynthesis system (Valentini et al., 1995).

7.2.8. Estimation of mesophyll conductance by gas exchange and chlorophyll fluorescence

Mesophyll conductance (g_m) was estimated according to the method of Harley et al. (1992), as follows:

$$gm = \frac{A_N}{(C_i - [\frac{\Gamma^*(J_F + 8(A_N + R_L))}{J_F} - 4(A_N + R_L)]}$$

Equation 7.1. Calculation of mesophyll conductance (gm) according to Harley methodology (Harley et al., 1992).

Where A_N and the substomatal CO_2 concentration (C_i) were taken from gas exchange measurements at saturating light, Γ^* (the chloroplastic CO_2 photocompensation

point in the absence of mitochondrial respiration) and R_L (the respiration rate in the light) were taken from Bernacchi et al. (2002).

The values of gm were used to convert A_N-C_i curves into A_N-C_c (chloroplastic CO_2 concentration) using the equation $C_c = C_i - A_N/g_m$. Maximum carboxylation rate (V_{cmax}), maximum electron transport capacity (J_{max}) and triose phosphate use (TPU) were calculated from the A_N-C_c curves, using the Rubisco kinetic constants and their temperature dependencies described by Bernacchi et al. (2002). The Farquhar model was fitted to the data by applying iterative curve fitting (minimum least-square difference) using the Solver tool from Microsoft Excel.

7.2.9. Analysis of partitioning changes in photosynthetic rate

We estimated the different limitations on A_N from stomatal conductance (*ls*), mesophyll conductance (*lm*) and biochemical capacity (*lb*), using the quantitative limitation analysis of Grassi and Magnani (2005) as applied by Tomás et al. (2013). Different fractional limitations, ls, lm and lb (*ls + lm + lb = 1*), were calculated as:

$$ls = \frac{\frac{g_{tot}}{g_s} \times \partial A_N/\partial C_c}{g_{tot} + \partial A_N/\partial C_c}$$

Equation 7.2. Calculation of stomatal limitations (*ls*) according to Grassi and Magnani (2005).

$$lm = \frac{\frac{g_{tot}}{g_m} \times \partial A_N/\partial C_c}{g_{tot} + \partial A_N/\partial C_c}$$

Equation 7.3. Calculation of mesophyll limitations (*lm*) according to Grassi and Magnani (2005).

$$ls = \frac{g_{tot} \times \partial A_N/\partial C_c}{g_{tot} + \partial A_N/\partial C_c}$$

Equation 7.4. Calculation of biochemical limitations (*lb*) according to Grassi and Magnani (2005).

Where g_s is the stomatal conductance to CO_2, g_m is the mesophyll conductance according to Harley et al. (1992; **Equation 7.1**) and g_{tot} is the total conductance to CO_2 from ambient air to chloroplasts (sum of the inverse CO_2 serial conductances gs and gm). $\partial A_N / \partial C_c$ was calculated as the slope of A_N-C_c response curves over a C_c range of 50–100 µmol mol^{-1}. Quantitative limitations of photosynthesis were estimated for at least six different leaves for each species and average estimates of the component photosynthetic limitations were calculated.

7.2.10. Statistical analyses

Statistical analysis (ANOVA, post-hoc Tukey test, Student's t test, normality Saphiro-wilk test and homoscedasticity Levene's test) were performed using R programming language in R studio (Team, 2018).

To visualize the dissimilarities between groups of plants with respect to the seasonal conditions and the treatment, a two-dimensional principal coordinate analysis (PCoA) calculated in a Euclidean dissimilarity matrix was performed. To confirm the effect of the two different factors, a permutational multivariate analysis (perMANOVA) was conducted in the same Euclidean matrix, using the adonis function of the vegan package (Oksanen et al., 2016), and 999 permutations. A post-hoc pairwise analysis with Bonferroni correction was conducted on the perMANOVA results (Martínez-Arbizu, 2017).

7.3. Results

A two-way perMANOVA analysis was applied to look for significant differences between groups of mycorrhizal plants, taking into account all the plant variables at the same time. The results confirmed that the seasonal conditions (F = 22.93, $p < 0.001$) and CO_2 treatment (F = 8.15, $p < 0.001$), as well as their interaction (F = 2.05, $p = 0.028$), significantly influenced the plant behavior, especially in terms of A_N, C_i, C_c, iWUE and V_{cmax} (**Figure 7.2**). The subsequent post-hoc pairwise analysis showed that, when comparing both treatments (CC and HC) there were significant differences between almost all the seasons (**Figure 7.3A**), while within each treatment, the number of

differences between seasons was higher in the HC treatment (4 statistical differences, **Figure 7.3B**) than in CC treatment (2 statistical differences, **Figure 7.3C**).
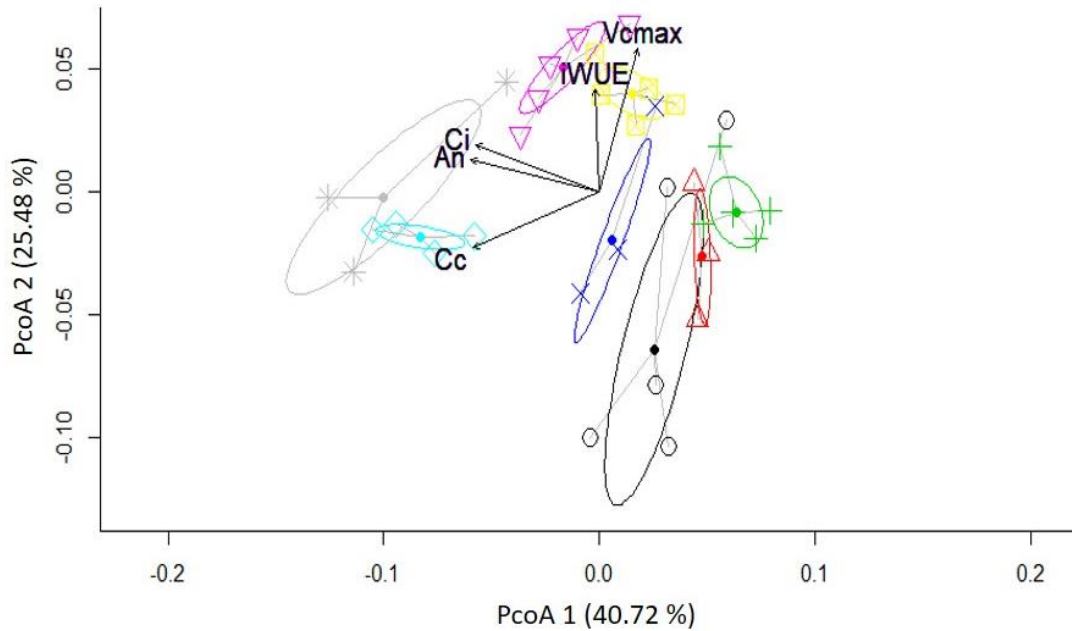
Figure 7.2. Principal coordinate analysis on plant behavior regarding CO₂ treatments and seasonal conditions. The arrows represent the greatest eigenvalues from a larger set of plant variables that better explain the differences in plant behavior across the different conditions. Dark blue = control chamber (CC) winter; black = CC early spring; red = CC late spring; green = CC summer; gray = high CO₂ chamber (HC) winter; light blue = HC early spring; pink = HC late spring; yellow = HC summer.
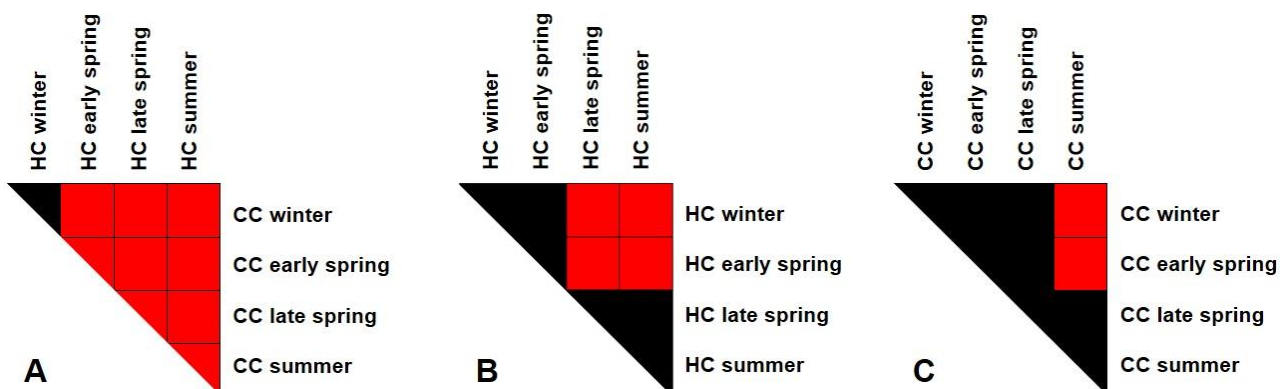
Figure 7.3. Post-hoc pairwise analysis of principal component analysis and perMANOVA from figure 7.1. Cells filled with red color represent significant p values ($p < 0.05$). (**A**) High CO₂ (HC) *vs* control (CC); (**B**) HC *vs* HC; (**C**) CC *vs* CC.

Leaf chlorophyll content was not affected by any of the treatments and/or conditions, while Ψ_{shoot} decreased from winter to summer conditions almost identically in both treatments (**Table 7.2**), and highly correlated with the increase of water-stress (decrease of Ψ_{soil} and increase of VPD) from winter to summer for both treatments (**Figure 7.4**). Plant biomass remained constant during the four scenarios in both treatments and was similar between them, but in summer conditions greater shoot dry weight was observed in HC treatment. Leaf area decreased in both treatments from winter to summer conditions, without differences between treatments. For both treatments, LMA was maximum in winter, decreased in early spring and then, increased gradually until summer (**Table 7.2**). Interestingly, neither floral buttons nor flowers were observed for any of the treatments until summer conditions, when the number of flower buds and flowers per plant was higher for HC treatment (**Table 7.2**).
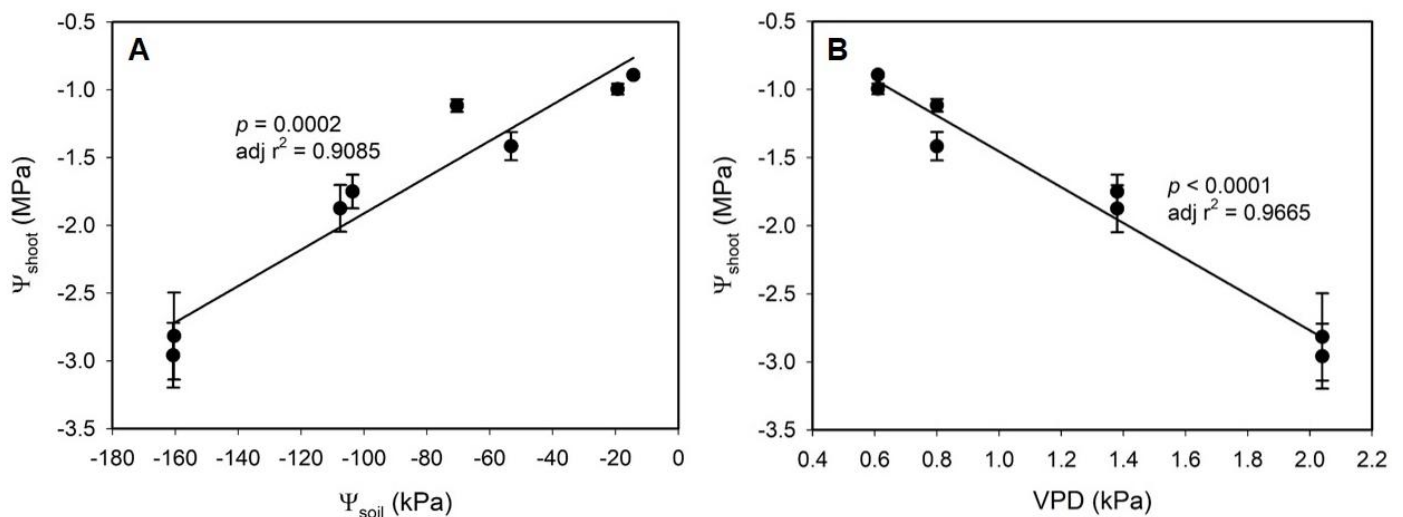
Figure 7.4. Relationships of shoot water potential (Ψ_{shoot}) with soil water potential (Ψ_{shoot}) (A) and vapor pressure deficit (VPD) (B).

Table 7.2. Plant biomass, hydraulic and leaf morphology variables in different seasonal conditions and CO$_2$ treatments. Mean values ± standard error are represented. Different letters represent statistical differences ($p < 0.05$) between seasonal conditions from the same CO$_2$ treatment when a variance analysis (ANOVA) and a Tukey's post-hoc test were performed. Asterisks represent statistical differences ($p < 0.05$) between different CO$_2$ treatments from the same season when a t-test was performed.

	CONTROL				HIGH CO$_2$			
	Winter	Early spring	Late spring	Summer	Winter	Early spring	Late spring	Summer
Shoot dry weight (g)	2.5±0.9a	2.3±0.4a	3.7±1.8a	1.3±0.2a	2.4±0.8a	4.1±1.4a	3.1±0.8a	3.4±0.4a*
Ψ_{shoot} (MPa)	-0.9±0.1a	-1.1±0.1a	-1.8±0.1b	-2.8±0.3c	-1.0±0.1a	-1.4±0.1b*	-1.9±0.2bc	-3.0±0.c
Chlorophyll (mg)	2.6±0.3a	3.2±0.2a	3.1±0.5a	3.1±0.3a	2.5± 0.3a	3.5±0.2b	2.4±0.3a	3.4±0.2b
Leaf area (mm^2)	20±1a	22±3ab	13±1b	16±3b	24±2a	14±1b	11±2b	10±1b
LMA (g m^{-2})	128±7a	45±6c	49±9bc	83±12b	143±12a	69±12c	72±8bc*	96±14b
Plants with flower buds (%)	nd	nd	nd	16	nd	nd	nd	33
Flower buds (per plant)	nd	nd	nd	1	nd	nd	nd	6.83*
Flowers (per plant)	nd	nd	nd	0.33	nd	nd	nd	3.83*

Mycorrhizal *T. claveryi* colonization increased from winter to summer conditions, but no differences were observed in starch and free sugar contents. In addition, no effect on the mycorrhizal status nor sugar content was found between any of the CO$_2$ treatments (CC vs HC) (**Table 7.3**).

Table 7.3. Root colonization and sugar content in different seasonal conditions and CO$_2$ treatments. Mean values ± standard error are represented. Different letters represent statistical differences ($p < 0.05$) between seasonal conditions from the same CO$_2$ treatment when a variance analysis (ANOVA) and a Tukey's post-hoc test were performed. Asterisks represent statistical differences ($p < 0.05$) between different CO$_2$ treatments, from the same season, when a t-test was performed.

	CONTROL				HIGH CO$_2$			
	Winter	Early spring	Late spring	Summer	Winter	Early spring	Late spring	Summer
Mycorrhiza (%)	21.2±3.7a	31.3±3.9a	38.3±7.2ab	46.7±1.8b	24.4±6.7a	26.9±2.7a	44.2±7.0b	39.3±3.6b
Root starch (mM glucose g^{-1})	2.2±0.6a	2.7±0.8a	3.3±0.6a	2.3± 0.1a	3.3±1.1a	2.2± 0.3a	2.5±0.4a	2.2±0.7a
Root free sugars (mM glucose g^{-1})	0.5±0.1a	1.0±0.3a	1.2±0.3a	0.8± 0.1a	0.9±0.2a	1.3± 0.2a	0.83±0.1a	0.8±0.1a

Gas-exchange parameters were highly affected by seasonal conditions and CO_2 treatments (**Table 7.4**). A_N, and gs presented maximum values in winter conditions, and then, decreased until summer conditions, both for CC and HC treatments. In the case of g_s, there were no differences in any condition between CC and HC, while for A_N, C_i and C_c, these values were higher in HC than in CC. The progressive decrease in g_s throughout the seasons supposed a significant increase in iWUE only in HC during early spring, late spring and summer, but not in winter. Unlike g_s, g_m reached its maximum in early spring and then decreased until summer in both treatments, although this appreciated decrease was significant only in CC. Positive correlations were found between A_N, gs and gm (**Figures 7.5A** and **7.5B**), and a good correlation was found at low values of g_s between g_s and g_m, but no correlation was found when taking into account all the data available (including winter) (**Figure 7.5C**). During the course of the seasons, V_{cmax} and TPU remained the same in CC treatment, but increased significantly in HC treatment, while J_{max} was the same in every treatment and condition, although J_{max}/V_{cmax} ratio decreased from winter to summer conditions in both treatments (**Table 7.4**).

Table 7.4. Gas-exchange variables in different seasonal conditions and CO_2 treatments. Mean values are represented $\pm$ standard error. Different letters represent statistical differences ($p < 0.05$) between seasonal conditions from the same CO_2 treatment when a variance analysis (ANOVA) and a Tukey's post-hoc test were performed. Asterisks represent statistical differences ($p < 0.05$) between different CO_2 treatments from the same season when a Student's t-test was performed.

	CONTROL (CC)				HIGH CO₂ (HC)			
	Winter	Early spring	Late spring	Summer	Winter	Early spring	Late spring	Summer
A_N (µmol CO_2 m^{-2} s^{-1})	11.4±0.8a	9.5±1.0ab	6.6±0.5bc	3.9±0.4c	20.6±2.3a*	17.9±0.8ab*	13.0± 1.6bc*	9.2±0.6c*
g_s (mmol H_2O m^{-2} s^{-1})	239± 43a	143± 8b	80± 7bc	55±14c	323±43a	150±20b	75±10bc	436±7c
g_m (mmol H_2O m^{-2} s^{-1})	82.8±4.9ab	139.5±38.2a	77.1±10.9ab	33.17±4.60b	77.1±31.9a	102.7±24.9a	51.1±14.4a	44.0±5.3a
V_{cmax} (µmol m^{-2} s^{-1})	58.8±17.7a	43.5±13.8a	63.3±6.1a	70.8±10.1a	51.2±9.9a	36.6±2.3a	93.5±7.6b*	91.0±7.5b
J_{max} (µmol m^{-2} s^{-1})	98.1±19.5a	86.0±19.6a	93.8±5.6a	89.6±6.5a	111.2±9.1a	91.9± 1.3a	107.2±3.8a	92.1± 4.9a
TPU (µmol m^{-2} s^{-1})	5.0±0.2a	4.7±0.9a	5.7±0.5a	3.4±0.4a	7.5±0.9a	7.0±0.2a	4.9±0.6b	3.4±0.3b
iWUE (µmol mmol^{-1})	51±7a	69±20a	83±7a	79±9a	66±11a	125±11ab*	180±17bc*	231±27c*
C_i (µmol CO_2mol^{-1}air)	301±13a	272±17a	251±10a	254±15a	671±21a*	540±33ab*	476±28bc*	389±24c*
C_c (µmol CO_2mol^{-1}air)	159±25a	181±21a	15765±11a	122±6a	333±92a	350±28ab*	186±20bc	156±6c*
J_{max}/V_{cmax}	1.8±0.2a	2.2±0.2ab	1.5±0.1ab	1.3±0.1b	2.4±0.7a	2.6±0.2a	1.2±0.1b	1.0±0.1b
J_{flu} (µmol m^{-2} s^{-1})	157±27a	118±18a	106±11a	105±6a	161±27a	114±2b	142±5ab	121±4ab
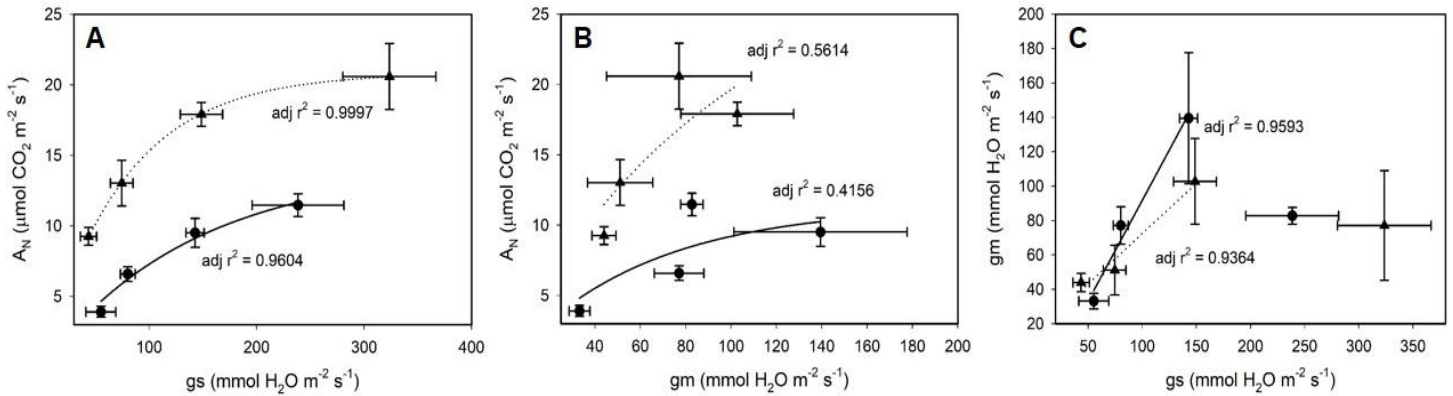
Figure 7.5. The relationship between A$_N$, g$_s$ and g$_m$ in *H. almeriense* mycorrhizal plants under different CO$_2$ treatments and seasonal conditions. Circles represent CC, while triangles represent HC. Data from figures (**A**) and (**B**) were fitted to a single rectangular hyperbola. Data from (**C**) fitted to a linear regression when only values from summer, late spring and early spring were taken into account.

When a two-way ANOVA was performed to the partition analysis on the photosynthetic limitations data, only seasonal influence ($p = 0.00822$), but no influence in the CO$_2$ treatment or the interaction between both factors were found. For both treatments, stomatal limitations increased and mesophyll limitations decreased as the seasonal conditions advanced from winter to summer (**Figure 7.6A**). Furthermore, when all the data were grouped, gs and the stomatal limitations were linearly correlated: the lower the gs, the greater the stomatal limitations (**Figure 7.6B**).
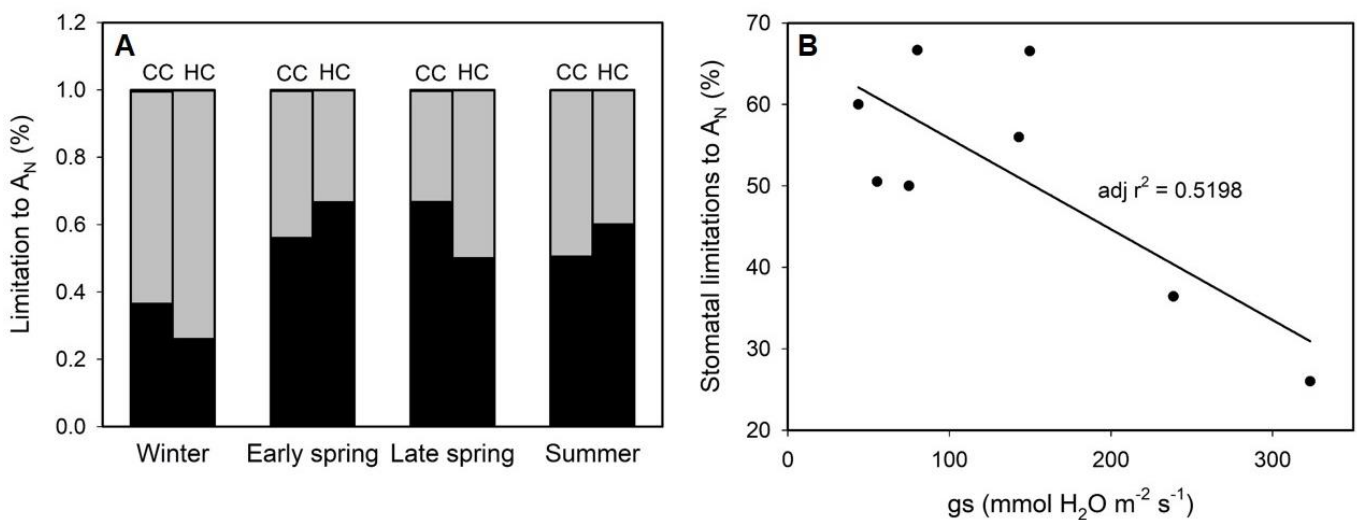
Figure 7.6. Partition analysis on the limitations to A$_N$. (**A**) stomatal (black) and mesophyll (grey) limitations to A$_N$ in every season and CO$_2$ treatment. Biochemical limitations were not represented as they were less than 0.5 % for each condition and treatment. CC = control chamber; HC = high CO$_2$ chamber. (**B**) Relationship between stomatal limitations to A$_N$ and g$_s$.

7.4. Discussion

Multivariate analysis methods, such as principal coordinate analysis (PCoA), allow data to be interpreted as a whole, instead of each variable independently, and together with statistical methods such as perMANONVA and post-hocs analysis, allows to infer statistical differences between groups. CO_2 treatment, the seasonal conditions and their interaction influenced the physiology of the mycorrhizal plant as a whole (**Figure 7.2; 7.3**). From the number of statistical differences within each treatment (**Figure 7.3B**; **7.3C**) it can be inferred that the generalized switch that goes from early to late spring described in **Chapter VI**, will be exacerbated under HC conditions.

As we hypothesized, the increase in atmospheric CO_2 concentrations improves A_N, and, ultimately, the iWUE of *T. claveryi* x *H. almeriense* plants. According to McCarrol et al. (2009), there are two kinds of responses to the increase in atmospheric CO_2 concentrations: active and passive. Active responses consist of an increase in A_N, without an effect or even a decrease in gs, resulting in an enhanced $_i$WUE. This is the most common response among C_3 plants, and is the one observed in *H. almeriense* mycorrhizal plants in this assay. The increase in A_N and $_i$WUE in HC plants only resulted in a greater biomass of shoots during the summer together with an increase in flowering events, but no other parameter, seemed to be affected (**Table 7.**2). These results show that the high concentration of atmospheric CO_2 helps plant cope, at least partially, with the negative effects of the water-stress and warming when these stresses are more severe, as in the summer scenario.

In both treatments, mycorrhization gradually increased from winter to summer (**Table 7.3**), in parallel to the increase in drought stress, a phenomenon that has been previously observed several times before in this particular mycorrhizal association (Navarro-Ródenas et al., 2013; Marqués-Gálvez et al., 2019). The active plant response to HC environment resulted in more carbon being assimilated, but this did not result in an increase in the content of root starch or free sugar or differences in mycorrhization levels for the HC treatment (**Table 7.3**). According to Alberton et al. (2005), a positive response could be expected, but their analysis were carried out with high CO_2 concentrations in absence of any other stressful condition. Everything indicates that the additional carbon assimilation achieved by HC plants could be reflected in increased flowering events, since both the number of flower buds and flowers are greater in HC

treatment (**Table 7.2**). Springer and Ward (2007) reviewed papers about this issue and concluded that the general response to the increase in atmospheric CO_2 concentration was earlier flowering, although unchanging flowering time has also been reported (Springer and Ward, 2007). Moreover, León-Sánchez et al. (2016) also described an earlier phenology under warmer and more water-stressful conditions. It is worth mentioning that during this experiment, flowering started between late spring and summer, while in field conditions this usually occurs in early spring. This temporary difference may be the consequence of shorter times in the chambers, since we simulated the transition between winter and summer (6 months) in just 3 months. This could also be the consequence of the unexpected LMA pattern presented by the plants (**Table 7.2**). In field conditions, an increase in LMA level has been reported (see **Chapter VI**) in parallel to the increase in water-stress conditions, but in this assay we found an initial decrease in LMA followed by a slight increase throughout the assay, for both treatments. Since LMA is known to respond to light (Poorter et al., 2009), the initial decrease may be the result of an adaptation to light in the chambers, and then slowly increases due to the gradual water-stress.

H. almeriense physiology has been studied mainly because of its interest as the host species for the cultivation of *T. claveryi*. These studies have been focused on its adaptation traits to arid environments and its responses to water-stress (Morte et al., 2000; 2010; Navarro-Ródenas et al., 2012; 2013; Marqués-Gálvez et al., 2019). However, due to the technical difficulties involved in the estimation of mesophyll conductance (mainly due to the low leaf size), this is the first time that mesophyll conductance of this species has been studied. In both CO_2 treatments (HC and CC), the maximum in A_N and g_s appears in the winter scenario, but maximum g_m was achieved in the early spring scenario. Based on annual trends, maximum A_N of mediterranean species usually occurs in spring and fall, while minimum values are found in winter and summer (Flexas et al., 2014). It is noteworthy that *H. almeriense* mycorrhizal plants find their maximum values of A_N and g_s during the winter scenario (**Table 7.4**). This has already been observed in the same species in field conditions (Navarro-Ródenas et al., 2015) and in other close species such as *C. albidus* (Gulías et al., 2009). The mild conditions of the winters of the ecological niches of this species could be the main responsible for this phenomenon.

As mentioned before, the maximum g_m was not found in winter, but in the early spring scenario for both treatments (**Table 7.4**) with a value around 140 mmol CO_2 m^{-2} s^{-}

[1] under CC conditions. This results in a dependence between A_N and g_s, and A_N and g_m, but not between g_m and g_s (**Figure 7.5**) overall, although, there is a relationship between g_s and g_m only at low values of gs (below 150 mmol H_2O m^{-2} s^{-1}). When Flexas et al. (2013) analyzed data from 44 species also found poor correlations between these two parameters. It seems that, although gm can be affected by environmental factors such as drought (Warren, 2008; Flexas et al., 2008; Flexas et al., 2012), when it reaches its maximum value (early spring scenario), it cannot increase more probably because of anatomical reasons such as LMA, leaf thickness or mesophyll and chloroplast surface area exposed to intercellular air space per unit of leaf area (*Sc / S*), as it happens in some Mediterranean oaks (Peguero-Pina et al., 2017). In our case, we did not found a clear relation between anatomical features (LMA) and g_m. Although maximum g_m is limited by LMA and it is assumed than the larger LMA, the lower gm, there are more anatomical features that can be playing a role and, therefore, disrupt this relationship between LMA and g_m, such as the cited *Sc / S* (Flexas et al., 2008; Peguero-Pina et al., 2017). Stomatal conductance seems to be determining more the photosynthesis of *H. almeriense* mycorrhizal plants especially when water-stress and temperature increase (**Figure 7.6**), and this limitation is correlated with the stomatal conductance, *i.e.* the more closed the stomas, the higher is the stomatal limitation, similarly to what happens in the rockrose *C. albidus* (Galle et al., 2011). *C. albidus* responded rapidly to the drought by reducing its g_s and maintained it even after re-watering events, while g_m decreased more slowly and more slightly than gs, being the stomatal limitations to photosynthesis more important than the mesophyll limitations. The authors proposed this as an drought adaptation mechanism that may have consequences for the fitness of this species within the frame of climatic change (Galle et al., 2011).

In conclusion, in this manuscript we proved that high CO_2 atmospheric concentrations affect the overall physiological parameters of the symbiosis *H. almeriense* x *T. claveryi* during spring. The improvement in net assimilation and water use efficiency of *H. almeriense* mycorrhizal plants and the fact that mycorrhizal is not affected will help this plant to cope with water-stress when atmospheric CO_2 concentration increases. Therefore, desert truffle cultivation could be a good alternative crop in the near future, since its adaptation to drylands under climatic change conditions will be, at least, as good as at present, and the potential crop areas are expected to increase. However, since the general phenological switch that occurs in spring, and specific phenological events, such

as flowering, that seem to be related to fructifications, are also affected under high atmospheric CO$_2$ concentrations, further field studies using different approaches such as free-air CO$_2$ enrichment experiments need to be explored to obtain further conclusions.

References

Ainsworth EA, Rogers A (2007) The response of photosynthesis and stomatal conductance to rising [CO_2]: mechanisms and environmental interactions. Plant Cell Environ. 30(3):258–70. https://doi.org/10.1111/j.1365-3040.2007.01641.x.

Alberton O, Kuyper TW, Gorissen A (2005) Taking mycocentrism seriously: mycorrhizal fungal and plant responses to elevated CO_2. New Phytol. 167:859-868. https://doi.org/10.1111/j.1469-8137.2005.01458.x.

Badeck FW, Bondeau A, Böttcher K, Doktor D, Lucht W, Schaber J, Sitch S (2004) Responses of spring phenology to climate change. New Phytol. 162(2):295–309. https://doi.org/10.1111/j.1469-8137.2004.01059.x.

Bartels D, Sunkar R (2005) Drought and salt tolerance in plants. Crit. Rev. Plant Sci. 24(1):23-58. https://doi.org/10.1080/07352680590910410.

Bernacchi CJ, Portis AR, Nakano H, von Caemmerer S, Long SP (2002) Temperature response of mesophyll conductance. Implications for the determination of Rubisco enzyme kinetics and for limitations to photosynthesis *in vivo*. Plant Physiol 130:1992–1998. https://doi.org/10.1104/pp.008250.

Chaves MM, Flexas J, Pinheiro C (2009) Photosynthesis under drought and salt stress: regulation mechanisms from whole plant to cell. Ann. Bot. 103(4):551-560. https://doi.org/10.1093/aob/mcn125.

Cleland E, Chuine I, Menzel A, Mooney H, Schwartz M (2007) Shifting plant phenology in response to global change. Trend Ecol. Evol. 22(7):357–65. https://doi.org/10.1016/j.tree.2007.04.003.

Corell R (2005) Arctic climate impact assessment. Bulletin of the American Meteorological Society. 86(6):860.

Crafts-Brandner SJ, Salvucci ME (2000) Rubisco activase constrains the photosynthetic potential of leaves at high temperature and CO_2. Proc. Natl. Acad. Sci. USA 97(24):13430-13435. https://doi.org/10.1073/pnas.230451497.

DaMatta, FM, Grandis A, Arenque BC, Buckeridge MS (2010) Impacts of climate changes on crop physiology and food quality. Food. Res Int. 43(7):1814-1823. https://doi.org/10.1016/j.foodres.2009.11.001.

Flexas J, Díaz-Espejo A, Berry JA, Galmés J, Cifre J, Kaldenhoff R, Medrano H, Ribas-Carbó M (2007) Analysis of leakage in IRGA's leaf chambers of open gas exchange systems: quantification and its effects in photosynthesis parameterization. J. Exp. Bot. 58:1533–1543. https://doi.org/10.1093/jxb/erm027.

Flexas J, Ribas-Carbó M, Diaz-Espejo A, Galmés J, Medrano H (2008) Mesophyll conductance to CO_2: current knowledge and future prospects. Plant Cell Environ. 31:602–621. https://doi.org/10.1111/j.1365-3040.2007.01757.x.

Flexas J, Barbour MM, Brendel O, Cabrera HM, Carriquí M, Diaz-Espejo A, et al. (2012) Mesophyll diffusion conductance to CO_2: an unappreciated central player in photosynthesis. Plant Sci. 193:70-84. https://doi.org/10.1016/j.plantsci.2012.05.009.

Flexas J, Niinemets Ü, Gallé A, Barbour MM, Centritto M, Diaz-Espejo A, et al. (2013) Diffusional conductances to CO_2 as a target for increasing photosynthesis and photosynthetic water-use efficiency. Photosynth Res. 117(1-3):45-59. https://doi.org/10.1007/s11120-013-9844-z.

Flexas J, Diaz-Espejo A, Gago J, Gallé A, Galmés J, Gulías J, Medrano H (2014) Photosynthetic limitations in Mediterranean plants: A review. Environ. Exp. Bot. 103: 12-23. https://doi.org/10.1016/j.envexpbot.2013.09.002.

Galle A, Florez-Sarasa I, Aououad HE, Flexas J (2011) The Mediterranean evergreen *Quercus ilex* and the semi-deciduous *Cistus albidus* differ in their leaf gas exchange regulation and acclimation to repeated drought and re-watering cycles. J. Exp. Bot. 62(14):5207-5216. https://doi.org/10.1093/jxb/err233.

Genty B, Briantais JM, Baker NR (1989) The relationship between the quantum yield of photosynthetic electron transport and quenching of chlorophyll fluorescence. Biochim. Biophys. Acta 990:87–92. https://doi.org/10.1016/S0304-4165(89)80016-9

Grassi G, Magnani F (2005) Stomatal, mesophyll conductance and biochemical limitations to photosynthesis as affected by drought and leaf ontogeny in ash and oak trees. Plant Cell Environ. 28(7):834-849. https://doi.org/10.1111/j.1365-3040.2005.01333.x.

Gulías J, Cifre J, Jonasson S, Medrano H, Flexas J (2009) Seasonal and interannual variations of gas exchange in thirteen woody species along a climatic gradient in the mediterranean island of Mallorca. Flora-Morphology, Distribution, Functional Ecology of Plants 204(3):169–81. https://doi.org/10.1016/j.flora.2008.01.011.

Gutiérrez A, Morte A, Honrubia M (2003) Morphological characterization of the mycorrhiza formed by *Helianthemum almeriense* Pau with *Terfezia claveryi* Chatin and *Picoa lefebvrei* (Pat.) Maire. Mycorrhiza 13(6):299–307. https://doi.org/10.1007/s00572-003-0236-7.

Harley PC, Loreto F, Marco G Di, Sharkey TD (1992) Theoretical considerations when estimating the mesophyll conductance to CO2 flux by analysis of the response of photosynthesis to CO₂. Plant Physiol. 98:1429–1436. https://doi.org/10.1104/pp.98.4.1429.

Honrubia M, Gutiérrez A, Morte A (2001) Desert truffle plantation from southeast Spain. In: Edible Mycorrhizal Mushrooms and Their Cultivation: Proceedings of the Second International Conference on Edible Mycorrhizal Mushrooms. Christchurch, New Zealand pp 3–5.

Huang J, Haipeng Y, Guan X, Wang G, Guo R (2016) Accelerated dryland expansion under climate change. Nat. Clim Change 6(2):166–71. https://doi.org/10.1038/nclimate2837.

Knudsen, KEB (1997) Carbohydrate and lignin contents of plant materials used in animal feeding. Anim. Feed Sci. Technol. 67(4):319-338. https://doi.org/10.1016/S0377-8401(97)00009-6.

Kovács G, Trappe J (2014) Nomenclatural history and genealogies of desert truffle. In: Kagan-Zur V, Roth-Bejerano N, Sitrit Y, Morte A, eds. Desert Truffles. Phylogeny, Physiology, Distribution and Domestication. Soil Biology, volume 38. Springer-Verlag, Berlin, Heidelberg pp. 57–67. https://doi.org/10.1007/978-3-642-40096-4_2.

Krall JP, Edwards GE (1992) Relationship between photosystem II activity and CO₂ fixation in leaves. Physiol. Plant. 86(1):180-187. https://doi.org/10.1111/j.1399-3054.1992.tb01328.x.

Lambers H, Chapin FS III, Pons JL (2008) Plant Physiological Ecology, 2nd edn. Springer-Verlag, New York.

Lavee H. Imeson AC, Sarah P (1998) The impact of climate change on geomorphology and desertification along a mediterranean-arid transect. Land Degradation and development 9(5):407–422. https://doi.org/10.1002/(SICI)1099-145X(199809/10)9:5<407::AID-LDR302>3.0.CO;2-6.

León-Sánchez L, Nicolás E, Nortes PA, Maestre FT, Querejeta JI (2016) Photosynthesis and growth reduction with warming are driven by nonstomatal limitations in a Mediterranean semiarid shrub. Ecol. Evol. 6 (9): 2725-2738. https://doi.org/10.1002/ece3.2074.

León-Sánchez L, Nicolás E, Goberna M, Prieto I, Maestre FT, Querejeta JI. (2018) Poor plant performance under simulated climate change is linked to mycorrhizal responses in a semi-arid shrubland. J. Ecol. 106(3):960-976.

Loescher WH, McCamant T, Keller JD (1990) Carbohydrate reserves, translocation, and storage in woody plant roots. HortScience. 25(3):274-281.

Lott JA, Turner K (1975) Evaluation of Trinder's glucose oxidase method for measuring glucose in serum and urine. Clin Chem. 21:1754–1760.

Marqués-Gálvez JE, Morte A, Navarro-Ródenas A, García-Carmona F, Pérez-Gilabert M (2019) Purification and characterization of *Terfezia claveryi* TcCAT-1, a desert truffle catalase upregulated in mycorrhizal symbiosis. PloS One. 14(7):e0219300. https://doi.org/10.1371/journal.pone.0219300.

Martínez-Arbizu, P (2017). Pairwise Adonis: Pairwise multilevel comparison using Adonis. R package version 0.0.1. https://github.com/pmartinezarbizu/pairwiseAdonis

IPCC (2018) Global warming: Summary for Policymakers. https://report.ipcc.ch/sr15/pdf/sr15_spm_final.pdf.

McCarroll D, Gagen MH, Loader NJ, Robertson I, Anchukaitis KJ, Los S, et al. (2009) Correction of tree ring stable carbon isotope chronologies for changes in the carbon dioxide content of the atmosphere. Geochim. Cosmochim. Acta 73(6)1539-1547. https://doi.org/10.1016/j.gca.2008.11.041.

Morte A, Lovisolo C, Schubert A (2000) Effect of drought stress on growth and water relations of the mycorrhizal association *Helianthemum almeriense-Terfezia claveryi*. Mycorrhiza. 10(3):115–119. https://doi.org/10.1007/s005720000066.

Morte A, Honrubia M, Gutiérrez A (2008) Biotechnology and cultivation of desert truffles. In: Varma A, ed. Mycorrhiza. Springer Berlin Heidelberg pp. 467–483. https://doi.org/10.1007/978-3-540-78826-3_23.

Morte A, Navarro-Ródenas A, Nicolás E (2010) Physiological parameters of desert truffle mycorrhizal *Helianthemun almeriense* plants cultivated in orchards under water deficit conditions. Symbiosis 52(2–3):133–139. https://doi.org/10.1007/s13199-010-0080-4.

Morte A, Andrino A (2014) Domestication: preparation of mycorrhizal seedlings. In: Kagan-Zur V, Roth-Bejerano N, Sitrit Y, Morte A, eds. Desert Truffles. Phylogeny, Physiology, Distribution and Domestication. Soil Biology, volume 38. Springer-Verlag, Berlin, Heidelberg pp. 345–365. https://doi.org/10.1007/978-3-642-40096-4_21

Morte A, Pérez-Gilabert M, Gutiérrez A, Arenas F, Marqués-Gálvez JE, Bordallo JJ, Rodríguez A, Berná LM, Lozano-Carrillo C, Navarro-Ródenas, A (2017) Basic and applied research for desert truffle cultivation. In: Varma A, Prasad R, Tuteja N, eds. Mycorrhiza-Ecophysiology, Secondary Metabolites, Nanomaterials. Springer International Publishing pp. 23–24. https://doi.org/10.1007/978-3-319-57849-1_2.

Murcia, MA, Martíne-Tomé M, Jiménez AM, Vera AM, Honrubia M, and Parras P (2002) Antioxidant activity of edible fungi (truffles and mushrooms): losses during industrial processing. J. Food Prot. 65:(10):1614–22. https://doi.org/10.4315/0362-028x-65.10.1614.

Murcia MA, Martínez-Tomé M, Vera A, Morte A, Gutierrez A, Honrubia M, Jiménez AM (2003) Effect of industrial processing on desert truffles *Terfezia claveryi* Chatin and *Picoa juniperi* Vittadini: proximate composition and fatty acids. J. Sci. Food Agric. 83(6):535-541. https://doi.org/10.1002/jsfa.1397.

Navarro-Ródenas A, Pérez-Gilabert M, Torrente P, Morte A (2012) The role of phosphorus in the ectendomycorrhiza *continuum* of desert truffle mycorrhizal plants. Mycorrhiza 22(7): 565-575. https://doi.org/10.1007/s00572-012-0434-2.

Navarro-Ródenas A, Bárzana G, Nicolás E, Carra A, Schubert A, Morte A (2013) Expression analysis of aquaporins from desert truffle mycorrhizal symbiosis reveals a fine-tuned regulation under drought. Mol. Plant Microbe Interact. 26(9):1068–78. https://doi.org/10.1094/MPMI-07-12-0178-R.

Navarro-Ródenas A, Nicolás E, Morte A (2015) Effect of irrigation on desert truffle mycorrhizal plants in field. XXI Reunión de la Sociedad Española de Fisiología Vegetal, Toledo, Spain.

Oksanen J, Blanchet FG, Friendly M, Kindt, P, Legendre P, McGlinn D, et al. (2016) Vegan: community ecology package. R version 3.2. 4. https://cran.r-project.org/web/packages/vegan/index.html.

Pastenes C, Horton H (1996) Effect of high temperature on photosynthesis in beans (II. CO$_2$ assimilation and metabolite contents). Plant Physiol. 112:1253–1260. https://doi.org/10.1104/pp.112.3.1253.

Peguero-Pina JJ, Sisó S, Flexas J, Galmés J, García-Nogales A, Niinemets Ü, et al. (2017). Cell-level anatomical characteristics explain high mesophyll conductance and photosynthetic capacity in sclerophyllous Mediterranean oaks. New Phytol. 214(2):585-596. https://doi.org/10.1111/nph.14406.

Poorter H, Niinemets U, Poorter L, Wright I, Villar R (2009) Causes and consequences of variation in leaf mass per area (LMA): a meta-analysis. New Phytol. 182(3):565–88. http://dx.doi.org/10.1111/j.1469-8137.2009.02830.x.

Robredo A, Pérez-López U, Miranda-Apodaca J, Lacuesta M, Mena-Petite A, Muñoz-Rueda A (2011) Elevated CO$_2$ reduces the drought effect on nitrogen metabolism in barley plants during drought and subsequent recovery. Env. Exp. Bot. 71(3):399-408. https://doi.org/10.1016/j.envexpbot.2011.02.011.

Rodrigues WP, Martins MQ, Fortunato AS, Rodrigues AP, Semedo JN, Simões-Costa MC, et al. (2016) Long-term elevated air [CO$_2$] strengthens photosynthetic functioning and mitigates the impact of supra-optimal temperatures in tropical *Coffea arabica* and C. canephora species. Global Change Biol. 22(1):415-431. https://doi.org/10.1111/gcb.13088.

Schlesinger WH, Reynolds JF, Cunningham GL, Laura F, Jarrell WM, Virginia RA, et al. (1990) Biological feedbacks in global desertification conceptual models for desertification. Science 247(4946): 1043–1048. https://doi.org/10.1126/science.247.4946.1043.

Scholander PF, Bradstreet ED, Hemmingsen EA, Hammel H (1965) Sap pressure in vascular plants. Science 148:339–346. https://doi.org/10.1126/science.148.3668.339.

Springer CJ, Ward JK (2007) Flowering time and elevated atmospheric CO$_2$. New Phytol. 176(2):243-255. https://doi.org/10.1111/j.1469-8137.2007.02196.x

Swann, ALS, Hoffman FM, Koven CD, Randerson JT (2016) Plant responses to increasing CO_2 reduce estimates of climate impacts on drought severity. Proc. Natl. Acad. Sci. USA 113(36):10019–24. https://doi.org/10.1073/pnas.1604581113.

Team RC (2018). R: A language and environment for statistical computing. R Foundation for Statistical Computing; Vienna, Austria.

Tomás M, Flexas J, Copolovici L, Galmés J, Hallik L, Medrano H, et al. (2013) Importance of leaf anatomy in determining mesophyll diffusion conductance to CO_2 across species: quantitative limitations and scaling up by models. J. Exp. Bot. 64(8):2269-2281. https://doi.org/10.1093/jxb/ert086.

Trinder P (1969) Determination of glucose concentration in the blood. Ann. Clin. Biochem. 6:24–27.

Valentini R, Epron D, De Angelis P, Matteucci G, Dreyer E (1995) *In situ* estimation of net CO2 assimilation, photosynthetic electron flow and photorespiration in Turkey oak (*Q. cerris* L.) leaves: diurnal cycles under different levels of water supply. Plant Cell Environ. 18:631–640. https://doi.org/10.1111/j.1365-3040.1995.tb00564.x.

Verdaguer D, Ojeda F (2002) Root starch storage and allocation patterns in seeder and resprouter seedlings of two Cape *Erica* (*Ericaceae*) species. Am. J. Bot. 89(8):1189-1196. https://doi.org/10.3732/ajb.89.8.1189.

Warren CR (2008) Stand aside stomata, another actor deserves centre stage: the forgotten role of the internal conductance to CO_2 transfer. J. Exp. Bot. 59(7):1475-1487. https://doi.org/10.1093/jxb/erm245

.

C H A P T E R

VIII

General discussion

Throughout the different chapters of this thesis, several main aspects related to the formation of mycorrhiza, biological adaptations to arid environments, response to water-stress, and the cultivation of *T. claveryi* in the the mycorrhizal symbiosis between *H. almeriense* and *T. claveryi* have been addressed.

8.1. On mycorrhizal symbiosis

Mycorrhizal fungi are still relatively unknown compared to other types of fungi such as pathogens or saprophytes, mainly because their dependence on the host plant makes it difficult to study their entire life cycle (Murat et al., 2008). Therefore, the most critical step in the life cycle of mycorrhizal fungi is the formation of the symbiosis. The mechanisms underlying this process have been studied primarily in AM and ECM, where it is known to consist of a bidirectional interaction between plants and fungi involving several molecules and signaling methods. There are several singularities and differences between AM and ECM. While molecules of plant origin, such as flavonoids, cutin and strigolactones, are important molecules for AM, the relevance and involvement of these or other molecules is still largely unknown for ECM. With regard to molecules of fungal origin, once again, the involvement of molecules such as lipo-chitooligosaccharides in AM has been reported, but it is still unknown whether they play a role or not in the ECM. The release of different volatile compounds such as sesquiterpenes and hormones such as auxins, ethylene and cytokinins, stimulates root development and, therefore, leads to a larger surface area to colonize in ECM. One thing in common is the presence of small secreted proteins (SSPs) that act as effectors for mycorrhizal symbiosis, both in AM (Koppholz et al., 2011) and in ECM (Plett et al., 2011) (Bonfante and Genre, 2015; Pellegrin et al., 2019a).

Knowledge about EEM, and more specifically about the mycorrhizal symbiosis established by desert truffles, is still poor, and in fact, EEM and ECM have traditionally been included in the same bag, suggesting that both have similar mechanisms for mycorrhizal symbiosis. In this thesis, we have revealed that the genomic features related to the symbiosis for EEM desert truffles are, in fact, similar to other features of ECM and AM previously reported, that is, the expansion of genome size accompanied by expansion on TE content, on orphan SSPs and a reduced set of PCWDE and CAZymes. In addition,

the number of genes encoding proteins related to secondary metabolism is low and in *T. claveryi* and other desert truffles it is similar to ECM *Tuberaceae*. Thanks to the genomic and transcriptomic assays carried out in **Chapter IV,** we have revealed the traits that compose the "desert truffle symbiosis toolkit". These features are similar to those described for ECM and AM, but it has some singularities such as, lower number of transposons, transporters or pectin targeting enzymes that are related to the arid environments inhabited by these species and to the EEM lifestyle (**Figure 8.1**).
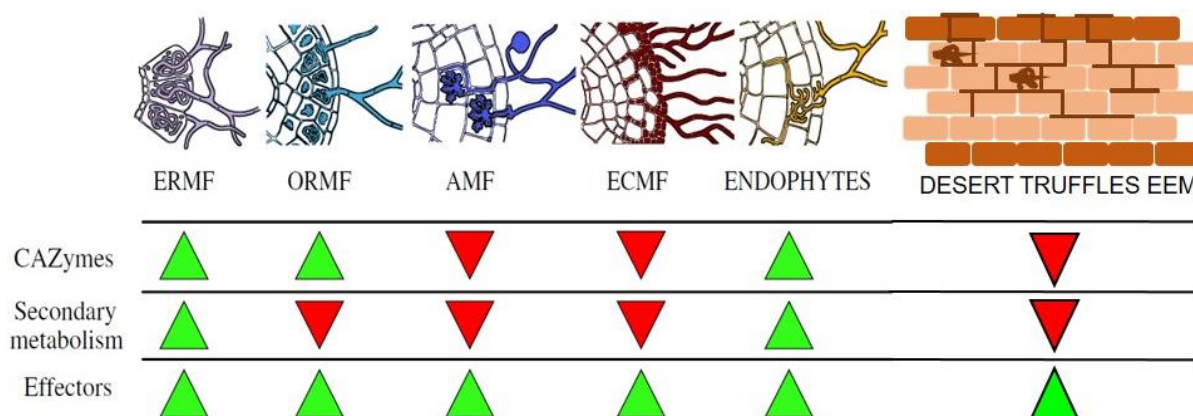
Figure 8.1. Schematic representation of important genomic features of mycorrhizal fungi and root endophytes, including desert truffles ectendomycorrhizal (EEM) fungi. Green and red arrows indicate either high or low abundance, respectively, for carbohydrate-active enzymes (CAZymes), secondary metabolism enzymes and effector encoding genes. ERMF = ericoid mycorrhizal fungi; ORMF = orchid mycorrhizal fungi; AMF = arbuscular mycorrhizal fungi; ECMF = ectomycorrhizal fungi. Figure adapted from Perotto et al. (2018).

In **Chapter IV**, a list of SSPs coding genes is proposed that, based on their upregulation in mycorrhizal tissue and in their unique presence in one or more desert truffles, are candidates to play a role in the mycorrhization of desert truffles (**Table 8.1**; **Figure 4.9**). As was previously the case with *Laccaria bicolor* MiSSP7 and MiSSP8 (Plett et al., 2011; 2014; Pellegrin et al., 2019b), or *Rhizophagus irregularis* SP7 (Kloppholz et al., 2011), the identification of the putative genes reported in this thesis could open the way for their future functional analysis, which could eventually lead to the understanding of this mycorrhizal symbiosis. Of all SSPs upregulated in *T. claveryi* x *H. almeriense* symbiosis, most of them (23 out of 27) are specific for desert truffles. A question that arises from **Table 8.1** is whether different host species will trigger the

upregulation of different effectors, and if the shared effectors are the result of sharing the same or very similar environments and hosts.

Table 8.1. List of candidate effectors to play a role in mycorrhizal symbiosis in *Terfezia claveryi* and homologs occurrence in other desert truffles.

Protein ID	Log2 fold-change in mycorrhiza	Interpro description	Homologs found in
1327700	2.66	Unknown	Tercla, Terbo, Tirniv and Kalpfe
1219779	4.52	Unknown	Tercla, Terbo, Tirniv and Kalpfe
1267151	4.66	Unknown	Tercla, Terbo, Tirniv and Kalpfe
1146117	3.56	Unknown	Tercla, Terbo, Tirniv and Kalpfe
1276641	4.26	Extracellular membrane protein, CFEM domain	Tercla, Terbo, Tirniv and Kalpfe
1142343	7.27	Unknown	Tercla, Terbo, Tirniv and Kalpfe
1140457	10.34	Protein of unknown function DUF4360	Tercla, Terbo, Tirniv and Kalpfe
1206964	8.63	Toxin 7	Tercla, Terbo, Tirniv
1276430	2.29	Unknown	Tercla, Terbo, Tirniv
1275594	5.45	Unknown	Tercla, Terbo, Tirniv
1241082	2.63	Unknown	Tercla, Terbo, Tirniv
1198056	4.20	Unknown	Tercla, Terbo, Tirniv
1204750	7.54	Unknown	Tercla, Terbo, Tirniv
489744	2.68	Unknown	Tercla, Terbo, Tirniv
1261819	5.35	Unknown	Tercla, Terbo, Tirniv
1272874	5.09	Unknown	Tercla, Terbo
1334622	5.71	Unknown	Tercla, Terbo
815809	7.59	Unknown	Tercla
696493	5.53	Unknown	Tercla
893313	3.71	Unknown	Tercla
1162621	2.54	Unknown	Tercla
320365	2.43	Unknown	Tercla
652145	2.05	Unknown	Tercla
1249596	10.25	Isochorismatase family	13 fungi
1189130	3.83	Ribotoxin	13 fungi
1085964	9.29	Ubiquitin 3 binding protein But2 C-terminal domain	13 fungi
1088250	2.63	Domain of unknown function (DUF4360)	13 fungi

As **Figure 4.10** shows, in symbiosis between *H. almeriense* and *T. claveryi*, from the fungal side, only two enzymes targeting the plant´s cell wall were upregulated: AA9 and CE8. With such a limited set of PCWDE upregulated in symbiosis, the question arises on how fungi are able to make space between the root cells to form the mycorrhizal

structure. One possibility may be that the plant is the main responsible for the remodeling of the cell wall, but, from the plant side, almost no enzymes upregulated in symbiosis have been found that could fulfill this purpose (**Figure 4.8**). Another option may lie in the importance of auxins and the "acid-growth theory". Indole-3-acetic acid (IAA) is considered one of the most important signaling molecules in the plant-fungus interaction (Barker and Tagu, 2000). Low amounts of IAA may be of importance in loosening plant cell wall (PCW) to accommodate the fungal partner. "Acid-growth theory" explains the loosening of the PCW at low pH (Majda & Robert, 2018; Rayle & Cleland, 1972). In plants, it has been shown that acid growth is promoted by auxins: directly, as a weak acid (Rayle & Cleland, 1972), by activating acidifying proteins such as proton pumps or potassium channels (Takahashi et al., 2012) and/or activating genes related to PCW biosynthesis, as expansins (Cosgrove, 2000), cellulose and xyloglucan modification genes (Cosgrove, 2005) and/or pectin methylesterases (Wakabayashi et al., 2000).

Tryptophan is considered the main precursor for the synthesis of IAA in plants. IAA is mainly synthetized *via* indole-3-piruvic acid (IPA) (Zhao et al., 2002), while bacteria can synthetize IAA using indole-3-acetadomide (IAM) as an intermediate (Patten and Glick, 1996). The routes of synthesis of IAA in fungi are poorly characterized. In *Ustilago maydis*, the genes involved in the IPA pathway have been isolated and characterized (Reineke et al., 2008); similarly, the genes of the IAM pathway in *Fusarium* species have been also identified and functionally characterized (Tsavkelova et al., 2012). On the other hand, in *Colletotrichum gleosporides,* IAA is synthesized primarily through the IAM pathway (Robinson et al., 1998). To date, no route of synthesis of IAA has been characterized in mycorrhizal fungi. There have been no previous studies regarding the role of in *T. claveryi*, but studies in the proximate species *Terfezia boudieri* (which also forms EEM) showed that IAA induces horizontal root development (Turgeman et al., 2015). In addition, auxins, in combination with phosphorous content, determines the type of mycorrhiza formed *in vitro*: ecto or endo (Zaretsky et al., 2006). In *T. claveryi*, two L-aminoacid oxygenases (E.C. 1.4.3.2) (protein IDs 281043 and 1227268), enzymes potentially responsible of the oxidative deamination of tryptophan to IPA, and an amidase (E.C. 3.5.1.4) (ID 1102465), potentially responsible of IAM transformation to IAA, are upregulated in symbiosis. These two enzymes are part of the two different IAA biosynthesis routes (IPA and IAM pathways), in principle, incomplete in *T. claveryi*, since there are no genes in the genome that encode the rest of enzymes. In addition, one

auxin efflux carrier (ID 1084486) is induced not only during symbiosis but also in DS *vs* WW, when the conditions favor endomycorrhizal relationships. In the future, special attention should be given to these enzymes and transporters to understand how *T. claveryi* biosynthesizes and transports IAA and the role of this hormone as a plant cell wall loosening agent, both in the mycorrhization process and in the switch between inter and intracellular structures.

Expansins (EXPNs) are extracellular proteins also related to the "acid-growth theory", since they induce pH-dependent plant cell wall loosening (Cosgrove, 2000). Plant expansins have been shown to have a role in AM colonization, accumulating in PCW and the interface zone between fungal cell wall (FCW) and PCW (Balestrini et al., 2005). In addition, in *L. bicolor* the role of fungal expansin-related genes in mycorrhization was studied, and localization assays showed a putative role of these enzymes in FCW, although some expansins were also located in PCW (Veneault-Fourrey et al., 2014). There is an EXPN gene upregulated in *T. claveryi* symbiosis (ID 1083860), suggesting a role in mycorrhization. Whether this protein acts in PCW, FCW or in the interface zone in the case of intracellular colonization, should be elucidated by functional assays.

Therefore, molecules related to the "acid-growth theory" induced in *T. claveryi* symbiosis should be taken into account when studying the effects of this fungus in the host PCW, especially in EEM symbiosis, where it seems that the PCWDE role may not be as important in mycorrhizal accommodation as in ericoid or orchid mycorrhizae, or even ECM (**Figure 4.10A**).

In **Chapter III**, we found, purified and characterized a catalase, TcCAT-1, which was upregulated in mycorrhizal symbiosis. However, according to the results of RNA-seq reported in **Chapter IV**, the gene encoding this enzyme, was not found to be equally upregulated, since while qPCR found a 14-fold upregulation (Chapter III), only a 2-fold upregulation was found by RNA-seq, a change that is below the 4 fold-change threshold established to consider significant upregulation. Since the results are from independent assays and obtained using different techniques these inconsistencies may be reasonable. The upregulation of the genes involved in the biotic stress response from the plant side (**Figure 4.8**) reveals a possible defense mechanisms of the host plant against the colonization by the mycorrhizal fungus; in this sense, the upregulation of *TcCAT-1* (**Figure 3.9**), together with the upregulation of several effectors (**Figure 4.9; Table 8.1**),

oxidorreductases and stress response genes from the fungal side (**Figure 4.8**) could represent the fungal strategies to ignore those plant responses and ensure a successful mycorrhization.

8.2. On water-stress responses and adaptation to arid environments

Drought stress plays an essential role in the biology of *T. claveryi*. This species is well-adapted to dry conditions, since it grows better under a moderate drought stress (Navarro-Ródenas et al., 2012). It is known that *T. claveryi* symbiosis brings several benefits to the water-stress tolerance of the host plant *H. almeriense*, such as improvement in its nutrient status, (Morte et al., 2000), survival capacity *in vitro* (Morte et al., 1994) and in field (Morte et al., 2010) or fine-tune regulation of their aquaporins under drought-stress (Navarro-Ródenas et al., 2013). In **Chapter III** we have shown that the mycorrhizal symbiosis between these two organisms also represents a beneficial response to the oxidative stress that relieves water-stress, since H_2O_2 levels are lower in mycorhizal roots under drought stress than in non-mycorrhizal roots (**Figure 3.10**). However, this decrease cannot be attributed to the expression levels of *TcCAT-1*. Everything points to the involvement of other enzymes and non-enzymatic compounds to lower reduce these H_2O_2 levels. In fact, in **Chapter IV**, up to 26 genes related to stress response, such as thioredoxins, superoxide dimutases or heat shock proteins were regulated in mycorrhizal symbiosis of *T. claveryi* x *H. almeriense* under water-stress. One of those genes is a catalase (ID 1248402) that was identified as a large subunit catalase L1 when a phylogenetic tree of fungal catalases was made (**Figure 3.8**). This catalase, which was upregulated 33.36-fold under water-stress may be one of the main responsible for the decrease in H_2O_2 levels under water-stress in mycorrhizal roots.

Another feature of *H. almeriense* x *T. claveryi* mycorrhizal symbiosis under water-stress is the change of mycorrhizal structures and the increased colonization. The increase in mycorrhizal colonization has been confirmed in different and independent assays throughout this thesis (**Table 8.2**), while the shift from intercellular to intracellular structures is also reported in **Chapter IV**, which supports previous assays such as Navarro-Ródenas et al. (2013). Furthermore, we have linked this morphological response

during drought with a molecular response. Since pectin targeting enzymes seem to be related to the degradation of the middle lamella and the formation of Hartig net, it seems that the favoring of intracellular structures in *T. claveryi* is accompanied by a general downregulation in PCWDE and MCWDEs in general, and pectin targeting enzymes in particular (**Figure 4.10B).** This is not only an adaptation to the gene-expression level, but it seems to be imprinted on the genomes of desert truffles, since they possess significantly less pectin degrading enzymes than other *Tuberaceae* mycorrhizal species. In **Chapter IV,** we describe more unique traits that set desert truffles apart from the mycorrhizal species of *Tuberaceae* and that seem to be related to their adaptation to arid and semiarid environments. The reduced, although still large, content in TEs compared to *Tuberaceae* mycorrhizas may be related to their plasticity and adaptability to their environment (Raffaele and Kamoun, 2012; Casacuberta and González, 2013), since all their hosts belong to the same family (*Cistaceae*) and most of them even to the same genus (*Helianthemum*) (Moreno et al., 2014). These species present less plasticity than, for example *Tuber* species, that are known to colonize hosts as diverse as *Populus*, *Quercus*, *Salix*, *Picea* or *Pinus* (Bonito et al., 2010).

The reduced amount of genes encoding for transporters, including aquaporins, may also reveal a conserved adaptive mechanism to optimize the hydraulic conductance in species that live in water-deficient environments. And last but not least, the expansion in pfam families involved in the processing of rRNA may be related to the unusal rRNA presented by some desert truffles called "hidden gap" (Navarro-Ródenas et al., 2018) which, in turn, may be related to specific mechanisms to withstand water-stress. With the results obtained in this thesis, we can suggest that desert truffles EEM are close, and may be considered as a type of ECM; therefore, their ability to form intracellular mycorrhiza, along with all the molecular traits described in **Chapter IV**, are evolutionary adaptations to the arid ecosystems that they inhabit.

Table 8.2. Summary of mycorrhizal colonization (%) in different assays of this thesis. Mycorrhization mean ± standard error of at least n=6 plants is represented. Different letters represent statistical differences between conditions in the Student's t-test.

	Chapter III	Chapter IV	Chapter IV (Intracellular colonization)	Chapter VII*
Well-watered mycorrhiza	27.8 ± 5.8a	21.34 ± 4.83a	2.73 ± 1.88a	21.17 ± 3.66a
Water-stressed mycorrhiza	48.8 ± 6.4b	45.37 ± 6.62b	41.91 ± 9.98b	46.67 ± 1.76b

*For Chapter VII, data from winter conditions was taken as well-watered, while from summer conditions as water-stressed.

With respect to the responses of the host plant *H. almeriense* to water-stress and its adaptations to arid environments, we have also found several features throughout the chapters of this thesis. Morte et al. (2010) described *H. almeriense* species as a **drought avoider**, with a conservative strategy of water-use by reducing transpiration and stomatal conductance. In **Chapter VI** we characterized the responses to the increase in water-stress that occurs in the Mediterranean climate during spring. We found a strong association between the level of expression of the Rubisco *RbcL* gene and the stomatal conductance (**Figure 6.6**), suggesting a stomatal control in the regulation of this gene, by controlling the concentration of CO_2 in the chloroplast (Flexas et al., 2006a; 2006b; Galmés et al., 2011). We also confirmed the fine-tuned regulation of aquaporins (AQPs) described by Navarro-Ródenas et al., (2013) also in field conditions (**Figure 6.7**). In addition, we found an intriguing expression pattern that shows that *HaPIP1.1* and *HaPIP2.1*, on the one hand, and *HaPIP1.2* and *HaPIP2.2*, on the other hand, are coexpressed, suggesting heteromerization for those genes (**Figure 6.8**) (Yaneff et al., 2014; Bienert et al., 2018). Furthermore, a sharp and generalized phenological switch has been described during spring, since all the parameters studied suddenly changed from early to late spring. The clearest example of this sudden change is the stomatal conductance that changes from 0.133 in early spring to 0.023 mol m^{-2} s^{-1} in late spring, and correlated in a sigmoidal form with the vapor pressure deficit (VPD) (**Table 6.2; Figure 6.4A**).

8.3. On desert truffle cultivation

In this thesis, there are several findings that will serve as powerful tools for the management of desert truffle cultivation.

The first has been to elucidate the reproduction mode of desert truffles, with special attention to *T. claveryi* (**Chapter IV**), which is one of the only two species of *Terfezia* that have been successfully cultivated. *T. claveryi*, together with *T. boudieri* and *T. nivea*, resulted to be **hetherothallic**, which means that outcrossing is obligatory for sexual reproduction. On the contrary, we have found two different *MAT* idiomorphs in the same strain of *K. pfeilii*, which means that this species could be homothallic (self-fertile). These findings open the way for several lines of research. First of all, functional assays are needed to confirm *in vivo* the heterothallism of *T. claveryi*, *T. boudieri* and *T. nivea* and the homothallism of *K. pfeilli*. In addition, an evolutionary study on the *MAT* genes of *Pezizaceae* could be of use because of the existence at the family level of two different reproduction modes (homothallism and heterotallism) in species that face similar environmental conditions. In the end, the increase of knowledge on this matter will have repercussion on how we understand the cultivation of these ascocarps and will force us to adopt new management models and production strategies of mycorrhizal plants, as has recently happened in the cultivation of black truffle (Rubini et al., 2011; Linde and Selmes, 2012; Murat et al., 2013; Rubini et al 2014; Le Tacon et al., 2014).

In **Chapter V** we unveiled the influence of climate on *T. claveryi* fructifications and we not only described the agroclimatic parameters, but also the time of the year when they are most important. Autumn seems to be the time of the year when more parameters have influence on fructifications, which suggests the early formation of truffle primordias in autumn and a slow development until spring (Bordallo, 2007; Pacioni et al., 2014). In a more applied field, these results allowed us to propose several management strategies that share the same goal: to establish and improve desert truffle productions to increase the profitability of this crop and its appeal to farmers. Not only is autumn important, but spring also seems to play a key role in the annual yield of *T. claveryi*. The results from **Chapter V** highlighted the importance of spring precipitations and vapor pressure deficit (VPD) (**Figure 5.4**). In addition, the accumulated knowledge coming from the experience of the research group plus the comments of farmers and gatherers made us think about the relationship between the plant status and phenology

during spring and the fructifications. In **Chapter VI** we characterized in depth the responses of the mycorrhizal plant *H. almeriense* to the increased drought and VPD that occurs in the Mediterranean climate from early to late spring. In addition to acquiring knowledge about the physiology of this species (discussed in **Section 8.2**), we found a marker that could serve as a tool for desert truffle cultivation. The sigmoidal relationship between stomatal conductance and VPD during spring (**Figure 6.4A**) revealed a threshold of VPD at which the plants undergo an abrupt change defined as phenology switch. The time of the year in which this switch occurred (*i.e.* the VPD threshold was reached) was correlated with truffle production for 18 years (**Figure 6.9**), meaning that the later this VPD threshold is reached, the greater the yiled is. Altogether, these results point to complex interactions between climate, plant phenology and desert truffle fructifications, which should be studied further. In order to test the applicability of these findings, we designed a simple shadowing device that, in theory, could dampen the increase in VPD in spring and, therefore, influence the desert truffle fructifications (**Figure 6.1**). Although reductions in VPD were achieved, the decrease in light (**Table 6.4**) could have countered the hypothetical improvements in the reduction in the VPD reduction.

Finally, in **Chapter VII** we also tested the effect of the atmospheric increase in the concentration of CO_2 on the physiology of this species of mycorrhizal plant, since this increase is predicted by the end of the century (IPCC, 2018). The results of this chapter foresee a bright future for this crop, since: 1) their potential cultivation areas will increase due to desertification (Schlesinger et al., 1990; Huang et al., 2016), and 2) the increased atmospheric CO_2 concentrations will help mycorrhizal *H. almeriense* plants to cope with water-stress, without affecting mycorrhiza intensity (**Table 7.2**; **7.3**; **7.4**). However, the effects on plant phenology and other factors such as potential changes in mycorrhizal communities due to climatic change (León-Sánchez et al., 2016; 2018) should also be considered.

In summary, the results in this thesis have allowed us to provide new management proposals that will improve the production of desert truffles from now on. At the same time, we have opened new paths for future research in order to transform this crop into an important economic resource in those areas where it is well adapted.

References

Balestrini R, Cosgrove DJ, Bonfante P (2005). Differential location of α-expansin proteins during the accommodation of root cells to an arbuscular mycorrhizal fungus. Planta 220(6):889–899. https://doi.org/10.1007/s00425-004-1431-2.

Barker SJS, Tagu D (2000). The roles of auxins and cytokinins in mycorrhizal symbioses. J. Plant Growth Regul. 19(2):144–154. https://doi.org/10.1007/s003440000021.

Bienert MD, Diehn TA, Richet N, Chaumont F, Bienert GP (2018) Heterotetramerization of plant PIP1 and PIP2 aquaporins is an evolutionary ancient feature to guide PIP1 plasma membrane localization and function. Front. Plant Sci. 9:382. https://doi.org/10.3389/fpls.2018.00382.

Bonfante P, Genre A (2015) Arbuscular mycorrhizal dialogues: do you speak 'plantish' or 'fungish'? Trends Plant Sci. 20(3):150–54. https://doi.org/10.1016/j.tplants.2014.12.002.

Bonito GM, Gryganskyi AP, Trappe JM, Vilgalys R (2010) A global meta-analysis of *Tuber* ITS rDNA sequences: species diversity, host associations and long-distance dispersal. Mol. Ecol. 19(22):4994-5008. https://doi.org/10.1111/j.1365-294X.2010.04855.x.

Bordallo JJ (2007) Estudio del ciclo biológico de *Terfezia claveryi* Chatin. Memoria de Suficiencia Investigadora del Programa de Doctorado de Biología Vegetal, Universidad de Murcia, Spain.

Casacuberta E, González J (2013) The impact of transposable elements in environmental adaptation. Mol. Ecol. 22: 1503–1517. https://doi.org/10.1111/mec.12170.

Cosgrove DJ (2000) Loosening of plant cell walls by expansins. Nature 407(6802):321–326. https://doi.org/10.1038/35030000.

Cosgrove DJ (2005) Growth of the plant cell wall. Nat. Rev. Mol. Cell Biol. 6(11):850–861. https://doi.org/10.1038/nrm1746.

Flexas J, Ribas-Carbó M, Bota J, Galmés J, Henkle M, Martínez-Cañellas S, Medrano H (2006a) Decreased Rubisco activity during water stress is not induced by decreased relative water content but related to conditions of low stomatal conductance and chloroplast CO_2 concentration. New Phytol. 172(1):73–82. https://doi.org/10.1111/j.1469-8137.2006.01794.x.

Flexas J, Bota J, Galmés J, Medrano H, Ribas-Carbó M (2006b) Keeping a positive carbon balance under adverse conditions: responses of photosynthesis and respiration to water stress. Physiol. Plant. 127:343–52. https://doi.org/10.1111/j.1399-3054.2005.00621.x.

Huang J, Haipeng Y, Guan X, Wang G, Guo R (2016) Accelerated dryland expansion under climate change. Nat Clim. Change 6(2):166–71. https://doi.org/10.1038/nclimate2837.

Kloppholz S, Kuhn H, Requena N (2011) A Secreted fungal effector of *Glomus Intraradices* promotes symbiotic biotrophy. Curr. Biol. 21(14):1204–9. https://doi.org/10.1016/j.cub.2011.06.044.

Le Tacon F, Marçais B, Courvoisier M, Murat C, Montpied P, Becker M (2014) Climatic variations explain annual fluctuations in French 'Périgord black truffle' wholesale markets but do not explain the decrease in 'black truffle' production over the last 48 years. Mycorrhiza 24(1):115–125. https://doi.org/10.1007/s00572-014-0568-5.

León-Sánchez L, Nicolás E, Nortes PA, Maestre FT, Querejeta JI (2016) Photosynthesis and growth reduction with warming are driven by nonstomatal limitations in a Mediterranean semiarid shrub. Ecol. Evol. 6 (9): 2725-2738. https://doi.org/10.1002/ece3.2074.

León-Sánchez L, Nicolás E, Goberna M, Prieto I, Maestre FT, Querejeta JI (2018) Poor plant performance under simulated climate change is linked to mycorrhizal responses in a semiarid shrubland. J. Ecol. 00(1):1–17. https://doi.org/10.1111/1365-2745.12888.

Linde, CC, Selmes H (2012) Genetic diversity and mating type distribution of *Tuber melanosporum* and their significance to truffle cultivation in artificially planted truffieres in Australia. Appl. Environ. Microbiol. 78(18):6534-6539. . https://doi.org/10.1128/AEM.01558-12.

Majda M, Robert S (2018) The role of auxin in cell wall expansion. Int. J. Mol. Sci. 19(4):951. https://doi.org/10.3390/ijms19040951.

IPCC (2018) Global warming: Summary for Policymakers. https://report.ipcc.ch/sr15/pdf/sr15_spm_final.pdf

Moreno G, Alvarado P, Manjón JL. (2014). Hypogeous desert fungi. In: Kagan-Zur V, Roth-Bejerano N, Sitrit Y, Morte A, eds. In: Kagan-Zur V, Roth-Bejerano N, Sitrit Y, Morte A, eds. Desert Truffles. Phylogeny, Physiology, Distribution and Domestication. Soil Biology, volume 38. Springer-Verlag, Berlin, Heidelberg pp. 3-20. https://doi.org/10.1007/978-3-642-40096-4_1.

Morte A, Cano A, Honrubia M, Torres P (1994) In vitro mycorrhization of micropropagated *Helianthemun almeriense* plantlets with *Terfezia claveryi* (desert truffle). Agric. Sci. Finl. 3: 309–314. https://doi.org/10.23986/afsci.72700.

Morte A, Lovisolo C, Schubert A (2000) Effect of drought stress on growth and water relations of the mycorrhizal association *Helianthemum almeriense-Terfezia claveryi*. Mycorrhiza 10(3):115–119. https://doi.org/10.1007/s005720000066.

Morte A, Navarro-Ródenas A, Nicolás E (2010) Physiological parameters of desert truffle mycorrhizal *Helianthemun almeriense* plants cultivated in orchards under water deficit conditions. Symbiosis 52(2–3):133–139. https://doi.org/10.1007/s13199-010-0080-4.

Murat C, Mello A, Abbà S, Vizzini A, Bonfante P (2008) Edible mycorrhizal fungi: identification, life cycle and morphogenesis. In: Varma A, ed. Mycorrhiza. Springer Berlin Heidelberg pp. 707–732. https://doi.org/10.1007/978-3-540-78826-3_33.

Murat C, Rubini A, Riccioni C, De la Varga, H, Akroume E, Belfiori B, et al. (2013) Fine-scale spatial genetic structure of the black truffle (*Tuber melanosporum*) investigated with neutral microsatellites and functional mating type genes. New Phytol. 199(1):176-187. https://doi.org/10.1111/nph.12264.

Navarro-Ródenas A, Pérez-Gilabert M, Torrente P, Morte A (2012) The role of phosphorus in the ectendomycorrhiza *continuum* of desert truffle mycorrhizal plants. Mycorrhiza 22(7): 565-575. https://doi.org/10.1007/s00572-012-0434-2.

Navarro-Ródenas A, Bárzana G, Nicolás E, Carra A, Schubert A, Morte A (2013) Expression analysis of aquaporins from desert truffle mycorrhizal symbiosis reveals a fine-tuned regulation under drought. Mol. Plant Microbe Interact. 26(9):1068–78. https://doi.org/10.1094/MPMI-07-12-0178-R.

Navarro-Ródenas A, Carra A, Morte A (2018) Identification of an alternative rRNA post-transcriptional maturation of 26S rRNA in the Kingdom Fungi. Front. Microbiol. 9(MAY):1–8. https://doi.org/10.3389/fmicb.2018.00994.

Pacioni G, Leonardi M, Di Carlo P, Ranalli D, Zinni A, De Laurentiis G (2014) Instrumental monitoring of the birth and development of truffles in a *Tuber melanosporum* orchard. Mycorrhiza 24(1):65-72. https://doi.org/10.1007/s00572-014-0561-z.

Patten CL, Glick BR (1996) Bacterial biosynthesis of indole-3-acetic acid. Can. J. Microbiol. 42(3):207–220. https://doi.org/10.1139/m96-032

Pellegrin C, Martin F, Veneault-Fourrey C (2019a) Molecular signalling during the ectomycorrhizal symbiosis. Biol Fungal Cell 1:95–109. https://doi.org/10.1007/978-3-030-05448-9_6.

Pellegrin C, Daguerre Y, Ruytinx J, Guinet F, Kemppainen M, Plourde MB, et al. (2019b) *Laccaria bicolor* MiSSP8 is a small-secreted protein decisive for the establishment of the ectomycorrhizal symbiosis. Environ. Microbiol. https://doi.org/10.1111/1462-2920.14727.

Perotto S, Daghino S, Martino E (2018) Ericoid mycorrhizal fungi and their genomes: another side to the mycorrhizal symbiosis?. New Phytol. 220(4):1141–47. https://doi.org/10.1111/nph.15218.

Plett JM, Kemppainen M, Kale SD, Kohler A, Legué V, Brun A, et al. (2011) A secreted effector protein of *Laccaria bicolor* is required for symbiosis development. Curr. Biol. 21(14):1197-1203. https://doi.org/10.1016/j.cub.2011.05.033.

Plett JM, Daguerre Y, Wittulsky S, Vayssieres A, Deveau A, Melton SJ, et al. (2014) Effector MiSSP7 of the mutualistic fungus *Laccaria bicolor* stabilizes the *Populus* JAZ6 protein and represses jasmonic acid (JA) responsive genes. Proc. Natl. Acad. Sci. USA. 111(22):8299–8304. https://doi.org/10.1073/pnas.1322671111.

Raffaele S, Kamoun S (2012) Genome evolution in filamentous plant pathogens: why bigger can be better. Nat. Rev. Microbiol. 10:417–430. https://doi.org/10.1038/nrmicro2790.

Rayle DL, Cleland R (1972) The *in vitro* acid-growth response: Relation to *in vivo* growth responses and auxin action. Planta 104(4):282–296. https://doi.org/10.1007/BF00386312

Reineke G, Heinze B, Schirawski J, Buettner H, Kahmann R, Basse CW (2008) Indole-3-acetic acid (IAA) biosynthesis in the smut fungus *Ustilago maydis* and its relevance for increased IAA levels in infected tissue and host tumour formation. Mol. Plant Pathol. 9(3):339–355. https://doi.org/10.1111/j.1364-3703.2008.00470.x

Robinson M, Riov J, Sharon A (1998) Indole-3-acetic acid biosynthesis in *Colletotrichum gloeosporioides* f. sp. *aeschynomene*. App. Environ. Microbiol. 64(12):5030–5032.

Rubini A, Belfiori B, Riccioni C, Tisserant E, Arcioni S, Martin F, Paolocci F (2011) Isolation and characterization of MAT genes in the symbiotic ascomycete *Tuber melanosporum*. New Phytol. 189(3):710–722. https://doi.org/10.1111/j.1469-8137.2010.03492.x.

Rubini A, Riccioni C, Belfiori B, Paolocci F (2014) Impact of the competition between mating types on the cultivation of *Tuber melanosporum*: Romeo and Juliet and the matter of space and time. Mycorrhiza 24(1):19-27. https://doi.org/10.1007/s00572-013-0551-6.

Schlesinger WH, Reynolds JF, Cunningham GL, Laura F, Jarrell WM, Virginia RA, et al. (1990) Biological feedbacks in global desertification conceptual models for desertification. Science 247(4946): 1043–1048. https://doi.org/10.1126/science.247.4946.1043.

Takahashi K, Hayashi K, Kinoshita T (2012).Auxin activates the plasma membrane H^+-ATPase by phosphorylation during hypocotyl elongation in *Arabidopsis*. Plant Physiol. 159(2):632–641. https://doi.org/10.1104/pp.112.196428.

Tsavkelova E, Oeser B, Oren-Young L, Israeli M, Sasson Y, Tudzynski B, et al. (2012) Identification and functional characterization of indole-3-acetamide-mediated IAA biosynthesis in plant-associated *Fusarium* species. Fungal Genet. Biol. 49(1):48–57. https://doi.org/10.1016/j.fgb.2011.10.005.

Veneault-Fourrey C, Commun C, Kohler A, Morin E, Balestrini R, Plett J, et al. (2014) Genomic and transcriptomic analysis of *Laccaria bicolor* CAZome reveals insights into polysaccharides remodelling during symbiosis establishment. Fungal Genet. Biol. 72:168–181. https://doi.org/10.1016/j.fgb.2014.08.007.

Wakabayashi K, Chun JP, Huber DJ (2000) Extensive solubilization and depolymerization of cell wall polysaccharides during avocado (*Persea americana*) ripening involves concerted action of polygalacturonase and pectinmethylesterase. Physiol. Plant. 108(4):345–352. https://doi.org/10.1034/j.1399-3054.2000.108004345.x

Yaneff A, Sigaut L, Marquez M, Alleva K, Pietrasanta LI, Amodeo G (2014) Heteromerization of PIP aquaporins affects their intrinsic permeability. Proc. Natl. Acad. Sci. USA 111(1):231–36. https://doi.org/10.1073/pnas.1316537111.

Zaretsky M, Sitrit Y, Mills D, Roth-Bejerano N, Kagan-Zur V (2006) Differential expression of fungal genes at preinfection and mycorrhiza establishment between *Terfezia boudieri* isolates and *Cistus incanus* hairy root clones. New Phytol. 171(4):837–846. https://doi.org/10.1111/j.1469-8137.2006.01791.x.

Zhao Y, Hull AK, Gupta NR, Goss KA, Alonso J, Ecker JR, et al. (2002) Trp-dependent auxin biosynthesis in *Arabidopsis*: involvement of cytochrome P450s CYP72B2 and CYP79B3. Genes Develop. 16:3100–3112. https://doi.org/10.1101/gad.1035402.5

CHAPTER IX

Conclusions

From the results obtained in the different chapters of this thesis and regarding the five specific objectives proposed, the following conclusions can be drawn:

Objective 1: To assess the role of fungal catalases in the T. claveryi x H. almeriense symbiosis, especially during mycorrhiza formation and in drought conditions.

1. A catalase from ascocarps of *Terfezia claveryi*, TcCAT-1, belonging to the large subunit size catalases (LSCs), has been identified, purified to homogeneity and biochemically characterized. It is a tetramer of approcimately 360 kDa, with maximum activity in a wide range of pH and temperature and it is inhibited by hydroxylamine, 2-mercaptoethanol and 3-aminotriazol. TcCAT-1 seems to play an important role in the mycorrhizal symbiosis between this species and its host plant *Helianthemum almeriense*, since it is upregulated 14 times in mature mycorrhiza compared to free living mycelium and ascocarp stage.

2. Mycorrhization has a beneficial effect in relieving oxidative stress, since the H_2O_2 levels in mycorrhizal roots under water-stress are approximately 2 times lower. The transcriptional profile of TcCAT-1 does not seem to be the responsible of the H_2O_2 decrease observed in the mycorrhizal plants under water deficit. Other enzymes that are upregulated under water-stress conditions such as the catalase JGI ID 1248402, which is 33 times upregulated under water-stress, and/or non-enzymatic molecules, could be the responsible of this phenomenon.

Objective 2: To describe the genomic features of desert truffles that are relevant to their cultivation, focusing on their reproductive mode, the development of the different symbiotic structures that these fungi form in the roots of their hosts, and their adaptations to semiarid environments.

3. The genomes of the desert truffles *Terfezia claveryi* and *Tirmania nivea* present similar features to the genomes of ectomycorrhizal and arbuscular mycorrhizal fungi previously sequenced: large genomes with a large

number of transposable elements, a large number of orphan genes coding for small secreted proteins that, in the case of *T. claveryi,* are upregulated in mycorrhizal symbiosis, and a reduced set of plant cell wall degrading enzymes (PCWDEs).

4. Desert truffle genomes present an expansion in gene families related to rRNA processing and a contraction in gene families related to the transport of water and metabolites compared to *Tuberaceae* mycorrhizas. These singularities may be related to adaptations to water-stress conditions.

5. We found a relationship between the morphological response of the mycorrhiza and the transcriptomic profile of PCWDEs in *T. claveryi* under water-stress: at the same time that the total mycorrhization increases and the intracellular mycorrhiza is favored, the plant and fungal cell wall degrading enzymes are downregulated, especially those that target pectin, because of its possible importance in the formation of the Hartig net.

6. *MAT* genes involved in the sexual reproduction of desert truffles are reported for the first time. All desert truffles studied (*Terfezia claveryi*, *Terfezia boudieri* and *Tirmania nivea*) are hetherothallic, except for *Kalarituber pfeilii*, that seems to be homothallic.

Objective 3: To determine which agroclimatic parameters can be positively or negatively correlated with the productivity of desert truffles and to know the critical periods along year when those agroclimatic parameters most importantly determine truffle crops.

7. The two key periods of time when agroclimatic parameters explain annual fluctuations of *T. claveryi* yields are autumn and spring. From the agroclimatic parameters studied, aridity index and soil water potential are the ones that most determine the annual yield of the desert truffle crop. With these findings, several management methods that consist in applying variable irrigation depending on aridity index, soil water potential or the combination of both in the key periods of time (autumn and spring) can be

used to maximize and stabilize the annual fluctuations in desert truffle yields.

Objective 4: To characterize the responses of the desert truffle plant H. almeriense to the environment in spring, to search for morpho-physio-molecular markers that could help us to track easily the changes in phenology, and to evaluate the relationships between the markers of the plant phenology and productivity of desert truffle.

8. Almost all the physiological parameters from desert truffle mycorrhizal plants (*Helianthemum almeriense*) are correlated with the vapor pressure deficit (VPD) or the soil water potential during the transition from early to late spring, indicating that these two factors and their interaction influence the *H. almeriense* physiological and phenological states. In addition, the abrupt change in all gas-exchange parameters, shoot water potential, Rubisco and aquaporins regulation reveal a generalized phenological switch in desert truffle plants during this period.

9. Transcriptional regulation of Rubisco large subunit size gene is highly correlated to stomatal conductance, suggesting that its expression is regulated by the CO_2 concentration in the substomatal cavities.

10. Aquaporin *HaPIP 1.1*, *HaPIP1.2*, *HaPIP2.1* and *HaPIP2.2* expressions are fine-tuned regulated in field conditions, since their expressions are only correlated with the vapor pressure deficit in late spring, when the water-stress is more extreme. In addition, these PIPs present an expression pattern that suggest their heteromerization, as *HaPIP1.1* and *HaPIP2.1*, on one hand, and *HaPIP1.2* and *HaPIP2.2* on the other hand, are co-expressed.

11. The vapor pressure deficit (VPD) is the environmental parameter that better explains the phenological switch of *H. almeriense* mycorrhizal plants in spring. The VPD-stomatal conductance relationship during spring has been selected as a marker of the phenological state of the plant and it partially

explains the interannual fluctuations in desert truffle production. This marker can and will be used as a tool for the design of management strategies.

Objective 5: To evaluate the effects of the increase in atmospheric CO_2 concentration and its interaction with the increasing drought of the Mediterranean springs to the physiological responses of the H. almeriense x T. claveryi mycorrhizal symbiosis.

12. High atmospheric concentrations of CO_2 and their interaction with drought conditions affect the overall physiological parameters of *Helianthemum almeriense* x *Terfezia claveryi* mycorrhizal plants. The most affected physiological parameters are the net CO_2 assimilation and the intrinsic water use efficiency, which increased up to 3 times under high atmospheric concentrations of CO_2, finding the maximum differences in summer conditions, when the water-stress was more extreme. At the same time, plant shoot biomass was 2.5 times higher at elevated CO_2 atmospheric concentrations only in summer, suggesting that the expected increase in atmospheric concentrations of CO_2 will help *H. almeriense* mycorrhizal plants to cope with the damaging effects of drought.

13. Mycorrhizal colonization and root sugar content remain unaffected, while *H. almeriense* plants have up to 10 times more flowers per plant under high atmospheric concentrations of CO_2. These results suggest that the extra income of carbon as a consequence of the enriched atmosphere in CO_2 is invested in the formation of flowers rather than in mycorrhizal modifications or sugar accumulation in the roots.

A P P E N D I X   A

Supplementary protocols

1. MMN and MMNo culture media

All the EEM fungi grown *in vitro* during the completion of this thesis have been grown in MMN or MMNo media (Arenas et al., 2018), at 23 ºC in the dark and with gentle agitation (75 rpm) in the case of liquid culture (**Table A1**).

Table A1. MMN and MMNo media composition. Adapted from Arenas et al. (2018).

Nutrients (g L^{-1})	MMN	Optimal MMN (MMNo)
$CaCl_2$	0.05	0.05
NaCl	0.025	0.025
KH_2PO_4	0.5	0.5
$(NH_4)_2HPO_4$	0.25	0.6
$MgSO_4 \cdot 7H_2O$	0.15	0.15
$FeCl_3 \cdot 6H_2O$	0.001	0.001
Thiamine	0.0001	0.0001
m-Inositol	-	0.05
Glycine	-	0.003
Nicotinic acid	-	0.0005
Pyridoxine	-	0.0003
Folic acid	-	0.0001
Biotin	-	0.00001
Malt extract	-	-
Glucose	10	15
Agar (in solid plates)	10	10

2. SDS-PAGE

Sodium dodecyl sulfate polyacrylamide gel electrophoresis (SDS-PAGE) was carried out on 10% gels prepared as described in **Table A2** (Laemmli, 1970). Each sample is mixed with 4X sample buffer (10% glycerol (v/v), 5% β-mercaptoethanol (w/v), 2.5% SDS (w/v), 0.0015% bromophenol blue (w/v) in 100 mM Tris-HCl buffer pH 6.8), heated at 95ºC for 4 minutes in order to dissociate the proteins and loaded in the stacking gel. Electrophoresis is carried out in a Mini-PROTEAN 3 system (Bio-Rad) at 200 V for 40 minutes with 25 mM Tris-HCl pH 8.3, 200 mM glycine and 0.1 (w/v) as running buffer and the gel is stained with a solution of 0.1% Coomassie Brilliant Blue R-250 solution (Sigma Aldrich) in a 40:10:50 methanol:glacial acetic acid:water solution for half an hour.

Once stained, the gel is unstained with 10% glacial acetic acid and the protein bands are visualized.

Table A2. SDS 10% polyacrylamide gel preparation protocol.

Compound	Volume
Running gel (10%)	
Tris-HCl 1.5M pH 8.8	2.5 mL
SDS 10% (w/v)	100 μL
Acrylamide/Bis-acrylamide 30/0.8% (w/v)	3.33 mL
Ammonium persulfate 10% (w/v)	50 μL
Tetramethylethylendiamine (TEMED)	20 μL
H₂O	Up to 10 mL (4.00 mL)
Stacking gel (4%)	
Tris-HCl 0.5M pH 6.8	1.25 mL
SDS 10% (w/v)	50 μL
Acrylamide/Bis-acrylamide 30/0.8% (w/v)	650 μL
Ammonium persulfate 10% (w/v)	25 μL
Tetramethylethylendiamine (TEMED)	10 μL
H₂O	Up to 5 mL (3.05 mL)

3.   Protein determination

For protein determination, the BCA method was used (Smith et al., 1965). This protocol is detailed below:

1.   Prepare "Reagent 1" by adding 1 volume of Cu (II) sulfate pentahydrate 4% with to 50 volumes of bicinchoninic acid (BCA) solution (Sigma Aldrich, USA).

2.   Prepare a standard curve (**Figure A1**) with known concentrations of bovine serum albumin (BSA). The problem sample/s are prepared in the same way (**Table A3**).

3.   After vortexing the samples, incubate them for 30 minutes at 37 ºC.

4.   Once the tubes are cooled, the absorbance at 562 nm is measured with an spectrophotometer.
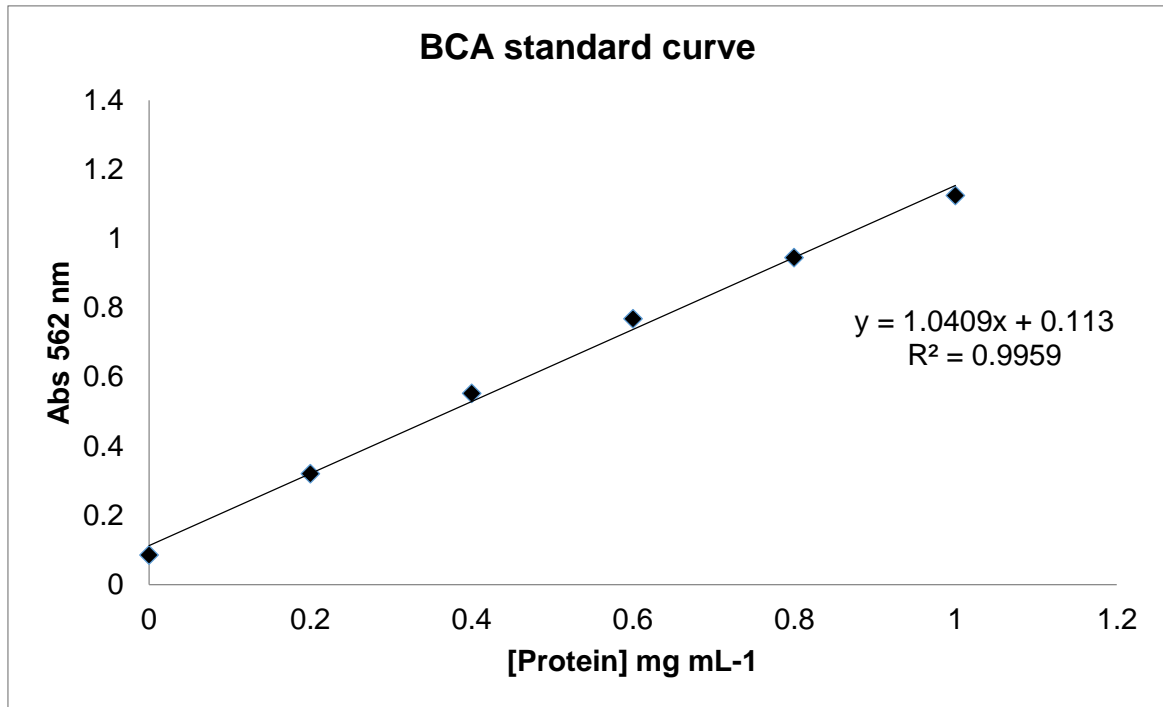
Figure A1. Standard curve for protein determination.

Table A3. Preparation of tubes for the determination of protein concentration with the BCA method.

Tube	H2O (μL)	BSA standard (1 mg/mL) (μL)	Sample (μL)	Reagent 1 (mL)
1	100	0	0	2
2	80	20	0	2
3	60	40	0	2
4	40	60	0	2
5	20	80	0	2
6	0	100	0	2
Sample	0	0	100	2

4. DNA and RNA extraction

Before DNA or RNA extraction, both from fungal and plant material, tissue is pulverized with liquid nitrogen with the help of a pestle and a mortar. All the material used must be freezing cold. In this thesis DNA was extracted either with DNAeasy plant minikit (Qiagen, Germany) or with the CTAB method (Chang et al., 1993), and RNA with RNAeasy plant minikit (Qiagen, Germany) or with the CTAB method (Chang et al., 1993). In the case of both kits, manufacturer's instructions were followed. CTAB protocol is detailed below:

1. Incubate 100 mg of frozen tissue with 1 mL of CTAB buffer (Table A2) at 65 ℃ for 10 minutes with constant agitation.

2. Add 1 volume of phenol : chloroform : isoamyl alcohol (25:24:1); vortex vigorously.

3. Centrifuge 20 minutes at 4 ℃, 10,000 g. Recover the supernatant carefully and transfer it to a new tube.

4. Add 1 volume of chloroform : isoamyl alcohol (24:1), and mix vigorously with a vortex.

5. Centrifuge 20 minutes at 4 ℃, 10,000 g. Recover the supernatant carefully and transfer it to a new tube.

6. Repeat steps 2-5 if necessary (only if the interphase is still visible or if the supernatant is still turbid).

7. Add 1/3 volumes of LiCl 8M, agitate the sample with a vortex and incubate overnight at 4 ℃.

8. Centrifuge 30 minutes at 4 ℃, 20,000 g. DNA should be present in the supernatant and RNA in the pellet.

DNA extraction

9.1. Transfer the supernatant to a new tube, add 1 volume of isopropanol and 0.1 volumes of sodium acetate 3M. Mix with a vortex and incubate it for 5 minutes on ice.

9.2. Centrifuge 30 minutes at 4 ºC, 20,000 g. Discard the supernatant and repeat a short centrifugation (2 minutes 20,000 g) to ensure removal of the supernatant.

9.3. Add 500 µL of cold 70 % ethanol.

9.4. Centrifuge 5 minutes at 4 ºC, 20,000 g. Discard the supernatant and repeat a short centrifugation (2 minutes 20,000 g) to ensure removal of the supernatant.

9.5. Add Tris : EDTA (TE) buffer (1:10) preheated to 50 ºC (**Table A4**). The amount of TE varies according to the needs of each extraction (usually between 30 to 100 µL).

9.6. DNA quantification (see **Appendix A: Section 4.1**)

RNA extraction

10.1. Resuspend the pellet from step 8 in 600 µL of preheated Sodium-SDS-Tris-EDTA (SSTE) buffer (**Table A4**).

10.2. Add 1 volume of chloroform : isoamyl alcohol (24:1), and vortex vigorously.

10.3. Centrifuge 20 minutes at 4 ºC, 10,000 g. Recover the supernatant carefully and transfer it to a new tube.

10.4. Add 0.1 volumes of sodium acetate 3M and 2.5 volumes of cold ethanol 100%. Mix with vortex and incubate for at least 3 hours at -20 ºC.

10.5. Centrifuge 30 minutes at 4 ºC, 20,000 g. Discard the supernatant and repeat a short centrifugation (2 minutes at 20,000 g) to ensure removal of the supernatant.

10.6. Centrifuge 5 minutes at 4 ºC, 20,000 g. Discard the supernatant and repeat a short centrifugation (2 minutes at 20,000 g) to ensure removal of the supernatant.

10.7. Add DEPC-H_2O. The amount of DEPC-H_2O varies according to the needs of each extraction (usually between 30 and 100 µL).

10.8. RNA quantification (see **Appendix A: Section 4.1**)

Table A4. Reagents needed for DNA and RNA extraction.

REAGENT	VOLUME	STOCK COMPOSITION	FINAL CONCENTRATION
TE (1:10) (TRIS-EDTA)	50 mL	0.5 mL Tris-HCl 1M pH:8 0.1 mL EDTA 0.5M pH:8 49.4 mL H_2O-DEPC	Tris-HCl 10 mM EDTA 1 mM
SSTE (SODIUM-SDS-TRIS-EDTA)	50 mL	10 mL NaCl 5M 2.5 mL SDS 10% 0.5 mL Tris-HCl 1M pH:8 0.1 mL EDTA 0.5M pH:8 36.9 mL H_2O-DEPC	NaCl 1 M SDS 0.5% Tris-HCl 10 mM EDTA 1 mM
C-TAB (2%)	50 mL	C-TAB 10% PVP (K30) 2% 1M Tris-HCl pH:8 0.5M EDTA pH:8 NaCl 5M	C-TAB 2% PVP (K30) 2% 100 mM Tris-HCl pH:8 25 mM EDTA pH:8 NaCl 2M
H_2O-DEPC	1 L	1 mL of DEPC per 1L of H_2O miliQ. Incubate with agitation overnight. Autoclave and eliminate gas (by opening the bottle in sterile conditions)	

4.1. DNA and RNA quantification

DNA and RNA were quantified using a spectrophotometric method (Sambrook and Russel, 2001). 1.2 μL were placed carefully inside a Nanodrop spectophotometer (Nanodrop 2000, Thermofisher). Each absorbance unit at 260 nm was considered as 50 μg cm μL^{-1} of DNA or 40 μg cm μL^{-1} of RNA. Absorbance at 230 and 280 nm was also measured to estimate carbohydrate, phenols and other compounds (230 nm) or protein (280 nm) contaminations. These ratios (260/230 and 260/280) should be between 1.8 and 2.2.

In addition, for genomic sequencing of DNA and RNA, fluorimetric quantification was performed using Qubit^{tm} fluorometer (Invitrogen, USA), following manufacturer's instructions.

5. Polymerase chain reaction (PCR)

For the correct identification of the strains used in the course of this thesis, PCR was performed using ITS1 (5'- TCCGTAGGTGAACCTGCGG-3') and ITS4 (5'-TCCTCCGCTTATTGATATGC-3') as forward and reverse primers. PCR product was purified using GeneJet PCR purification kit (Thermofisher MA, USA), following

manufacturer's instructions, and sequenced in "Servicio de Biología Molecular" from University of Murcia. The sequences obtained were compared with the-NCBI-nr (NCBI non redundant) database. PCR mix is detailed, below:

In 0.2 mL eppendorf tubes the following reaction was prepared:

H_2O miliQ	16.5 μL
Buffer 10X	2.5 μL
MgCl2 (50 mM)	0.75 μL
dNTPs (5 mM)	1 μL
BSA 1%	1 μL
Primers (10 μM each)	F (1 μL) + R (1 μL)
Taq DNA polymerase 5 U $μL^{-1}$ (Invitrogen)	0.1 μL
DNA template	1 μL (10-100 ng)

Positive (with known sample) and negative (with H_2O miliQ) controls were always performed. Typical conditions of the PCR cycle were as follows:

Initial denaturation	5 min at 95 °C
Denaturation	5 sec at 95 °C
Annealing (depends on Tm of the primers)	10 sec at X °C
Elongation per kb)	1 min at 72 °C (1 min
Repeat steps 2-5 for 35 additional cycles	
Final elongation	10 min at 72 °C
Keep sample at 4 °C until agarose gel loading.	

6.   Agarose gel electrophoresis (1%)

For the preparation of agarose gel, dissolve 0.35g of agarose in 35 mL of TAE 1X (40 mM Tris, 20 mM acetic acid, 1mM EDTA) and heat until-turbidity is lost. Let it cool at room temperature and add 1 μL of SYBR^{tm} safe. Before solidifying, pour the gel into the gel box and cover in the dark until the gel is completely solid. Before loading,

mix 2 µL of sample with 10 µL of loading buffer 6X (sacarose 50 % (w/v), Bromophenol blue 0.3% (w/v)). Load the samples and run the gel for 40 minutes at 80 V. To reveal the results, expose the gel to UV light (260 nm); the samples were compared with 1 Kb Plus Ladder (Invitrogen, USA).

8. Fungal colonization

Root staining, mycorrhizal observation and counting under the microscope are adaptations of protocols from Gutiérrez et al. (2003) and Derkowska et al. (2008).

8.1. Root staining

The harvested roots were placed in containers with pores of a size that allowed the passage of the different solutions without losing any piece of root. The protocol for staining was the following:

1. Roots were incubated with 10% KOH (w/v) for one hour at 100 ºC.

2. After the incubation, roots were rinsed with tap water three to five times to remove the remaining of KOH and then, were incubated with H_2O_2 freshly prepared, for five to eight minutes at 100 ºC.

3. Again, the roots were rinsed with tap water three to five times and incubated during 5 minutes with 1M HCl at room temperature.

4. Without rinsing, roots were incubated with a mix of trypan blue ink and 5% acetic acid for twenty minutes.

5. The roots were kept at 4 ºC in a mixture of glycerol an water 1:1 (v:v) until they were observed under a microscope.

8.2.   Fungal colonization

To determine the mycorrhization status, the roots were observed under an Olympus BH2 microscope. From each root sample three calculations were made: total mycorrhization percentage, mycorrhization intensity and intracellular mycorrhiza percentage.

8.2.1.   Mycorrhization percentage

To calculate the mycorrhization status, 100 sections of secondary and tertiary roots were observed per sample under the microscope and classified as mycorrhizal or non-mycorrhizal depending on the presence/absence of *T. claveryi* mycorrizal structures. The results were given as percentage of the total sections observed.

8.2.2.   Mycorrhization intensity

To calculate mycorrhization intensity, each *T. claveryi* mycorrhizal structure observed was classified as low, low-medium, high-medium and high, with respect to the mycorrhiza observed in a single section. Then, the mycorrhization intensity was calculated in the following way:

$$Mycorrhization\ intensity\ (out\ of\ 4) = \frac{(1 \times n\ low) + (2 \times n\ low, medium) + (3 \times low, high) + (4 \times high)}{4}$$

8.2.3.   Intracellular colonization percentage

Each *T. claveryi* mycorrhizal structure observed was also classified as intercellular or intracellular depending on whether it was forming a clear Hartig net ("intercellular") or the hyphae observed were clearly inside the cortical cell ("intracellular").

References

Arenas F, Navarro-Ródenas A, Chávez D, Gutiérrez A, Pérez-Gilabert M, Morte A (2018) Mycelium of *Terfezia claveryi* as inoculum source to produce desert truffle mycorrhizal plants. Mycorrhiza 28(7):691-701. https://doi.org/10.1007/s00572-018-0867-3.

Chang S, Puryear J, Cairney J (1993) A simple and efficient method for isolating RNA from pine trees. Plant Mol. Biol. Rep. 11(2):113–116. https://doi.org/10.1007/BF02670468.

Derkowska E, Sas-Paszt L, Sumorok B, Szwonek E, Gluszek S (2008) The influence of mycorrhization and organic mulches on mycorrhizal frequency in apple and strawberry roots. J. Fruit Ornamental Plant Res. 16:227-242.

Gutiérrez A, Morte A, Honrubia M (2003) Morphological characterization of the mycorrhiza formed by *Helianthemum almeriense* Pau with *Terfezia claveryi* Chatin and *Picoa lefebvrei* (Pat.) Maire. Mycorrhiza 13(6):299–307. https://doi.org/10.1007/s00572-003-0236-7.

Laemmli UK (1970) Cleavage of structural proteins during the assembly of the head of bacteriophage T4. Nature 227:680-685.

Sambrook J, Russell D (2001) Molecular cloning: a laboratory manual, 3rd ed. Cold Spring Harbor Laboratory Press, New York.

Smith PK, Krohn RI, Hermanson GT, Mallia AK, Gartner FH, Provenzano MD, et al. (1985) Measurement of protein using bicinchoninic acid. Anal Biochem. 150:76–85. https://doi.org/10.1016/0003-2697(85)90442-7

APPENDIX B

Supplementary Tables

Table S1. 13 fungi used for genome comparison.

JGI_ID	SpeciesName	Phylum	Class	Order	Genus
Tubme1v2	*Tuber melanosporum*	*Ascomycota*	*Pezizomycetes*	*Pezizales*	*Tuber*
Tubae1	*Tuber aestivum*	*Ascomycota*	*Pezizomycetes*	*Pezizales*	*Tuber*
Tubbor1	*Tuber borchii*	*Ascomycota*	*Pezizomycetes*	*Pezizales*	*Tuber*
Chove1	*Choiromyces venosus*	*Ascomycota*	*Pezizomycetes*	*Pezizales*	*Choiromyces*
Gyresc1	*Gyromitra esculenta*	*Ascomycota*	*Pezizomycetes*	*Pezizales*	*Gyromitra*
Morco1	*Morchella importuna*	*Ascomycota*	*Pezizomycetes*	*Pezizales*	*Morchella*
Wilmi1	*Wilcoxina mikolae*	*Ascomycota*	*Pezizomycetes*	*Pezizales*	*Wilcoxina*
Pyrco1	*Pyronema confluens*	*Ascomycota*	*Pezizomycetes*	*Pezizales*	*Pyronema*
Tercla1	*Terfezia claveryi*	*Ascomycota*	*Pezizomycetes*	*Pezizales*	*Terfezia*
Terbo2	*Terfezia boudieri*	*Ascomycota*	*Pezizomycetes*	*Pezizales*	*Terfezia*
Tirniv1	*Tirmania nivea*	*Ascomycota*	*Pezizomycetes*	*Pezizales*	*Tirmania*
Kalpfe1	*Kalaharituber pfeilii*	*Ascomycota*	*Pezizomycetes*	*Pezizales*	*Kalaharituber*
Ascim1	*Ascobolus immersus*	*Ascomycota*	*Pezizomycetes*	*Pezizales*	*Ascobolus*

Table S2. Genes involved in pheromone biosynthesis and signalling in desert truffles. *T. magnatum* genes identified in Murat et al., 2018 were used to blast against *T. claveryi* and *T. nivea*, and score, E value, % of identity and % of subject cover are showed. ND = Not Detected

T. magnatum protein ID	Definition	T. claveryi					T. nivea				
		Protein ID	Score	Evalue	% Identity	% Subj. Coverage	Protein ID	Score	Evalue	% Identity	% Subj. Coverage
287376	a-pheromone processing metalloptidase Ste23	1192807	3,047	0.00E+00	61.8	79.7	632311	3,056	0.00E+00	61.6	85.3
309398	pheromone processing carboxypeptidase KexA (Kex1) putative	1150695	2,046	0.00E+00	67.7	85.9	186368	2,044	0.00E+00	67.8	86.1
291739	CAAx prenyl protease 2	383855	614	7.89E-64	55.7	63.2	715022	618	3.42E-69	56.5	63.1
208117	protein farnesyltransfexase subunit beta	1271593	1,052	5.25E-108	63.6	38.3	703666	1,068	1.20E-110	57.6	54.1
273258	pheromone processing endopropease KexB (Kex2)	1164104	2,446	0.00E+00	65.4	79.2	712477	2,403	0.00E+00	64.9	80.1
288494	pheromone maturation dipeptidyl aminopeptidase A	1166044	2,625	0.00E+00	62.1	81.5	715637	2,681	0.00E+00	60.5	83.5
321911	CAAX prenyl protease 1	ND	ND	ND	ND	ND	579358	1,571	0.00E+00	67.7	98.4
351221	DNA-binding protein Mcm1 (MADS box family transcription factor)	1064833	373	1.84E-37	82.4	97.8	335775	501	1.48E-49	61.8	76.9
164943	mitogen-activated protein kinase, Fus3	539905	1,723	0.00E+00	94	99.2	632973	1,726	0.00E+00	94.3	99.2
183436	mitogen activated protein kinase kinase kinase Ste11	1271913	1,980	0.00E+00	69	64	631343	2,048	0.00E+00	67.7	74.2
343331	sexual development transcription factor Ste12 (Homeodomain DNA binding)	1271895	2,160	0.00E+00	73.2	84	585075	2,174	0.00E+00	75.7	81.7
340923	serine/threonine-protein kinase Ste20	1090810	1,784	0.00E+00	90.6	56.3	248689	1,785	0.00E+00	90.6	43.9
359048	pheromone alpha-factor receptor PreB/Ste2	1099354	615	3.57E-59	48.1	66.3	634491	623	2.86E-60	50.4	65.2
169273	heterotrimeric G-protein beta subunit	1327174	4,477	1.86E-33	32.9	207.6	713803	3,791	8.16E-31	33.5	162.7
341689	protein kinase regulator Ste50	1051184	987	2.30E-98	62.3	78.9	62577	902	2.18E-96	59.8	58.8
200542	heterotrimeric G-protein alpha subunit (type 1 G-alpha, GPA1)	787358	1,664	0.00E+00	90.1	100	215037	1,667	0.00E+00	90.4	100
357565	mitogen activated protein kinase kinase, Dual specificity protein kinase, STE7-like	1275962	1,431	0.00E+00	85.5	75	537180	1,437	0.00E+00	85.1	76.3

Table S3. Aquaporins from the 13 fungi analyzed.

Ascobolus inmersus (3)	**Terfezia boudieri (1)**
jgi|Ascim1|201278|gw1.21.193.1	jgi|Terbo2|813167|estExt_Genewise1.C_440040
jgi|Ascim1|211724|e_gw1.62.43.1	**Terfezia claveryi (1)**
jgi|Ascim1|325701|gm1.5701_g	jgi|Tercla1|1292087|MIX10105_167413_47
Choiromyces venosus (3)	**Tirmania nívea (1)**
jgi|Chove1|1827977|fgenesh1_pm.36_#_62	jgi|Tirniv1|208015|CE208014_7037
jgi|Chove1|1844542|estExt_fgenesh1_pg.C_500074	**Tuber aestivum (2)**
jgi|Chove1|970854|CE970853_4344	jgi|Tubae1|1799|GSTUAT00001200001
Gyromitra esculenta (4)	jgi|Tubae1|8318|GSTUAT00009239001
jgi|Gyresc1|619320|estExt_fgenesh1_pg.C_590004	**Tuber borchii (3-4)**
jgi|Gyresc1|459760|e_gw1.7.177.1	jgi|Tubbor1|1124382|gm1.6505_g
jgi|Gyresc1|550632|fgenesh1_kg.17_#_735_#_TRINITY_DN2700_c0_g2_i1	jgi|Tubbor1|1188962|estExt_Genemark1.C_10124
jgi|Gyresc1|517966|gm1.9637_g	jgi|Tubbor1|1063107|fgenesh1_pg.54_#_36
Kalaharituber pfeilii (1)	**Tuber melanosporum (3)**
jgi|Kalpfe1|796112|gm1.8764_g	jgi|Tubme1v2|178|GSTUMT200000179001
Morchella importuna (2)	jgi|Tubme1v2|8688|GSTUMT200005969001
jgi|Morco1|547947|fgenesh1_pg.47_#_9	jgi|Tubme1v2|1698|GSTUMT200001847001
jgi|Morco1|494943|e_gw1.67.23.1	**Wilcoxina mikolae (3)**
Pyronema confluens (2)	jgi|Wilmi1|606841|estExt_Genewise1Plus.C_1600042
jgi|Pyrco1|4121|PCON_05121m.01	jgi|Wilmi1|661730|estExt_fgenesh1_pg.C_660016
jgi|Pyrco1|8120|PCON_09121m.01	jgi|Wilmi1|664343|estExt_fgenesh1_pg.C_1490003

Appendix B

Table S4. Fungal reads present in plant

Taxa_genus	DSMP_2	DSMP_3	DSMP_9	Average	%	NMP_1	NMP_2	NMP_3	Average	%	WWMP_1	WWMP_4	WWMP_6	Average	%
Acaromyces	0.00117816	0.0013853	0.00104639	0.00120328	0.12032817	0.0011697	0.00139799	0.00121595	0.00126121	0.12612117	0.00152495	9.40E-04	8.68E-04	0.00111084	0.11108427
Ascosphaera	0.001316	2.66E-04	9.35E-04	0.00083908	0.08390761	7.73E-07	5.24E-06	2.10E-06	2.7021E-06	0.00027021	2.49E-04	4.22E-04	3.96E-04	0.00035585	0.03558534
Ceratobasidium	0.00391831	4.45E-05	0.00277279	0.00224521	0.22452111	1.11E-05	2.81E-05	1.01E-05	1.6433E-05	0.00164331	7.03E-05	7.92E-05	8.45E-05	7.7972E-05	0.00779721
Exophiala	9.43E-04	4.73E-04	8.66E-04	0.00076064	0.07606442	1.49E-06	3.23E-05	5.32E-06	1.3032E-05	0.00130316	4.39E-04	0.00108249	9.85E-04	0.0008355	0.08355011
Kalaharituber	0.00256368	0.00150787	0.00209367	0.00205507	0.2055072	1.63E-05	4.71E-05	1.93E-05	2.7543E-05	0.00275433	9.48E-04	0.00146473	0.00138	0.00126425	0.12642502
Myrothecium	7.98E-05	2.19E-05	4.81E-05	4.9931E-05	0.00499312	1.51E-04	1.90E-05	1.03E-04	9.0894E-05	0.00908939	2.29E-05	0.00118403	0.00104246	0.00074978	0.07497819
Paracoccidioides	0.00187112	0.0022924	0.00110674	0.00175675	0.17567516	3.34E-04	0.00241436	0.00137157	0.00137328	0.13732845	5.00E-04	5.48E-04	4.36E-04	0.00049511	0.04951121
Peziza	0.00168694	6.22E-04	0.00149573	0.00126819	0.12681919	8.96E-06	1.67E-06	7.40E-06	1.1033E-05	0.00110335	5.22E-04	6.98E-04	6.93E-04	0.00063771	0.0637713
Pyrenochaeta	0.00151813	5.32E-05	0.00109898	0.00089011	0.08901091	2.97E-05	7.93E-05	4.75E-05	5.2171E-05	0.00521713	2.29E-04	7.28E-05	8.40E-05	0.00012871	0.01287142
Pyronema	5.66E-05	5.86E-05	3.43E-05	4.9821E-05	0.0049821	4.04E-05	0.00278475	0.00103642	0.00128719	0.12871913	9.09E-05	3.00E-05	4.38E-05	5.4913E-05	0.00549132
Rhizoctonia	0.01510023	0.00166936	0.01068958	0.00915306	0.91530599	2.40E-04	3.30E-04	3.13E-04	0.00029427	0.02942714	5.85E-04	8.71E-04	9.09E-04	0.00078841	0.07884147
Terfezia	0.26457378	0.14029115	0.21993841	0.20826778	**20.8267784**	0.00303184	0.00589439	0.00298718	0.00397114	**0.3971136**	0.08291942	0.13581972	0.12658333	0.11510749	**11.5107487**
Thanatephorus	0.00421344	3.91E-04	0.00302815	0.00254428	0.2544277	1.84E-04	2.22E-04	1.96E-04	0.00020069	0.02006947	2.20E-04	2.28E-04	2.78E-04	0.00024177	0.02417724
Tricharina	3.55E-04	3.77E-04	3.29E-04	0.00035382	0.03538173	4.61E-04	0.035851	0.01362619	0.01664617	1.66461739	6.20E-04	4.46E-04	5.70E-04	0.00054523	0.05452273
Trichophaea	1.15E-04	1.72E-04	1.14E-04	0.00013376	0.01337595	1.78E-04	0.00599567	0.00232531	0.00283301	0.28330065	0.00016892	1.15E-04	1.45E-04	0.00014291	0.01429129
Wilcoxina	1.72E-04	1.75E-04	1.64E-04	0.00017038	0.01703783	2.34E-04	0.00765191	0.00298516	0.0036238	0.36238035	1.99E-04	2.00E-04	2.18E-04	0.00020575	0.02057498
Others	0.00861101	0.00708226	0.00645648	0.00738325	0.73832519	0.00251708	0.01018405	0.00555513	0.00608542	0.60854205	0.00475977	0.00414507	0.0038433	0.00424938	0.424938
Total fungal reads					**23.9124417**					**3.77900028**					**12.6991598**

Table S5. Environmental design of the chambers for the transition from winter to summer simulation.

Table S1. Environmental desing of the chambers for the transition from winter to summer simulation

Environmental data retrieved from the meteorological station La Alberca MU62 (http://siam.imida.es)

	Average temperature (ºC)	Maximum temperature (ºC)	Minimum temperature (ºC)	Average relative humidity (%)	Light hours (h)	VPD (kPa)	Soil water potential (Mpa)
Winter (1999-2017)	10.585	15.91166667	5.956666667	67	10	0.608	-30
Early spring (1999-2017)	14.18888889	19.18888889	9.344444444	60	12	0.832	-60
Late spring (1999-2017)	20.80888889	25.51777778	16.21944444	53	14	1.386	-100
Summer (1999-2017)	27.50666667	30.58611111	24.78277778	53	14	2.046	-120

Experimental data for chambers

Winter

Schedule	Temperature (ºC)	Weighted temperature average (ºC)	Irradiation (lux)	Light hours (h)	Relative humidity	Calculated VPD (kPa)	Soil water potential (Mpa)
04.00-12.00	12	12.64	4000	07.00-17.00	60	0.585031083	-16.83
12.00-16.00	16			0 17.00-07.00	60		
16.00-24.00	12				60		
24.00-04.00	12				60		

Early spring

Schedule	Temperature (ºC)	Weighted temperature average (ºC)	Irradiation (lux)	Light hours (h)	Relative humidity	Calculated VPD (kPa)	Soil water potential (Mpa)
04.00-12.00	14	14.47	4000	06.00-18.00	60	0.6590769	-61.83
12.00-16.00	19			0 18.00-06.00			
16.00-24.00	14						
24.00-04.00	12						

Late spring

Schedule	Temperature (ºC)	Weighted temperature average (ºC)	Irradiation (lux)	Light hours (h)	Relative humidity	Calculated VPD (kPa)	Soil water potential (Mpa)
04.00-12.00	21	20.958	4000	05.00-19.00	50	1.240033662	-105.62
12.00-16.00	26			0 19.00-05.00			
16.00-24.00	21						
24.00-04.00	16						

Summer

Schedule	Temperature (ºC)	Weighted temperature average (ºC)	Irradiation (lux)	Light hours (h)	Relative humidity	Calculated VPD (kPa)	Soil water potential (Mpa)
04.00-12.00	27	27.278	4000	05.00-19.00	50	1.811540954	-160.5
12.00-16.00	31			0 19.00-05.00			
16.00-24.00	27						
24.00-04.00	25						

A P P E N D I X   C

Supplementary Figures

Figure S1. *Terfezia claveryi* **distribution and density of normalised log2 transformed read counts of 9,247 genes from 9 replicates, 3 per treatment.** Flm = free living mycelia; wwm = well watered mycorrhizae; dsm =drought-stressed mycorrhizae.

Figure S2. Correlation of *Terfezia claveryi* transcriptomes among 9 replicates, 3 per treatment. (**A**) Hierarchical clusters of biological replicates based on thedistances of transcriptomic similarities. (**B**) Adjacent matrix of the correlation coefficients (p < 0.0001). Flm = free living mycelia; wwm = well watered mycorrhizae; dsm = drought stressed mycorrhizae.

```
                10        20        30        40        50        60        70        80        90       100
        ....|....|....|....|....|....|....|....|....|....|....|....|....|....|....|....|....|....|....|....|
Pc        MSAFASLITLGFRNPIGQERDQVIQSHYVRAKDFMGTIPSGNSG--------------EEIPGPEQQVTAGAN-------------------
Taest     -------MSTLTALEMAIEAEAFIHQRYGGISFHEYLPLLTDG--------------TFCFEGSDGAQLQVSHMLP----------------
Tmagn     -------MSSLSVLQMAVEAGPLIHQRYHGVNLSQYLSMFANK--------------TFSFNGSDGAQLSVLHMLP----------------
Tmel      -------MTALSMLNMAVEAGPLIHQRYDGIGLAEYIPLLANG--------------TFFFDGSDGAPLQVRHLLP----------------
Terbo     ----MNIQPQNNLPAFSAMQSFHLTNYLQQIGTDDFQATHNIGPD------GIFPIWDVRQQAQPNLKLGPLENPN----------------
Homa      --MENFLIDPTLMGPAHLETSALETAGLDPLVYFTVQQQQILQS----------AWAAATVQISPFSKVAALH--------------------
Ustvirens]  --MTSETNWPEVSQWSPDQLRTLWNQLQAQVNPFAQVLCLD--------------------------------------------------
Kp        MKMKDSFVRIFSIKAMRKEDRDTVRNIRPRVLSCRTQSSMINAAVISKCINTQNVRFYDQGQDGVPVYHDHILNREQARNQFAAQYFHPQIEDVHHINQD

                110       120       130       140       150       160       170       180       190       200
        ....|....|....|....|....|....|....|....|....|....|....|....|....|....|....|....|....|....|....|....|
Pc        ----------------EKITRFICLSPEEIVQSYN--------------------TSTDPAALKAVPCFSPVSVFATGDSVSSLVLLASDGSIVICVEELNKSY
Taest     ----TKWKPTP--------EPLRVSFNPSPHTIVGT------------HLTLHDRPVYKLSDGSILVVSDPTTSPTSFQLTDITFDDP----QHEVTNENR
Tmagn     ----ADWKPAS--------GPLSVSFDSAPHTIVGT------------HHTIRSRPVYKLSDGSILLVFDPVVTDVDFQLTDRSFEDP----QHEIIGLTR
Tmel      ----ADWKPVN--------GPLTVLFDSAPHTIIGT------------HFSIHNHPIYKLNDGSIFVVLD-LATKMGFEFTNQSFMDP----QLEVSGENR
Terbo     ----------------KHHIGRVVYGVPKQYSCNHGYGFDYEN---LVEQGFEPDYANEVVATEALNAHNATLEEIDHMTLWAISKQNGIQYVPAALCP
Homa      ----------------ANMVLALSEDSQKSLLAD--------------------FTNVIGAPALLVRDSSDLDRFFIGSLQEFSSTNQSLIIMPGYDHF
Ustvirens]  -------------------GNLYRMLDNGAKAFIAQN-------------------FINHVKESVLYCIDGTGHDRVFLGAPRHFVAG-CGMILQPRGSEP
Kp        KYLPAWDLDQPKQPHVILGPLEAPQDAVARVVHGIPVQYQANECSVPRLTTYDNVQYGLIRKTINELHALQGNQEEIQEMKFWALKQGTGTQLPPAGLSP

                210       220       230       240       250       260       270       280       290       300
        ....|....|....|....|....|....|....|....|....|....|....|....|....|....|....|....|....|....|....|....|
Pc        LTSDYEDPVEHNMAQRPKATTKQASAH----------------------HIPRPDNAFILYRNHKTGEIKAKYDHLGNNDIS--------------
Taest     FLRFFIKAGQDLSSHEISVRKIQEKG-----------------------IKRPANAFILFRTERMGSIKSQYPGIGNNDIFS-------------
Tmagn     FLRLATDE-QDFASHGASLSLIRAKG-----------------------VKRPANAFILFRTENMRTIKTRVPQMGNNDIS-------------
Tmel      FLRLVTND-QDFAYHGSSLSMIHDKG-----------------------VKRPANAFILFRTDKMKPLKAQYPEMGNNDIS-------------
Terbo     EINEAARSGNWYEANQAAKSITAAGAVVVFDNSTRPDMPKLDKHVDGSYDEEQNGIKRPPNSWILYRRDAHKQIVKLYPKMKNTDIS--------
Homa      FLVSTGDASIQSGLPSPISVQGHESDD------------------SNKDDVKQKLPRPPNAYILYRKERHHSVKDEFPGICNNEIS--------
Ustvirens]  FWIVRSETKVKIATVCPPSIPEKTTK-----------------------IPRPPNAYILYRKERHNTVKEANPGITNNEIS--------
Kp        ALNYAAEEGGGWEAVKEASQTLMAAGNAVSP-----WSSQRKPFMVTAKEEWPNLMRRPPNAWIIYRRDYHKIIAKLFPGMRNTDIS--------
                                                                                          _____

                310       320       330       340       350       360       370       380       390       400
        ....|....|....|....|....|....|....|....|....|....|....|....|....|....|....|....|....|....|....|....|
Pc        ----------KVIGRLWHQEDEALKQSYRQMAKLQTEELLRKFPDYHYQPRRSSEIIPRPG-------------------AQKKDRVRKAKAITRRKSILQ
Taest     --------IAKILGRMNRDSPDEAKEVYKAKARQLAISHKLIYPNYKYTPRAPYEILRRLN------GNVDP----------EIVNEPGN-TVANDLGALT
Tmagn     --------KILGRMWQNSSNEAKEVYKARARQLAISHKLVNPNYKYTPRRSHEIRRRAY------ARKGLSNYVDLHSPGAERDARE-RATTHLGTLT
Tmel      --------KILGRMWQNSSDEVKNVYKARAHQLAVSHKLINPDYKYSPRRSREIMRRGS------GNKGPSARIDLHRAGVAKRGKK-RIITHLGFLT
Terbo     --------KVVSLMWKRESEQVKKYYIDYADEINQNFRQHHPNYRFSPRRPGDRQRRTAR-----ASAADANPADATTQAIQNAADAAQVAQDAAHVA
Homa      --------RILGRRWKEESETVRAFYKEQSENYKQNFMNTHPDYQYRPRKAGEKKKRNR---------------------RVQPKDPENTGLQSPVSAKG
Ustvirens]  --------QILGRAWNLESREVRQKYKDMADRIKQALLEKHPDYQYKPRKPSEKKRRTR-------------------RNTQAQIVVSSTADDFPISSPESGIP
Kp        --------KIIARMWQEEKSEVKMNYKERSDELAQMHKMMNPNYKFNPRKAGERKRRATRERSVLGSADVDALMETLSPVTSHTSNNNSVDCHLENIN
        _____

                410       420       430       440       450       460       470       480       490       500
        ....|....|....|....|....|....|....|....|....|....|....|....|....|....|....|....|....|....|....|....|
Pc        FN---------------SLIVWPHANSYKV--------------------------------------------------------------------
Taest     QR-------------FIAHPTAAT--------LNEIIAEAGQIMSALGYTE-----------------------------------------------
Tmagn     AQ-------------FASEPSTVT--------LGEIIEEAEKVLGSFGLIN-----------------------------------------------
Tmel      QR-------------FATHPTANN--------LGDIIEEAEKVLKAFGMVN-----------------------------------------------
Terbo     AQDAAQVAAQDAAQVAAQDAAQDAAQDEAQDAAQDAAQDAALPLSDYIHILAQIPAQALINTIADAVVSDAEVASSASDVEIASSASDVEVASSASAASS
Homa      TPKVS----------FAESPI----------------------------------------------------------------------------
Ustvirens]  LT--------------ASPPSTHDAN-----------------------------------------------------------------------
Kp        REKISFEPRYNNPSYSSSPSTAHSYSSGECCWETLEQPTNDILTKMQASNTFYDDLGALMLSEPQFFCMSP---------------------------
```

Figure S3. Alignment of the MAT 1-2-1 gene of K. pfeilii with other Pezizomycotina species. Pc = *Pyronema confluens*; Taest = *Tuber aestivum*; Tmagn = *Tuber magnatum*; Tmel = *Tuber melanosporum*; Terbo = *Terfezia boudieri*; Homa = *Huntiella omanensis*; Ustvirens = *Ustilaginoidea virens*; Kp = *Kalaharituber pfeilii*. Underlined section represents HMG box domain and the arrows the conserved intron position.
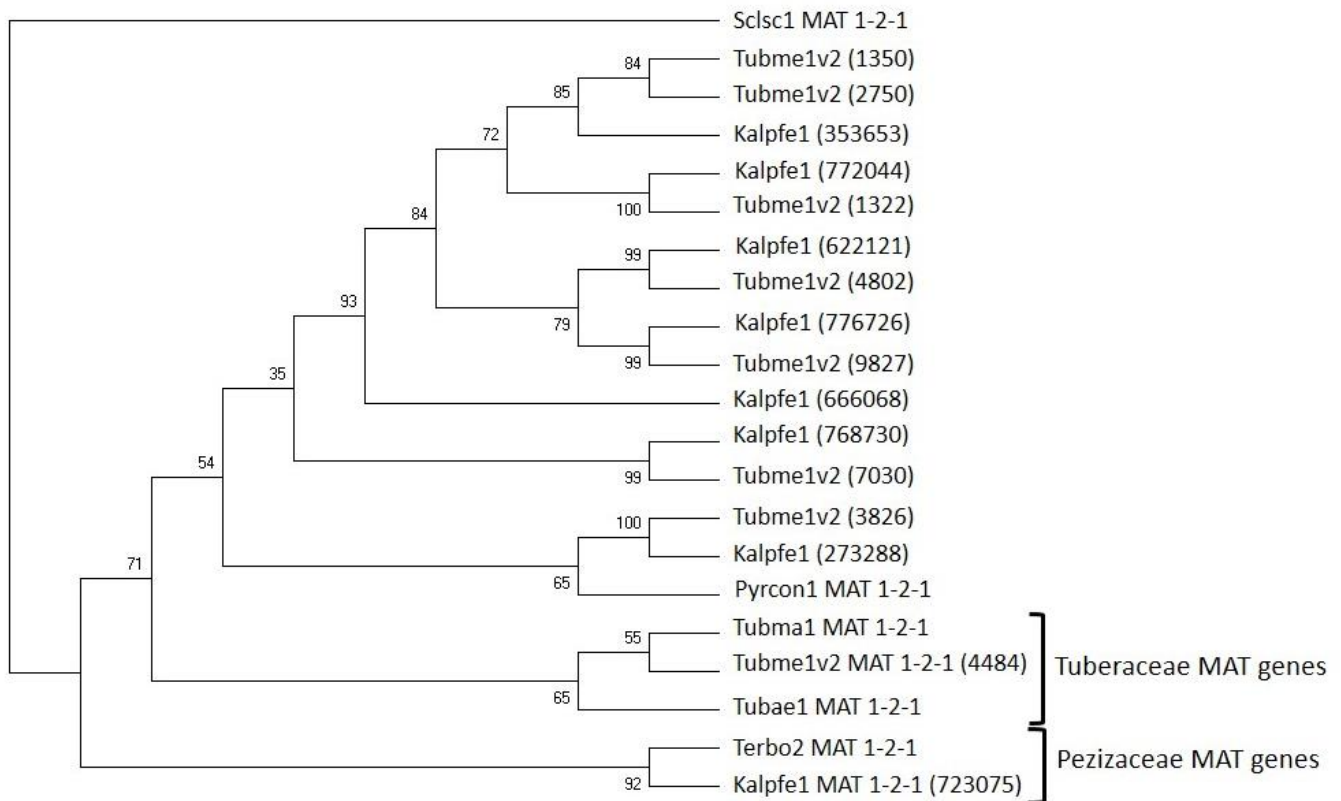
Figure. S4. Phylogeny tree of putative HMG domain containing proteins from *Kalaharituber pfeilii* and *Tuber melanosporum*, togheter with known MAT 1-2-1 genes from Tuberaceae and Pezizaceae. Sequence alignment was performed only on HMG domains, using methods described in M&M section. The numbers in brackets are protein IDs from HMG containing proteins of *T. melanosporum* and *K. pfeilii*. Sclsc1 = *Sclerotinia sclerotiorum*; Tubme1v2 = *Tuber melanosporum*; Kalpfe1 = *Kalaharituber pfeilii;* Pyrcon1 = *Pyronema confluens;* Tubma1 = *Tuber magnatum*; Tubae1 = *Tuber aestivum*; Terbo2 = *Terfezia boudieri.*
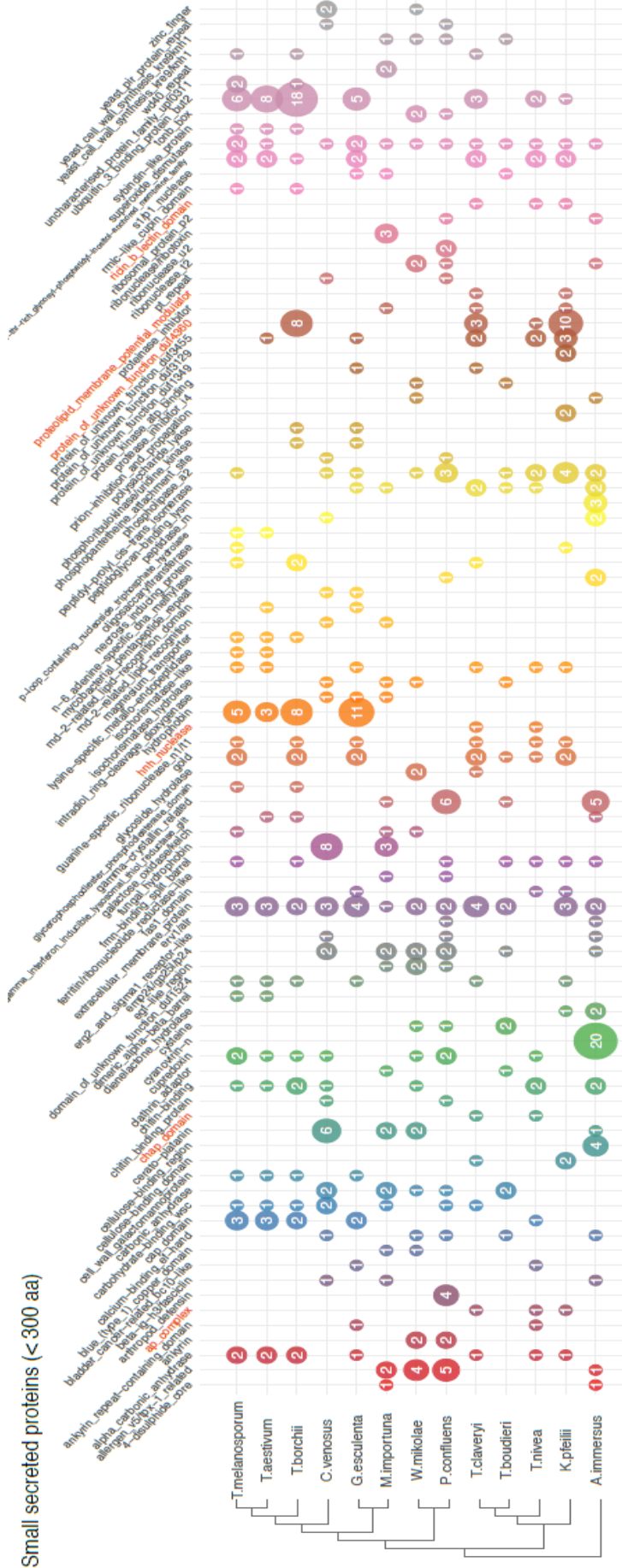
Figure S5. Presence and absence of genes for small secreted proteins (SSPs). Terms of genes unique to desert truffles among the genomes compared are in orange. The count of genes is shown in bubbles with numbers. The species are sorted in evolutionary order.
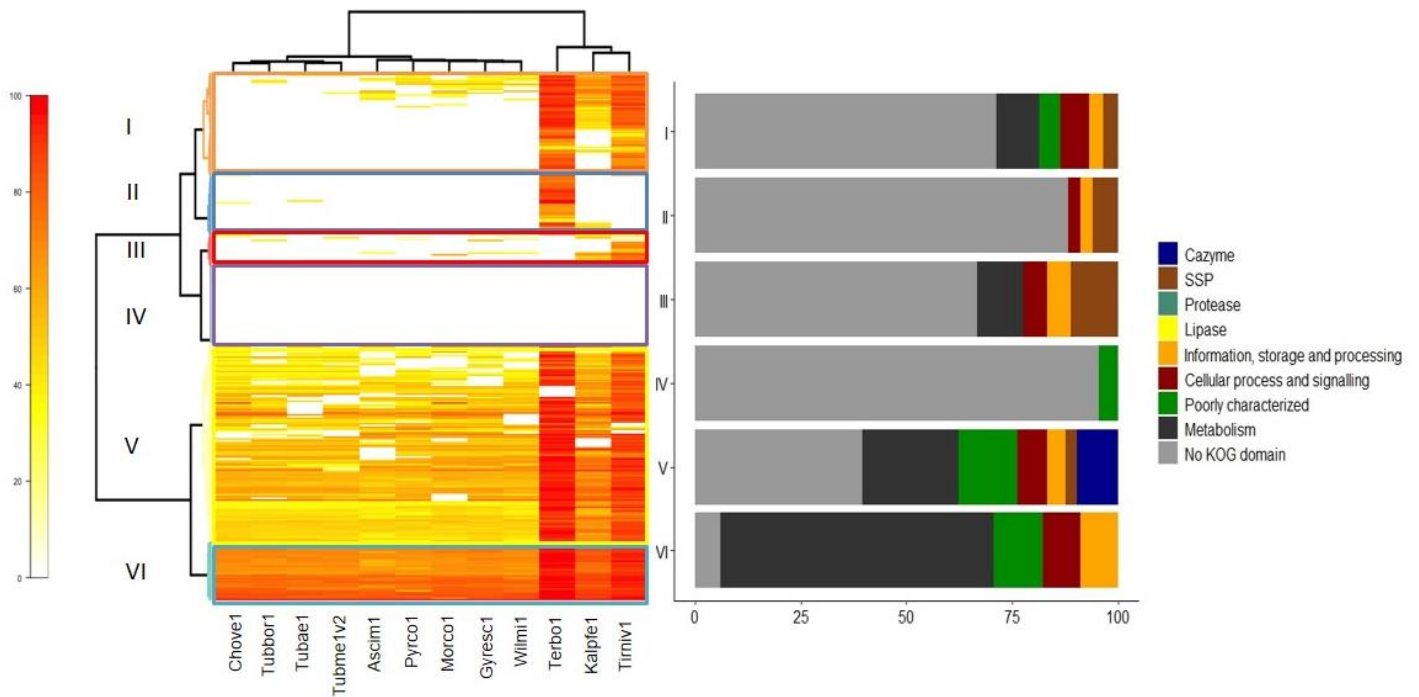
Figure S6. Sequence conservation and functional analysis of symbiosis repressed transcripts. The heatmap depicts a double hierarchical clustering of the symbiosis-downregulated *Terfezia claveryi* genes (rows, fold-change < 4, FDR-corrected < 0.05). Symbiosis-represed genes were blasted (BLASTP) against the genomes of the thirteen genomes analyzed. Homologues are coloured from yellow to red depending on the percentage of similarity. Clusters are numbered and highlighted with different colors. Right of the heatmap, the percentages of putative functional categories are given for each cluster as bar plots. Terbo2 = *Terfezia boudieri*; Kalpfe1 = *Kalaharituber pfeilii*; Tirniv1 = *Tirmania nivea*; Chove1 = *Choiromyces venosus*; Tubme1v2 = *Tuber melanosporum*; Morco1 = *Morchella importuna*; Pyrcon1 = *Pyronema confluens*; Tubbor1 = *Tuber borchii*; Tubae1 = *Tuber aestivum*; Wilmi1 = *Wilcoxina mikolae*; Gyresc1 = *Gyromitra esculenta*; Ascim1 = *Ascolobus immerses*.
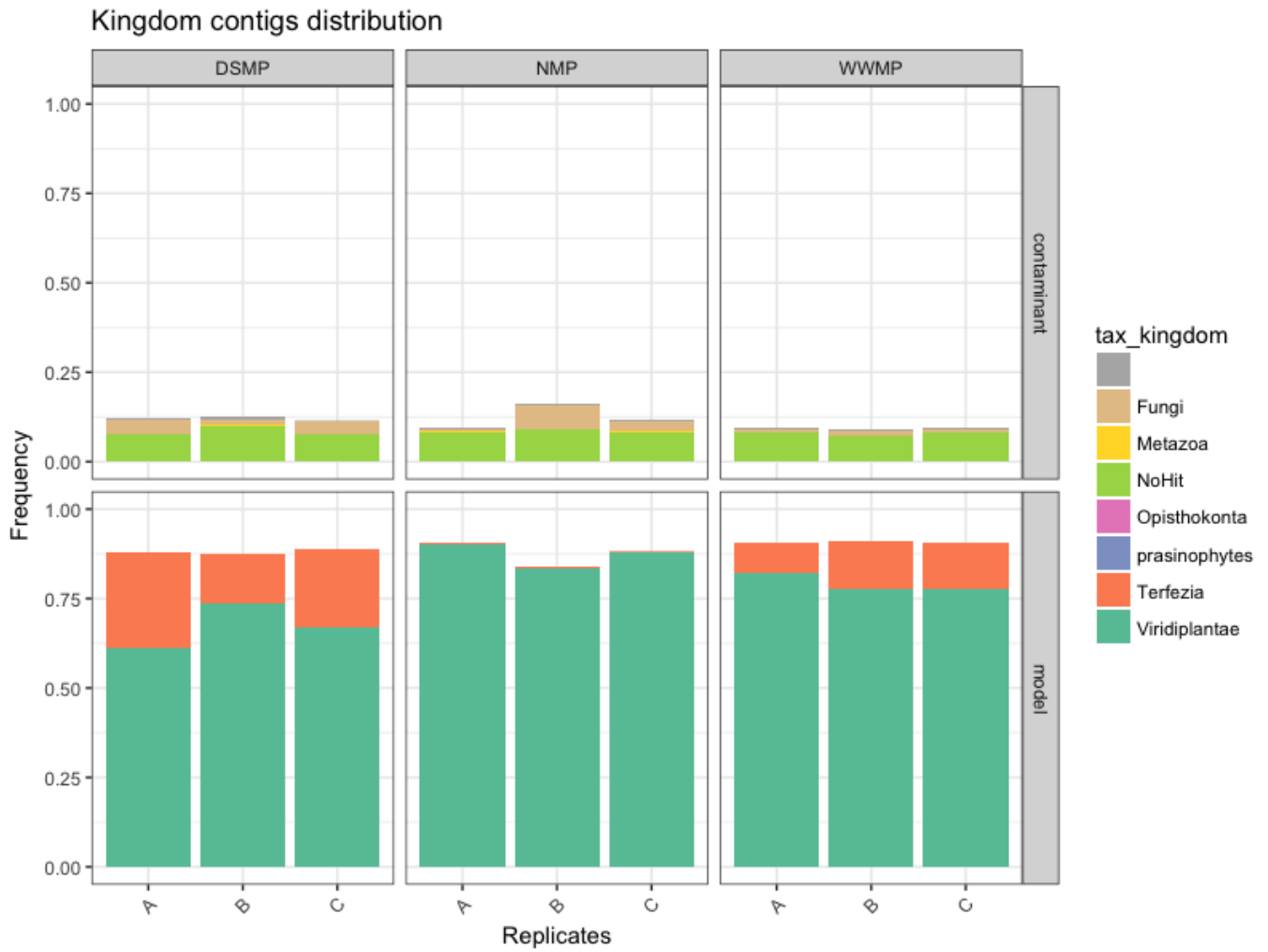
Figure S7. Kingdom contig distribution from reads of the metatranscriptome of *T. claveryi x H. almeriense* roots. DSMP = drought-stressed mycorrhizal plant; NMP = non mycorrhizal plant; WWMP = well-watered mycorrhizal plant. A, B or C refers to each replicate from the 3 different treatments.
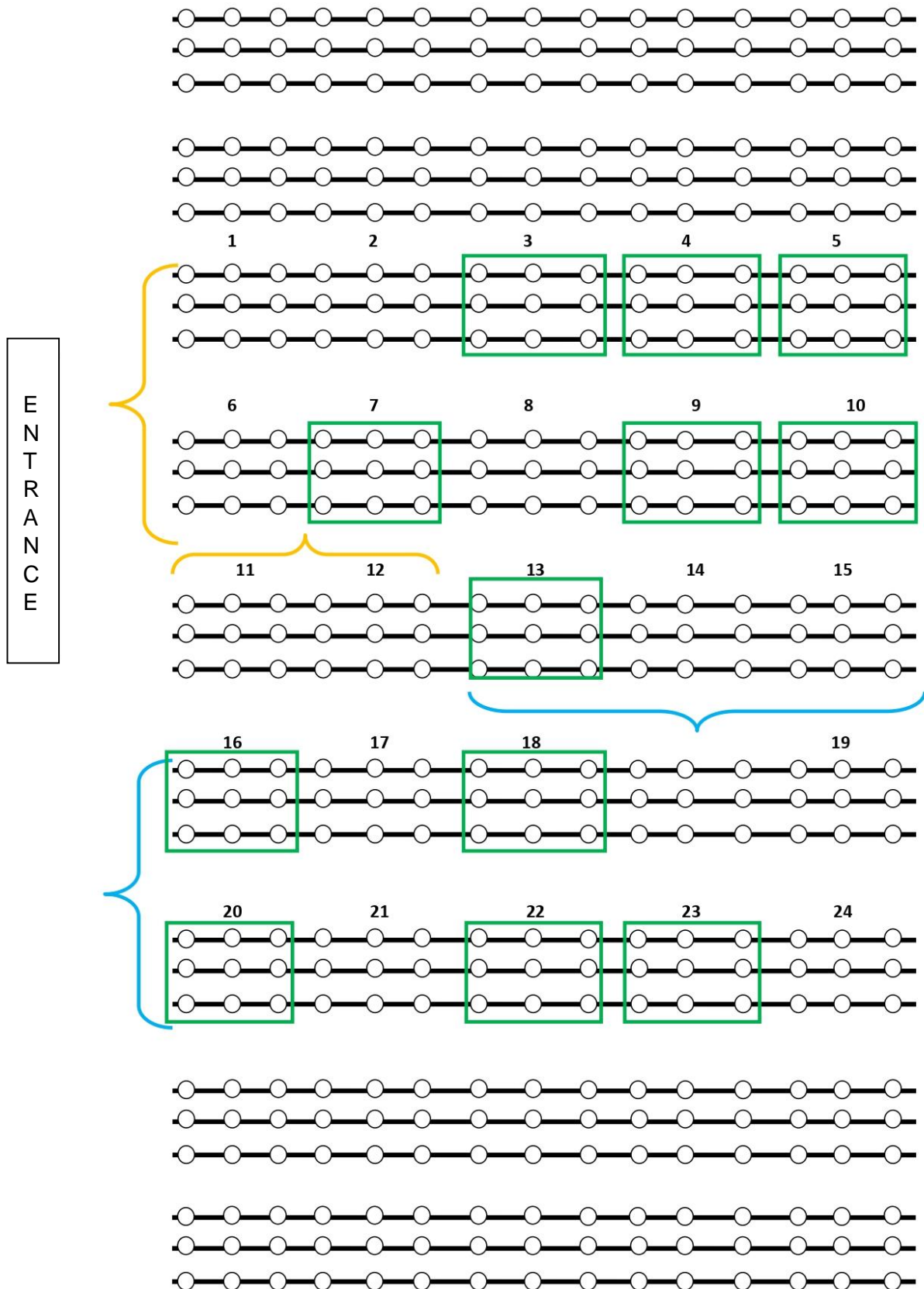
Figure S8. Schematic representation of the experimental site used in Section 6.2.2. Each circle represents a plant, green boxes represent the location of the shadowing devices. Plants inside brackets in yellow were control (non-irrigated), while those inside blue brackets were irrigated.